



Universidade de Brasília

En cotutelle avec l'Université de Paris

Programa de Pós- Graduação em Ciências da Saúde – Universidade de Brasília

Laboratório de Histopatologia Oral, Universidade de Brasília

École doctorale MTCl – Médicament – Toxicologie – Chimie – Imageries ED563

Laboratoire Physiopathologie Orale Moléculaire INSERM UMR_S1138

DECIPHERING RANKL SIGNALING IMPLICATIONS IN CRANIOFACIAL SKELETON GROWTH THROUGH ITS PERMANENT AND TRANSIENT INVALIDATIONS

Andrea Cristina da Silva Gama Cerqueira

Tese de doutorado em Ciências da Saúde/ *Pharmacologie*

Dirigida pela Dra. Ana Carolina Acevedo e pela Dra. Beatriz Castañeda

Apresentada e defendida publicamente em 29/11/2019

Banca examinadora

Pr. Jean-Christophe Fricain - Universidade de Bordeaux

Relator

Pr. Ricardo Della Coletta – Universidade Estadual de Campinas

Relator

Doutor Frédéric Lézot - Inserm

Examinador

Doutor Paulo Marcio Yamaguti – Universidade de Brasília

Examinador

Pra. Ana Carolina Acevedo – Universidade de Brasília

Orientadora

Pra. Beatriz Castañeda - Universidade Paris Diderot

Co-orientadora



Except where otherwise noted, this is work licensed under <https://creativecommons.org/licenses/by-nc-nd/3.0/fr/>

ACKNOWLEDGEMENTS

My sincere thanks goes to Dr. Ariane Berdal and Dr. Sylvie Babajko, who have provided me the opportunity to join their team, and who gave me access to the laboratory and research facilities. Without their precious intellectual support and priceless contribution it would have not been possible to conduct this research.

I am deeply grateful to my supervisors Dr. Beatriz Castañeda and Dr. Ana Carolina Acevedo for all the patience, support, encouragement, supervision, and kind advices which gave me confidence and made the completion of this work possible. I have benefited from every single valuable moment, their expertise and immense knowledge in research. Thank you so very much for your guidance and insightful comments.

I owe my deepest and utmost gratitude to Dr. Frédéric Lézot for his relentless scientific support and engagement in all phases of the project providing me with all the required technical facilities from the INSERM UMR-1238 Laboratory of Bone Sarcoma and Remodeling of Calcified tissues, Team 1 Microenvironment of Primary Bone Tumors: signaling and therapeutic targeting at the Faculty of Medicine in Nantes University, Nantes, France. I would like to extend my gratitude to the whole team 1 with a very special mention to Mr. Jérôme Amiaud, Dr. Jorge William Vargas Franco and Dr. Benjamin Navet for their good willing and sympathy without whom it would have never been possible to come to a good end. Thank you all for your invaluable, priceless contribution!

I am grateful to Professor Jean-Christophe Fricain and Professor Ricardo Della Coletta for agreeing to review my PhD work and manuscript.

I thank Dr. Paulo Marcio Yamaguti for accepting to be full part of the jury.

I thank Mr. Christophe Klein for his kindness and expertise in confocal microscopy.

All my gratitude to the lovely people with whom I had the joy and honor to get along in the Laboratory of Oral Histopathology at the University of Brasília and in the Molecular Oral Physiopathology Laboratory at the *Centre de Recherche des Cordeliers* in Paris.

My thanks to my parents for supporting me spiritually throughout writing this thesis and my life in general. You have given me a wonderful model of hard work and perseverance. I am indebted for an education of which I am proud. To my brother for his encouragement and for the good moments of a lifetime. To my baby sister, you are always in my heart.

To my husband Luiz Felipe for his tireless support.

To my daughters Luíza and Sofia simply because you exist and blindly accept to follow me in my adventures. Our team is unbeatable!

Special thanks to *Fundação de Apoio à Pesquisa do Distrito Federal (FAPDF)*, *Coordenação de Aperfeiçoamento de Pessoal de Nível Superior (CAPES)* in the name of CAPES COFECUB Project, *Polícia Militar do Distrito Federal (PMDF)* and the *Société Française d'Orthopédie Dento-Faciale (SFODF)* for providing the funding for my research and scholarship.

ABSTRACT

Observations relative to osteopetrotic pathologies, showed that the most common oro-dental features in patients with osteopetrosis include osteomyelitis of the jaws, eruption defects and dental anomalies. These observations have raised the question of the origin of such variations in the dento-alveolar phenotype associated to osteopetrosis other than just a defective osteoclastic function. The aim of this project was to assess the importance of the impact of RANKL/RANK/OPG/LGR4 signaling pathway invalidations and its effects on the craniofacial bone growth, the dental development and eruption. We have chosen to work with osteopetrosis models in mouse corresponding to permanent and transient invalidations of the master protein of the osteoclastogenesis, RANKL. The series of experiments performed in an osteopetrotic context of permanent invalidation of RANKL enabled to state that the maternal soluble RANKL is able to cross the placenta barrier and so may participate in the development of the craniofacial skeleton, mostly through its implications in cell-to-cell communications and the osteoclast differentiation control. During tooth later development, the *Rankl* null mutant mice showed important root alterations. Our comparative analyses of the dento-alveolar consequences of transient and permanent invalidations of RANKL has enabled to demonstrate that in addition to the defective osteoclastogenesis, perturbations of the cell-to-cell communications are present with a gradual severity in relation with the penetrance of the RANKL invalidation in terms of intensity and timing. Our results obtained in mouse models demonstrated that defective molar eruptions, more specifically molar retentions, are part of general craniofacial growth alteration. This was confirmed by our clinical data evidencing that primary eruption retentions are associated with a particular craniofacial phenotype. This study suggests that any retained teeth in patients could be the consequence of spatio-temporal perturbations of the RANKL signaling by exogenous actors that remain to be characterized.

KEYWORDS: Osteopetrosis, Tooth eruption, Root elongation, RANKL/RANK/OPG/LGR4 signaling pathway.

RESUME

Les observations relatives aux pathologies ostéopérotiques ont montré que les résultats bucco-dentaires les plus fréquents chez les patients consistaient en une ostéomyélite des mâchoires, des anomalies d'éruption et des anomalies dentaires. Ces observations ont soulevé la question de l'origine de tels défauts du phénotype dento-alvéolaire associés à l'ostéopérose, en plus d'une fonction ostéoclastique défectueuse. L'objectif de ce projet était d'évaluer l'importance de l'impact des invalidations de la voie de signalisation RANKL/RANK/OPG /LGR4 et ses effets sur la croissance osseuse crâniofaciale, le développement dentaire et l'éruption. Nous avons choisi de travailler avec différents modèles d'ostéopérose chez la souris correspondant à des invalidations permanentes et transitoires d'un facteur maître de l'ostéoclastogenèse, RANKL. L'ensemble des expériences effectuées dans un contexte ostéopérotique d'invalidation permanente de RANKL a permis d'affirmer que le RANKL maternelle soluble est capable de franchir la barrière placentaire. Il peut donc participer au développement du squelette crâniofacial, principalement par ses implications dans des communications cellulaires et le contrôle de la différenciation des ostéoclastes. Au cours du développement ultérieur des dents, les souris mutantes pour *Rankl* présentaient des altérations importantes des racines. Nos analyses comparatives des conséquences dento-alvéolaires des invalidations transitoires et permanentes de RANKL ont permis de démontrer qu'outre l'ostéoclastogenèse défectueuse, des perturbations des communications cellulaires sont présentes avec une sévérité progressive en relation avec la pénétrance de l'invalidation RANKL en termes d'intensité et de fenêtre temporelle. Nos résultats obtenus sur des modèles murins invalidés pour *Rankl* ont démontré que les éruptions molaires défectueuses, plus particulièrement les rétentions primaires molaires, font partie de l'altération générale de la croissance crâniofaciale. Ceci a été confirmé par nos données cliniques démontrant que les rétentions d'éruptions primaires sont associées à un phénotype crâniofacial particulier. Cette étude suggère que toutes les dents incluses chez les patients pourraient être la conséquence de perturbations spatio-temporelles de la signalisation RANKL par des acteurs exogènes qui restent à caractériser.

MOTS-CLES : Ostéopérose, Eruption dentaire, Elongation radiculaire, Voie de signalisation RANKL/RANK/OPG/LGR4.

RESUMO

Observações relativas a patologias osteopetróticas mostraram que os achados oro-dentais mais frequentes em pacientes consistiam em osteomielite dos maxilares, defeitos de erupção e anomalias dentárias. Essas observações levantaram a questão da origem de tais variações no fenótipo dento-alveolar associado à osteopetrose, além de apenas uma função osteoclástica defeituosa. O objetivo deste projeto foi avaliar a importância do impacto das inativações da via de sinalização RANKL/RANK/OPG/LGR4 e seus efeitos no crescimento ósseo craniofacial, no desenvolvimento dental e na erupção. Optamos por trabalhar com modelos de osteopetrose em camundongos correspondentes a inativações permanentes e transitórias da proteína mestre da osteoclastogênese, RANKL. A série de experimentos realizados em um contexto osteopetrótico de inativação permanente do RANKL permitiu afirmar que o RANKL solúvel da mãe é capaz de atravessar a barreira placentária e, portanto, pode participar do desenvolvimento do esqueleto craniofacial, principalmente por suas implicações na comunicação célula-célula e controle da diferenciação dos osteoclastos. Durante o desenvolvimento posterior do dente, os camundongos *Rankl* knock out mostraram importantes alterações nas raízes. Nossas análises comparativas das consequências dento-alveolares das inativações transitórias e permanentes do RANKL permitiram demonstrar que, além da osteoclastogênese defeituosa, as perturbações das comunicações célula-célula estão presentes com uma gravidade gradual em relação à penetrância da inativação de RANKL em termos de intensidade e tempo. Nossos resultados obtidos em modelos de camundongos demonstraram que erupções molares defeituosas, mais especificamente retenções dos molares, fazem parte da alteração geral do crescimento craniofacial. Os achados clínicos, evidenciaram que as retenções primárias de erupção estão associadas a um fenótipo craniofacial específico. Esse estudo sugere que dentes retidos em pacientes podem ser consequências de perturbações espaço-temporais da sinalização RANKL por atores exógenos que ainda precisam ser caracterizados.

PALAVRAS-CHAVE : Osteopetrose, Erupção dentária, Elongação radicular, Via de sinalização RANKL/RANK/OPG/LGR4.

TABLE OF CONTENTS

1. PREAMBLE.....	17
2. INTRODUCTION – STATE OF THE ART	21
2.1.Development of the dentoalveolar complex	21
2.1.1.Tooth crown formation.....	22
2.1.1.1.Initiation.....	22
2.1.1.2.Morphogenesis.....	23
2.1.1.3.Histogenesis/ Mineralization	24
2.1.2.Tooth root formation	24
2.1.2.1.Hertwig’s epithelial root sheath (HERS).....	24
2.1.2.2.Cementogenesis	27
2.1.2.2.1.Acellular cementum.....	27
2.1.2.2.2.Cellular cementum.....	28
2.1.3.Alveolar bone formation	29
2.1.3.1.Cellular components	31
2.1.3.1.1.Osteoblastic cells	31
2.1.3.1.1.1.Osteoblasts	31
2.1.3.1.1.2.Osteocytes	33
2.1.3.1.2.Osteoclastic cells.....	34
2.1.3.2.Matrix components.....	36
2.1.3.2.1.Collagen	36
2.1.3.2.2.Non-collagenous proteins	37
2.2.Tooth eruption and alveolar bone remodeling	37
2.2.1.Definition and terminology.....	37
2.2.2.Tooth eruption theories	38

2.2.3.Dental follicle role and bone microenvironment interactions	39
2.2.4.Etiology and diagnosis of tooth eruption disorders	42
2.3.RANKL/RANK/OPG signaling pathway and the dento-alveolar complex	
development	46
2.3.1.RANKL (TNFSF-11)	47
2.3.2.RANK (TNFRSF-11A).....	48
2.3.3.Osteoprotegerin - OPG (TNFRSF-11B)	48
2.3.4.LGR4	49
2.3.5.RANKL/RANK/OPG expression during dento-alveolar complex	
development	50
2.3.6.Phenotypes associated to alterations of the RANKL/RANK/OPG	
signaling pathway	52
2.3.6.1.Genetic alterations.....	53
2.3.6.1.1.Loss of function - Osteopetrosis	53
2.3.6.1.2.Gain of function - Osteolysis	56
2.3.6.2.Therapeutic alterations.....	57
2.3.6.2.1.Inhibitions of RANKL/RANK/OPG/LGR4 signaling.....	57
2.3.6.2.1.1.RANKL inhibition.....	57
2.3.6.2.1.2.Bisphosphonates	59
2.3.6.2.2.Activations of RANK signaling pathway	62
2.3.6.2.2.1.RANK-Fc and OPG-Fc	62
3. HYPOTHESIS	63
4. OBJECTIVES	64
4.1.GENERAL OBJECTIVE.....	64
4.2.SPECIFIC OBJECTIVES	64
5. MATERIALS AND METHODS	66

5.1.Oro-dental features in patients with osteopetrosis: A systematic review of 95 cases .	66
5.2.Experimental study	68
5.3.Clinical study	74
6. RESULTS	78
6.1.Oro-dental features in patients with osteopetrosis: A systematic review of 95 cases (Paper to be submitted)	78
6.1.1.Study selection	78
6.1.2.Study characteristics	78
6.1.3.Quality assessment.....	79
6.1.4.Results of individual studies.....	81
6.2.Maternal RANKL Reduces the Osteopetrotic Phenotype of Null Mutant Mouse Pups evidencing the implication of RANKL signaling in cell-to-cell communications necessary to craniofacial skeleton morphogenesis – Published papers section – paper 1	86
6.3.Origins of Rankl null mutant mouse dental root developmental alterations (Paper to be submitted)	91
6.4.Molar primary retention as part of craniofacial development alteration associated to transitory inhibition of the RANKL signaling	101
6.5.Craniofacial morphology features of patients with Molar primary retention.	111
7. DISCUSSION.....	116
8. CONCLUSION	133
9. PERSPECTIVES.....	135
10. REFERENCES	136
11. ANNEXES	149
12. PUBLISHED PAPERS	167

LIST OF ILLUSTRATIONS

- Figure 1.** Epithelio-ectomesenchymal signaling in tooth development.
- Figure 2.** Schematic representation of enamel knots throughout development.
- Figure 3.** Schematic representation of root morphogenesis.
- Figure 4.** Schematic representation of tooth-alveolar bone complex development.
- Figure 5.** Schematic representation of different steps of osteoclastogenesis.
- Figure 6.** Radiographic imaging of human second molar eruption process.
- Figure 7.** Schematic representation of the signaling pathway during eruption.
- Figure 8.** Schematic representation of signaling in Dental Follicle and Stellate Reticulum of a first rat mandibular molar during tooth eruption.
- Figure 9.** Radiographic imaging of mechanical retention of human second lower molar.
- Figure 10.** Radiographic imaging of secondary retention of human right first lower molars.
- Figure 11.** Clinical photograph of primary failure of eruption. Lateral view of a patient with a classic primary failure of eruption.
- Figure 12.** Schematic representation of RANKL/RANK/OPG/LGR4 signaling pathway.
- Figure 13.** Schematic representation of RANKL / RANK and OPG expression during early stages of dental development.
- Figure 14.** Mechanism of action of denosumab.
- Figure 15.** History of development of RANKL antagonists.
- Figure 16.** Injection protocols of anti-RANKL antibody IK22-5 in mice.
- Figure 17.** Cephalometric landmarks used in growth analysis.
- Figure 18.** Micro CT imaging of dental eruption in mice.
- Figure 19.** Radiographic imaging of cephalometric radiography measurements according to Tweed.

Figure 20. Delaire's qualitative parameters.

Figure 21. Flow diagram of literature search and selection criteria.

Figure 22. Quality assessment graph.

Figure 23. Number of cases distribution according to the type of Osteopetrosis.

Figure 24. Reported eruption anomalies and dental anomalies.

Figure 25. Micro-CT comparative analysis of the craniofacial skeletons of first- and second-generation.

Figure 26. Histological comparative analysis of the craniofacial skeletons of first- and second generation *Rankl* null mutant mice.

Figure 27. Micro-CT imaging of the craniofacial skeleton of pups born from null mutant females and heterozygous males.

Figure 28. Micro-CT imaging of the skeletons of wild type, heterozygous, and first-generation *Rankl* null mutant pups.

Figure 29. Histological comparative analysis of the skeletons of wild type, heterozygous, and first-generation *Rankl* null mutant pups.

Figure 30. Histological comparative analyses of the dental phenotype related of RANKL genotypes.

Figure 31. Comparative analyses of the Hertwig's epithelial root sheath length in the different RANKL genotypes.

Figure 32. RANKL, RANK, OPG and LGR4 expression patterns in the mandible first molar of 5 day-old wild-type mice.

Figure 33. PCNA and P21 expression patterns in the mandible first molar of 5 day-old wild-type mice.

Figure 34. Comparative analyses in 35 days-old mice of the consequences on dental phenotype versus the transient invalidations of RANKL.

Figure 35. Sagittal micro-CT sections comparative analysis of molar eruption in mice.

Figure 36. Masson's trichrome staining histological analysis of the first, second and third lower molars phenotypes.

Figure 37. TRAP histoenzymology evidencing one month after the end of treatment.

Figure 38. TRAP histoenzymology of first lower molar frontal sections of wild type control group mice and PND1 group mice.

Figure 39. Comparative analysis of craniofacial morphometric parameters.

Figure 40. Comparative analysis of Tweed's craniofacial measurements.

Figure 41. Delaire's cephalometric analysis.

LIST OF TABLES

Table 1. Evaluated patients of the Orthopedics-Dentofacial Orthopedics Department of the La Pitié-Salpêtrière hospital

LIST OF ABBREVIATIONS

AB	Alveolar bone
ADO	Autosomal dominant osteopetrosis
AEFC	Acellular extrinsic fiber cementum
ARO	Autosomal recessive osteopetrosis
BMP2	Bone morphogenetic protein 2
BPS	Bisphosphonates
BSP	Bone sialoprotein
CAII	Carbonic Anhydrase II
CBCT	Cone beam computed tomography
c-fos	Fos Proto-oncogene, AP-1 transcription factor subunit
CIFC	Cellular intrinsic fiber cementum
CLCN7	Chloride channel gene 7
CSF-1	Colony stimulating factor 1
DAPI	4',6-diamidino-2-phenylindole
DC	Dental cementum
DF	Dental follicle
DLX	Distal-less homeobox gene
ECM	Extracellular matrix
EGF	Epithelial growth factor
ERM	Epithelial rests of Malassez
Fc-OPG	RANKL-binding domains of osteoprotegerin and an IgG Fc fragment
FGF	Fibroblast growth factor
HERS	Hertwig's Epithelial Root Sheath
HGF	Heparin growth factor
IEE	Inner enamel epithelium
IGF	Insulin growth factor
IL-1 α	Interleukin – 1 α
IP	Intraperitoneally

KO	knock out
LGR4	Leucine-rich repeat-containing G protein-coupled receptor 4
LRP5	Low density lipoprotein receptor-related protein 5
MCP-1	Monocyte chemoattractant protein-1
MCS-F	Macrophage-colony stimulating factor
MSX2	Muscle segment homeobox transcription factor
NCPs	Non-collagenous proteins
NEMO	NF- κ B essential modulator
NFATc1	Nuclear factor of activated T-cells, cytoplasmic 1
NF- κ B	Nuclear transcriptional activator
OC	Osteocalcin
OCIF	Osteoclastogenesis Inhibitory Factor
OEE	Outer enamel epithelium
OPG	Osteoprotegerin
OPG-Fc	RANKL inhibitor
OSX	Osterix
P21	Cdk (Cyclin-dependent Kinase) interacting protein
PBS	Phosphate buffered saline
PCNA	Proliferating cell nuclear antigen
PDL	Periodontal ligament
PFE	Primary Failure of Eruption
PICOS	P: Participant ; I: Intervention ; C: Comparison ; O: outcomes ; S: Study design
PLAP-1	Periodontal ligament associated protein-1
PLEKHM1	Pleckstrin homology domain-containing protein, family M, member 1
PRISMA	Preferred Reporting Items for Systematic Reviews and Meta-analysis
PROSPERO	International Prospective Register of Systematic Reviews
PTH1R	Parathyroid hormone 1 receptor
PTHrP	Parathyroid hormone-like hormone
PTHrp	Parathyroid hormone-related protein
PTM	Post-translational modification

RANK	Receptor Activator of Nuclear Factor- κ B
RANK-Fc	Recombinant RANK-L antagonist
RANKL	Receptor Activator of Nuclear Factor- κ B ligand
RSPO	R-spondin
RUNX2	Runt-related transcription factor 2
SI	Stratum Intermedium
SMAD4	Mothers against decapentaplegic homolog 4
SNX10	Sorting nexin 10
SOST	Sclerostin
SR	Stellate reticulum
TBI	Tooth-bone interface
TCIRG1	T cell immune regulator 1
TGF β	Transforming growth factor β
TNFR	Tumor necrosis factor receptor
TNFSF	Tumor necrosis factor ligand superfamily
TNF α	Tumor necrosis factor α
TRAF6	TNF receptor-associated 6
TRAIL	TNF-related apoptosis-inducing ligand
TRAP	Tartrate-resistant acid phosphatase
WNT	Wingless gene

1. PREAMBLE

Teeth are epithelial-mesenchymal organs developing and functioning in intimate coordination with bone and periodontal tissues. This complex develops in continuous interactions between the oral ectoderm and the ectomesenchymal cells of neural crest origin [1].

Tooth development involves the crown and the root formation. When crown formation is nearly complete, the tooth root begins to develop with the guidance of the Hertwig's epithelial root sheath (HERS), a double epithelial layer formed from the outer and inner enamel epithelium at the cervical loop of the crown which grows in the apical direction. The HERS is located between the two regions of neural crest-derived mesenchyme: the dental papilla and the dental follicle. Later, the dental papilla cells adjacent to the inner epithelial layer of the HERS and the epithelial basement membrane differentiate into odontoblasts, and thus to form root dentin. Studies have shown that odontoblasts communicate with the cells of the bone microenvironment throughout the root elongation process [2,3].

The eruption mechanism depends on the spatial relationship between the eruption pathway created by the crown dental follicle, on the bone remodeling in the apical region and, on the root adaptation of the periodontal ligament to eruptive movements. At a cellular level, the eruption process depends on the reciprocal interactions between HERS, the follicle and alveolar bone cells [4]. Cellular mobilization in the remodeling of the bone implies a process of apposition and bone resorption by specialized cells, osteoblasts, and osteoclasts [5,6].

The RANKL/RANK/Osteoprotegerin (OPG) triad is one of the main signaling pathway of bone remodeling that enables direct communication between osteoblasts and osteoclasts. Additionally, the triad plays a major role in the course of alveolar bone remodeling required for dental eruption and root formation as shown in the studies of Castañeda et al., 2011, 2013 [7,8].

Other studies on the RANKL/RANK/OPG pathway in dentoalveolar growth confirmed its importance in maintaining the integrity of the set formed by the tooth and the alveolar bone in the physiological and pathological context. The RANKL and BMPs are regulated by the MSX2 transcription factor to coordinate the allometric growth of the crown, the elongation of the root, and the eruption [9–12].

Since early 2000s, the Oral Molecular Physiopathology team INSERM UMR_S 1138 in Paris, France led by Pr. Ariane Berdal and Dr. Sylvie Babajko has been studying the correlation of tooth development and the surrounding alveolar bone. Within this framework, the team evaluated the role of the RANKL/RANK/OPG signaling pathway in postnatal growth in mice overexpressing RANK. The results showed increased osteoclasts in the alveolar bone, early root formation, and accelerated dental eruption when compared to wild littermates. RANK overexpression stimulated cell proliferation follicle and HERS cells, which accelerated root elongation, especially on the fifth postnatal day [7].

To deepen the understanding of the role of RANK/ RANKL/ OPG signaling in the dentoalveolar complex, the dentoalveolar phenotype in knockout mice (KO) for the *Rankl* gene was studied during my master's degree under the direction of Dr. Beatriz Castañeda. The *Rankl*^{-/-}, the *Rankl*^{+/-}, the wild type, and the overexpressing RANK mice were assessed and they showed no root formation and gradual tooth inclusion within the bone suggesting ankylosis in the molars of the *Rankl*^{-/-} mice. In contrast, these results were not observed in heterozygote, wild, and RANK overexpressed mice. These observations highlighted the crucial role of the RANK/RANKL/OPG signaling pathway for the formation of dental roots and confirmed the relation between the adjacent dental and non-dental tissues in the pathophysiology of dentoalveolar complex.

The present study is the continuation of my master's degree. It is a part of the CAPES/COFECUB international collaboration project. It was developed in the Molecular Oral Pathophysiology laboratory (INSERM UMR_S 1138 – Paris – France) and in the Laboratory of Oral Histopathology, Health Sciences Faculty, University of Brasília (Brasília, Brazil) in collaboration with Unit 1238 of INSERM, Faculté de Médecine, Université de Nantes (France), in accordance to the international agreement signed between the Universities of Brasília and Paris Descartes.

The general aim of the present study is to assess the importance of the impact of RANKL/RANK/OPG/LGR4 signaling pathway through permanent and transient invalidation and its effects on the craniofacial growth and on the dental development, from the initial stages of morphogenesis to the functional molar eruption.

The aim of the experimental study was to develop a murine model of tooth eruption inhibition and root formation through injections of a neutralizing anti-RANKL antibody for the comparison with the model of *Rankl* KO. The evaluation of transient inhibition of RANKL in murine models depending on the teeth affected may determine the period during which the eruptive process and root growth are compromised and how the modulation in bone resorption induces blockage of the eruption as well as elongation of the roots.

The key clinical research question of this study was whether there is a specific craniofacial phenotype in patients affected by the primary failure of eruption and if both conditions are directly related. In order to address this question, the experimental strategy regarding the murine model injected with a neutralizing antibody anti-RANKL was used. Besides, a systematic review of the oro-dental manifestations in patients with osteopetrosis as well as a clinical study that compared and evaluated 42 patients presenting tooth eruption defects, with mechanical etiology or primary retention, were performed.

The results of the present study provide a better understanding of eruption pathologies and could guide the clinical management of patients helping to establish well adapted orthodontic therapeutic strategies.

2. INTRODUCTION – STATE OF THE ART

2.1. Development of the dentoalveolar complex

Dental development is a complex physiological process that includes the crown formation through the stages of bud, cup and bell, late bell and root development. These events are followed by tooth eruption which gives rise to the tooth functional position in the mouth [13].

Teeth are epithelial-mesenchymal organs consisting of oral ectoderm and ectomesenchymal cells derived from neural crest in functional coordination with periodontal tissues and surrounding bone [1]. All the odontogenesis phases are under the coordination of different signaling pathways that regulate the expression of important genes in the initiation, the morphogenesis and the cytodifferentiation stages [14]. Factors and associated signaling pathways that mediate communication between cells, from the tooth development initiation to root formation, belong to the families: BMP (bone morphogenetic protein), FGF (fibroblast growth factor), Hedgehog and WNT. They are crucial for tooth development all along the different developmental stages [9,15–17]. Paracrine signal molecules of several conserved families mediate cell communication during tooth development and it was conclusively shown

that the same signals are used sequentially throughout morphogenesis, and many factors are often co-expressed (Figure 1).

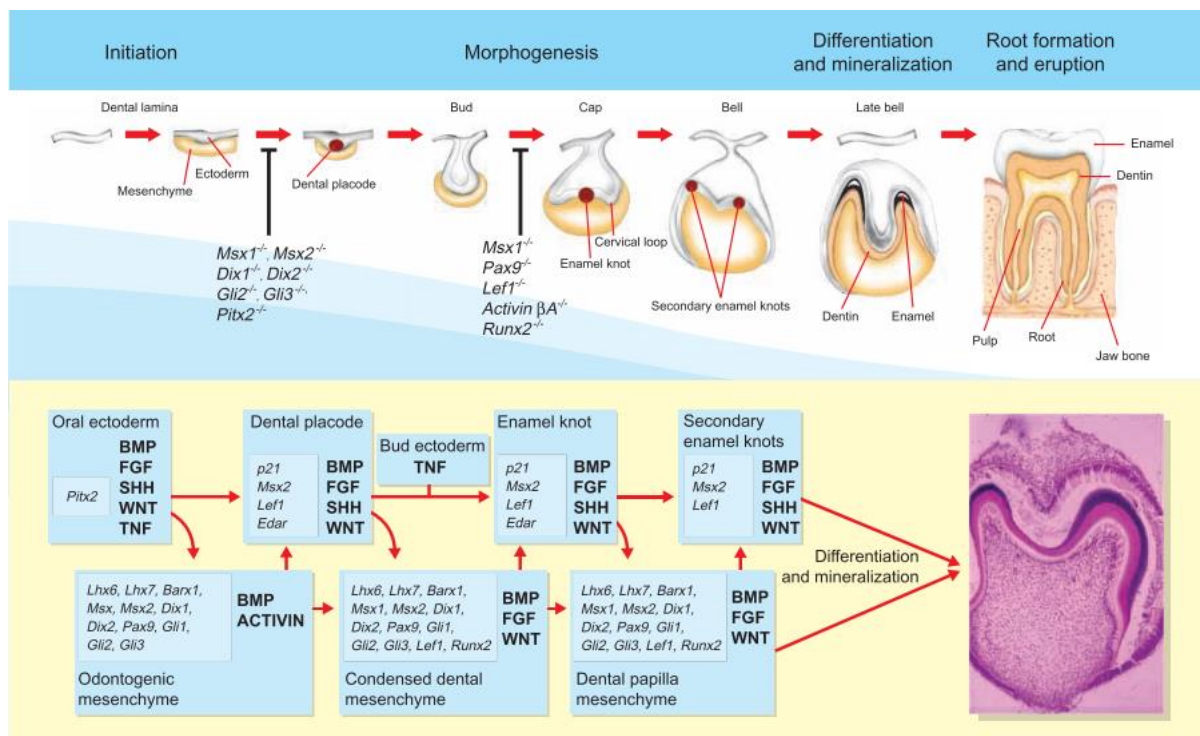


Figure 1. The signaling in tooth development Adapted from Thesleff, 2003.

The understanding of the interactions between dental cells and those of the surrounding bone is very important since an intricate cascade of gene expression directs the cells to the right place and into the proper differentiation pathway [13]. The slightest disruption in the development of one of the tooth tissues and its supporting bone has repercussions on the other and it may lead to defects of the complex tooth/periodontium at several levels.

2.1.1. Tooth crown formation

2.1.1.1. Initiation

Odontogenesis begins very early during embryonic development, when the initial maxillomandibular complex are developed. A spatial-temporo combination of transcription factors determines the intra- and inter-maxillary typology and position of each dental unit and the alveolar bone. This is what Paul Sharpe assimilated in the mid-1990s to a "dental

homeocode” that was reviewed by Suryadeva in 2015 [18,19]. Teeth form from the ectoderm surface of the first branchial arch and the frontonasal prominence as well as from the underlying ectomesenchyme that is derived from the neural crest [16]. A key feature during tooth initiation is the ectoderm thickening forming a placode within the primary epithelial bands that buds to the underlying neural-crest-derived ectomesenchyme [13]. The oral epithelium initiates tooth development thanks to FGFs (Fibroblast Growth Factors), BMPs (Bone Morphogenetic Proteins), WNTs and SHH (Sonic hedgehog) interacting with the underlying neural crest-derived mesenchyme [20].

2.1.1.2. Morphogenesis

Following the epithelium thickening during the first steps of tooth formation, the epithelium interacts with the ectomesenchyme which then condenses around the epithelial bud [21]. In the subsequent stage of development, the epithelium folds and grows to surround the dental papilla ectomesenchyme (cap stage). During the bell phase, the internal epithelium of the enamel organ doubles and determines the shape and number of cusps guided by the signaling of the enamel knots [22] (Figure 2).

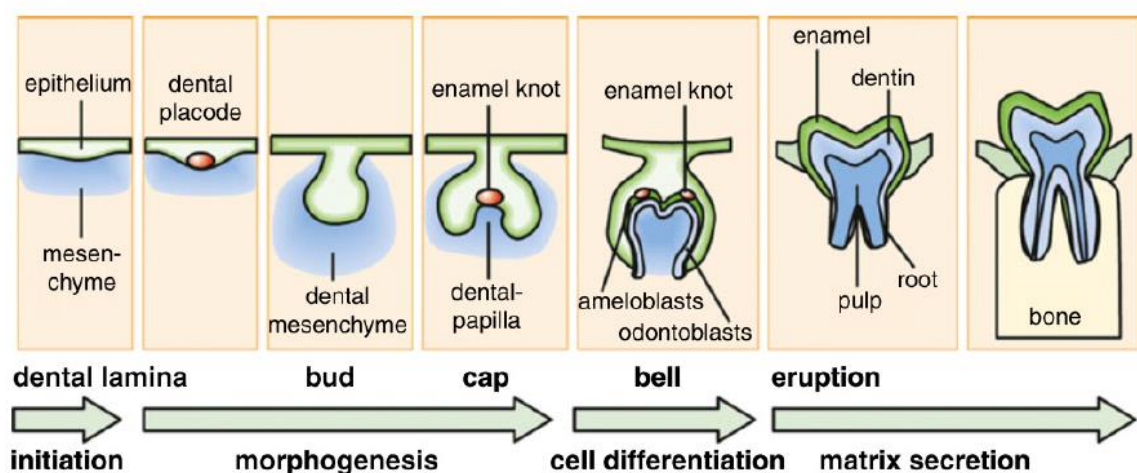


Figure 2. The dental placode and enamel knots are signaling centers regulating tooth morphogenesis. Adapted from Thesleff, 2014.

2.1.1.3. Histogenesis/ Mineralization

The late bell stage involves cytodifferentiation events. The mineralized dental crown tissues, dentin and enamel, are formed by specialized cells, the odontoblasts and ameloblasts differentiating from the ectomesenchyme and epithelium, respectively. Ectomesenchymal cells facing the basement membrane differentiate into dentin-producing odontoblasts and start to secrete organic dentin matrix that serves as a scaffold for the deposition of hydroxyapatite crystals. Shortly after initial predentin deposition, the adjacent layer of epithelial cells differentiates into ameloblasts and they secrete organic enamel matrix necessary for the three-dimensional organization of enamel and subsequently mediate enamel maturation. Histodifferentiation in the crown region is followed by histodifferentiation in the root [23]. Dental and periodontal histogenesis corresponds to an important volumetric growth of these tissues, more precisely regarding root formation [24].

2.1.2. Tooth root formation

2.1.2.1. Hertwig's epithelial root sheath (HERS)

After the completion of crown formation, the apical ectomesenchyme continues to proliferate to form the developing periodontium. Also, the inner and outer enamel organ epithelia fuse below the level of the crown cervical loop to produce a bilayered epithelial sheath termed Hertwig's epithelial root sheath (HERS) that grows apically. [25]. The classic theory of root formation states that, as these cells divide, there is an apical migration of HERS cells through the underlying dental ectomesenchymal tissues (dividing them into dental papilla and dental follicle). During tooth root development, all functional hard tissues are formed by three kinds of cells: HERS, dental papilla mesenchymal and dental follicle cells, which form developing apical complexes [2].

As the root develops, the first radicular mantle dentin is formed, the epithelial sheath fenestrates, and individual cells migrate away from the root into the region of the future periodontal ligament to form the rests of Malassez [2,26,27]. These dental follicular cells differentiate into cementoblasts (Cb) to form the cementum. Simultaneously, the collagen fibers of the periodontal ligament secreted by the periodontal fibroblasts are integrated into the new cementum matrix and anchors the root in the alveolar bone [2] (Figure 3). HERS, when guiding root formation, secretes growth factors that contribute to odontoblastic differentiation, suggesting that HERS is a signaling center [9,28,29]. After HERS is fragmented, clusters of epithelial cells involved by a basal lamina, called epithelial rests of Malassez (ERM), remain in a quiescent state in the periodontium and seem to be responsible for root repair/regeneration [30].

The HERS plays an important role in root elongation via tissue interactions with pulpal ectomesenchyme on the one hand and the dental follicle on the other hand. HERS cells express epithelial molecules such as cytokeratin, E-cadherin, and ameloblastin, as well as mesenchymal molecules such as BSP, vimentin, and N-cadherin [31]. The mechanism of interaction between the epithelial cells of the sheath and the mesenchymal cells, as well as the signaling pathways involved, are currently poorly understood. Indeed, while the interactions between epithelium and mesenchyme cells have been extensively studied during early development as previously described [22], only a few studies focused on communications between root (dental epithelial cells) and bone cells during late development.

Recent studies in rodents have shown the cellular dynamics and expression levels of growth factors and their receptors, namely: FGFs (fibroblast growth factors), EGF (Epithelial growth factor), HGF (Hepatocyte growth factor) and IGFs (Insulin growth factors) in the root-crown transition region [32]. New evidence demonstrated that *Nfic*, the main gene in root formation, interacts directly or indirectly with the Osx-Wnt/ β -catenin and Tgf β -Bmp-Smad4

signaling pathways through the interaction between HERS and the dental ectomesenchyme [33].

HERS at the apex of the developing root becomes fragmented, allowing cementoblasts or fibroblasts derived from the dental follicle to contact the outer surface of the root. In 2013, Sakano et al.[32] suggested that HERS was mainly composed with outer enamel epithelium, and interacted with dental follicle cells for root and periodontal ligament (PDL) development after fragmentation [34].



Figure 3. Root morphogenesis scheme in 2 stages: root initiation and root elongation. HERS is formed by fusion of outer enamel epithelium (OEE) and inner enamel epithelium (IEE), which marks the initiation of root formation. Some HERS cells eventually become epithelial rests of Malassez (ERM). DFC, dental follicle cells; HERS, Hertwig's epithelial root sheath; SI, stratum intermedium; SR, stellate reticulum. Adapted from Wang et al., 2017

2.1.2.2 Cementogenesis

The tooth root cementum is a thin, mineralized tissue covering the root dentin surface, critical for anchoring the tooth to the surrounding alveolar bone (AB) via the periodontal ligament. It has historically been classified into cellular and acellular cementum by inclusion or non-inclusion of cementocytes. Generally, acellular cementum is thin and covers the cervical root, whereas thick cellular cementum covers the apical root [35]. Cementum is primarily made up of two parts, the acellular extrinsic fiber cementum (AEFC, acellular or primary cementum) and the cellular intrinsic fiber cementum (CIFC, cellular or secondary cementum), though mixed stratified cementum exhibits layers of both types in some species [36]. Dental cementum (DC) and AB share common progenitor cells in the ectomesenchymal dental follicle. Moreover, DC is often described as bone-like, therefore questions remain whether cementoblasts are merely positional osteoblasts. DC is avascular, non-innervated. It grows by apposition with no significant turnover or remodeling. [37,38].

The HERS' cells of the inner epithelium take part directly in the formation of the first acellular cementum layer. This process is carried out under the double influence of epithelial cells and mesenchymal cells [35].

2.1.2.2.1.Acellular cementum

Acellular cementum anchors collagen fibers from the periodontal ligament (PDL), promoting attachment to the surrounding alveolar bone (AB) [38]. Acellular cementum covering the cervical portion of the root is critical for tooth attachment to the adjacent periodontal ligament (PDL), while cellular cementum covering the apical root is supposed to play a role in post-eruptive tooth movement and adaptation to occlusion [36].

The acellular extrinsic fiber cementum is morphologically uniform and it is cell-free consisting of a tight bundle of fibers (Sharpey's fibers), inserted from the outside and anchored

in the mineralized parts of the cementum. The presence of a large amount of these fibers demonstrates the importance of its function in anchoring teeth. It is located in the cervical third of the root and may extend more apically to the anterior teeth. Acellular cementum is forming very slowly but at a constant rate. Consistency and arrangement of acellular cementum layers respond to changes in Sharpey's fiber orientation which adapts and changes continuously throughout life during post-eruptive tooth movement. Part of the acellular cementum is afibrillar. It is located at the cervical border of the enamel and is formed after the end of the pre-eruptive maturation of the enamel and possibly during the dental eruption. It is generated by cementoblasts and its function remains poorly understood [39].

2.1.2.2.2. Cellular cementum

The first cementum layer in the cervical portion of the root is acellular. More apically, toward the root apex, cementum becomes both thicker and cellular. Cementoblasts, tooth root lining cells, are responsible for laying down cementum on the root surface, a process that is indispensable for establishing a functional periodontal ligament. These cells are responsible for synthesizing the extracellular matrix (ECM) and promoting mineralization of the cementum. When they become entrapped within the matrix layer, they are termed cementocytes [40]. Cao et al in 2014 documented a close relationship between the temporal and spatial expression pattern of Osterix (OSX) and the formation of cellular cementum [41]. The following year, Kim et al. stated that OSX is required for root formation by regulating odontoblast differentiation, maturation, and root elongation [42]. Later, He et al. in 2016 suggested that OSX functions promote odontoblast and cementoblast differentiation and root elongation, but not crown formation [43,44].

Some authors suggest that cementoblasts can have three origins:

- During the early stages of root formation, the HERS cells convert into mesenchymal cells and then into cementoblasts.

- Then, during the root elongation, the dissociation of the HERS would allow the fibroblasts of the dental follicle to access the formed dentin and to differentiate into cementoblasts.

- Later, when the tooth is erupted and contact its antagonist in the oral cavity, the progenitor cells of the periodontal ligament differentiate into cementoblasts under the influence of the growth factors of the cementum. While cementoblasts are phenotypically similar to osteoblasts, and cementum resembles bone in mineral composition and hardness, cementum is not known to undergo any significant turnover during lifetime [31].

2.1.3. Alveolar bone formation

The development of the alveolar bone is coordinated with that of the tooth (Figure 4). More precisely, the volumetric tooth growth at both the coronal and radicular levels as well as the displacements of the growing dental germs, relative to each other, involve a process of modeling the peripheral bone [5,9]. Despite the dental eruption does not depend on root formation, the bone crypt must adapt to the crown and root formation, hence bone remodeling linked to the phenomenon of eruption [45–48]. The mechanism of eruption depends on the spatial relationship of the eruption pathway created by crown dental follicle cells, the eruption pressure caused by the apical innervation of the root membrane, and the periodontal ligament adaptation to the movement [4]. This bone mobilization for the eruption involves the processes of resorption and apposition with the emergence of the notion of site specificity [6]. These two well-known coupled processes rely on the recruitment and activation of highly specialized cells osteoclasts and osteoblasts, the involvement of cells in the osteoblastic pathway, progenitor commitment, their proliferation, osteoblast differentiation and function, are governed by a

precise genetic program that includes transcription factors and members of four major families: WNT (Wingless-like), TGF- β (Transforming growth factor β), Hedgehog (Sonic, Indian and Desert) and FGFs (fibroblast growth factors) [49–51]. Proliferation and differentiation of osteoblastic precursors are also under the control of several hormones: Parathyroid hormone, sex steroid hormones, glucocorticoids, growth hormone and vitamin D are the main ones. Their direct or indirect effects on osteoblasts vary according to the stage of maturation and the microenvironment of the bone. The cells involved in tooth development from ectoderm and ectomesenchyme derived from the neural crest form the alveolar bone, the periodontal ligament and the cementum constituting the functional unit of mastication [1,52]. The region between the alveolar bone and the cementum of the tooth is defined as the tooth-bone interface (TBI) [5,52].

During crown development, this functional unit is located between the dental germ and the surrounding alveolar bone and creates the space necessary for tooth growth while during the development of the root, there is a space composed of a soft tissue in which the periodontal ligament can develop [52]. If the TBI is not maintained, the bone fuses with the resulting tooth giving rise to ankylosis, hence the importance of osteoclasts that maintain the TBI and the non-mineralization of the TBI in order to avoid disturbance of tooth growth [53] (Figure 4).

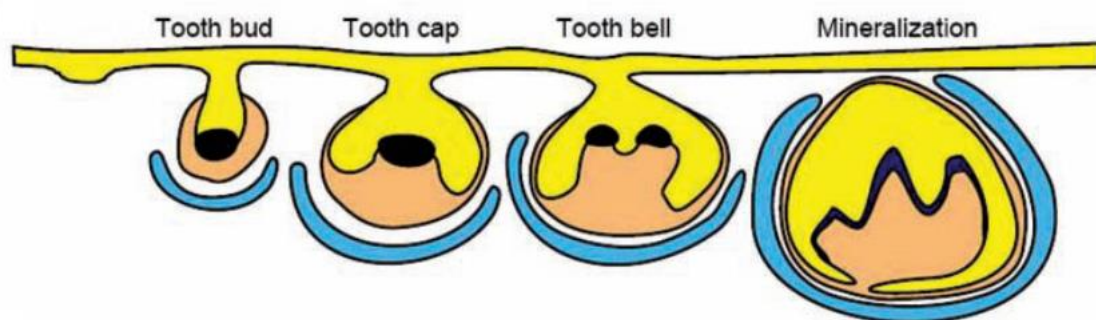


Figure 4. Schematic representation of tooth-alveolar bone complex development. Yellow: oral and dental epithelium; Orange: dental mesenchyme; Blue: developing alveolar bone; Black: enamel knots. Adapted from Fleischmannova et al., 2010.

Considering the above concept of TBI, Yamada et al. in 2007 attested that PLAP-1/ asporin plays a crucial role in the periodontal ligament (PDL) as a negative regulator of

cytodifferentiation and mineralization. Aspirin regulates BMP-2 activity to prevent the PDL non-physiological mineralization such as ankylosis. As a matter of fact, the authors suggested that some mechanisms exist to constitutively prevent unorchestrated osteogenesis and cementogenesis by PDL cells [54]. The actual mechanism to maintain the TBI involves the aspirin direct binding to BMP-2, and inhibition of TGF- β /SMAD signaling, resulting in the inhibition of bone formation [55].

2.1.3.2. Cellular components

2.1.3.2.2. Osteoblastic cells

2.1.3.2.2.1. Osteoblasts

The osteoblasts have a mesodermal origin in most of the skeleton, but derived from the neural crest in most of skull and face bones. The osteoblastic progenitors are mesenchymal cells present in the medullary stroma, the periosteal and endosteal surfaces.

The osteoblast, confined for a long time to its bone building function, is actually a very eclectic cell, actively regulating osteoclast formation and function as well as hematopoietic stem cells homeostasis. It is also an endocrine cell, affecting energy metabolism, male fertility and cognition through the release of osteocalcin, a perfect definition-fitting hormone in its uncarboxylated state [56].

The involvement of cells in the osteoblastic pathway, their proliferation, differentiation and function are governed by a precise genetic program controlled by several transcription factors, including the homeoproteins of the MSX family which allows the acquisition of the osteoblastic phenotype. RUNX2 is the main factor regulating osteoblastic differentiation. It is a transcription factor belonging to the Runt family, which includes three members: RUNX1-3. The expression of *RUNX2* begins at the level of mesenchymal condensations preceding osteoblastic differentiation [57]. *Runx2*^{-/-} mice die at birth and present a total absence of bone

tissue by default of osteoblasts. The skeleton is normal but completely cartilaginous [57,58]. Recent studies suggest that *RUNX2* may play a major role in the engagement of mesenchymal stem cells in the osteoblast lineage [59]. It has also been shown that overexpression of *RUNX2* in preosteoblasts inhibits their proliferation [60] and that overexpression of *RUNX2* in non-osteoblastic cells induces the expression of osteocalcin (OC) and sialoprotein bone (BSP) [61,62]. Expression of the *Runx2* gene is regulated by many factors, such as BMPs, some WNTs, and several homeodomain transcription factors including *MSX2*, *DLX3* and *DLX5*. Matrix-synthesizing osteoblasts are recognized by their cuboidal shape, their location on newly formed bone matrix, and the expression of relatively osteoblast-specific genes such as osteocalcin. During the process of bone formation, matrix-synthesizing osteoblasts have at least three potential fates. Some of them become embedded within the bone.

The WNT pathway plays an important role in early embryonic development, tissue inductions, dental morphogenesis, skeletal development, cell growth regulation and osteoblast differentiation [63,64], and also in the regulation of osteoclast differentiation by inhibition of expression of RANKL in osteoblasts [63].

Osteoblasts have two major interdependent functions during growth and in adults. On the one hand, bone formation by synthesis and mineralization of the collagen-based bone matrix, and on the other hand, control of recruitment and differentiation of osteoclasts via the RANKL/RANK/OPG signaling pathway [64].

Accumulating evidence also implies that osteoblastic RANKL regulates osteoblastogenesis [65–67]. Interestingly, Ikebuchi et al. in 2018 revealed that RANKL- RANK signaling regulates osteoblastogenesis in addition to its role in osteoclastogenesis [68].

2.1.3.2.2.2. Osteocytes

Osteocytes are derived from osteoblasts, which in turn are derived from osteogenic precursors residing in the bone marrow. The mature osteocyte represents a terminally differentiated stage of the osteoblast lineage. However, the precise mechanisms by which an osteoblast becomes embedded in bone matrix to begin a new life as an osteocyte and the genetic and molecular mechanisms that regulate the differentiation and maturation of the osteocyte are not yet fully understood [69]. Osteocytes are the most abundant cell types in bone and arguably the least well understood. The technical advances that greatly accelerated research into osteoblast and osteoclast biology in the 1970s and 1980s, such as the identification of cell type-specific markers, development of techniques for bone cell isolation and culture, and the establishment of phenotypically stable cell lines, have only lately proved fruitful for osteocytes. Until the last decade, osteoblasts and osteoclasts the effector cells that carry out bone formation and resorption remained the focus of research aimed at understanding bone modeling and remodeling [70].

Recent studies suggest that osteocytes are the major source of RANKL in physiological and pathologic osteoclastogenesis. The osteocyte death associated with bone microdamage leads to upregulation of the RANKL/OPG ratio in osteocytes adjacent to the damaged site, which explains the localized formation of mature osteoclasts. Osteocytes provide RANKL to osteoclast precursors through direct interactions at the extremities of dendritic processes. In addition, OPG functions not only as a secreted decoy receptor for RANKL but also as a regulator of RANKL intracellular traffic, restricting RANKL presentation to the cell surface, which likely determines the magnitude of signal input [71–73].

Several evidences show that the osteocytes do not merely represent the osteoblasts fate, but they are instead very active cells that, besides a mechanosensorial function, they actively contribute to the bone remodeling by regulating bone formation and resorption. The regulation

is exerted by the production of sclerostin (SOST), which in turn inhibits osteoblast differentiation by blocking WNT/beta-catenin pathway. At the same time, osteocytes influence bone resorption both indirectly, by producing RANKL, which stimulates osteoclastogenesis, and directly by means of a local osteolysis, which is observed especially under pathological conditions [56,73].

2.1.3.2.3. Osteoclastic cells

Osteoclasts are multinucleated giant cells essential for physiologic remodeling of bone and also play important physiologic and pathologic roles in the dentofacial complex that differentiate from myeloid precursors under the influence of the cytokines macrophage colony stimulating factor (MCS-F) and receptor activator of NF- κ B ligand (RANKL) supplied by osteoblasts and/or osteocytes. These osteoclastic precursors differentiate into pre-osteoclasts, mononuclear cells possessing all of the osteoclastic markers (TRAP activity, alphaV-beta3 integrin, calcitonin receptor, etc.), which merge with each other to give the functional multinucleate osteoclast [74,75]. A decoy receptor for RANKL called osteoprotegerin (OPG), which is also secreted by the osteoblast lineage, tempers osteoclast differentiation. Osteoclasts degrade bone by the polarized secretion of proteolytic enzymes (e.g. cathepsin K) and acid, which hydrolyze and solubilize the organic and inorganic components of bone, respectively. Proton and enzyme secretion are directed into a resorption lacunae, which is partitioned from rest of the bone microenvironment by a sealing zone of densely packed podosomes that surrounds the apical membrane of the osteoclast. Subsequent to the osteoclastic resorptive phase, coupling mechanisms promote the recruitment and differentiation of mesenchymal derived osteoblast progenitors at the resorption lacunae. After these cells mature into osteoblasts, they line the eroded bone surface and secrete the organic component of bone, termed osteoid, which is mineralized over time by the incorporation of hydroxyapatite [75].

Differentiation of osteoclasts, like that of any hematopoietic cell, requires close interactions with stromal cells or osteoblasts. These interactions involve not only molecules synthesized by the stromal cells, active on the precursors of osteoclasts, but also direct contacts between these two cell types. When those two cells interact, they can form gap junctions and small water-soluble molecules can pass through the two cell types [76]. Everts et al. 2009 have shown that bone lining cells, a subpopulation of the osteoblast, are in close contact with osteoclasts attached to bone. The initiation of osteoclastogenesis mainly depends on the interaction between those two cell types [6]. The factors involved, some of which have recently been identified, are either expressed on the surface of the stromal cells from which they can be released by proteolysis [74], or directly secreted. The two major signaling factors implicated in these differentiation steps are presented in Figure 5.

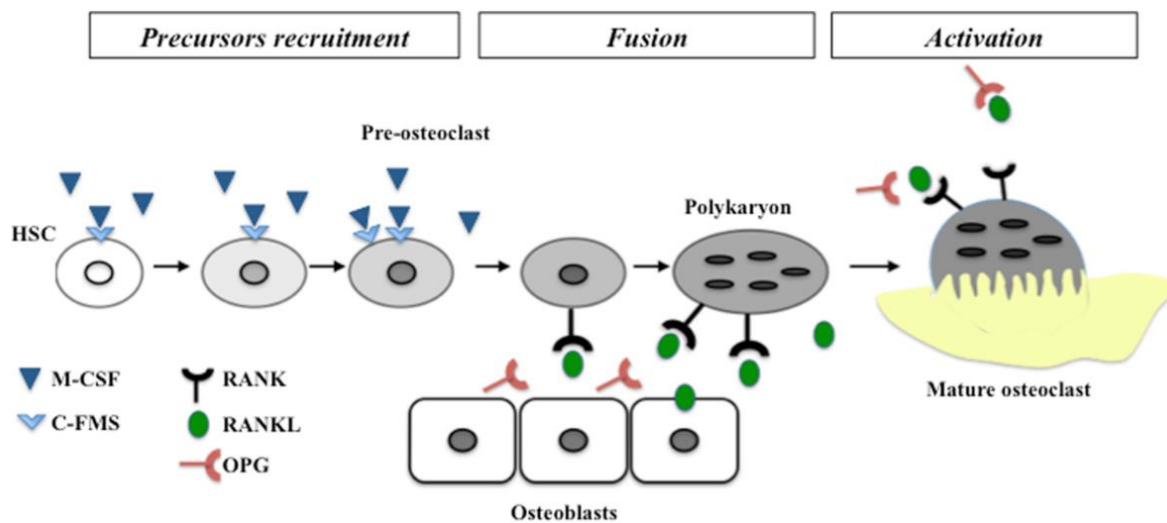


Figure 5. Schematic representation of different steps of osteoclastogenesis. The two main factors controlling the differentiation called M-CSF and RANKL are represented with their receptors. M-CSF is necessary to recruitment and expression of RANK at the surface of pre-osteoclasts. RANKL enable the fusion of pre-osteoclasts in polykaryon and the final differentiation in mature osteoclasts. HSC, hematopoietic stem cell. Adapted from Gama et al., 2015.

2.1.3.3. Matrix components

2.1.3.3.2. Collagen

Collagens are essential for cell-cell interactions and cell attachment to the basement membrane. They are indispensable for skin formation, the organization of cells into tissues, and tissue function [77]. The collagen superfamily contains at least 27 types of collagens that together constitute the most abundant proteins found in the body. All collagens are composed of three polypeptide alpha chains coiled around each other to form the typical collagen triple-helix configuration. Common features include the presence of the amino acid glycine in every third position (Gly-X-Y repeating sequence), of hydroxyproline and hydroxylysine, and of non-collagenous domains, and a high proportion of proline residues. Variations among the collagens include differences in the assembly of the basic polypeptide chains, lengths of the triple helix, interruptions in the helix, and the terminations of the helical domains [13].

The organic phase of bone is primarily a network of interlinked type I collagen. Specifically, tropocollagen (300 nm × 1.6 nm in diameter) is a triple helix consisting of two α -1 chains and one α -2 chain with a distinct motif (Glycine-X-Y) n in which X is often proline (~28% in collagen I) and Y is often Hydroxyproline (~38% in collagen I). Post-translational modifications (PTMs) of collagen are important to the overall structure and stability and, in turn, the mechanical behavior of bone. Hydroxylation of proline is one type of PTM that forms hydroxyproline, which facilitates hydrogen bonding with both water and other amino acids within the collagen chain. The collagen-rich matrix of bone confers toughness to an otherwise brittle mineral phase (i.e., ceramics like hydroxyapatite exhibit little post-yield deformation) [78].

2.1.3.3.3. Non-collagenous proteins

Although collagen I is the most abundant protein in the organic matrix (~90%), non-collagenous proteins (NCPs) also participate in the control of mineralization as well as in the quality and the biomechanical properties of bone. The NCPs include glycoaminoglycan containing molecules (aggrecan, biglycan, decorin), glycoproteins (alkaline phosphatase, osteonectin, periostin, tenascin), Small Integrin Binding Ligand N-Glycosylated Proteins-SIBLINGs (bone sialoprotein, dentin sialoprotein, dentin matrix protein I, matrix extracellular phosphoprotein, osteopontin), RGD containing glycoproteins (fibronectin, vitronectin), Matrix-Gla proteins, osteocalcin, and serum proteins such as albumin. Some debate still continues as to whether the non-collagenous proteins are contained within the collagen secretory granules or in a distinct population of granules. Irrespective of this aspect, non-collagenous proteins also are released mainly along the surface of osteoblasts apposed to osteoid and diffuse from the osteoblast surface toward the mineralization front where they participate in regulating mineral deposition [13,78].

2.2. Tooth eruption and alveolar bone remodeling

2.2.2. Definition and terminology

Dental eruption is defined as the movement of the tooth from its site of development in the alveolar bone to its functional position in the oral cavity. It is a localized event that requires the dental follicle (DF) to regulate the resorption of alveolar bone to form an eruption pathway [79,80]. The dental germ carries out a three-dimensional path through the alveolar bone which undergoes a peripheral remodeling due to the volumetric growth of the tooth.

According to Marks and Schroeder (1996) [45], the dental eruption process is conventionally divided into 5 stages:

- 1) the pre-eruptive tooth movements (figure 6. 1);

2) the intra-osseous eruption allows redirection of alveolar growth: there is evidence of bone resorption at the crown level and bone formation at the root level (Figure 6. 2);

3) the transmucosal eruption begins after the tooth has passed through the alveolar bone crest and has penetrated the oral epithelium. This stage is marked by the appearance of the junctional epithelium on the surface of the tooth (Figure 6. 3);

4) the pre-occlusal movements correspond to the stage where the tooth appears in the oral cavity and adopts its functional position (Figure 6. 4);

5) the post-eruptive movements allow the tooth to have a functional and adaptive position according to occlusal attrition and facial growth (Figure 6. 5).

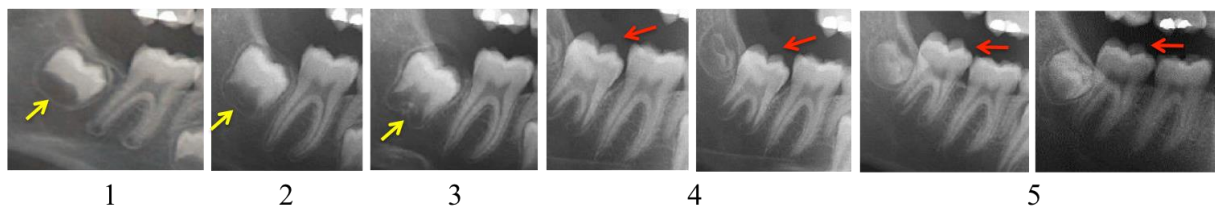


Figure 6. Panoramic radiographies evidencing the second lower molar eruption process according to Marks and Schroeder's classification (1996). Yellow arrows: 1. Pre-eruptive movement; 2. Intraosseous eruption movement; 3. Transmucosal eruption movement. Red arrows: 4. Pre-occlusal eruption movement; 5. Post-eruptive movement.

Each step requires a reciprocal interaction between the tooth and its surrounding tissues, while being coordinated in time and space with the growth of the jaws and those of other teeth, via specific molecular and genetic actors.

2.2.3. Tooth eruption theories

Dental eruption is a complex phenomenon and results from a balance between eruptive forces (mechanisms to "push" the germ) and resistance forces (mechanisms for "pulling" the germ) [81]. No consensus on the origin of the eruption process has been determined, but several theories have been evoked over the years [82].

These theories can be classified into two categories:

- Theories related to periodontal tissues: contraction of collagen within the periodontal ligament, traction of periodontal fibroblasts, hydrostatic and vascular pressure;
- Theories related to other factors: root edification, proliferation of pulp cells, alveolar growth and the role of the dental follicle.

Some of these assumptions have been refuted over time, others lack suitable scientific evidence to confirm them. For example, the theory that root elongation allowed tooth eruption was invalidated since rootless tooth can continue to erupt [46,48]. Similarly, after irradiation of the root growth zone (Hertwig's epithelial root sheath) in the monkey, the tooth still erupts [83].

The studies concluded that the process was too complex to be explained by the simple involvement of a single tissue.

2.2.4. Dental follicle role and bone microenvironment interactions

The dental follicle is the precursor of the periodontal ligament and other periodontal components such as cementum and alveolar bone. It is connected to the gingiva via an extension/canal called the dental gubernaculum [84]. It is at the level of this canal that the bone resorption necessary for the formation of the eruption path takes place. Studies have shown that molars in osteopetrotic rats do not erupt because bone resorption in these animals is reduced [85]. The role of the dental follicle in the eruptive process was mainly studied during a series of experiments by Marks and Cahill using the mandibular premolar teeth of dogs as a model.

In 1980, they conducted a study to analyze the role of the root, the dental crown, the follicular sac and the gubernaculum canal in the process of dental eruption. Their results demonstrate that tooth eruption is not affected by the removal of the gubernaculum, that of the roots or that of the dental pulp. Similarly, when the follicle is dissociated from the dental crown and replaced elsewhere without the crown, the path of eruption is still formed (via bone resorption) and bone apposition at the basal level of the crypt is present.

On the other hand, removal of the dental follicle prevents the creation of a pathway and the tooth does not erupt. In order to understand the dental crown role on eruption, the same authors repeated the experiment in 1984 by analyzing 29 dog premolars. They replaced the tooth with a metal replica while keeping the dental follicle intact and they showed that the replica erupted. Therefore, they demonstrated that the dental follicle plays a primordial role in the eruptive process, whereas the tooth itself does not contribute to it.

After validating the theory of dental follicle involvement in eruption, they took a closer look at its cytology (and that of the bony crypt) by examining the dental follicles of dog premolars at 2 week intervals for 12 weeks during their eruption. The objective was to characterize qualitatively and quantitatively the cells present at different eruption times. They described a strong increase of mononuclear cells in the coronary part of the dental follicle just before the eruption. These cells had the same histological characteristics as those of monocytes, precursors of osteoclasts. At the same time, there was an accumulation of osteoclasts and monocytes on the surface of the bone crypt, *i.e.* at the beginning of the formation of the eruption pathway (Figure 7).

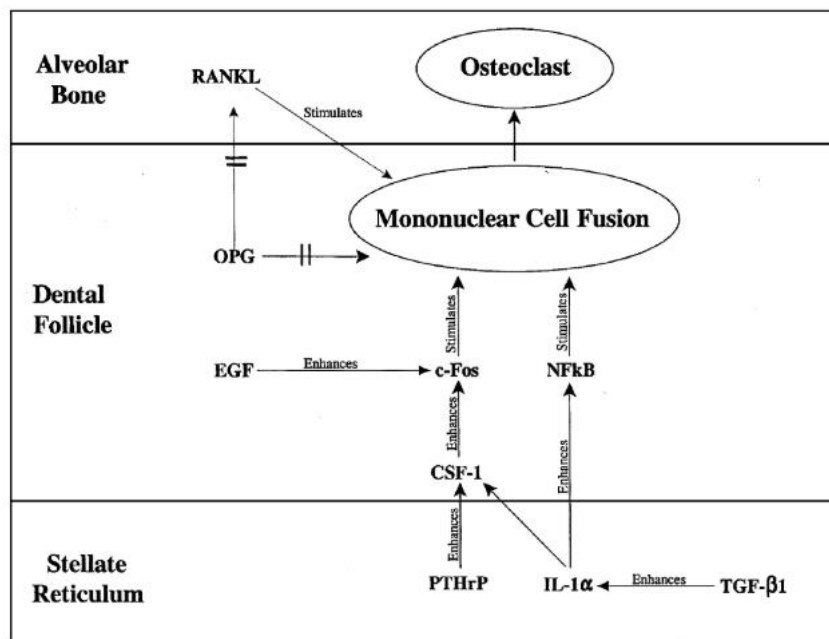


Figure 7. Signaling pathway - osteoclast formation during eruption. Adapted from Wise et al., 2002

Marks et al. in 1987 [86] showed that these monocytes are immediately adjacent to osteoclasts, and also often located near the microvasculature of the dental follicle. This particular location and morphology suggest that monocytes leave the bloodstream to migrate to the bone crypt where they differentiate and fuse to form the osteoclasts required for coronary bone resorption. In the basal part of the bone crypt, there is a significant number of osteoblasts, associated with a strong bone cell proliferative activity. Other studies have demonstrated the presence of regional differences in the tooth follicle [86]. Specifically, when the coronal half of the follicle is removed (leaving the basal part intact), the eruption path is not formed because bone resorption is blocked. Conversely, if the basal half of the follicle is removed, the tooth does not erupt due to the absence of alveolar bone formation.

These studies of the intraosseous stage of tooth eruption show that this phase is characterized by the translocation of the tooth through the developing alveolus by a coordinated resorption and formation of bone and that this process can be plastic and asymmetrical to accommodate root growth and tooth drift. All these metabolic events likely begin in the enamel epithelia and are continued and coordinated by the dental follicle through local signals which involve proteins and growth factors made in the follicle or adjacent tissues. According to the literature, this signaling cascade is summarized in Figure 8.

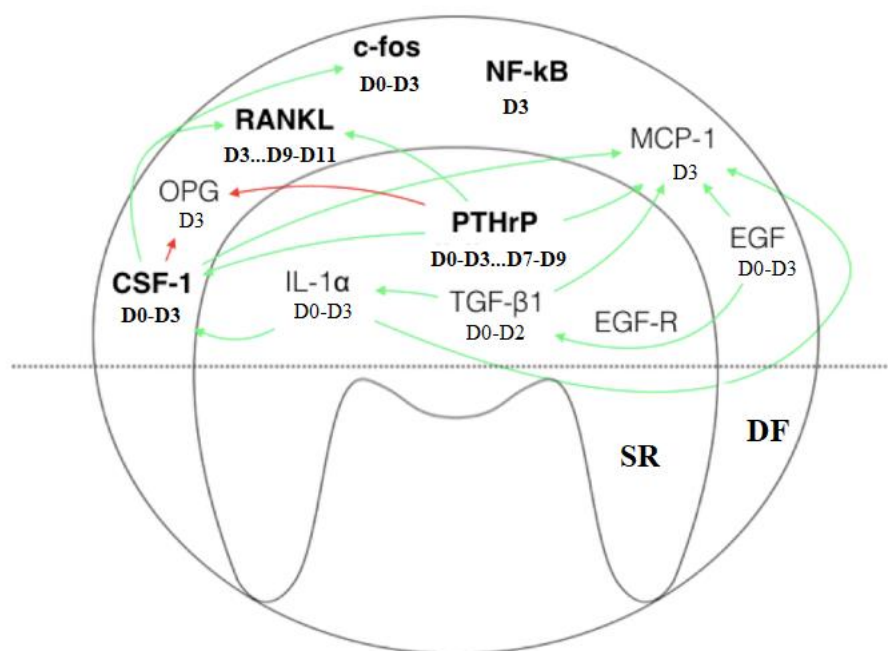


Figure 8. Schematic representation of Dental Follicle (DF) and Stellate Reticulum (SR) of a first rat mandibular molar. The signaling cascade occurring in the coronal portion of the crypt initiates the eruption. The words in bold represent essential actors to eruption. The green arrows indicate a stimulating action, and the red arrows an inhibiting action. Adapted from Choukroune, 2016.

A better understanding of the unique aspects of osteoclastogenesis and osteoclast function will facilitate effective development of new therapeutic approaches [87]. Dental eruption is therefore a polarized process.

2.2.5. Etiology and diagnosis of tooth eruption disorders

Prevalence studies of eruption anomalies of permanent molars were conducted in the department of Dentofacial Orthopedics of *La Pitié-Salpêtrière* Hospital between 2013 and 2015 on 1432 patients followed up in the department. These alterations were present in 1.68 % of the patients of the service. In 2017, these data were updated and showed a prevalence of 2.02 % affected patients. According to Bondemark, all second molar eruption abnormalities account for 2.3% of orthodontic patients [88].

Regarding general etiologies, two main categories are found: systemic etiologies and genetic etiologies [89]. Tooth eruption disorders were found associated to endocrine disorders

such as hypothyroidism, hypoparathyroidism and hypopituitarism (pituitary insufficiency) and also to specific treatments such as anti-cancer treatments (chemo or radiotherapy), the use of antibiotics and bisphosphonates. They are also found in malnutrition with vitamin A and D (rickets) deficiencies, HIV infection, anemia, renal failure and premature birth.

Regarding the genetic etiology, several conditions associated with delayed eruption are reported [89]: abnormalities of dental structure such as hereditary amelogenesis imperfecta (enamel-renal syndrome), dentine dysplasia; ectodermal dysplasia such as congenital dyskeratosis and anhidrotic ectodermal dysplasia; bone diseases such as cleidocranial dysplasia, osteopetrosis, sclerosteosis, osteogenesis imperfecta, cherubism, osteoglophonic dwarfism, gingival fibromatoses, endocrine diseases such as Turner's syndrome, McCune-Albright syndrome and hereditary vitamin-resistant rickets; neurological diseases such as Down Syndrome and Carpenter Syndrome; some dysmorphic syndromes (Apert syndrome, Goldenhar syndrome) and primary failure of eruption.

For other etiologies, the origin implies environmental factors intervening after birth. Thus, the transient alteration of dental eruption by some environmental factors and conditions is of particular interest in the kinetics of the effects obtained on dental eruption.

Eruption alterations can present a broad spectrum of severity, they can concern simple eruption delays up to retentions and severe tooth inclusions of the tooth. It is considered that the tooth has a delayed eruption when it has not erupted while $2/3$ of the root is formed.

In 1991, Raghoobar [90] defined the different eruption anomalies according to their etiology:

- Impaction is defined as the blockage of tooth eruption caused by a clinically or radiologically detectable obstacle to the eruption pathway or because of an abnormal tooth (e.g. a change in angulation of the eruption path). In this sense when the obstacle

is removed, the evolution of the tooth is favorable [91]. The most common etiologies are: lack of space in the arches and the presence of supernumerary teeth, odontogenic tumors or cysts [92,93] (Figure 9).

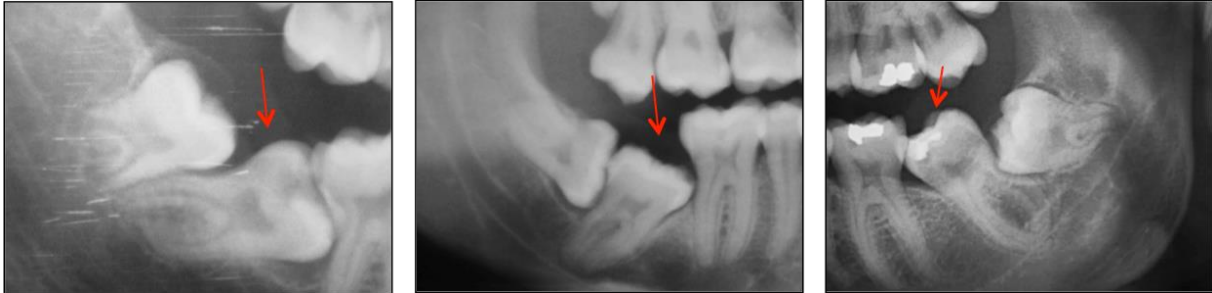


Figure 9. Panoramic radiographies evidencing lack of space and a mechanical obstacle to normal eruption process. Red arrows: Second lower molars impaction.

- Primary retention is a term that defines the eruption interruption of a normally positioned tooth in the absence of a physical barrier on its eruption path, before its emergence into the oral cavity. An eruption path is formed and visible radiographically. Primary retention is probably caused by a disturbance in the dental follicle that fails to initiate the metabolic events of osteoclastogenesis necessary for the eruptive phenomenon [91,92]. Primary retention is suspected when it has not erupted two years after the normal age of eruption.
- Secondary retention is described as the tooth eruption interruption after gingival emergence, in the absence of a physical barrier on its eruption path (Figure 10).



Figure 10. Panoramic radiography evidencing a secondary retention in which tooth eruption is interrupted after gingival emergence, in the absence of a physical barrier on its eruption path.

Among the primary retentions, the primary failure of eruption (PFE) is an anomaly in the eruptive phenomenon leading to the absence of the eruption of the tooth [94]. This alteration can be symmetrical or asymmetrical, uni- or bilateral. The posterior teeth are most often affected and the teeth posterior to the first affected tooth are usually affected. The tooth is not ankylosed and an eruption pathway is observed. Temporary and permanent dentition may be affected, a decrease in the growth of the alveolar bone and a severe open bite are observed in the affected area.

Nevertheless, in some patients it is unclear whether PFE is present or not. They present a local eruption disturbance of permanent first or second molar with no consequence on the neighboring teeth. (Figure 11).



Figure 11. Lateral view of a patient with a classic Primary Failure of Eruption(PFE). Local eruption defect of permanent first or second molar with no consequence on the neighboring teeth.

Part of the PFE origin has been associated to familial/genetic forms, with mutations in the PTH1R gene [95] but the underlying mechanism is still unknown. PTH1R, the parathyroid hormone 1 receptor, is a protein encoded by the PTH1R gene and PTH1R is the receptor for the parathyroid hormone (PTH) and the parathyroid hormone-related protein PTHrP, also called parathyroid hormone-like hormone (PTHLH). PTH1R is expressed at high levels in the bone and the kidney and is involved in several processes as chondrogenesis, bone remodeling, osteoclastogenesis, and in the regulation of certain organ function as the renal function [96]. When the receptor is activated through PTH binding, osteoblasts express RANKL (Receptor Activator of Nuclear Factor κ B Ligand), which binds to RANK (Receptor Activator of Nuclear Factor κ B) on osteoclasts. This mechanism activates the osteoclasts and thus increases bone resorption. Regarding the non-genetic forms, their origins remain elusive.

2.3. RANK/RANKL/ OPG signaling pathway and the dento-alveolar complex development

The identification of the RANKL/RANK/OPG signaling pathway was a crucial breakthrough in understanding the regulation of osteoclastogenesis in remodeling cycle and provided the pharmacological target for the novel antiresorptive.

The TNF superfamily members (TNFSF) are expressed in a variety of tissues and organs and, recently, studies related to this family have clarified important cellular and molecular mechanisms in dental development [97]. RANKL and OPG are members of the TNF and TNF receptor (TNFR) superfamilies, respectively, and link to RANK. They not only regulate osteoclast formation, activation and survival in physiological bone remodeling but also in various pathological conditions [98,99]. The RANKL/RANK/OPG system was discovered in the late 1990s by four different groups and has proved to be important in the immune response

via the interaction of the triad with dendritic cells in rheumatoid arthritis, periodontal disease, osteoporosis, osteoarthritis, multiple myeloma and metastatic bone tumours over the years [99]. A permissive concentration of M-CSF, which is expressed by osteocytes and osteoblasts and stimulates RANK expression, is required prior to the action of RANKL.

RANKL binding to its receptor, RANK, on osteoclastic precursor cells, drives further osteoclast differentiation and facilitates fusion, activation and survival. RANKL/RANK binding induces downstream signaling molecules including mitogen-activated protein kinase, TNF-receptor associated factor, NF- κ B and c-fos and ultimately activation of key transcription factors, including NFATc1, that regulate the expression of osteoclast genes.

2.3.2. RANKL (TNFSF-11)

The receptor activator of nuclear factor kappa-B ligand (RANKL) is a cytokine and transmembrane protein essential for osteoclast differentiation and bone resorption whose coding gene is *TNFSF11* (ID: 8600), located on chromosome 13q14.11. Human and murine RANK ligands are glycoproteins synthesized with 317 and 316 amino acids, respectively, and have great homology among them [100]. RANKL is strongly expressed in skeletal and extra-skeletal sites, such as mammary epithelial cells, keratinocytes, synovial fibroblasts, chondrocytes, endothelial vascular cells, and by T and B lymphocytes. In bone sites, it is produced by mesenchymal cells, osteoblasts, hypertrophic chondrocytes and stromal cells [99,101]. During development, the RANKL mRNA expression may be detected in murine embryos' brains, hearts, kidneys, skeletal muscles and skin. Among the three different RANKL isoforms identified, one of them does not have the transmembrane and intracellular domains, it may be secreted and has inhibitory functions. Moreover, it has been demonstrated that soluble RANKL is less effective as a mediator of osteoclastogenesis [100,102]. Many studies suggest that osteocytes are a major source of RANKL [69,70,72,103,104].

2.3.3. RANK (TNFRSF-11A)

The receptor activator of nuclear factor kappa-B (RANK) is the RANKL membrane receptor, part of the TNF receptor family (TNFRSF 11A), whose human gene that encodes it is the *TNFRSF11A* (ID: 8792), located on chromosome 18q21.33. Human and murine RANK mRNAs code for type I transmembrane glycoproteins with 616 and 625 amino acids, respectively (55). The expression of RANK RNAs is ubiquitous, but protein expression in bone tissue seems to be limited to osteoclasts and their precursors. RANKL/RANK interaction occurs by stimulation of the M-CSF (Macrophage colony stimulating factor) and it is enough for osteoclast differentiation [99].

2.3.4. Osteoprotegerin - OPG (TNFRSF-11B)

Osteoprotegerin (OPG) also called osteoclastogenesis inhibitory factor (OCIF), is a bone resorption inhibiting factor secreted by the cell as a soluble glycoprotein member of the TNF receptor superfamily (TNFRSF11B), whose human gene that encodes it is the *TNFRSF11B* (ID: 4982), located on chromosome 8q24.12. OPG is produced by many cell types besides osteoblasts, such as cells in the heart, liver and spleen. B lymphocytes are the major source of OPG in the bone marrow of mice, which account for 64% of total bone marrow OPG production. OPG, as a decoy receptor, can bind with RANKL and block its bind and activation with RANK [105]. It is believed that its primary function as a receptor is to modulate the interactions between binding RANKL and RANK. Human and murine osteoprotegerin isoform sequences have 85% homology. It is ubiquitous and is present in the brain, liver, lungs, heart, kidneys, skeletal muscles, skin, intestines, calvaria, stomach, testicles and placenta. The OPG expression is still detected in mesenchymal cells, stromal medullary cells and osteoblasts [100].

Stimulation of differentiation, activation and survival of osteoclasts mediated by RANKL and inhibition of RANKL/RANK interaction by osteoprotegerin are the key mechanisms that control bone homeostasis. The whole set is also controlled by several other

osteoclast factors including glucocorticoids, vitamin D3 [1,25(OH)₂D₃], interleukin-1, TNF- α , TGF- β , WNT ligands and other hormonal, local and systemic factors [100].

2.3.5. LGR4

The leucine-rich repeat-containing G-protein-coupled receptor 4 (LGR4, also called GPR48) is a novel receptor for RANKL, that competes with RANK for RANKL binding in osteoclasts, and that negatively regulates osteoclast differentiation and bone remodeling [106]. LGR4 regulates canonical RANKL-RANK signaling through the decreasing interaction between RANK and the downstream component TRAF6 and also LGR4 abrogates RANKL-induced NF- κ B signaling. A mechanistic understanding of RANKL-LGR4 interaction has provided new insights into LGR4 mediated RANKL signaling in osteoporosis and other diseases [106,107].

LGR4 is also associated with Wnt receptors and it mediates R-spondin signaling. R-spondins (RSPOs) have been reported as functional ligands for LGR4 in adult stem cell maintenance and activity [106]. (Figure 12).

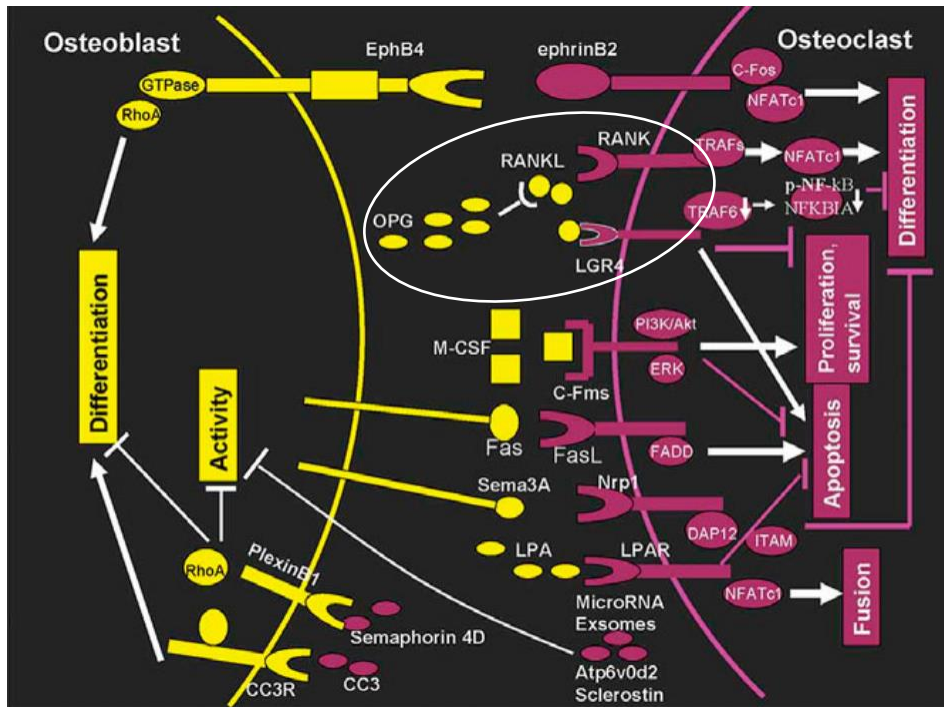


Figure 12. Schematic presentation of osteoblast-osteoclast interactions emphasizing the main actors - RANKL/RANK/OPG/LGR4 - in the osteoclastogenesis canonical pathway. White circle evidencing the osteoblast-osteoclast interface. Adapted from Chen et al., 2017.

2.3.6. RANKL/RANK/OPG expression during dento-alveolar complex development

The RANKL/RANK/OPG signaling pathway has been studied in the development of the dentoalveolar complex and thus Castaneda *et al.* have demonstrated that remodeling of the bone crypt is necessary for tooth eruption as well as for root formation [7,8], to accommodate the tooth that is being formed, thus demonstrating the communication between bone and dental cells [24].

The involvement of bone remodeling factors in terms of morphogenesis and dental germ histogenesis has not been studied a lot. It has been demonstrated that in the bud stage, there is an OPG and RANK co-expression in the epithelium and a RANKL co-expression in the underlying ectomesenchymal cells.

In the cap, bell and crown stages, OPG and RANKL are expressed by the dental papilla, ameloblasts, odontoblasts, and in the dental follicle [9,10]. This expression suggests local and temporal-spatial communication between the ectomesenchymal cells that originate the tooth and bone during early development. In 2011, Castaneda *et al.* demonstrated, in mice with RANK over-expression (RANK-Tg), that the crypt presented an increase in TRAP-positive cells as well as in root elongation and accelerated dental eruption [7] (Figure 13).

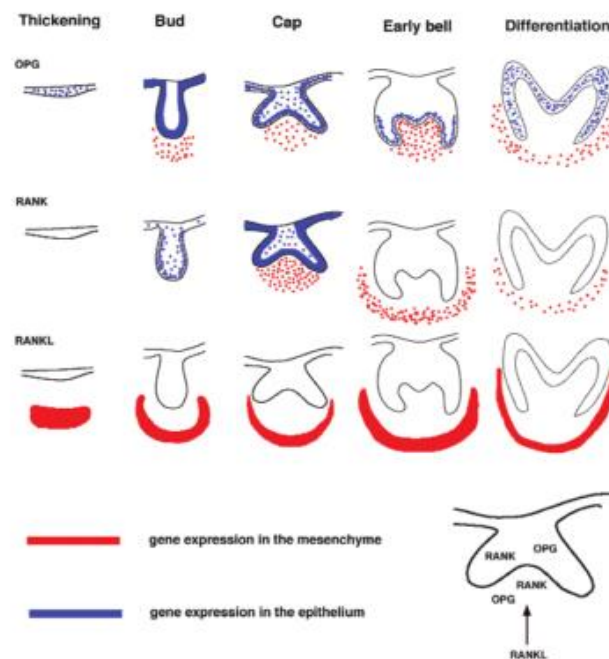


Figure 13. Schematic representation of RANKL / RANK and OPG expression during early stages of dental development. Expression of RANK, RANKL, OPG in blue at the level of the epithelium and in red at the level of the mesenchyme. Adapted from Ohazama *et al.*, 2004.

Other studies on the RANKL/RANK/OPG signalling pathway in dentoalveolar development confirmed the importance of maintaining the integrity of the complex formed by the tooth and surrounding bone in a physiological and pathological context [9–12]. They also showed that, under physiological conditions, RANKL and RANK are expressed in the dental follicle during dental eruption. OPG was also identified as an important factor to control homeostasis of the dentoalveolar complex [3,80]. In 2014, Kawasaki *et al.* demonstrated the dynamic spatio-temporal expression of R-spondins and Lgrs in murine odontogenesis. They performed in situ hybridization of R-spondins on frontal head sections at embryonic days from

the molar crown initiation up to the onset of cytodifferentiation. *Lgr4* was found to be expressed in bud tooth epithelium [108]. There is still a lot to learn about the spatial protein expression distribution in post-natal ages regarding LGR4.

The interdependence between alveolar bone remodelling and early tooth development has been established, but there is still much to be clarified about the role of the triad in late tooth development and, more precisely, in root formation.

Therapeutic approaches with antiresorptive drugs that act by blocking RANKL (anti-RANKL antibody) and the osteoclast function (bisphosphonates) are of special interest since numerous studies, in humans and in animal models, describe changes in the development of the stomatognathic system when used continuously in the treatment of systemic bone pathological conditions. Eruptive defects are among the most common findings, since bone mobilization around the forming tooth is essential for its emergence in the mouth [12,24,117–122,109–116].

2.3.7. Phenotypes associated to alterations of the RANK/RANKL/OPG signaling pathway

The dento-alveolar complex actors are all interdependent in such a way that any alteration of the formation or maintenance of one of the constituents of this complex inevitably has repercussions on the others. Thus, an alteration of the bone modeling causes a more or less premature deterioration of the dental development in relation to the severity of the bone involvement [53]. The growth pathologies of the alveolar bone having an implication on the dental development are of two types, according to whether their origin is related to a decrease of the bone resorption, osteopetrosis, or to an increase of bone resorption, osteolysis.

2.3.7.2. Genetic alterations

2.3.7.2.2. Loss of function: Osteopetrosis

Osteopetrosis (OP) is a group of heterogeneous inherited rare metabolic bone diseases also known as “marble bone disease”. It was first described in 1904 by Albers-Schonberg, a German radiologist whose eponym is also a name for the condition. Phenotypically, it is radiographically characterized by a general increase in bone density [123], leading to skeletal fragility and a predisposition to low impact fractures. This osteosclerotic disorder is due to impaired osteoclast differentiation or function [124,125].

OP consists of a clinical spectrum ranging from very mild to severe disease phenotypes that may be fatal in the first year of life [126]. Due to this variability in severity and the associated complications, the clinical classification of OP is challenging. Nevertheless, there are three forms of osteopetrosis defined based on their clinical features, the age at onset, and the pattern of inheritance, consisting of autosomal recessive (ARO), autosomal dominant (ADO), and X-linked osteopetrosis [124,125,127,128].

ADO has an incidence of 1:20,000 births and two types of dominant forms of ADO (Type I and Type II) are described in the literature. ADO type 1, classified as mild osteopetrosis, is now considered a misclassification. Indeed, it has been established that ADO type I is associated with defects in osteoblasts resulting from a gain-of-function mutation in the *LRP5* gene which enhances bone formation [129]. Therefore, it should instead be considered a high bone mass disease [123,124,128]. ADO type II (also known as Albers-Schönberg disease; OMIM#166600) has a mild bone phenotype and results from mutations in the *CLCN7* gene affecting the function of osteoclasts. This form is mainly seen in adults, since clinical onset typically occurs in adolescence or adulthood [130]. However, cases which were diagnosed at a young age have been also reported [131–133].

ARO, also known as malignant bone osteopetrosis, exhibits more severe phenotypes and is rarer than ADO, with an incidence of 1:250.000 births [134]. It is diagnosed soon after birth and is often lethal in infancy or childhood.

Amongst the ARO forms, two subsets of osteopetrosis can still be distinguished, consisting of the first, osteoclast-rich forms in which deficits arise from the inability of mature, multinucleated, but nonfunctional cells to perform resorption, and the osteoclast-poor forms in which deficits arise from a failure in osteoclast differentiation which directly affects the number of osteoclasts [132]. Osteopetrotic patients affected with recessive osteoclast-rich forms may have a high number of non-functional osteoclasts due to loss of function mutations in genes implicated in the mechanisms of bone resorption, such as *TCIRG1* (OMIM#259700), *CLCN-7* (OMIM#611490), *OSTM1*(OMIM#259720), *SNX10* (OMIM#615085), *PLEKHMI* (OMIM#611497) and *CAII* (OMIM#259730). The CA-II dependent form was the first human osteopetrosis with a recognized molecular defect identified and is easily diagnosed since its bone phenotype is also associated with renal tubular acidosis [135].

Alternatively, the recessive osteoclast-poor forms may lack osteoclasts due to mutations in genes implicated in the process of osteoclast differentiation, such as *TNFSF11* (OMIM#259710) and *TNFRSF11A* (OMIM#612301), which encode the RANKL and RANK proteins, respectively [127,136]. Bone biopsies from these patients are nearly entirely depleted of osteoclasts.

A so-called intermediate recessive form, also of childhood onset, and is different from ARO because the outcome is less severe and life expectancy is much higher [137]. Del Fattore et al. [123] and Coudert et al. [125] considered CAII-deficient osteopetrosis to be an intermediate form. The X-linked form (XLO) is extremely rare and lethal, and involves mutations in the *NEMO* (NF- κ B essential modulator) gene which encodes the regulatory subunit of the IKK complex, essential for NF- κ B pathway activation [138,139]. Based on

current knowledge of osteoclast differentiation pathways and the cellular mechanisms leading to bone resorption, a number of additional genes may also be involved, which is a matter of active research in the field of bone genetics.

At present, there is no treatment available for the ADO forms. Nonetheless, the only established treatment for severe ARO forms is hematopoietic stem cell transplantation (HSCT), the success of which depends on human leukocyte antigen matching and host compatibility. HSCT cannot be used to treat patients with recessive forms caused by mutations in the *TNFRSF11* gene. Therefore, special interest has been given to the discovery of alternative therapeutic options [140]. Osteoclasts and osteoblasts are the main agents of bone growth and self-renewal and the impact of osteoclast activity on dental and alveolar bone development has been previously analyzed in the context of severe osteopetrosis in animal models [11]. Indeed, transgenic mice for a number of genes involved in osteoclast differentiation and function harbour eruption defects and tooth malformations culminating in the generation of odontoma-like structures despite the presence of normal teeth [87]. Since some of these genes may also be mutated in osteopetrotic patients, oro-dental alterations are expected to be a frequent finding. Indeed, clinical reports have shown that oro-dental alterations in osteopetrotic patients are a frequent finding. Common oral features reported include unerupted teeth and osteomyelitis, particularly affecting the mandible in association with dental abscesses or dental caries [126,134]. Clinically, since osteopetrosis clearly appears to affect many aspects of whole orofacial development, this condition negatively alters patients' quality of life. Therefore, an overall understanding of the osteopetrotic dental phenotypic spectrum is relevant to clinical diagnosis and management. In addition, such a study would update the criteria used for routine dental surveillance and maintenance of proper oral hygiene in this high-risk population by identifying, preventing, and managing the myriad complications at the maxillofacial site, consequently improving patient health care [126].

2.3.7.2.3. Gain of function – Osteolysis

In contrast to osteopetrosis, there are hyper-resorptive bone diseases, characterized by hyper-activation of osteoclasts. Paget's disease (Paget's Bone Disease, OMID PBD # 602080) is a relatively common and asymptomatic disease until the sixth decade of life. It is a complex disease involving genetic predispositions and environmental factors that have not yet been fully identified [141,142]. On the other hand, Paget's juvenile disease (Juvenile Paget Disease, OMIM # 239000), Early-onset Paget Disease of Bone (PDB2, OMIM # 602080), Expansive Skeletal Hyperphosphatasia (ESH), and familial expansive osteolysis (Familial Expansile Osteolysis, OME, OMIM # 174810) are rare bone dysplasias with local or general skeletal alterations whose predominant peripheral distribution manifests itself from the second decade of life on. The most obvious clinical features are progressive osteolytic lesions accompanied by severe spinal cord expansions, causing pain, early deafness, and deformities accompanied by pathological fractures. Histologically, intense and uncontrolled bone remodeling is observed with significant osteoblastic and osteoclastic activity. Osteoclasts are numerous, larger and accompanied by intense areas of osteoformative activity by osteoblasts. The lamellar bone structure is replaced by abnormal bone tissue, with irregular mosaic-shaped trabeculae and interstitial fibrous tissue between the newly formed trabecular bone and the residual lamellar bone. Biochemically, these pathologies are characterized by an increase in the level of bone markers, confirming a rapid bone remodeling activity [143–145].

Concerning dental alterations, the first clinical and radiological manifestations appear during adolescence. The pathognomonic sign of Expansive Familial Osteolysis is an intense root resorption of the apical region and the dental cervical region. These alterations cause fractures, abnormal mobility and premature avulsions [146]. These alterations are associated with a reduction of the pulp space and root canals narrowing by secondary apposition of dentin. Gradually, the pulp is replaced by fibrous tissue and the cementum, especially in the molars

and in the apical zones. The periodontal ligament is very narrow. Nevertheless, the alveolar bone remains normal for radiological and histological examination [147].

For skeletal expansive hyperphosphatasia and juvenile Paget's disease, the craniofacial manifestations reported in the literature are more restricted. Early loss of temporary and definitive teeth has been described while structural abnormalities occur only occasionally. Concerning Paget's juvenile disease, osteolytic focal lesions of the maxillary and mandible with loss of teeth from the second decade of life have been described [145].

2.3.7.3. Therapeutic alterations

2.3.7.3.2. Inhibitions of

RANK/RANKL/OPG/LGR4 signaling

2.3.7.3.2.1. RANKL inhibition

The identification of the RANK/RANKL signaling pathway in the 1990s allowed the development of new pharmacological targets to reduce osteoclast activity and, consequently, bone resorption through RANKL inhibition. Such inhibition was explored by the use of denosumab, a humanized monoclonal antibody anti- RANKL [148] that has IK22-5 as its murine analogue.

Denosumab is a new class of antiresorptive drugs and RANKL inhibitors that became an alternative to the treatment of osteoporosis, malignant conditions and other skeletal disorders [149]. This humanized monoclonal antibody is a natural IgG2 immunoglobulin with significant non-absorbent activity that mimics osteoprotegerin (OPG) by binding to the RANKL, a cytokine essential for osteoclast differentiation, activation and survival [150], preventing cellular events of osteoclast differentiation and, therefore, bone resorption [151].

The main difference between denosumab and bisphosphonates (BPs) is that, for them to perform their inhibitory function, osteoclasts must internalize the drug at the resorption site, while denosumab acts in the extracellular environment [148] (Figure 14).

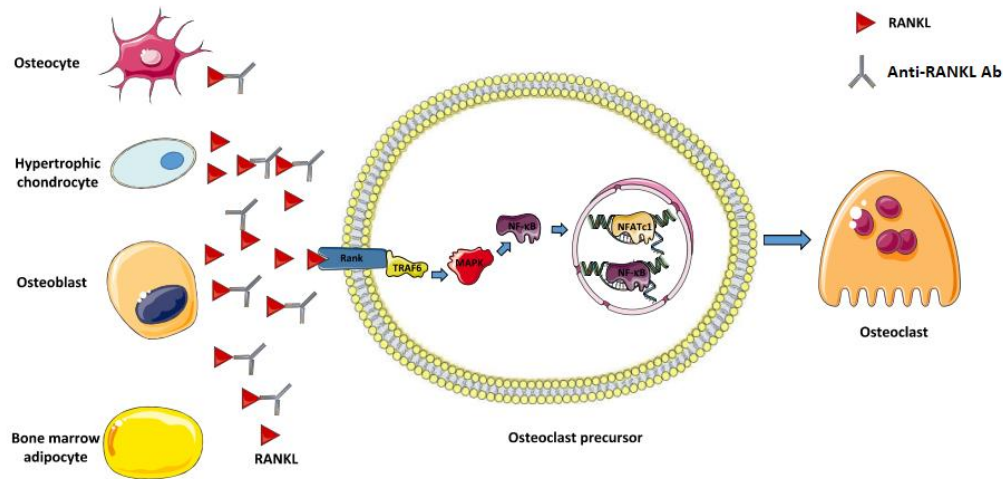


Figure14. Mechanism of action of denosumab. Adapted from Portal-Núñez *et al.*, 2017.

RANKL inhibition prevents monocyte-macrophage fusion and subsequent formation of multinucleate osteoclasts. Treatment with BPs presents high stability in osteoclast inhibition, may interfere with patient growth, induces accumulation of TRAP-positive cells on the bone surface [117], and, in the long term, giant, hypernucleated osteoclasts, with prolonged apoptosis may be observed [152].

The advantage of the anti-RANKL antibody lies in the efficiency of the resorption inhibition, the rapid reversal and the absence of TRAP-positive cells on the bone surface; however, it does not present a direct antitumor effect. Despite the difference mentioned, the side effects are similar with regard to tooth eruption. In 2012, Semler *et al.* published a study in which 4 patients with type VI *osteogenesis imperfecta* were treated with denosumab, which proved to be well accepted, with excellent laboratory control parameters and no complications [153]. Two years after the treatment started, the same group of patients was evaluated and their general clinical condition was stable, with no history of treatment interruption due to various

side effects. They concluded that denosumab appears to be safe in the medium term and that other clinical trials should be prospectively assessed [154].

In 2016, Hoyer-Kuhn *et al.* extended anti-RANKL antibody treatment to a group of 10 children with OI. In this phase II clinical trial, the safety and efficacy of osteoclast inhibition were evaluated. The authors concluded that, on average, the drug analysed significantly increased bone mineral density in the lumbar spine, suppressed bone resorption for 10 to 12 weeks, and appeared to be safe in the one-year treatment, with good calcium and vitamin D supplementation, besides increasing the children's absolute height, the ones included in the study [155].

Although denosumab has not been approved to be used in children, clinical trials are progressing with good results, significant improvement in the parameters considered, and greater control and reduction of side effects due to the complete degradation of the antibody after a few months [149].

2.3.7.3.2.2. Bisphosphonates

BPs and Denosumab are antiresorptive drugs that, when acting on bone metabolism, prevent unwanted events, such as pathological fractures, due to osteolytic systemic conditions [148].

The clinical efficacy of bisphosphonates derives from two key properties: the ability to bind strongly to calcium crystals in mineral bone [156] and their inhibitory effects in mature osteoclasts through intracellular effects [157]. For these reasons, they are useful in the treatment of skeletal disorders, such as osteoporosis, Paget's disease, *osteogenesis imperfecta* and metastatic bone diseases [148,158–161].

BPs inhibit bone resorption and are divided into two main groups: non-nitrogen-containing and nitrogen-containing bisphosphonates, and the latter have greater *in vitro*

antiresorptive effects [156,162]. Non-nitrogen-containing bisphosphonates are metabolized in cytosol in adenosine triphosphate (ATP) analogues that block the osteoclast function and induce apoptosis in osteoclasts. On the other hand, nitrogen-containing bisphosphonates act mainly by inhibiting an enzyme from the mevalonate pathway: farnesyl pyrophosphate synthase, which prevents post-translational modification (prenylation) of small guanosine triphosphate binding proteins (GTP) essential for osteoclast function and survival [148].

Among so many other clinical uses in pathological conditions, BPs, notably pamidronate, appear as the gold standard in the treatment of *osteogenesis imperfecta* (OI), which is a group of connective tissue disorders inherited with heterogeneous phenotypic and molecular patterns, and which share similar skeletal abnormalities causing bone fragility and deformities [118,163]. The beneficial effects observed in children with OI are increased bone mineral density (BMD), reduction in fracture rate, and substantial improvement in their functional status [164]. In a systematic review conducted by Rijks *et al.*, the authors concluded that, despite evident good long-term results, especially in the first year of treatment, the optimal duration of therapy with bisphosphonates is still unknown [165].

Since BPs are recommended for bone pathologies and administered to pregnant women or children during the development of their deciduous and permanent teeth [166], disorders in the odontogenesis are expected and, therefore, dental anomalies. Such hypothesis was confirmed by studies with zoledronic acid, pamidronate and alendronate during the development of murine teeth that caused eruption failures [110,112,114,117]. Clinically, a French team accompanied 33 children with *osteogenesis imperfecta*, whose ages varied between 6.2 to 14.6 years, and they concluded that bisphosphonate therapy is responsible for defects in tooth eruption, and that this event was independent from therapy duration, but it was dose-dependent [114].

In addition to eruption disorders, a recent study conducted by a Turkish team observed enamel and dentin malformations in erupted and developing teeth, myxomatous degeneration, morphological disorders in tooth germs, and narrow pulp chambers in groups treated with pamidronate, besides altered mandibular growth patterns [111]. In a recent cross-sectional study, the chronology of dental development in patients with OI and treated with BPs was compared with two control groups, untreated and healthy OI patients. The authors concluded that children treated with BPs had a normal tooth development rate, which was indistinguishable from the development of healthy children, and this was due to a compensatory mechanism given by the use of BPs, since OI grants patients accelerated tooth development [120].

From another perspective, in an experimental study in murine animal models submitted to high doses of zoledronic acid (Zoledronate), the development and eruption of teeth were severely and irreversibly compromised, presenting abnormal amelogenesis with disorganized ameloblasts, root ankylosis, hypercementosis, and, with time, root resorption [117]. An interesting fact that gives Zoledronate superior efficacy in relation to other bisphosphonates is that, according to evidence, it not only inhibits osteoclast activity, but it also promotes anabolic activity by stimulating osteoblastic differentiation [164].

In a prospective observational study with patients that were followed up for 2 years, zoledronic acid positively impacted the quality of life of paediatric patients with OI, and it proved to be safe. However, the optimal dose, duration of therapy and long-term safety still need to be defined [167].

2.3.7.3.3. Activations of RANK signaling pathway

2.3.7.3.3.1. RANK-Fc and OPG-Fc

The effect of RANKL inhibition was first evaluated in preclinical and clinical studies using Fc fusion proteins. With Fc-OPG and OPG-Fc, OPG was fused to the Fc portion of human immunoglobulin G1 (IgG1). A third molecule, RANK-Fc was formed by fusing the extracellular domain of RANK (amino acids 22–201) to the Fc portion of IgG1. Later studies investigated RANKL inhibition using denosumab, a fully human monoclonal antibody that targets RANKL. Denosumab has several advantages over OPG-Fc or Fc- OPG constructs. First, in terms of its selectivity, denosumab does not bind to TRAIL (TNF-related apoptosis-inducing ligand) or to other TNF family members including TNF- α , TNF- β , and CD40 ligand, whereas TRAIL binding has been observed with OPG. Second, due to its molecular mass, its half life is prolonged compared to the Fc constructs. Finally, neutralizing antibodies against OPG-Fc could have neutralizing effects on both the drug and OPG, which would not be expected with denosumab. Indeed those two molecules represent an evolutionary step towards the anti-RANKL antibody concept [148,168,169] (Figure 15).

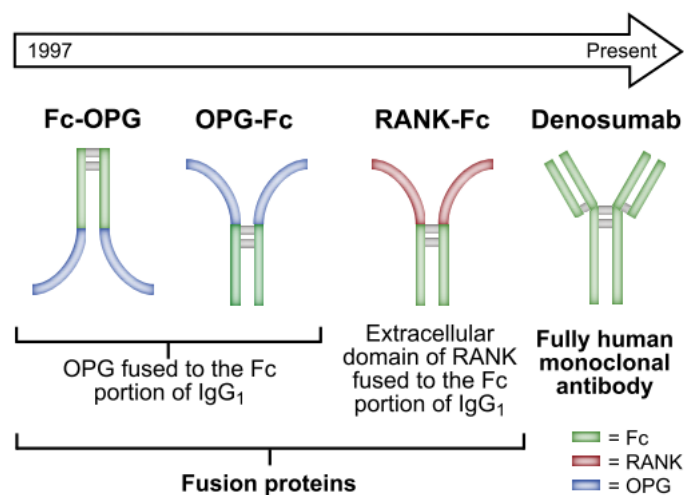


Figure 15. History of development of RANKL antagonists. Adapted from Baron et al., 2011.

3. HYPOTHESIS

The activity of osteoclasts, controlled by the RANKL/RANK signaling pathway, is known to have effects on the eruption process as on the root elongation and morphology. Indeed, the presence of an increased number of osteoclasts during alveolar bone growth (*Rank Tg* mice) was associated with an earlier eruption and an advanced root elongation while the reduction of osteoclasts (in *Rankl^{+/-}* mice) was associated with a delayed root elongation. Moreover, the over-activation of the osteoclastogenic pathway was shown to stimulate the proliferation of epithelial cells of the Hertwig's epithelial root sheath, in coordination with mesenchymal cells of the apical papilla, suggesting the existence of local communications between dental and alveolar bone cells during the craniofacial development. Such a communication function of the RANKL/RANK signaling pathway was validated during the dental morphogenesis through the analysis of the craniofacial phenotype of *Rankl^{-/-}* mice from the second generation that did not survive after birth. However, a validation during the post-natal growth was missing.

Consequently, the main hypothesis of the present project was that during the post-natal growth of the craniofacial skeleton, the RANKL/RANK signaling pathway has at least two different functions which are the control of the osteoclast differentiation/activity and the implication in the cell to cell communications necessary to the harmonious and functional growth of the different elements of this skeleton.

4. OBJECTIVES

4.1. GENERAL OBJECTIVE

To assess the importance of the impact of RANKL/RANK/OPG/LGR4 signaling pathway through permanently and transitory invalidation and its effects on the craniofacial growth and on the dental development, from the initial stages of morphogenesis to the functional molar eruption.

4.2. SPECIFIC OBJECTIVES

Taking into account that RANKL/RANK/OPG/LGR4 signaling perturbations in the way of loss of function are associated to an osteopetrotic phenotype, the specific objectives of this study are:

To perform a deep analysis of the available literature relative to the oro-dental features associated with osteopetrosis taking into account its occurrence in affected individuals. To establish, using *Rankl* null mutant mice (*Rankl*^{-/-}), that the RANKL/RANK/OPG/LGR4 signaling is not only implicated in the osteoclastogenesis control and the osteoclast activity regulation, but also in cell-to-cell communications necessary for tooth development up to its functional eruption. The analysis of the importance of the RANKL of maternal origin onto the phenotype of *Rankl* null mutant mice is an elegant strategy to complete such a demonstration.

To assess and compare the early stages of the mouse first molars roots development in the osteopetrotic contexts induced respectively by total and transitory RANKL invalidation.

To assess and compare the eruption process of the mouse first molars in the osteopetrotic contexts induced respectively by total and transitory RANKL invalidation.

To assess and compare the alveolar bone growth in the osteopetrotic contexts induced respectively by total and transitory RANKL invalidation.

To link the molar eruption disorders associated with perturbations of the RANKL/RANK/OPG/LGR4 signaling to a larger craniofacial growth phenotype.

5. MATERIALS AND METHODS

The materials and methods presented in this section were described according to each specific objective and they are ordered in the results section as follows:

5.1. Oro-dental features in patients with osteopetrosis: A systematic review of 95 cases

Systematic Review Methods:

Protocol and registration

The systematic review (SR) was conducted in accordance with the Preferred Reporting Items for Systematic Reviews and Meta-analysis (PRISMA) checklist [170,171], whose protocol was registered with the International Prospective Register of Systematic Reviews (PROSPERO) [172] database (number CRD42018097266).

Eligibility criteria

The “PICOS principle” was followed to provide a standardized approach in formulating the questions of this study, according to the following guidelines: P – participants (individuals with osteopetrosis), I – intervention (not applicable), C – comparison (not applicable), O – outcomes (proportion of oro-dental features), S - study design (observational studies). In addition, the maxillomandibular findings in individuals with osteopetrosis of any age or gender, without a time restriction, were taken into consideration.

The following studies were excluded from this SR: (1) reviews, letters, personal opinions, book chapters, conference abstracts, posters, short communications, patents and editorials, (2) studies without maxillomandibular manifestations, dental, and/or oral findings, (3) studies published in non-Roman languages, (4) studies using the same sample, (5) *in vivo*, *ex vivo*, and *in vitro* studies, (6) osteopetrosis associated with other syndromes or pathological conditions, (7) studies in which the only oral findings reported were caries, (8) studies without any clinical

and/or radiological exams, and (9) case reports consisting of 3 or fewer cases, due to the weak inferences and high likelihood of bias inherent to these studies.

Information sources and literature search

Studies considered for inclusion were identified using a customized search strategy for each of the following electronic databases: Pubmed, Scopus, Web of Science, Latin American and Caribbean Health Science (LILACS) and Livivo. The gray literature was explored through Google Scholar, ProQuest and OpenGrey. All databases were searched for studies published prior to February 7th, 2019 (Appendix 1). Additionally, reference lists of selected articles were hand-screened for potentially relevant studies that could have been missed during the electronic database searches or by consultation with experts in the field. Duplicate references were removed using reference manager software EndNote® X7 (Thomson Reuters, Philadelphia, PA, USA), and the review was managed by Rayyan QCRI, Qatar [173].

Study selection and data collection process

The eligibility criteria were assessed in two phases. In phase 1, two authors (A.G. and F.T.A.) independently screened the titles and abstracts identified in all electronic databases. These authors selected articles that appeared to meet the inclusion criteria based on their abstracts. In phase 2, the same authors (A.G. and F.T.A.) read the full text of all selected articles and excluded studies that did not meet the inclusion criteria. Disagreements between them were solved by consensus. When they did not reach a consensus, a third author (A.C.A.) was involved in making a final decision. One author (A.G.) collected the key information related to each included article, such as authors, year of publication, country, study design, number of reported cases, individuals' gender, median ages of diagnosis or first exam, mode of inheritance, gene(s) implicated, when available, diagnostic methods and oral findings. A second author (F.T.A.)

cross-checked all the collected data. Once again, disagreements between them were solved by consensus, and the third author (A.C.A.) was involved, as required, in making a final decision.

Quality assessment in individual studies

For the quality assessment of each study, the Methodological Quality and Synthesis of Case Series and Case Reports proposed by Murad et al., 2018 [174] in association with the Case Series and Prevalence Studies from the Joanna Briggs Institute (JBI) critical appraisal tools [175,176] were used. Therefore, this quality assessment was applied to all selected articles. Two reviewers (A.G. and F.T.A.) scored each item with a “yes,” “no,” “unclear,” or “not applicable” label, independently assessing each included study. Disagreements between both reviewers were resolved by consensus and via the opinion of a third reviewer (A.C.A.).

5.2. Experimental study

Animals and Drug Administration

All C57BL/6J mice used in the experiments were housed in pathogen-free conditions at the Experimental Therapy Unit at the medical faculty at the University of Nantes (Nantes, France), in accordance with the institutional guidelines of the French Ethical Committee (CEEA-PdL-06, accepted protocol number 00165.01) and under the supervision of authorized investigators. New born mice were used for the experiments. The *Rankl* heterozygous mice were generated by homologous recombination. Genotyping was carried out using PCR with the following primers :

50-*Rankl*: CCAAGTAGTGGATTCTAAATCCTG;

30-*Rankl*: CCAACCTGTGGACTTACGATTAAAG; and

30 insert: ATTCGCAGCGCATCGCCTTCTATC as previously described [177].

At least 5 mice per group have been analysed.

In order to analyze the effects of RANKL maternal in phenotype of osteopetrotic mice, *Rankl* null mutant pups from null mutant parents were generated. First- and second-generation null mutant pups were obtained by mating heterozygous and homozygous animals, respectively.

The skeletal phenotype of *Rankl* null mutant mice was compared at one day post-natal between mouse pups obtained from heterozygous *versus* homozygous parents. Some heterozygous pregnant mice were injected IP three times during the second part of gestation with 2 mg/kg of a mouse-specific RANKL-blocking antibody, IK22.5, following the established protocol [177].

In order to assess the effects of RANKL invalidation on dental and craniofacial development, two experimental models were used, *Rankl* null mutants (*Rankl*^{-/-}), *Rankl* heterozygous (*Rankl*^{+/-}) and a RANKL transitory blockage with a RANKL neutralizing antibody according to the following protocol:

The C57BL/6 mice received a series of 4 injections of RANKL neutralizing monoclonal antibody (IK22-5) from the 1st postnatal day (D1 protocol) and the 7th postnatal day (D7 protocol). The injection shots are made every two days with an injection of 25 µg (50 µl to 0.5 µg/µl) for the first two injections, then 50 µg (50 µl to 1 µg/µl) for the two other injections subcutaneously between the shoulder blades. The mice are euthanized one month after the last injection (Figure 16). In this study sex was not considered.

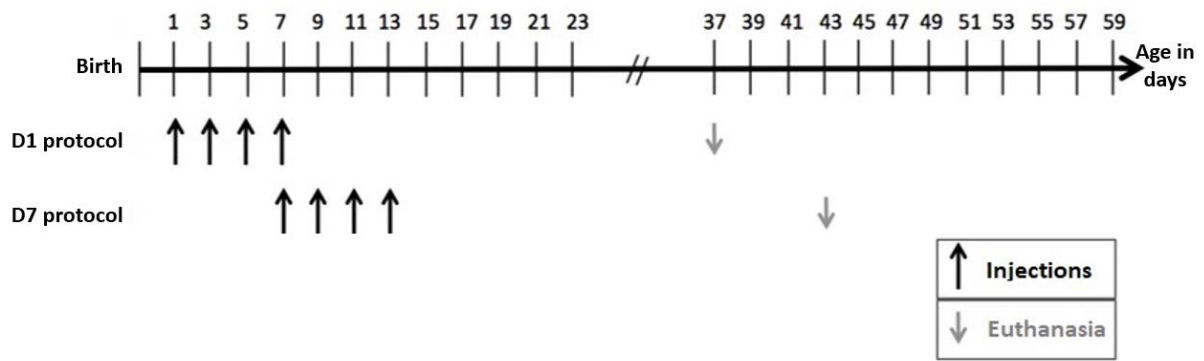


Figure 16. Chronograph of the two protocols used to evaluate the RANKL invalidation. Protocol D1 (Anti-RANKL antibody: 4 injections, first two injections of 25 μg and last two injections of 50 μg , with 2 day intervals, beginning at day 1 after birth) and Protocol D7 treatments (Anti-RANKL antibody: 4 injections, first two injections of 25 μg and last two injections of 50 μg , with 2 day intervals, beginning at day 7 after birth) presenting times of injection and euthanasia.

Micro CT Analysis

Analyses of the bone microarchitecture were performed using a Skyscan 1076 in vivo microCT scanner (Skyscan, Kontich, Belgium). Tests were performed after sacrifice on the tibias and heads of each animal. All tibias and heads were scanned using the same parameters (pixel size 9 μm , 50 kV, 0.5 mm Al filter, 10 minutes of scanning). The reconstructions were analyzed using NRecon and Ctan software (Skyscan, Kontich, Belgium). 3D visualizations of the tibias and heads were made using ANT software (Skyscan, Kontich, Belgium).

The morphologies of the skull and upper and lower jaws were evaluated in relation to some vertical and sagittal cranial measurements.

The choice of landmarks is based on an already existing analysis [178,179]. The analysis presented enabled the measure of several points on the same section in order to facilitate the study (Figure 17). The statistical analysis of the data was performed using the Tukey test with a significance level corresponding to $p \leq 0,05$.

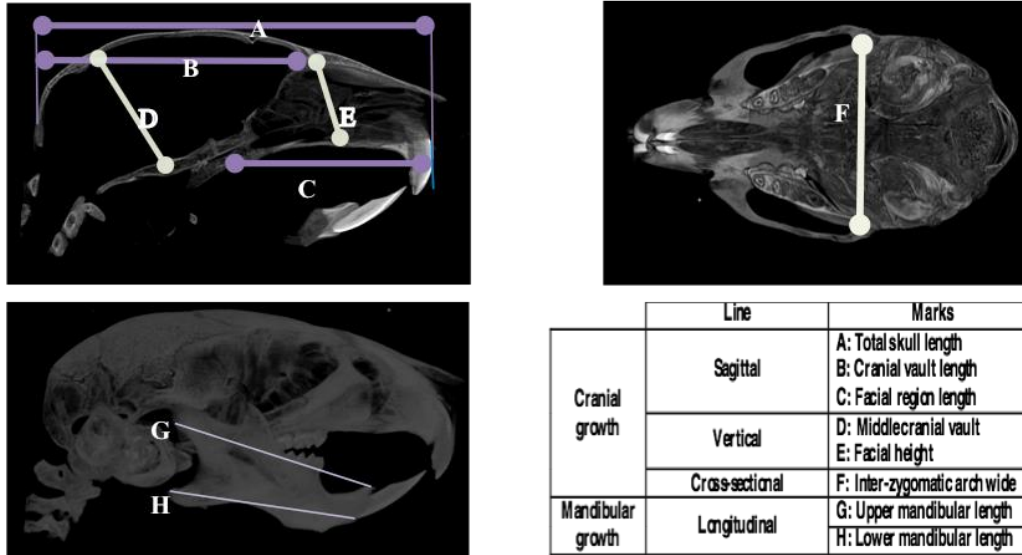


Figure 17. Craniofacial landmarks used in growth analysis.

The molar eruption defect in the mouse model was evaluated according to two parameters:

1. Relative to the normal mouse eruption sequence: Upper M1 (first molar), lower M1, upper M2 (second molar), lower M2, upper M3(third molar) and lower M3.

2. Relative to the distance between the occlusal surface with retained molars and the occlusal plane in control mice (Figure 18 A, B, C, D).

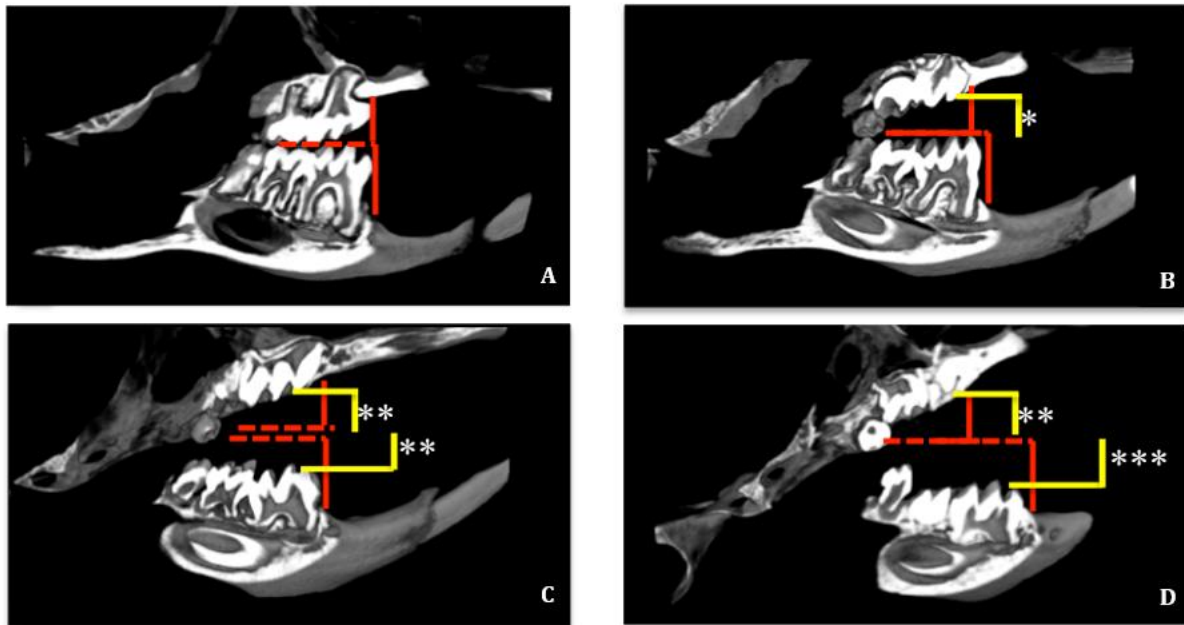


Figure 18. Micro CT parameters used to evaluate tooth eruption defects subsequent to the anti-RANKL antibody treatments.

Histology

Whole skeletons and heads were collected from euthanized mice were fixed in 4% buffered paraformaldehyde. Samples were decalcified in 4.13% EDTA/0.2% paraformaldehyde pH 7.4 over 4 days in KOS sw10 (Milestone, Sorisole, Italy). The specimens were dehydrated and embedded in paraffin. Then, 3 μ m-thick sagittal sections stained with Masson's trichrome were observed using a DMRXA microscope (Leica, Nussloch, Germany). Tartrate-resistant acid phosphatase (TRAP) staining was performed on sample sections to identify multinucleated osteoclast-like cells after 90 min' incubation in 1 mg/mL of Naphthol AS-TR phosphate, 60 mmol/L *N,N*-dimethylformamide, 100 mmol/L sodium tartrate, and 1 mg/mL Fast Red TR Salt solution (all from Sigma Chemical Co., St. Louis, MO, USA), and counterstained with hematoxylin.

Immunohistochemistry

The paraffin was removed by immersion in toluene and the sections were rehydrated by immersing them in decreasing grades of ethanol solutions (100, 95 and 70%), followed by immersion in water and PBS 1X. When peroxidase-conjugated antibodies have to be used, the endogenous peroxidases were preliminary inactivated by an H₂O₂ (hydrogen peroxide) treatment. The sections were then saturated with serum (10%) and incubated with the primary antibody using concentration indicated by the manufacturer (Supplementary table 1) .

One section in each slide was incubated without antibody to serve as a negative control. After rinsing, sections were incubated with the secondary antibody at the dilution indicated by the manufacturer (Supplementary Table 1). Then the reaction to evidence the Horseradish peroxidase (HRP) enzymatic activity was realized using the NovaRED kit (Vector, Laboratories, Burlingame, USA) and the DAB kit (DAKO). The sections were then dehydrated and mounted with Eukitt (K, Freigburg, Germany). For the RANK, RANKL, OPG, LGR4, CD146, SOX9 and CD68 antibodies the Biotine-Streptavidine peroxidase system was used as previously described [177]. In order to compare the number of epithelial cells present in the Hertwig's epithelial root sheath between the molars of *Rankl*^{-/-} mice and the controls, a quantification of cells marked with cytokeratin-14 was done for each molar and averaged according to the number of sections. The obtained numbers were compared between groups at all ages. The statistical analyses were performed with the t-test of the Prism (6.01) software (GraphPad Software, La Jolla, CA, USA).

Immunofluorescence

The decalcified mouse heads were immersed sequentially in 15% and 30% sucrose in PBS 1X and mounted on Freeze Gel (Labonord, Z.I. de Templemars, France) for further cryostat sections. Sections were air dried and then saturated with 1% BSA in PBS for 30 minutes to block nonspecific binding sites. Slides were incubated with a rabbit

polyclonal primary antibody directed against keratin-14 (Covance AF64, Princeton, NJ, USA) diluted 1/500 in PBS at room temperature for 1 hour. After rinsing three times with PBS, the sections were incubated with a goat polyclonal anti-rabbit IgG secondary antibody coupled to Alexa Fluor 594 (A-11072, Life Technologies) at room temperature for 1 hour and then rinsed and incubated for 10 minutes with DAPI (4,6-Diamidino-2-phenylindole dihydrochloride). After rinsing with PBS, the slides were mounted with cover slips and the fluorescence-mounting medium, Fluoprep (BioMérieux, Marcy l'Etoile, France). DAPI staining was used to evaluate the cell density.

5.3. Clinical study

In order to analyze the relationship between Molar Primary Retention (MPR) and craniofacial growth, we compared the craniofacial phenotypes of the patients presenting MPR with patients with impactions or mechanical retentions. Orthodontic records of the patients of the Orthopedics-Dentofacial Orthopedics Department of the *La Pitié-Salpêtrière* hospital have been evaluated in accordance with the *Commission National de l'Informatique et des Libertés* under the number g8w2314849D.

Inclusion criteria:

- Patients who have interrupted eruption of at least one permanent first or second molar (excluding third and temporary molars);
- Patients with or without physical obstacle on the eruption path (visible clinically or radiographically);
- Patients at least at the stage of the young adult teeth.

Exclusion criteria:

- Patients with medical syndromes involving eruption defects were not included in this study like cleidocranial dysplasias or bone diseases such as osteopetrosis;

- an antecedent of orthodontic treatment;

- an incomplete orthodontic file (missing x-rays).

Studied sample

42 patients with first and second molar eruption alterations. They were divided into two groups:

- Group MPR consists of 24 patients with primary retention of eruption: no mechanical obstacle to the eruption visible clinically or radiographically. The molar is normally positioned. Patients in this group are, on average, 16.75 years old.

- Group C consisting of 18 patients with mechanical impactions, representing the control group: a physical obstacle or an axis unfavorable to the eruption of the molar could be objectified at the clinical or radiological level. The average age of these patients is 16.25 years.

The patients are listed by age, sex, ethnicity, the presence of family antecedents (alteration of molar eruption), the uni or bilateral character; the type of arcade affected, the type of tooth affected, supra or infra-crestal position, the presence of a radiological eruption path (for infra-crestal molars), other associated anomalies and the dental diagnosis. Chosen criteria following Sharma et al., 2016 [180]. Statistical analyses were performed using the Fisher test. A difference is significant between the groups if $p \leq 0.05$.

A retrospective teleradiographic study of these patients was conducted using two different cephalometric analyzes:

- Tweed quantitative analysis – CEPH (Orqual) (Figure 19)

Data statistical analysis will be performed using Student's t-test. The significance level for this

test is $p \leq 0.05$.

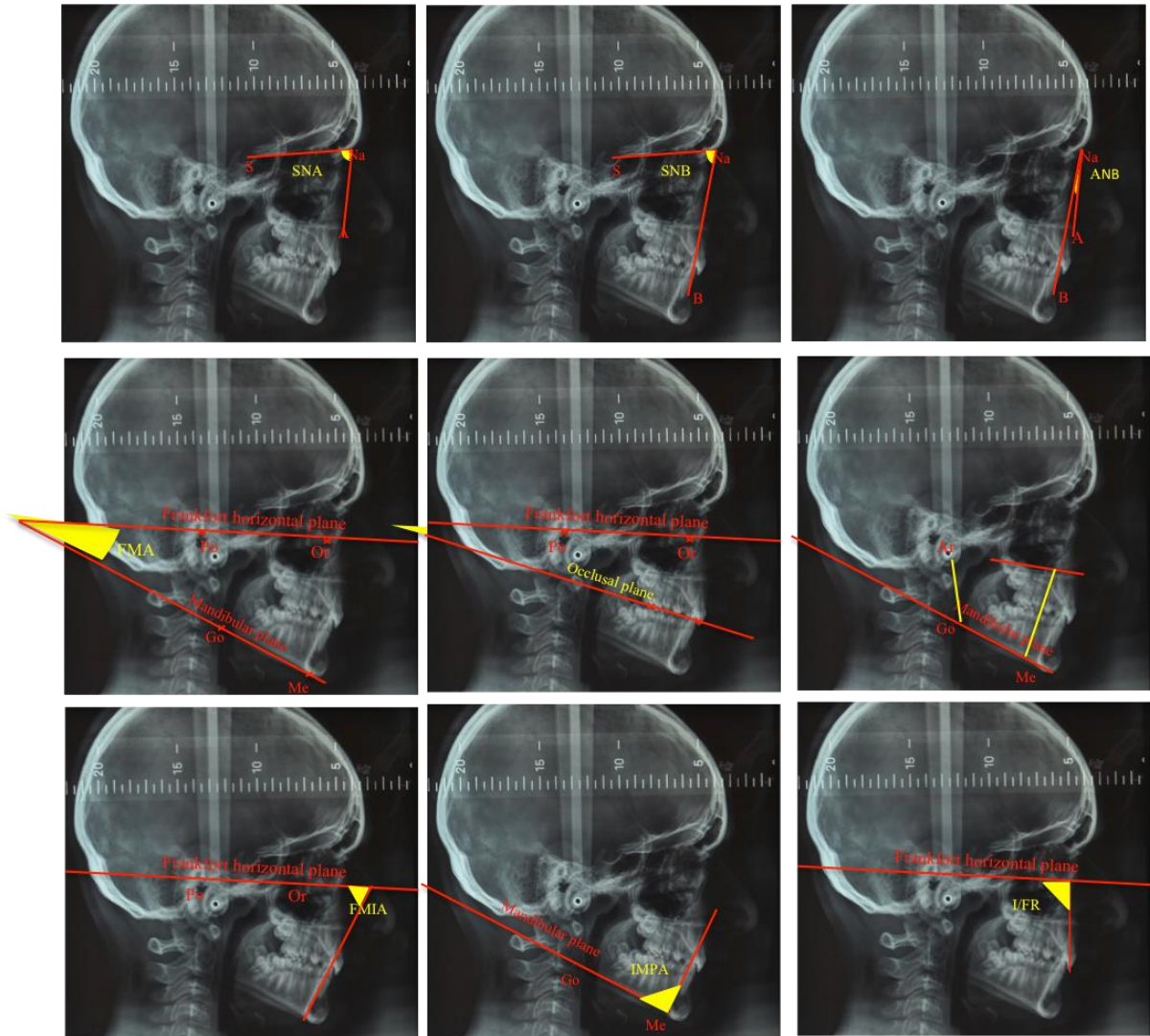


Figure 19. Cephalometric radiography measurements considered for the clinical study and growth evaluation.

- Delaire qualitative analysis (Software Delaire 2015 Evolution®). The statistical analysis of the qualitative data will be performed using the Fisher test with a significance level set at $p \leq 0.05$ (Figure 20).

Maxillary (Mx)			Relative position MxMb		
Orientation (IM / F1)		0,88°	F1M/f1m	Skeletal class II	0,88°
Pti / F4		0,2 mm	Incisors		0,2 mm
IM/F6	Ascension	-2,9 mm	Maxillary incisor apex orientation	Palatoversion	-2,9 mm
Mandible (Mb)					
Symphysis sagittal sense (f1m/F1)	Mandibular retrusion	-3,2°			-3,2°
vertical sense (Me/Met)		1,2 mm			1,2 mm
Ramus (R/F3)	Condylar posterior position	-0,6 mm	mandibular incisor Apex orientation	vestibuloversion	-0,6 mm
position of the condyle head orientation of posterior edge		-4,0°			-4,0°
Cp-Go/Cpt-Got		0,2 mm			0,2 mm
Cp-Go/N-ANS		-1,3 mm	Height ib-Me/ibt-Met		-1,3 mm
Cp-Go/Cpt V2		-1,9 mm	Angle C1/F1		-1,9 mm
Cos-Go/Cos-Got		-0,1 mm	Vertical proportions ANS-Me/N-Me		-0,1 mm
Gonial angle Cp-Go/Go-Me	opening	1,8°	Mandibular ramus/N-ANS		1,8°
Corpus, No-Me/Not-Me		0,5 mm	Axiological potential Hyoid bone position	Decrease abasement	
Mandible total length Cp-Me/Cpt-Met :	brachygnathism				

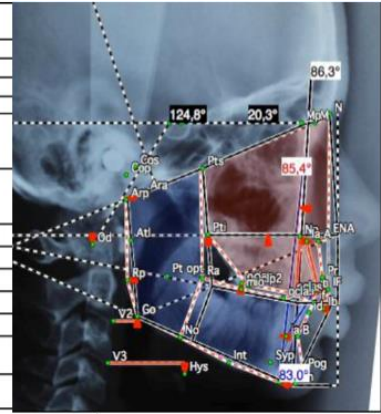


Figure 20. Delaire's qualitative parameters considered in this study.

6. RESULTS

My PhD set of results included a Systematic Review on dental features of osteopetrotic patients and experimental data which gave rise to 5 papers, 2 already published (Published papers section – paper 1 and 2) and 3 in preparation.

6.1. Oro-dental features in patients with osteopetrosis: A systematic review of 95 cases (Paper to be submitted)

6.1.1. Study selection

In phase 1 of the study selection, 1,242 citations were identified across the five electronic databases. After adjusting for duplicates, 826 citations remained. Of these, 777 were excluded after reviewing the abstracts as they did not meet the inclusion criteria or met one or more of the exclusion criteria. Six additional studies were considered from the grey literature and from the additional reference lists. In phase 2, the full-texts of the 55 remaining studies were evaluated, leading to the exclusion of 43 articles (Supplementary table 2). Thus, a total of 12 studies were included in this review, spanning a total of 95 patients. A flow diagram detailing the process of identification, inclusion, and exclusion of studies is shown in Figure 21.

6.1.2. Study characteristics

The studies were conducted in 11 different countries: France [181], Norway [182], Belgium [183], Iran [184], USA [185,186], India [187], Canada [188], Saudi Arabia [189], South Africa [190], Tunisia [191], and England [192]. The total sample from the 12 studies included 95 individuals affected by osteopetrosis and the size of each sample ranged from 3 [192] to 31 subjects [181]. Only one article was written in French [191]. All studies were published between 1968 [192] and 2016 [183] and they consisted of case series describing the oro-dental findings related to this genetic condition based on radiographic and clinical

examinations. A summary of the descriptive characteristics of the included studies is provided in Supplementary table 3.

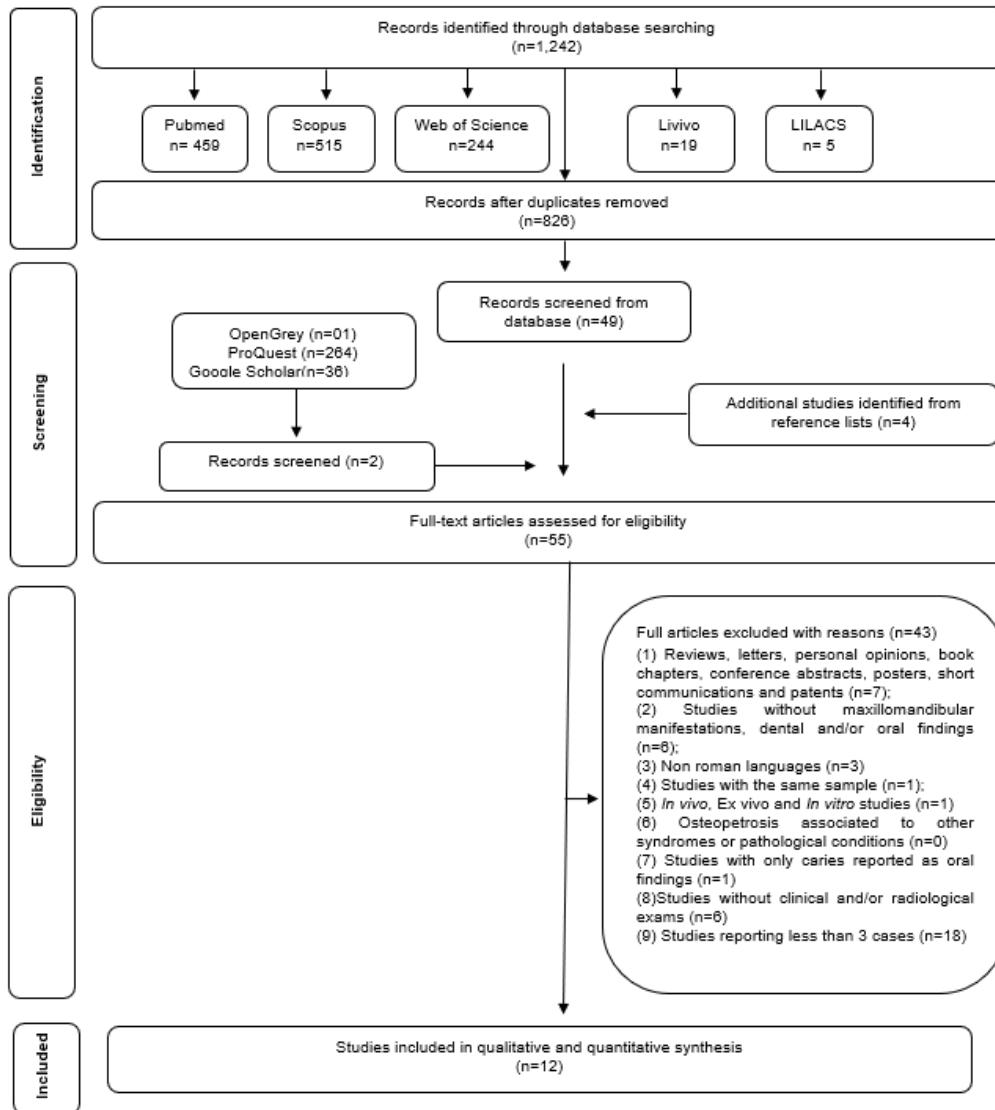


Figure 21. Flow Diagram of literature search and selection criteria adapted from PRISMA [170,171].

6.1.3. Quality assessment

The results of the quality assessment of the 12 included studies are outlined in Supplementary table 4 and analyzed in Figure 22. The main identified methodological weaknesses consisted of the lack of clear criteria for the inclusion of patients in the case series. Since osteopetrosis is a rare genetic condition, the representative sample of each study was not

a matter of concern, resulting in a lack of statistical data, except for one study that provided weak prevalence data [181]. In addition, the overall studies included in this SR are highly heterogeneous and fail to provide a detailed description of the oral findings. The design study rationale is highly descriptive and its subjectivity responds to this high risk of methodological bias. As demonstrated in Figure 22B, we found that the studies selected for this SR had a poor reporting quality.

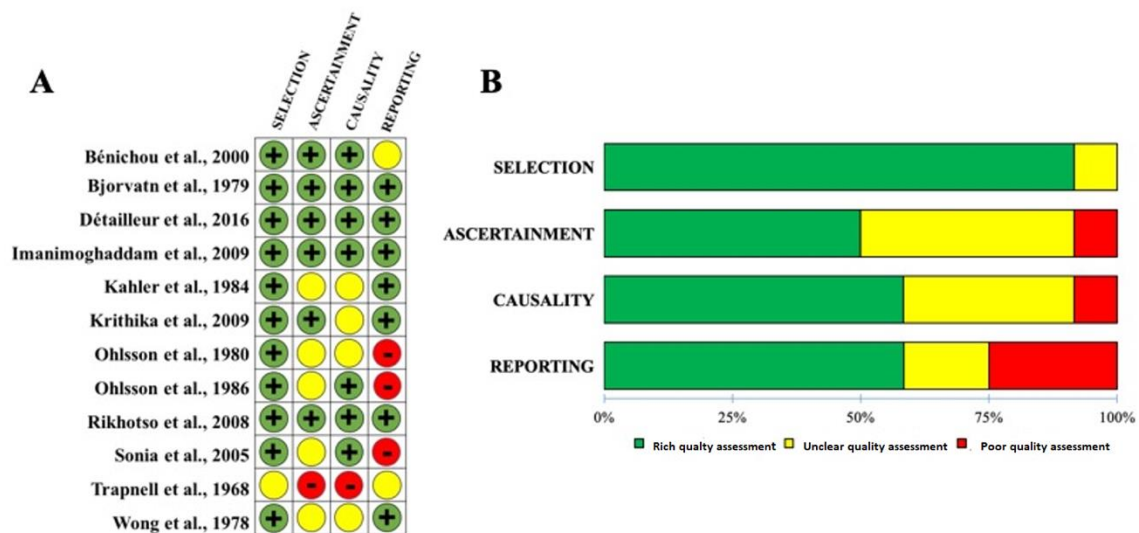


Figure 22. A- Quality assessment graph based on the JBI critical appraisal modified checklist for case series and prevalence studies. B- Quality assessment summary. Score: 100-76% Rich quality assessment (green); 51-75% Unclear quality assessment (yellow); 26-50% Poor quality assessment (red).

6.1.4. Results of individual studies

The descriptive characteristics of the 12 included studies are summarized in Supplementary table 3. Included patients were between 23-days and 47-years-old. The demographic information of the studied patients was not clearly detailed in all studies. For all patients, the osteopetrosis diagnosis was based on clinical and radiographic data, and molecular analyses were only performed in two studies [183,191]. With regards to the type of osteopetrosis and mode of inheritance, one study exclusively reported ADO cases [181], 8 studies reported a series of ARO cases [182–186,188,189,191], and cases of ARO associated with renal tubular acidosis were identified in 3 studies [188,189,191]. In one study, Rikhotso et al., 2008 described 2 cases of ADO type II and 1 ARO case [190]. Two studies did not describe the type of osteopetrosis nor the mode of inheritance of the patients [187,192]. The distribution of the number of patients according to the type of osteopetrosis is shown in Figure 23.

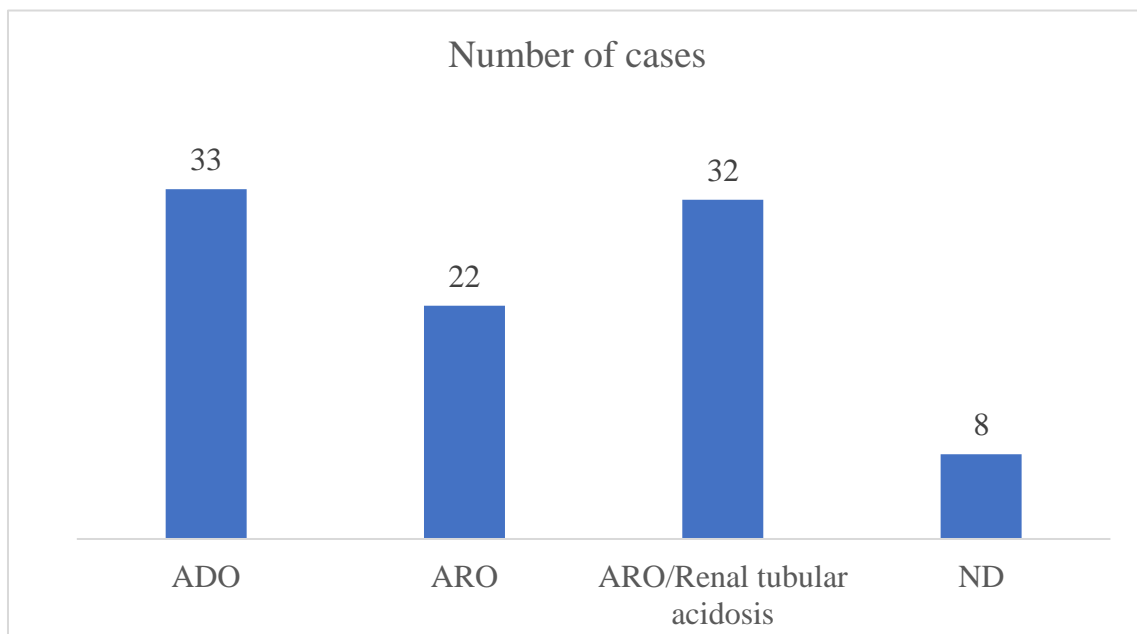


Figure 23. Number of cases distribution according to the type of Osteopetrosis. ADO: Autosomal Dominant osteopetrosis; ARO: Autosomal Recessive osteopetrosis; ND: Diagnosis not defined

Détailleur et al. reported 3 different variants in the *TCIRG1* gene (homozygous G19106A, homozygous C404G, R669X) in ARO patients [183]. All 24 ARO/renal tubular acidosis patients described by Sonia et al. 2005 presented a G>A splice junction point mutation in intron 2 of the *CAII* gene [191].

The reported oro-dental features are summarized in Supplementary table 5 and detailed hereafter.

Maxillary and mandibular osteomyelitis

Maxillary and mandibular osteomyelitis was by far the most cited oral finding in all forms of osteopetrosis. Out of 12 studies, 9 reported osteomyelitis of the jaws corresponding to a total of 21 patients (22,10%), of which 7 presented with maxillary osteomyelitis (7,36%), 13 presented with mandibular osteomyelitis (13,68%), and one presented with osteomyelitis in both jaws (1,05%). Of these 21 patients, 12 were children and adolescents aged 7- to 18-years-old and had mostly recessive forms [182,184,185,190]. The study with the largest number of cases described presented 31 ADO type II individuals whose most common oral manifestation was osteomyelitis of the mandible, found in 4 affected adults [181]. Two studies with no defined osteopetrosis types presented patients affected by osteomyelitis [187,192]. With regards to the AR form of osteopetrosis with renal tubular acidosis and cerebral calcifications, as few as only 3 patients presented with osteomyelitis [189,191].

Ohlsson et al.[189], Rikhotso et al. [190], Trapnell et al. [192] and Sonia et al. [191] reported the occurrence of maxillary osteomyelitis. Sonia et al. [191] reported a series of 24 cases of ARO with tubular renal acidosis, only 2 of which developed osteomyelitis, while Rikhotso et al. and Ohlsson et al. [189,190] reported only one case, accounting for 33% and 25% of the sample in each study, respectively. Five studies reported osteomyelitis after tooth

extraction followed by poor healing [185,187,189,190,192]. Three studies did not specify the causative relation between extraction and osteomyelitis [181,182,191] and, finally, one study described two cases with spontaneous onset of infection [184].

Dental eruption defects

Tooth eruption defects were the second most common reported oral feature. These were classified according to 6 groups: delayed eruption, unerupted teeth, ankylosis, infra-occlusion, primary tooth retention and general tooth eruption defects with no specific pattern. Eight studies outlined these dental anomalies [183–188,190,191]. Seven of them were reported in ARO and ARO/renal tubular acidosis patients [182,183,185,186,188,190,191], while the type of osteopetrosis was not determined in one of the studies [187]. Bjorvatn et al.[182] and Sonia et al.[191] mentioned the existence of eruption defects but did not provide any descriptive details. Most patients presented delayed eruption and unerupted teeth as a type of eruption anomaly (Fig. 24A and Supplementary table 6).

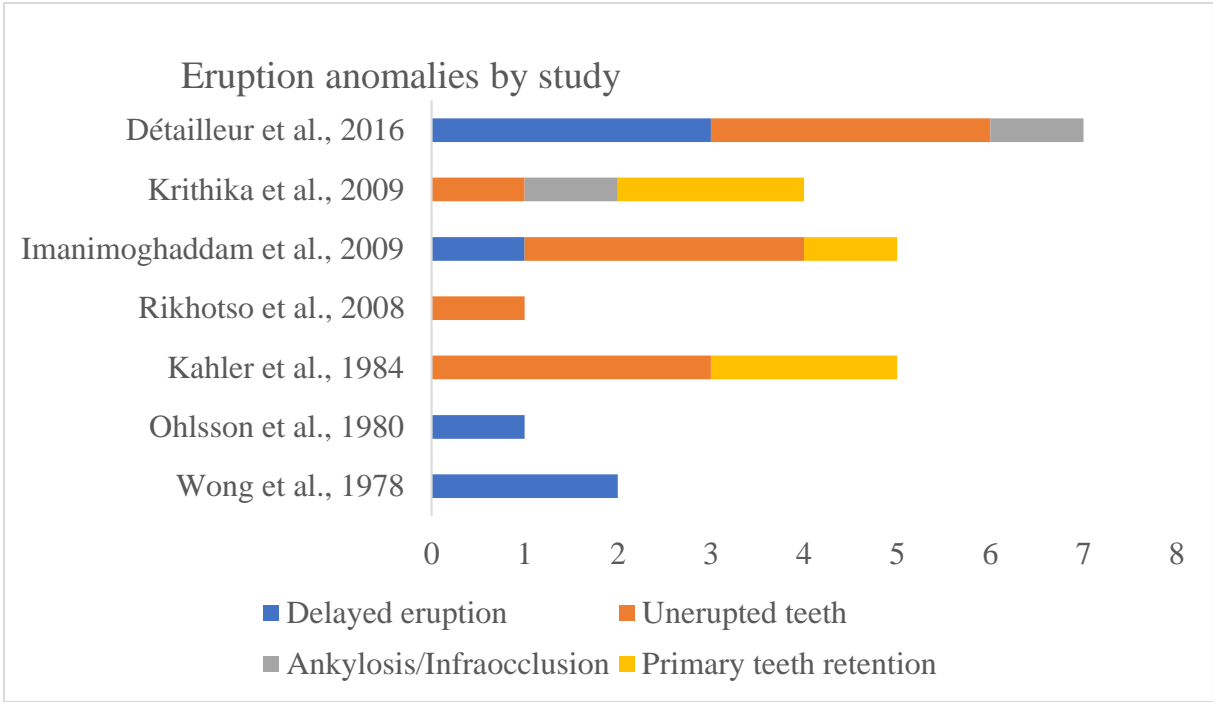
Both dentitions, primary and permanent ones, seemed to be affected by eruption defects and only in two studies [183,187] they were enough detailed highlighting retained molars, molar agenesis, molar ankylosis and infraocclusion. A generalized slower eruption rate and even no eruption at all were also reported.

Dental anomalies

Nine studies reported at least one type of dental anomaly (number, size, shape or enamel defect) in ARO patients, ARO/renal tubular acidosis patients, or patients affected by an undefined type of osteopetrosis [182–185,187–191]. The distribution of the different types of dental anomalies is shown in Figure 24B and Supplementary table 7. Tooth agenesis of various degrees of severity was reported in 9 patients [183–185,187,189,190] and shape anomalies in primary and permanent teeth (15 patients) were also observed [183–185,188,189,191]. In 2

studies, all individuals presented with malformed teeth [183,185]. Hypoplasia in 7 patients (4 studies) was the main reported enamel developmental defect (EDD) [183,187–189]. Of the 95 included patients, only 1 patient had supernumerary teeth [183]. Root malformations were pointed out in 3 studies [182–184] and the occurrence of hypercalcified and fused teeth was described by Détaillieur et al. in two different patients [183]. In a large series of 24 patients, Sonia et al. [191] only highlighted the presence of odontoma-like structures.

A



B

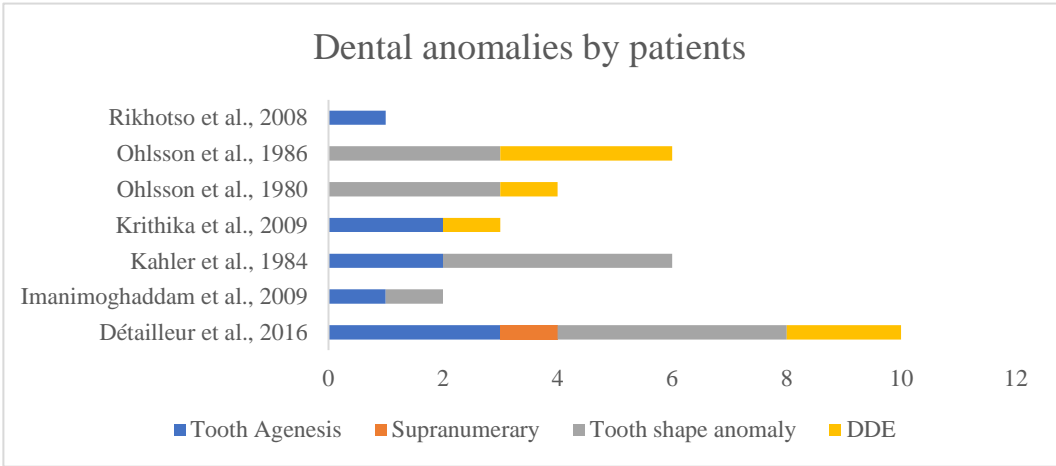


Figure 24. Reported eruption anomalies (A) and dental anomalies(B).

Other oral findings

Other oral findings were noted such as non-trauma related tooth fractures [181], reduced temporomandibular joints (TMJ) movements [182], broad alveolar ridges [182,186,190], lower palate vault [182], high arched palate [186], periodontitis [182] and bone expansion [184]. The sclerotic mandible and maxilla [184,187,190,191] accounted for the compression of the inferior alveolar nerve [190] and the facial dysmorphias [191] such as prognathism [185,190], small lower jaw [189,191] and midface deficiency [190]. The most prevalent features are detailed in Supplementary table 7.

6.2. Maternal RANKL Reduces the Osteopetrotic Phenotype of Null Mutant Mouse Pups evidencing the implication of RANKL signaling in cell-to-cell communications necessary to craniofacial skeleton morphogenesis – Published papers section – paper 1

Second-Generation Rankl Null Mutants Had a More Severe Craniofacial Phenotype:

At birth, the Micro-CT and histological analyses showed that first-generation *Rankl* null mutants (N = 5) had a craniofacial osteopetrotic phenotype with an open foramen, due to delayed mineralization of the calvaria and delayed tooth development, associated with an absence of osteoclasts (Figures 25 and 26). Since part of the craniofacial skeleton develops during the second half of gestation, and taking into account that secreted forms of RANKL of maternal origin may be active in the embryo, the question of an attenuated craniofacial phenotype in first-generation *Rankl* null mutants was raised. In order to answer this question, second-generation *Rankl* null mutant pups were generated by mating male and female *Rankl* null mutants. The craniofacial phenotype of the second-generation null mutants (N = 5) was more severe than the phenotype of the first-generation mutants, with a more open foramen (Figure 25) and more delayed tooth morphogenesis (Figure 26). In addition, a loss in mandible curvature was observed (Figure 25), associated with defective disruption of the Meckel cartilage (Figure 26). A similar craniofacial phenotype was observed in null mutant pups (N = 2) from null mutant females mated with heterozygous males (Figure 27), confirming the importance of RANKL of maternal origin.

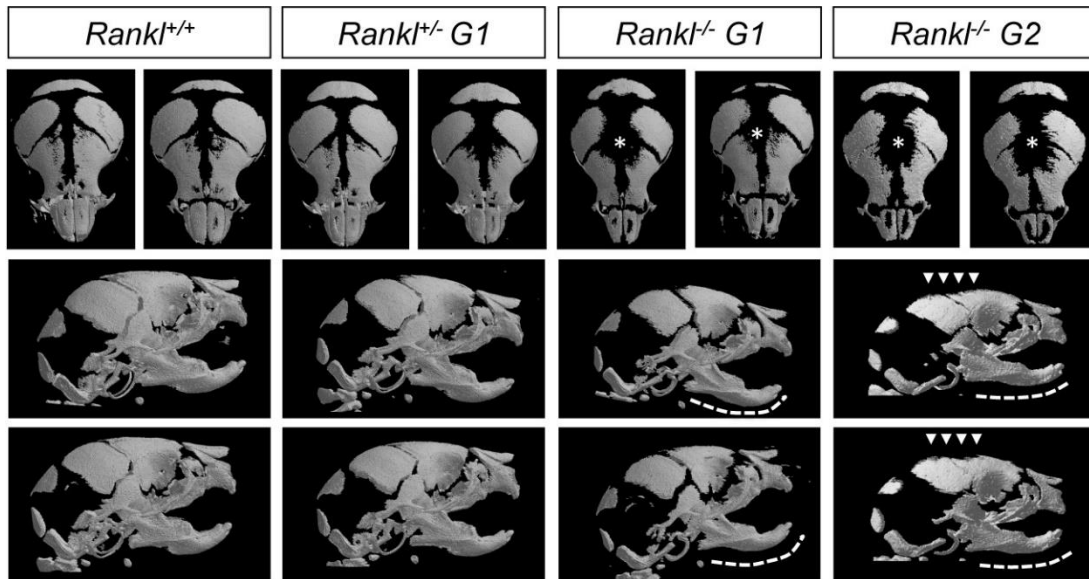


Figure 25. Micro-CT comparative analysis of the craniofacial skeletons of first- and second-generation. Percentage of closure measures (surface) for the different genotypes are 89 ± 2 for +/+, 84 ± 3 for +/-, 67 ± 4 for G1-/- and 57 ± 5 for G2-/. Moreover, the mandibles of second-generation null mutants appeared flat, with missing proximo-distal curvature (dotted lines). Angle of the mandible curvature measures (opening degrees) for the different genotypes are 134 ± 9 for +/+, 136 ± 11 for +/-, 139 ± 9 for G1-/- and 163 ± 7 for G2-/. No difference was observed between the wild type and heterozygous pups. Numbers of pups: 4 +/+, 8 G1+/-, 5 G1-/-, and 5 G2-/-.

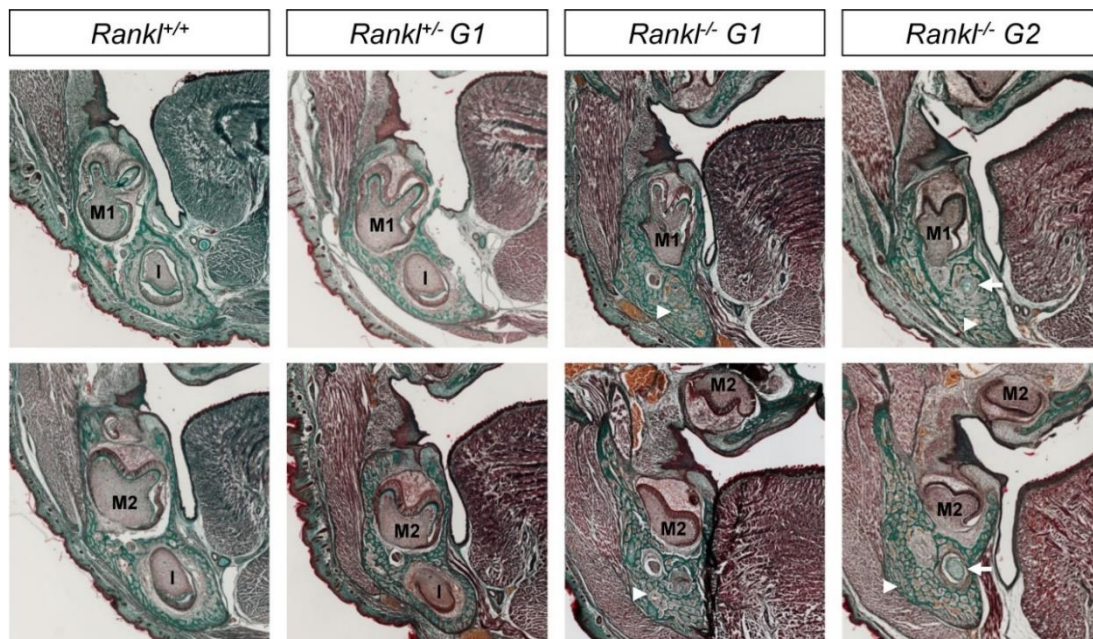


Figure 26. Histological comparative analysis of the craniofacial skeletons of first- and second generation Rankl null mutant mice. Frontal sections of the head in planes of first (M1) and second (M2) molars revealed more severe osteopetrosis in the second-generation (Rankl^{-/-} G2) compared to the first-generation (Rankl^{-/-} G1) null mutants. While both null mutants revealed increased bone density compared to wild type and heterozygous mice (arrowheads), the second-generation null mutants had a remnant Meckel cartilage (arrow) and a very significant delay in the development of first and second molars, with the second molar appearing to be blocked between the cap and bell stages. Comparison of sections from wild type and heterozygous pups revealed a pre-osteopetrotic phenotype in the heterozygous mice, with increased bone density and delayed moving back of the

incisor (I) in the mandible. Magnification 40× for all images. Numbers of pups: 4 +/+, 8 G1+/-, 5 G1-/-, and 5 G2-/-.

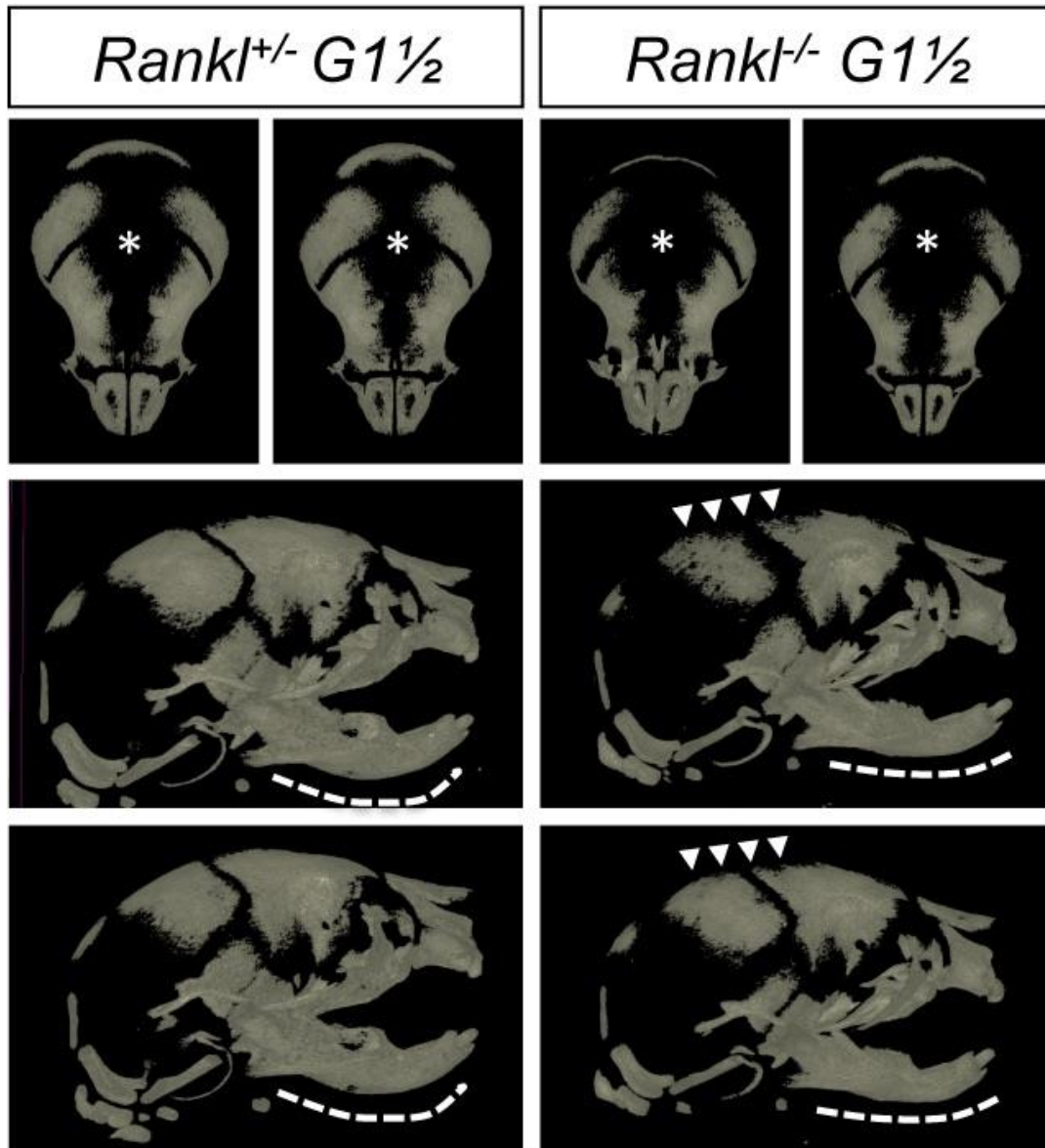


Figure 27. Micro-CT comparative analysis of the craniofacial skeleton of pups born from null mutant females and heterozygous males. Heterozygous and null mutant pups revealed craniofacial phenotypes that were respectively similar to first- and second-generation null mutants. Enlarged foramina (stars) were present, more pronounced in the null mutants (arrowheads), and the mandibles of the null mutants appeared flat (dotted lines) as in the second-generation null mutants. Percentage of closure measures (surface) for the two genotypes are 65 ± 4 for +/- and 54 ± 7 for -/-. Angle of the mandible curvature measures (opening degrees) for the two genotypes are 133 ± 10 for +/-, 159 ± 12 for 1 -/-. Numbers of pups: 4 +/- and 2 -/-.

IK22-5 RANKL-Blocking Antibody Injections in Pregnant Heterozygous Mice Induced a Second-Generation-Like Phenotype in Null Mutant Pups

In order to validate the importance of RANKL of maternal origin in the attenuated osteopetrotic phenotype of the null mutant pups, IK22-5-blocking antibody was injected into heterozygous pregnant females during the second part of gestation, and the consequences on the whole skeleton of the pups were analyzed (Figures 28 and 29). A noticeable aggravation in either craniofacial or long bone phenotypes was observed for the different genotypes, with WT being comparable to first-generation heterozygous mutants and first-generation to second-generation null mutants. Surprisingly, while a more open foramen (Figure 28) and severe tooth morphogenesis delay (Figure 29) was observed in the null mutants from injected mothers, the curvature of the mandible appeared unaffected (Figure 28), suggesting that this craniofacial osteopetrotic feature was secondary to a loss of RANKL function before mid-gestation.

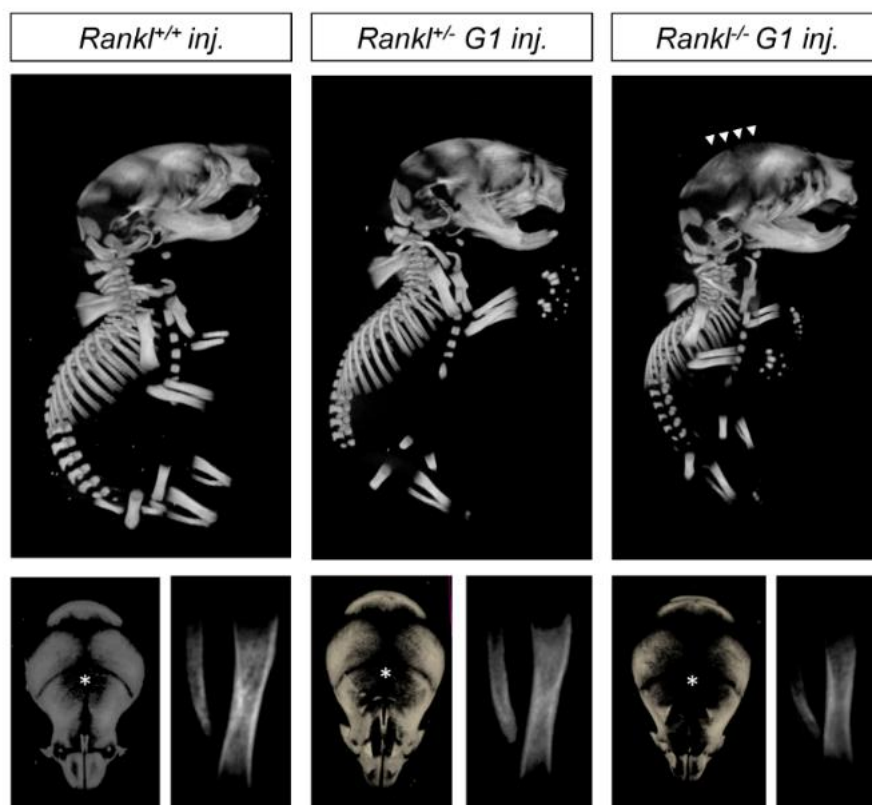


Figure 28. Micro-CT comparative analysis of the skeletons of wild type, heterozygous, and first-generation Rankl null mutant pups born from females treated with IK22-5 during the second half of pregnancy. A graduated skeleton phenotype was observed from wild type to null mutant pups, with the presence of an enlarged foramen (star and arrowheads) in all genotypes. Percentage of closure measures (surface) for the different genotypes are 87 ± 3 for +/+, 68 ± 4 for +/-, and 60 ± 4 for -/-. Globally, it seems that injections

of IK22-5 increased the phenotype of each genotype to the next in terms of severity, wild type being comparable to non-injected heterozygous, heterozygous to non-injected first-generation null mutants, and first-generation null mutants to second-generation phenotypes. Numbers of pups: 3 +/+, 6 +/-, and 2 -/-.

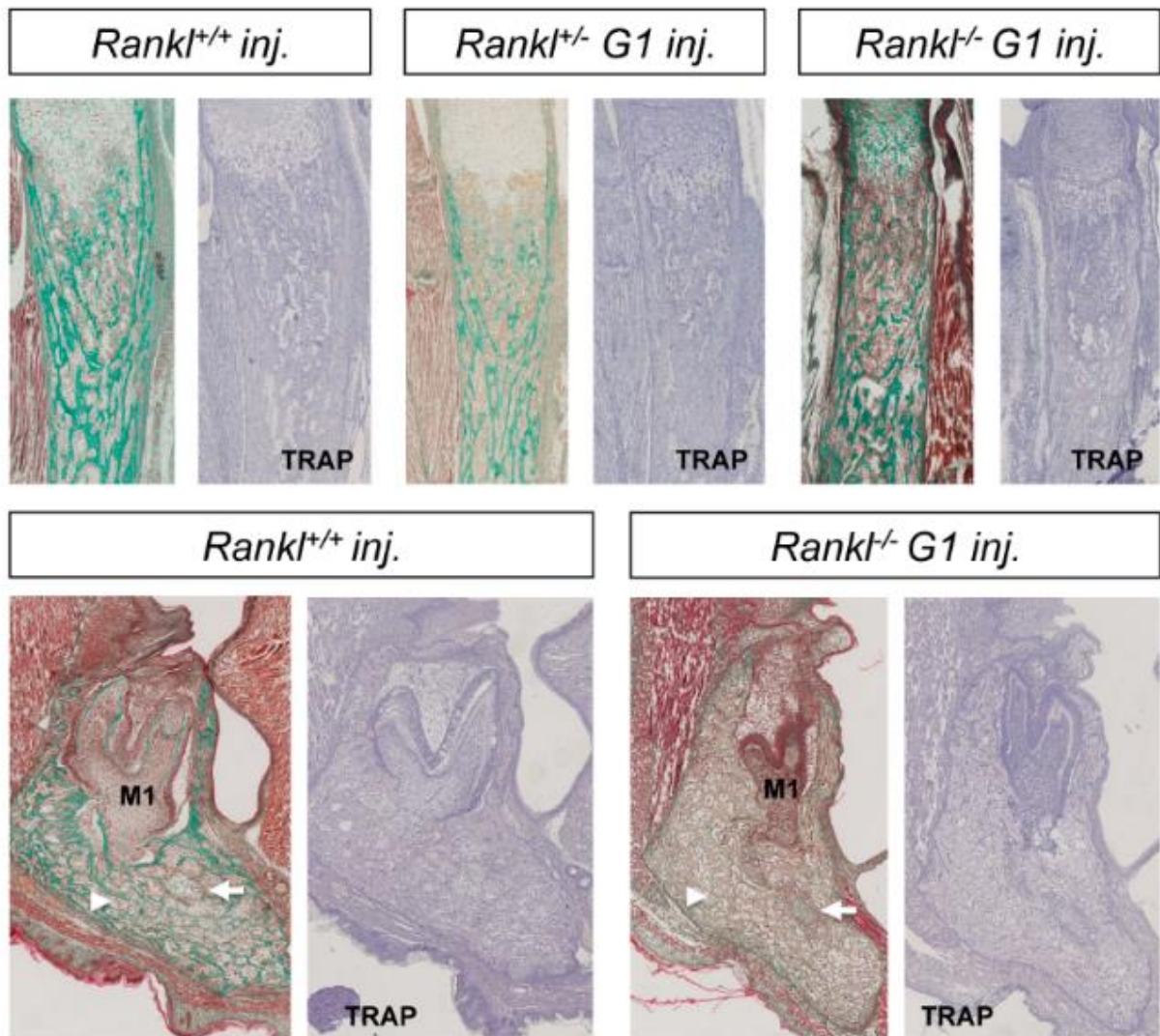


Figure 29. Histological comparative analysis of the skeletons of wild type, heterozygous, and first-generation *Rankl* null mutant pups born to females treated with IK22-5 during the second half of pregnancy. Masson trichrome staining of longitudinal sections of tibias made it possible to observe an osteopetrotic phenotype in all genotypes with, however, graduated severity from wild type to null mutant. TRAP staining was negative in all sections, signaling the absence of osteoclasts, induced by the IK22-5 injections. Masson trichrome staining of mandible frontal sections in the plane of the first molar (M1) revealed the induction of an osteopetrotic phenotype in the wild type pup with significant mandibular bone density (arrowhead), an absence of incisor in this section plane, remnant Meckel cartilage (arrow), and abnormal tooth morphology. TRAP staining of adjacent sections revealed a total absence of osteoclasts. Concerning the null mutant pups, a phenotype similar to the second-generation mutant pup was observed, with significant mandibular bone density (arrowhead), remnant Meckel cartilage (arrow), and abnormal tooth morphology. Magnification 40 \times . Numbers of pups: 3 +/+, 6 +/-, and 2 -/-.

6.3. Origins of Rankl null mutant mouse dental root developmental alterations

(Paper to be submitted)

Phenotypic alterations of the dento-alveolar bone complex associated to the different Rankl genotypes

The phenotype of mouse mandibular first molar and the underlying alveolar bone was histologically characterized for the three different *Rankl* genotypes (*Rankl*^{+/+}, *Rankl*^{+/-} and *Rankl*^{-/-}) from post-natal day 3 to 7 (Figure 30A). Whatever the age considered, no histological difference was observed between the *Rankl*^{+/+} and *Rankl*^{+/-} mice (Figure 30A). In contrast, the *Rankl*^{-/-} mice presented a severe osteopetrotic phenotype with alterations of both the crown and the root tissue histogenesis, associated to a grade entrapment in the surrounding hypertrophic alveolar bone (Figure 30A). Regarding the root, the formation of the Hertwig's epithelial root sheath (HERS) was initiated as visible at day 5 but rapidly constrained by the hypertrophic alveolar bone presence more obviously in the buccal region (Figure 30A). The TRAP histo-enzymology was realized on adjacent sections (presented for day 5 in Figure 30B) evidencing a total absence of staining in the *Rankl*^{-/-} mouse whatever the age. Interestingly while a similar repartition of TRAP positive cells was observed around the tooth in the alveolar bone of *Rankl*^{+/+} and *Rankl*^{+/-} mice, the number of positive cells and the intensity of the staining appeared lower in the heterozygous mice suggesting the existence of an haploinsufficiency effect at least concerning the osteoclastogenesis (Figure 30B).

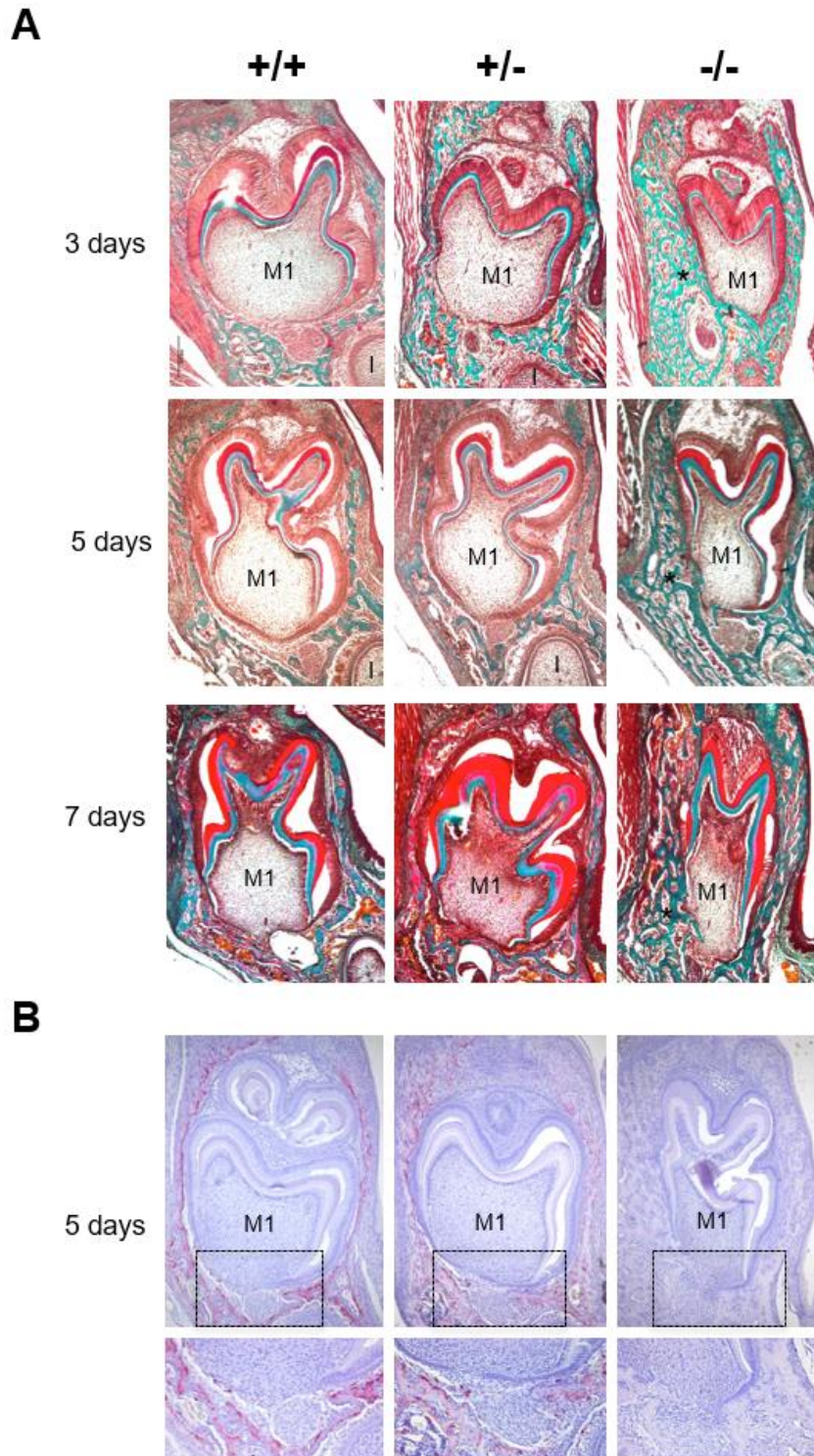


Figure 30: Histological comparative analyses of the dental phenotype related to the different *Rankl* genotypes. (A) Masson's trichrome staining performed in 5µm thick frontal sections of the *Rankl*^{+/+}, *Rankl*^{+/-} and *Rankl*^{-/-} C57BL6 mouse heads at the ages of 3, 5 and 7 days post-natal. An equivalent distribution of the bone matrix around the first molars (M1) was observed for *Rankl*^{+/+} and *Rankl*^{+/-} genotypes whatever the age considered. In contrast, concerning the *Rankl*^{-/-} genotype, a gradual increase of the bone matrix deposition was observed with age (stars), so that the tissue boundary between the dental follicle and the apical papilla was interrupted more specifically in the buccal region. Moreover, the *Rankl*^{-/-} mouse molar presented over-time a progressive crown narrowing. I: incisor. Scale: 20X/100 µm. (B) TRAP histoenzymology at post-natal day 5 evidenced a regular distribution of TRAP positive osteoclasts around the first molar (M1) for the *Rankl*^{+/+} and *Rankl*^{+/-} genotypes. As expected no TRAP staining was observed on the section of the *Rankl*^{-/-} mice. A close view of the apical papilla (black rectangles) highlighted a reduction of the TRAP staining in the *Rankl*^{-/-} section comparatively to the *Rankl*^{+/+} section. Scale 20X/100 µm.

Alterations of the Hertwig's epithelial root sheath elongation associated to the different Rankl genotypes

The Hertwig's epithelial root sheath (HERS) elongation that constitutes the main root developmental event was characterized for the three different *Rankl* genotypes (*Rankl*^{+/+}, *Rankl*^{+/-} and *Rankl*^{-/-}) from post-natal day 3 to 7 using the epithelial marker keratin-14 immunohistochemistry (Figure 31A). Measurements of the number of cells constituting the HERS were realized in the lingual and the buccal regions of the mandible first molar mesial root for the different *Rankl* genotypes as for the RANK over-expressing (*Rank*^{Tg}) mouse that present an accelerated root elongation (Figure 31B and Supplementary table 8). Whatever the region considered, the number of cells was higher in the *Rank*^{Tg} mice at days 3 and 5 compared to the control while lower at day 7 signing as expected an earlier HERS elongation and disruption. A contrario, the number of cells was lower than control for the *Rankl*^{-/-} mouse whatever the day considered evidencing a defective HERS elongation. Interestingly, the number of cells was nevertheless continuously growing for the *Rankl*^{-/-} mouse from day 3 to 7 at least in the lingual region signing a reduction rather than a blockage of the HERS cells proliferation. Concerning the *Rankl*^{+/-} mouse, a cells-number similar to the control was observed, except at day 5 in the buccal region for an unexpected reason.

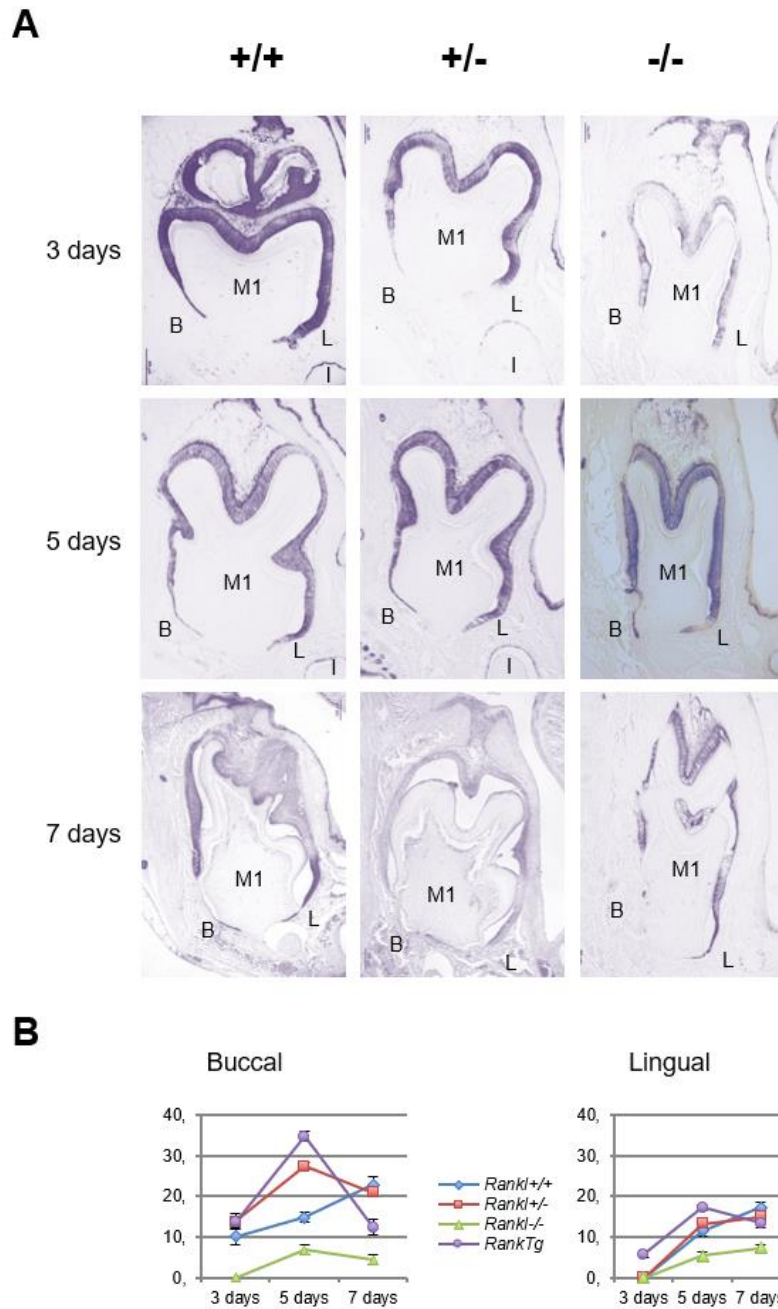


Figure 31: Comparative analyses of the Hertwig's epithelial root sheath length in the different *Rankl* genotypes based on cytokeratin-14 immuno-staining. (A) Cytokeratin-14 immunohistochemistry was performed on 5µm thick frontal sections of the *Rankl*^{+/+}, *Rankl*^{+/-} and *Rankl*^{-/-} C57BL6 mouse heads at the ages of 3, 5 and 7 days post-natal. The *Rankl*^{-/-} sections evidenced an important reduction of the number of Hertwig's epithelial root sheath cells with interruptions of the sheath continuity by the bone matrix deposition with a progressive invasion of the pulp. In the lingual (L) region, the sheath appeared less altered morphologically than in the buccal (B) region. Scale: 20X/100 µm. (B) Graphic representation of the quantitative analyses of the Hertwig's epithelial root sheath cells number in the buccal and lingual regions realized on the sections of the *Rankl*^{+/+}, *Rankl*^{+/-} and *Rankl*^{-/-} C57BL6 mouse heads at the ages of 3, 5 and 7 days post-natal. Similar quantitative analysis performed for *Rankl*^{Tg} mouse that present an accelerated root elongation was added. *Rankl*^{-/-} sections presented a low number of epithelial cells, whatever the lingual or buccal regions, comparatively to either the two other *Rankl* genotypes that appeared very close except at day 5 in the buccal region, or the *Rankl*^{Tg} genotype. X axe: mice age in days. Y axe: number of root sheath epithelial cells.

Expression patterns of RANKL and its three receptors namely RANK, OPG and LGR4 in the mandible first molar mesial root of 5 days-old mouse supported the implication of RANKL in the proliferation of HERS cells.

In order to characterize the potential direct implication of RANKL signaling in the HERS elongation through modulation of the proliferation of epithelial cells from the apical area, the expression patterns of RANKL and its three known receptors RANK, OPG and LGR4 were established by immunohistochemistry on frontal sections of 5 days-old wild type mouse mandible first molar (Figure 32). RANKL expression was observed in mesenchymal cells of the dental pulp facing the HERS, in cells from the apical follicular mesenchyme and in few cells at the alveolar bone surface (Figure 32A). The main receptor RANK was highly expressed in mesenchymal cells of the dental pulp, in epithelial cells of the HERS and in various large cells at the bone surface (Figure 32A). Interestingly, no RANK expression was detected in cells of the apical follicular mesenchyme. The decoy receptor OPG expression was detected at low level in mesenchymal cells of the dental pulp facing the HERS and also in cells from the apical follicular mesenchyme (Figure 32A). Finally, the alternative receptor LGR4 expression was detected at low level in few epithelial cells of the HERS and at high level in cells from the apical follicular mesenchyme and in cells at the alveolar bone surface (Figure 32A). The four expression patterns were shown in Figure 32B for comparison. Regarding the potential HERS cells proliferation modulation by RANKL signaling, it seems that such a control implicates the receptor RANK, the most expressed by those cells. Interestingly concerning the two mesenchymal compartments, differential situations were observed. In the pulp compartment RANK was the main expressed receptor whereas in the apical follicular mesenchyme LGR4 was the main expressed (Figure 32B) suggesting different impact of RANKL on mesenchymal cells of those two compartments. Regarding the alveolar bone compartment, RANK was

expressed in large cells at the bone surface supposed to be osteoclasts while LGR4 in rather small and numerous cells at the bone surface suspected to be osteoblasts.

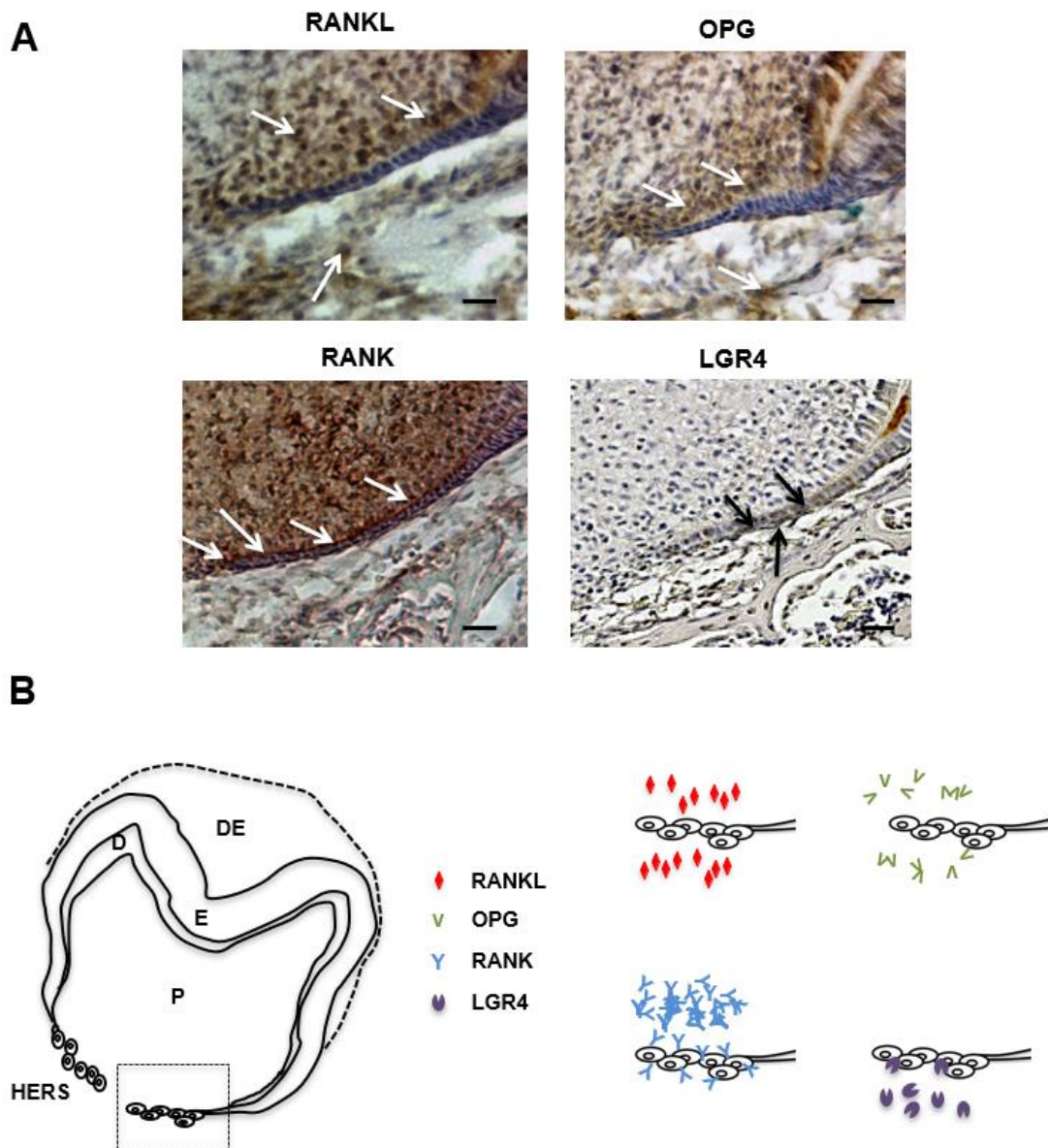


Figure 32: RANKL, RANK, OPG and LGR4 expression patterns in the mandible first molar of 5 day-old wild-type mouse. (A) Immunohistochemistry experiments were realized on 5 μ m thick frontal sections of 5 day-old wild-type C57BL6 mice heads for RANKL, RANK, OPG and LGR4. RANKL and OPG expressions were observed in some mesenchymal cells of the pulp mainly facing the Hertwig's epithelial root sheath, in mesenchymal cells of the apical papilla and in certain alveolar bone cells (arrow-heads). RANK expression was highly detected in the pulp, in the Hertwig's epithelial root sheath and in cells at the bone surface. A soft LGR4 expression was evidenced in some cells of the Hertwig's epithelial root sheath and the apical papilla (arrow-heads), and in most cells at the alveolar bone surface. Scale: 20X/100 μ m. (B) Schematic representations of established RANKL, RANK, OPG and LGR4 expression patterns in 5 day-old wild-type C57BL6 mouse mandibular first molar root. Cells of the Hertwig's epithelial root sheath expressed only RANK and LGR4 with an important difference in the number of stained cells and the staining intensity in the favor of RANK. DE: dental epithelium; E: enamel; D: dentine; P: pulp; HERS: Hertwig's epithelial root sheath.

Alterations of HERS cell proliferation associated to the different Rankl genotypes.

In order to characterize the potential modulation of HERS cell proliferation by RANKL signaling, the expression patterns of the proliferation marker PCNA and the proliferation inhibitor P21^{Waf-1/Cip-1/Sdi-1} (P21) were established by immunohistochemistry on frontal sections of the mandible first molar mesial root of mice from the three different *Rankl* genotypes (*Rankl*^{+/+}, *Rankl*^{+/-} and *Rankl*^{-/-}) at post-natal day 3 to 7. Histological results obtained at day 5 are presented in Figure 33 and the quantification/evaluation staining intensity in the HERS cells at all ages were presented in Supplementary tables 9 and 10. Concerning PCNA expression, in the *Rankl*^{-/-} mouse, no expression was detected from day 5 whereas a low staining was observed in a minority of mice at days 3 and 4 (Figure 33A and Supplementary table 9). In the *Rankl*^{+/+} and *Rankl*^{+/-} mice, a PCNA staining was observed at all age in the HERS cells with a gradual decrease in intensity from day 3 to day 7 (Figure 33A and Supplementary table 10). Interestingly the intensity of the staining was globally lower in the *Rankl*^{+/-} than in the *Rankl*^{+/+} mice in agreement with a haploinsufficiency effect.

Concerning P21 expression, in the *Rankl*^{-/-} mice, a high intensity was observed in HERS cells from days 3 to 7 (Figure 33B and Supplementary table 10). In *Rankl*^{+/+} mice, a low intensity P21 expression was observed in HERS cells except at day 3 evidencing an intermediary staining intensity (Figure 33B and Supplementary table 10). In *Rankl*^{+/-} mice, a low intensity P21 expression was observed in HERS cells except at day 3 for which P21 was not detected and surprisingly at day 6 evidencing in most mice an intermediary staining intensity (Figure 33B and Supplementary table 10).

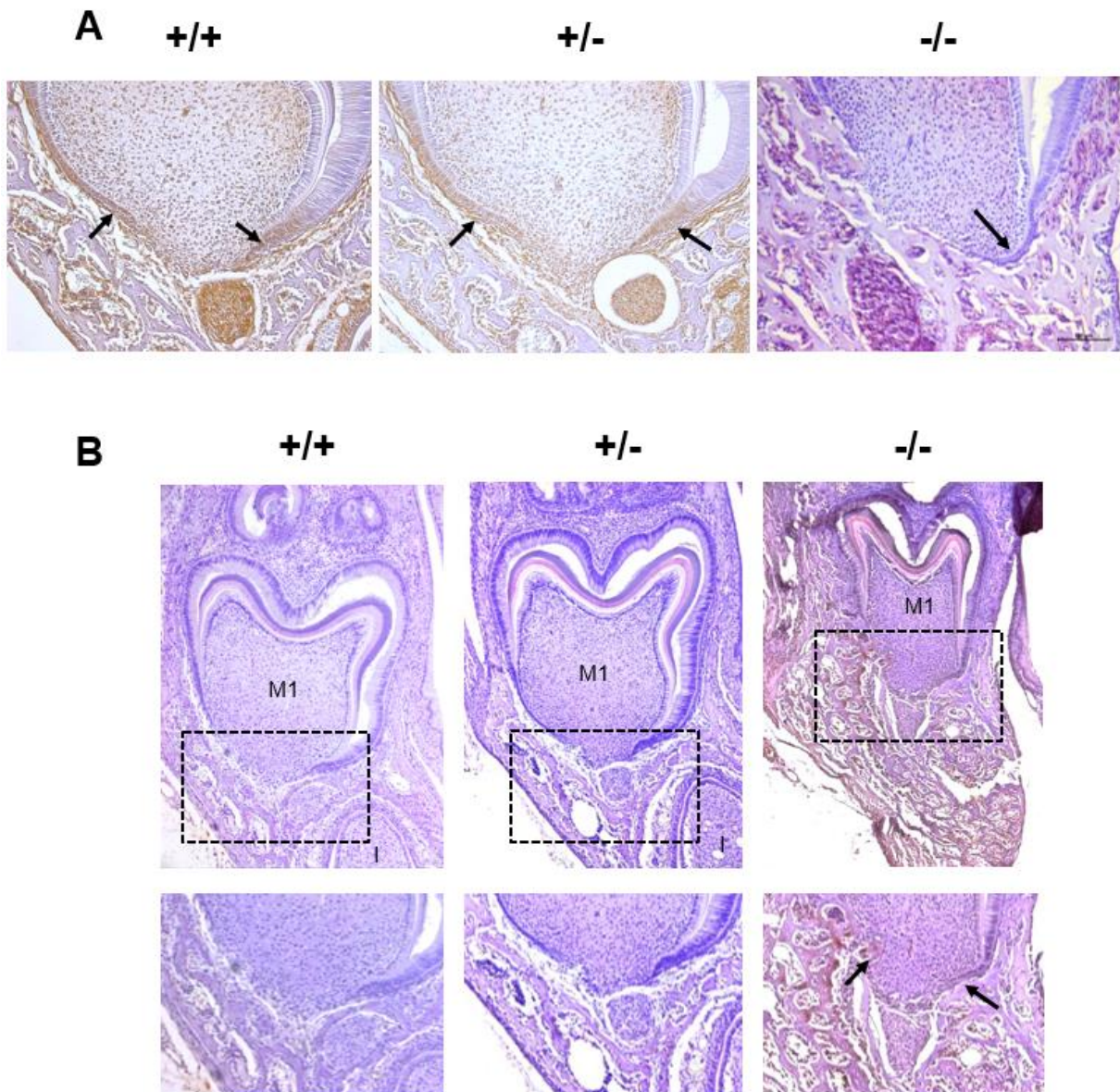


Figure 33: PCNA and P21 expression patterns in the mandible first molar of 5 day-old wild-type mouse. Immuno-histochemistry experiments were realized on 5 μ m thick frontal sections of 5 day-old wild-type C57BL6 mouse head for PCNA (A) and P21 (B). The PCNA expression was similarly detected for the $Rankl^{+/+}$ and $Rankl^{+/-}$ mice in cells of the Hertwig's epithelial root sheath (arrows) and cells of the apical papilla. In contrast, in the $Rankl^{-/-}$ mouse the PCNA staining was extremely reduced in those cells while important in alveolar bone cells. The P21 expression was close to absent in sections of $Rankl^{+/+}$ and $Rankl^{+/-}$ mice while important for $Rankl^{-/-}$ mouse in cells of the Hertwig's epithelial root sheath (arrows), the apical papilla and the alveolar bone. Black squares correspond to the region enlarged below. Scale 20X/100 μ m. M1: first molar.

Comparison of the mandible first molar phenotypes between 35 days-old wild type, Rankl^{-/-} and RANKL transitory defective mice.

Comparatively to wild type mouse, in permanently or transiently RANKL invalidated mice, the dental eruption (Figure 34A-C) and the root elongation (Figure 34B and C) were severely affected. Concerning the root elongation, the presence of HERS cells was observed in the two types of invalidated mice (Figure 34C), more specifically in rests of Malassez (arrows in Figure 34C) and the most apical region of the sheath (arrow-heads in Figure 34C and Figure 34D) structures, suggesting an unaccomplished root elongation further supported by the absence of cellular cementum formation (Figure 34B). The number of HERS cells was more important in the transiently invalidated mice than in the permanently invalidated mice (Figure 34C) with an evident relationship to the length of the root that appeared more important in the transiently deficient mouse (Figure 34B and C). Interestingly other differences were noticed between mice with global and transient RANKL invalidations. Indeed, an ankylosis was only observed in the globally RANKL invalidated mice as a narrowed eruption pathway (Figure 34B). Altogether these results evidenced that RANKL transitory invalidation during the first post-natal week was sufficient on the one hand to block the first molar eruption despite a large eruption pathway, and on the other hand to freeze the root elongation in the absence of either ankylosis or compression inside a hypertrophic osteopetrotic alveolar bone.

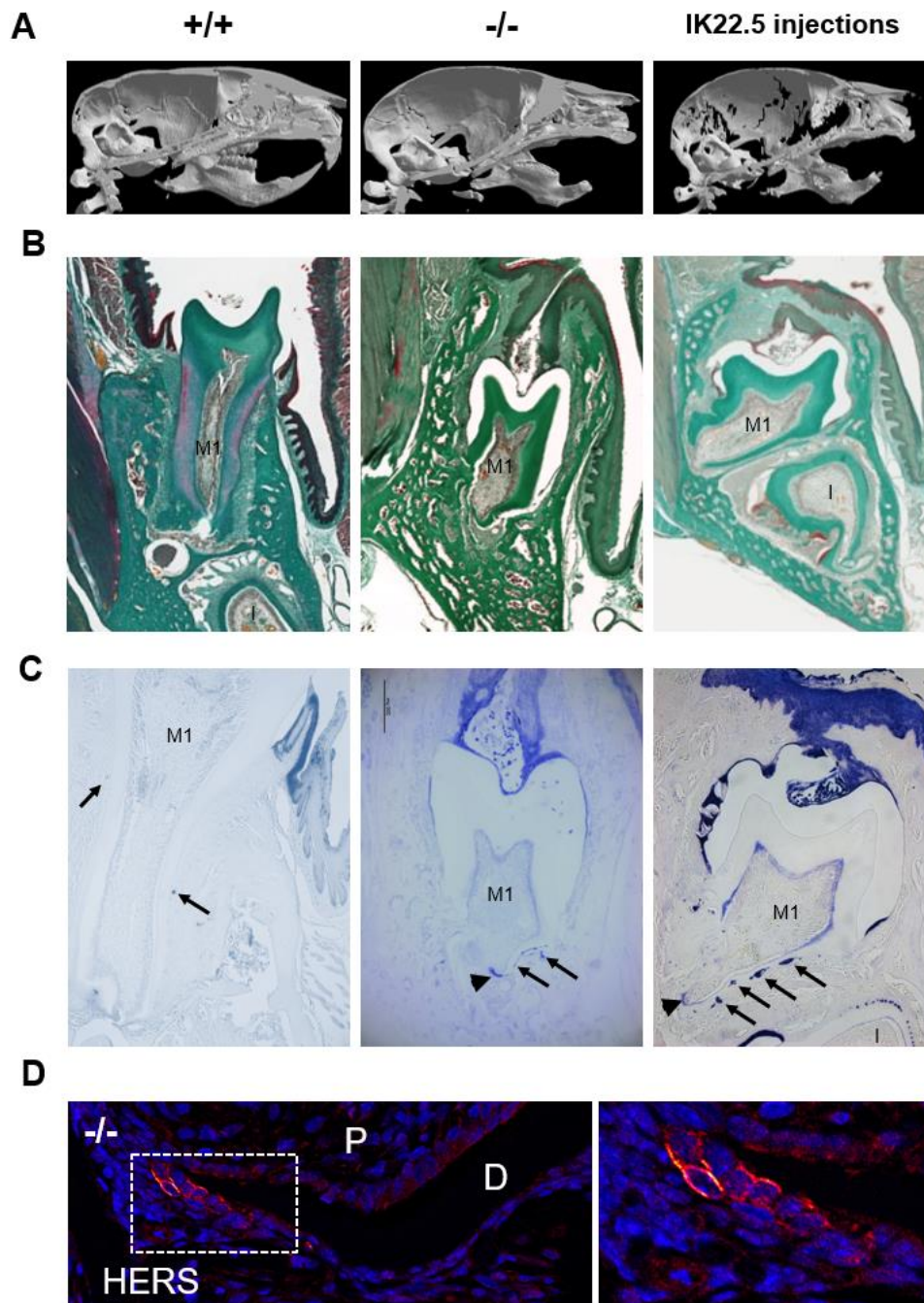


Figure 34. Comparative analyses in 35 days-old mice of the consequences on dental phenotype of the global ($Rankl^{-/-}$) versus the transient (4 injections of IK22.5 neutralizing antibody from postnatal day 1 to 7) invalidations of RANKL. (A) Micro-tomography 3-D reconstructions of the heads of $Rankl^{+/+}$, $Rankl^{-/-}$ and RANKL transiently invalidated mice enabled to observe close phenotypes between the RANKL invalidated mice comparatively to control ($Rankl^{+/+}$) with presence of a more curve skull associated to dental eruption defects. (B) Masson's trichrome staining realized on frontal sections in the plan of the first molar (M1) of $Rankl^{+/+}$, $Rankl^{-/-}$ and RANKL transiently invalidated mouse heads confirmed the defective eruption and evidenced similar dysmorphic lower molar for the RANKL invalidated mice in comparison to the control. However, a more pronounced phenotype was visible for the global invalidation with the presence of an ankylosis in the buccal region. Interestingly, the incisor (I) was absent in this section's plan only for the mouse globally invalidated for RANKL. Scale: 20X/100 μ m. (C) The keratin-14 immuno-labeling evidenced the presence of HERS cells and hypertrophic epithelial rests of Malassez cell (arrows) despite the dysmorphic root formation and elongation in both RANKL invalidated mice. Scale: 20X/100 μ m. (D) The keratin-14 immunofluorescence confirmed the presence of HERS cells in the most apical region of the root (apex) in the $Rankl^{-/-}$ mouse at 35 days. D: dentin; P: pulp. The square corresponds to the region enlarged. Scale 20X/100 μ m. M1: first molar; I: incisor.

6.4. Molar primary retention as part of craniofacial development alteration associated to transitory inhibition of the RANKL signaling

Molar primary retention observed in clinic corresponds to a still non-explained absence of molar eruption despite a large eruption pathway with no existing physical obstacle. Interestingly, this resembles to the situation associated to transient inhibition of RANKL described above (Figure 34) raising the question of RANKL implication signaling in the occurrence of molar primary retention. In order to demonstrate such involvement, the experimental strategy used was first to assess in mouse the impact of different transient inhibitions of RANKL, through injections of IK22.5 antibody during different post-natal periods, onto the eruption and the root elongation processes of molars and secondly to compare the obtained craniofacial phenotypes with those of human patients.

Concerning the mice experiments, two periods of RANKL inhibitions were chosen, from postnatal days 1 to 9 (PND1 group) and 7 to 15 (PND7 group) in order to respectively target the first and the second molars. The wild type and the *Rankl* KO mice were used as negative and positive controls.

Micro-CT analysis of the consequences of RANKL post-natal transient inhibitions onto mouse molars eruption.

The eruption profiles of the different groups obtained by micro-CT are presented in (Figure 35). Interestingly, while mice of the PND1 group had an homogenous phenotype, mice from the PND 7 group presented a variable pattern of eruption with several levels of defects concerning the first and second molars that were classified as light (Figure 35d), moderate (Figure 35e) and severe (Figure 35f).

In mice of PND1 group, it was possible to observe the presence of severe primary retentions of all the M1 and M2 that were in an intraosseous position. M1 appeared more severely affected than M2. Despite the severity of the M1 and M2 phenotypes, the M3 was clearly unaffected (Figure 35f). Interestingly, in all mice of the PND7 group, the M3 were also not affected, what validate the fact that the two chosen periods target only M1 and M2.

In the PND7 mice with a light retention pattern, the first (M1) and second (M2) upper molars were retained while the lower molars did not appear to be affected (Figure 35d). In the PND7 moderate group, all the M1 and M2 showed eruption alteration but with different levels of severity. Indeed, the lower molars showed a delay of eruption or a secondary retention with an infraocclusion as molars were visible in the oral cavity. On the other hand, the upper molars had primary retentions and remained intraosseous. Upper second molars were the most severely affected (Figure 35e).

In the PND7 severe group, all M1 and M2 were retained, almost all intraosseous except for the cuspid points of the lower molars. Also, upper molars were more severely affected than lower molars.

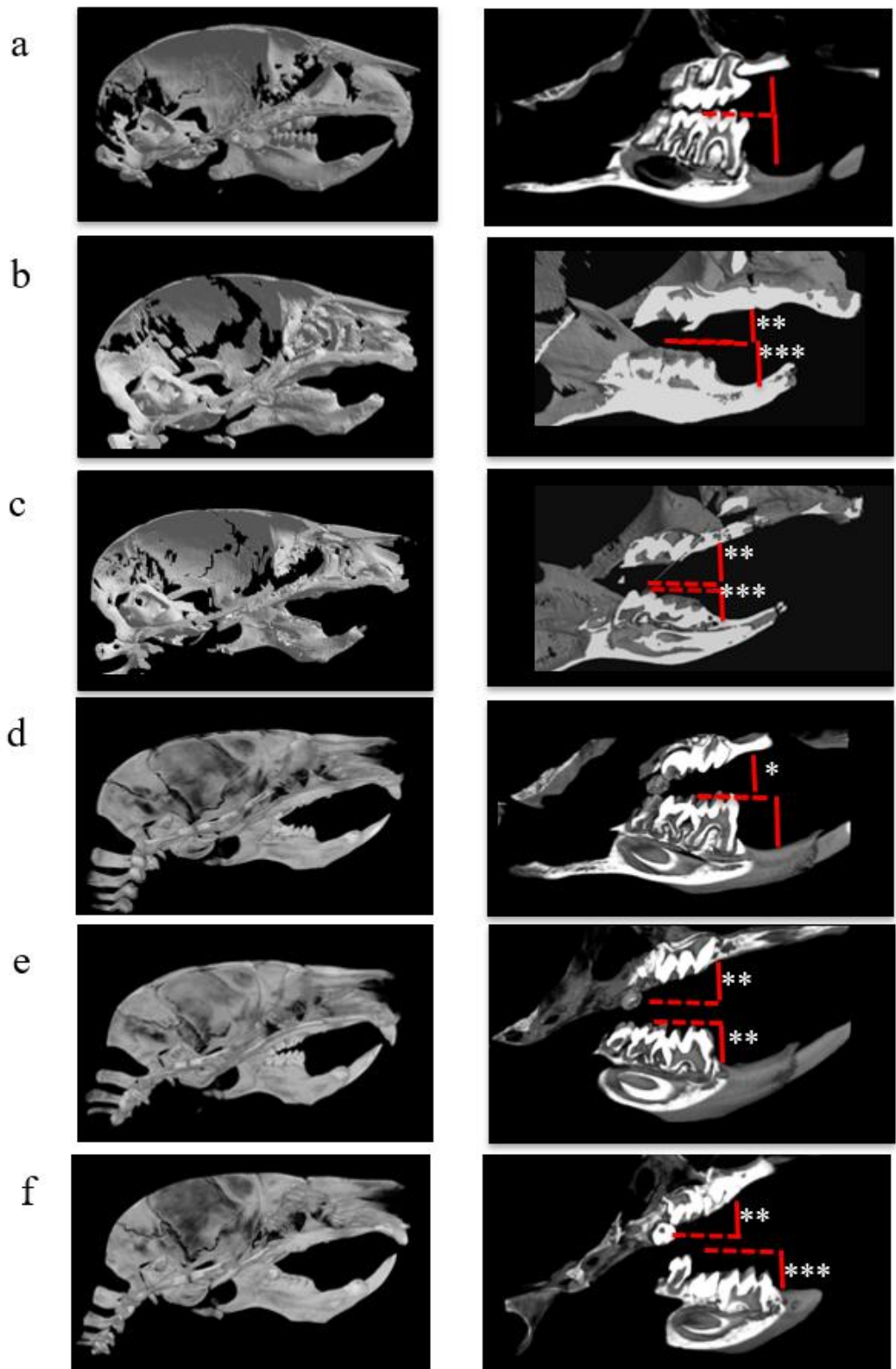


Figure 35. Sagittal micro-CT sections comparative analysis of molar eruption in mice: a. Wild type. b. Rankl^{-/-}. c. D1: PND1 group, d. PND7 group light retention, e. PND7 group moderate retention, f. PND7 group severe retention. Red dotted line: Occlusal plane level. White stars: highlight the heterogenous eruption defects in PND7 group (d-f).

Histological analysis of the consequences of RANKL post-natal transient inhibitions onto mouse mandible molars eruption.

A histological analysis was performed to study the effects of the transient inhibitions of RANKL on the mandible alveolar bone remodeling necessary to molar eruption and on the mandible molars organogenesis. The Masson's trichrome staining (Figure 36) evidenced that comparatively to mice from the wild type group, mice from the PND1 group have the most severe phenotype with the first and the second molars in retention with severe tissue disturbances (Figure 36, D-F). As evidenced by micro-CT, the third molars appeared histologically unaffected whatever the protocol considered. Mice from the PND7 group evidenced variable and heterogeneous phenotypes with mild/light forms (G-I) and severe forms (J-L). In the severe forms, the first molars were mainly retained but severe tissues disturbances were observed for both first and second molars. In the mild/light forms limited tissues disturbances are visible in the molar root area (Figure 36).

The TRAP histoenzymology staining (Figure 37) remarkably evidenced that the number of TRAP positive cells were more important in the alveolar bone than in the severe molar phenotype. Indeed, the higher TRAP staining was visible around the first and second molars of mice from the PND1 group (Figure D-F) then around those of mice from the PND7 group (J-L) with severe phenotype. The TRAP histoenzymology also enabled to observe, in the coronary region, the formation of an eruption pathway in mice of the PND1 group despite the molar intra-osseous retention (Figure 38).

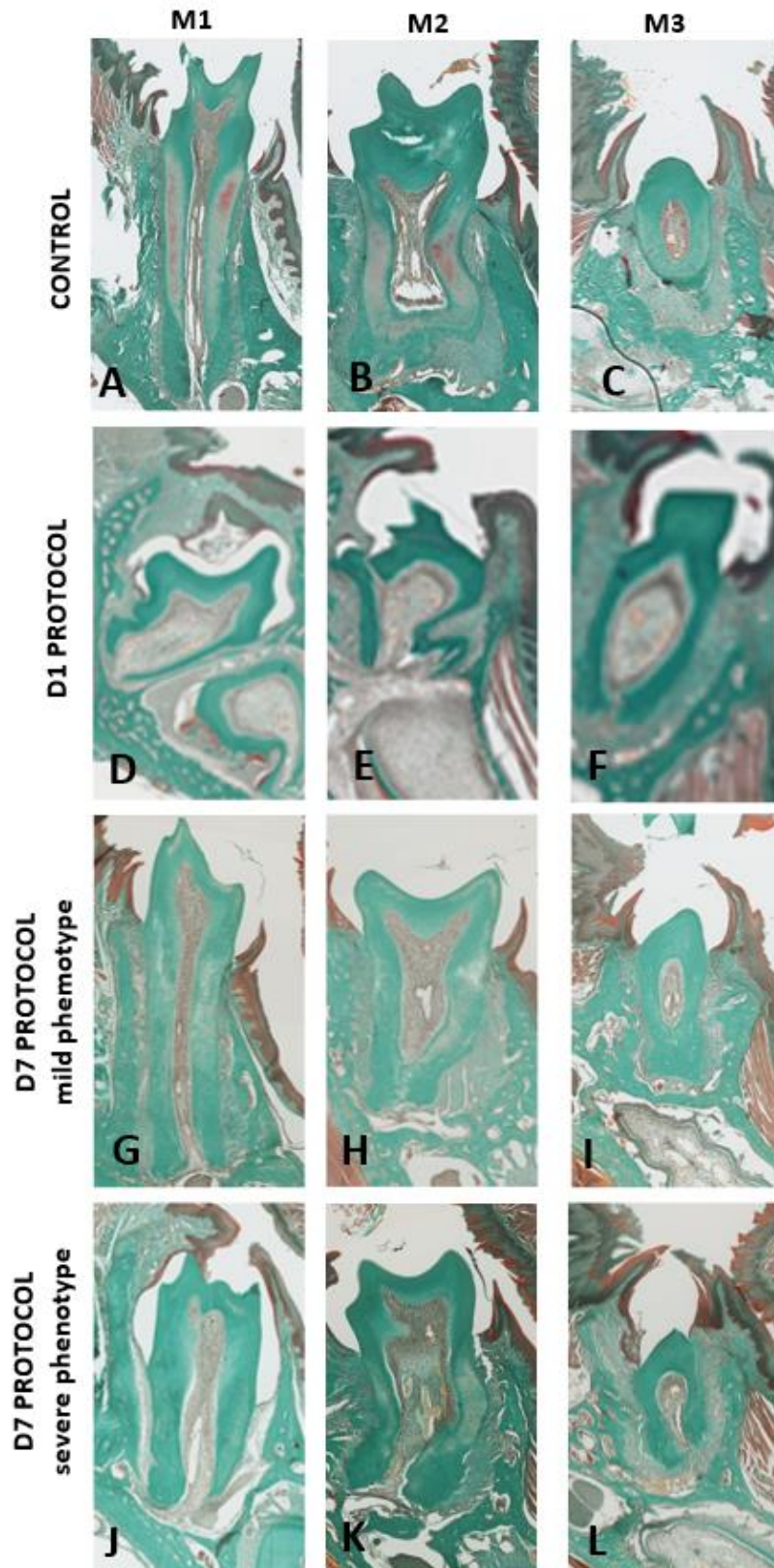


Figure 36. Masson's trichrome staining histological analysis of the first, second and third lower molars phenotypes. (A-C) Untreated mice group (Control); (D-F) Mice of the PND1 group (D1 protocol); (G-L) Mice of the PND7 group (D7 protocol) with mid/light phenotype (G-I) and severe phenotype (J-L). M1: first lower molar; M2: second lower molar; M3: third lower molar. Scale: 200 μ m

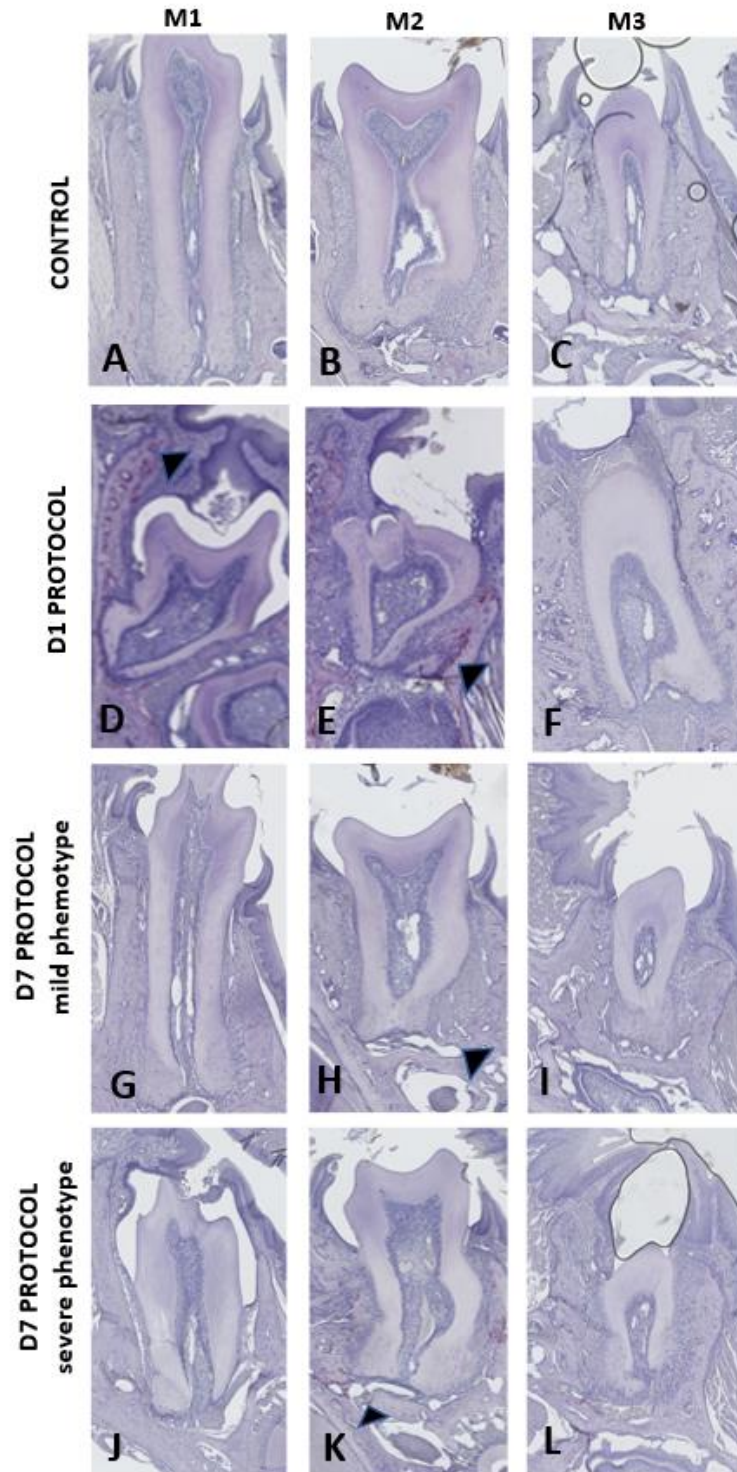


Figure 37. TRAP histoenzymology evidencing one month after the end of treatment an important TRAP positive cells concentration in the alveolar bone around the first and second molars of mice from the PND1 group that present the most severe phenotype. To a lower instance, TRAP positive cells were also observed in the alveolar bone around the first and second molars of mice from the PND7 group with severe phenotype. (A-C) Untreated mice group (Control); (D-F) Mice of the PND1 group (D1 protocol); (G-L) Mice of the PND7 group (D7 protocol) with mid/light phenotype (G-I) and severe phenotype (J-L). M1: first lower molar; M2: second lower molar; M3: third lower molar. Black arrows: evidence the TRAP positive cells. Scale : 200µm.

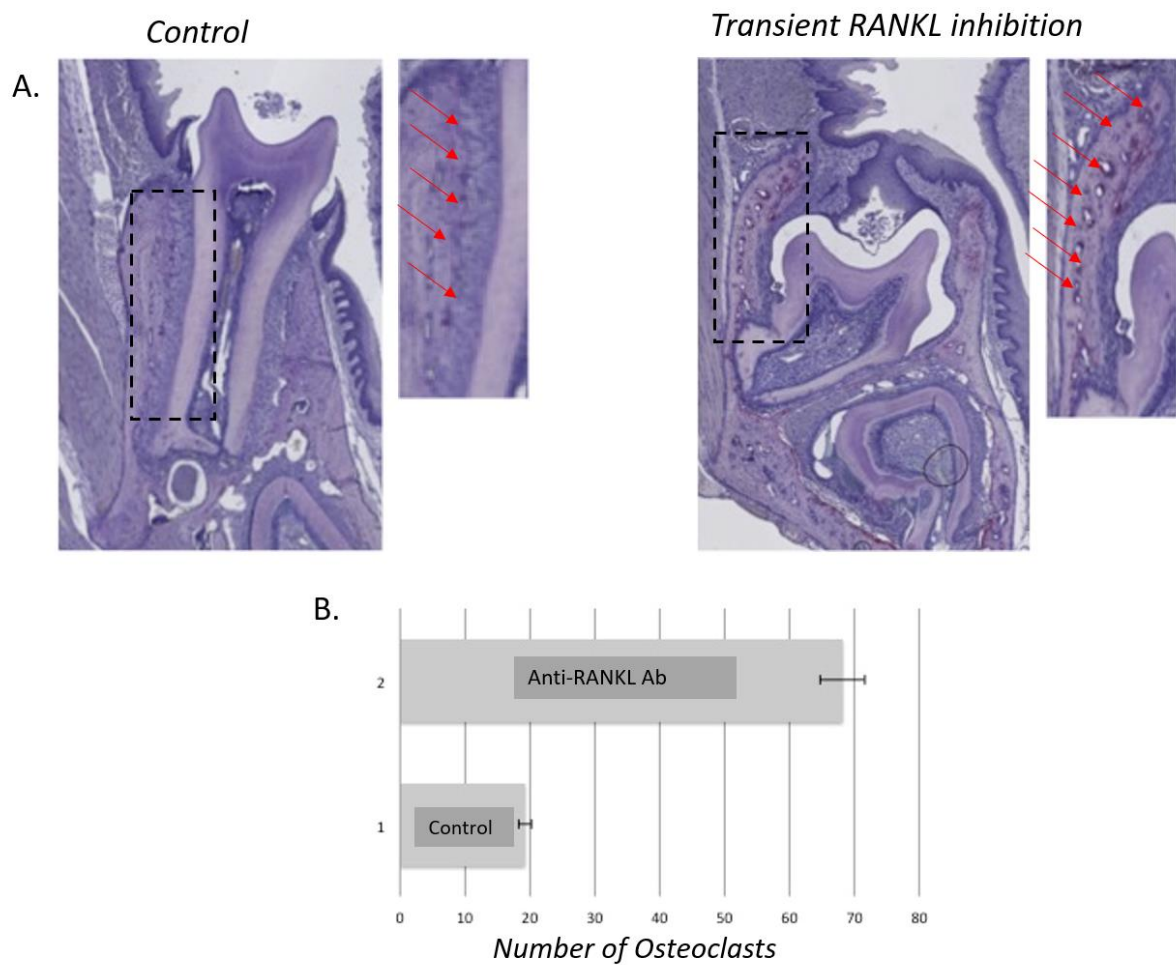


Figure 38. TRAP histoenzymology of first lower molar frontal sections of wild type control group mice and PND1 group mice. **A.** 10X image and 20X magnification. The arrows show the TRAP positive cells present in alveolar bone adjacent to the periodontal ligament. **B.** Graph of the quantification of the number of TRAP positive cells present in the alveolar bone adjacent to the periodontal ligament. The bar represents the average with the standard deviation corresponding to each group of mice (Published papers section – paper 2).

Analyses of the craniofacial morphometric consequences of RANKL post-natal transient inhibitions onto mouse molars eruption

In order to assess the effects of the transient RANKL invalidations on the craniofacial development, the skull and the upper and lower jaws morphologies were characterized by the measurements of some horizontal, vertical and sagittal morphometric parameters based on micro-CT scans following Vora et al., 2016 and Xiaoxi et al., 2017 analysis [178,179]. Similar measurements were performed for wild type and *Rankl*^{-/-} mice to serve respectively as the negative and the positive controls concerning the RANKL invalidation.

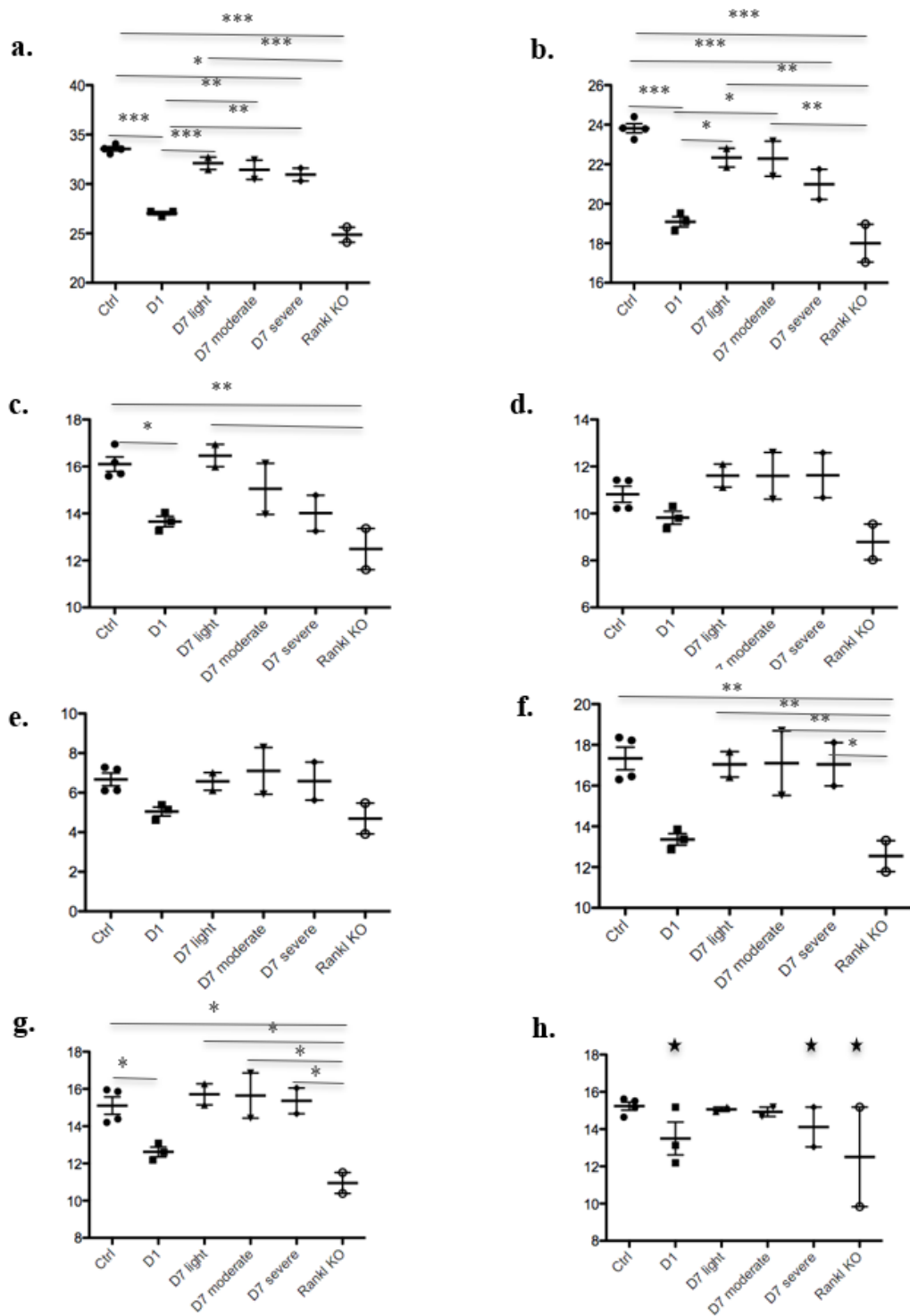


Figure 39. Comparative analysis of craniofacial morphometric parameters between mice transiently invalidated for RANKL from group PND1 (D1) and group PND7 (D7) with references wild type mice and Rankl KO mice. **a:** Total skull length; **b:** Cranial vault length; **c:** Facial length; **d:** Middle cranial length; **e:** Facial height; **f:** Inter-zygomatic arch wide; **g:** Upper mandible length; **h:** Lower mandible length.

When compared to wild type group, most of the measurements evidenced a statistically significant difference in the *Rankl*^{-/-} group (Figure 39). Indeed, the total skull length (a), the cranial vault length (b), the facial length (c), the inter-zygomatic arch wide (f) and the upper mandible length (g) measurements were significantly reduced ($p \leq 0.05$). Concerning the other measurements, namely the middle cranial length (d), the facial height (e) and the lower mandible length (h), despite the absence of significance, a decrease tendency was observed in the the *Rankl*^{-/-} groups (Figure 39).

Concerning the PND1 group, all mice evidenced a reduction of the craniofacial measurements compared to control mice and very close to the reduction observed in the *Rankl*^{-/-} group (Figure 39). Indeed, a significative decrease was reported for the same measurements than for *Rankl*^{-/-} group (Figure 39). Interestingly, whatever the parameters considered no significant difference has been observed between these two groups.

Regarding the PND7 group, measurements were performed taking into consideration the different phenotypes in term of severity. Interestingly, the parameters did not significantly change in the the *Rankl*^{-/-} group and the PND1 group were also unaffected in all mice of PND7 group (Figure 39). In addition, the facial length (c), the inter-zygomatic arch wide (f) and the upper mandible length (g) parameters were unaffected in all mice of the PND7 group comparatively to mice of the wild type group (Figure 39). Finally, only the total skull length (a) and the cranial vault length (b) measurements evidenced differences comparatively to the wild type group. The differences were significant only for mice of the most severe phenotype group (Figure 39).

Consequently, it seems that parameters in the most phenotypically affected mice by transient RANKL inhibitions tend toward the values observed for the *Rankl*^{-/-} group whereas the parameters remained close from the wild type group values in less affected mice.

6.5. Craniofacial morphology features of patients with Molar primary retention.

In order to analyze the relationship between Molar Primary Retention (MPR) and craniofacial growth, and to establish a relationship with the mice craniofacial morphology analysis, the craniofacial phenotypes of patients of the Orthopedics-Dentofacial Department of *La Pitié-Salpêtrière* hospital presenting MPR with patients with impactions or mechanical retentions were compared.

A first evaluation of orthodontic records allowed us to make the following classification:

	Control Group	MPR Group	p (Fisher test)
Sex			0,756
	F	9	10
	M	9	14
Ethnic group			0,063
	Caucasian	7	5
	African	6	15
	North-African	2	4
	Asian	3	0
Family background			0,014*
	Presence	0	7
	Absence	18	17
Uni/bilateral			0,532
	Unilateral	9	9
	Bilateral	9	15
Dental arch			0,033*
	One dental arch	13	9
	Two dental arch	5	15
Teeth involved			0,0008***
	First (M1)	0	2
	Second (M2)	18	13
	M1 and M2	0	9
Supra/ infra- osseous			1
	Supra.	9	11
	Juxta.	2	4
	Infra.	7	9
Eruption pathway (X rays)	(N= 7 infra-crestal)	(N= 9 infra-crestal)	0,0087**
	Visible	1	8
	not visible	6	1

Associated anomalies		4	8	0.506
	Impacted canines	4	4	
	Inclusions	0	1	
	Tooth agenesis	0	2	
	Ankylosis	0	1	
	No anomalies	14	16	
Angle's Malocclusion classification	Class II/2 overbite	5	18	0,0043**
	Other	13	6	

Table 1. Evaluated patients of the Orthopedics-Dentofacial Orthopedics Department of the La Pitié-Salpêtrière Hospital (in accordance with the "Commission National de l'Informatique et des Libertés").

A telerradiographic retrospective study of these patients was conducted using Tweed and Delaire's cephalometric analysis.

The Tweed's analysis showed a statistically significant difference between them concerning the SNB angle ($p = 0.0060$) with an average of 76.6° for the MPR group versus 80.2° for the C group (norm = 80°); ANB angle ($p = 0.0112$) with an average of 5.6° for the primary retentions group against 3.5° for the control group (norm between 0 and 4°); the I / FR angle ($p = 0.0001$) with an average of 104.7° for the MPR group versus 116° for the C group (norm = 107°). No statistically significant difference was found between the two groups for all other measures (Figure 40).

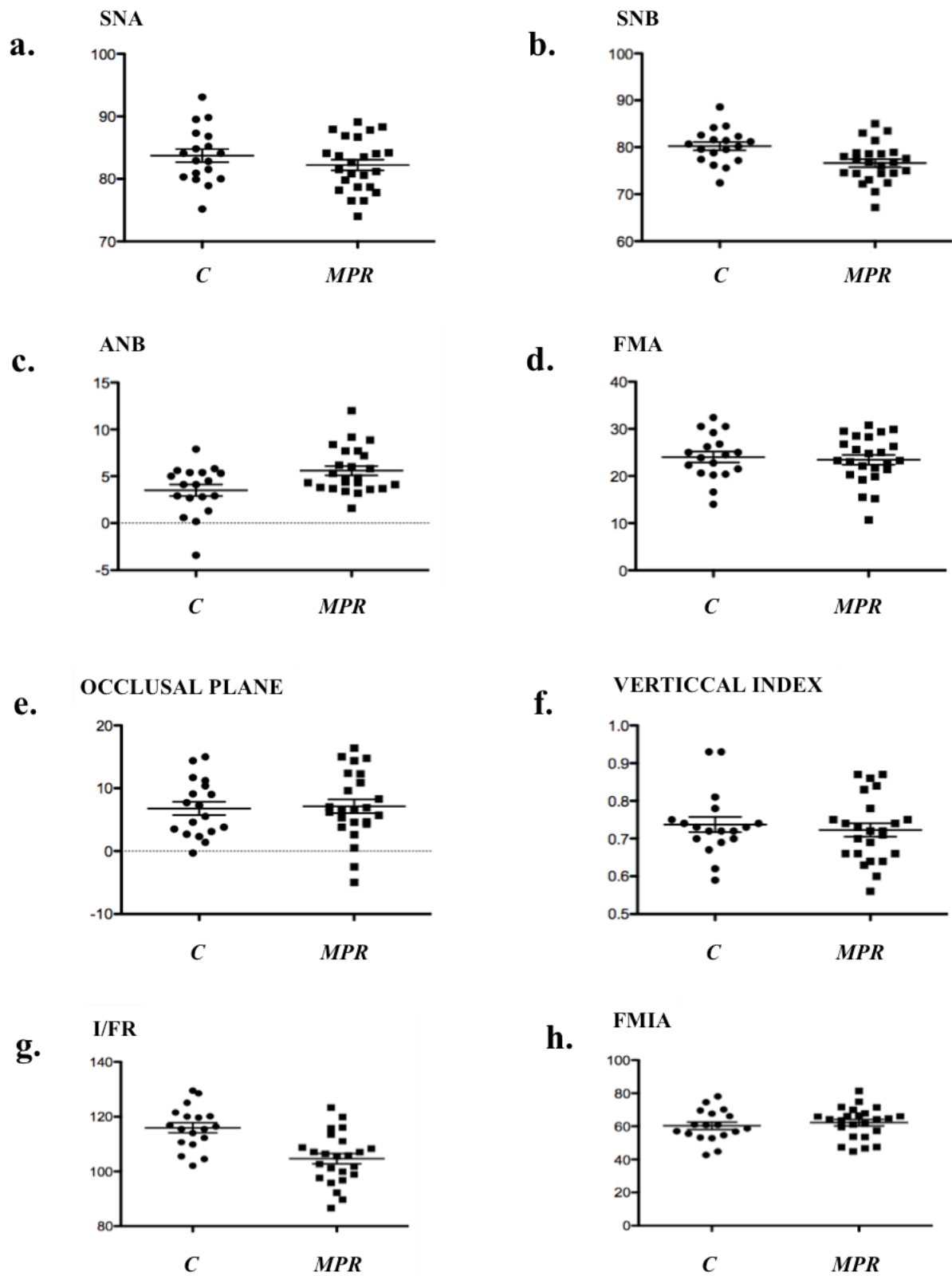


Figure40. Comparative analysis of Tweed's quantitative craniofacial measurements between control patients (C) and Molar Primary Retention (MPR) Relative position maxillary-mandible : a. SNA ; b. SNB ; c. ANB. Vertical analysis : d. FMA ; e. occlusal plane ; f. vertical index Dental analysis : I/FR (upper incisor) ; FMIA (lower incisor)

Delaire's analysis provided the general craniofacial and dental features of the population studied (Figure 41):

			Group C	Group MPR	P (Fisher test)	
Sagittal	Skeletal class	Class I Class II Class III	4 14 2	0 23 1	0,0378*	
	Mandibular position	M. retrusion M. protrusion	7 11	18 6	0,0274*	
Mandibular morphology	ramus	Dolicho-ramus Brachy-ramus normal	7 7 4	7 17 0	0,0266*	
		Corpus (mandibular body)	Dolico-corpus Brachy-corpus normal	12 6 0	11 11 2	0,390
			Gonial angle	Opening Closing normal	13 4 1	19 5 0
	Mandibular length	Dolico-mandible Brachy-mandible		9 9	4 20	0,041*
vertical	Lower height	Increase Decrease normal	8 5 5	14 6 4	0,603	
incisors	Upper incisor	Palatoversion vestibuloversion	8 10	20 4	0,018*	
	Lower incisor	Linguoversion vestibuloversion	7 11	11 13	0,757	

Figure 41. Delaire's cephalometric analysis. Comparison between patients of Control group C and Molar Primary Retention group MPR.

Concerning the skeletal class, in the "Molar primary retention" group, the majority of patients presented a class II (96%), 4% a class III and none found in class I. In the "control" group, 67% of patients are in class II, 22% in class I and 11% in class III. The distribution of skeletal classes between the two groups is statistically significant ($p = 0.0378$).

In regard to mandibular position, in the "control" group, 39% of patients presented retrognathism compared to 75% for patients with primary retentions ($p = 0.0274$). Interestingly, among the skeletal class II control patients, only 36% present retrognathism whereas in the "primary retention" group, 78% of patients in skeletal class II have associated retrognathism (Figure 41).

Regarding mandibular morphology, in the "control" group, the gonial angle is closed at 22% versus 17% for the "primary retentions" group ($p = 0.697$). In the "primary retention" group, the mandibular dimensions were smaller than for the "control" group, and statistically significant for ramus ($p = 0.0266$) and mandibular length ($p = 0.041$). In fact, 67% of short

ascending ramus, 39% of short mandible body 79% of brachygnathism are found in patients with primary retention of molars against 39% short ascending ramus, 33% of short mandible body and 50% brachygnathism in control subjects (Figure 41).

In respect to lower height, no statistically significant difference was found between the two groups ($p = 0.603$). Nevertheless, subjects with primary retentions of the molars still show a slightly increased height of the lower stage in 58% of the cases compared to 44% for the control subjects.

Concerning the dental measurements, 83% of patients with primary retentions had palatoversion upper incisors versus 44% for control patients ($p = 0.018$). For the lower incisors no significant difference was found between the two groups.

7. DISCUSSION

The research developed in my PhD followed two axes : a systematic review compiling the oro-dental features in patients with osteopetrosis and its frequency in affected individuals, an experimental study which was focused on the RANKL/RANK/OPG/LGR4 signaling implication in orofacial physiopathology based on the use of RANKL genetically (loss of function) or transiently (anti-RANKL blocking antibody) invalidated mice and finally a clinical study focused on mechanical and primary failure of eruption relating osteopetrotic phenotypes with RANKL loss of function and eruption issues.

The systematic review investigated the available literature on oro-dental features in patients with osteopetrosis. Although there are studies describing the oro-dental features associated with this condition, no SR has been performed before this thesis emphasizing the oral manifestations and their frequency in affected individuals.

Osteopetrosis, a genetic osteosclerotic disorder, affects osteoclastic differentiation or its function. It is expressed by a generalized reduced bone resorption and consequently an increased bone density [123–125,134,136,193] and the clinical spectrum ranges from very mild to severe disease phenotypes. The genetic heterogeneity contributes to the wide phenotypic spectrum that can be seen even within kinships, limiting the ability to correlate the genotype and clinical phenotype [126]. Here we reviewed only the ones in which osteoclasts were impaired, known as the autosomal recessive and dominant osteopetrosis forms, according to the Osteopetrosis Consensus Guidelines for diagnosis, therapy and follow-up [194]. All the gathered studies in the SR were case series with more than 3 cases. Despite the weak inferences and the high likelihood of bias to which these studies are subject, they have been deeply impacting the rare diseases medical literature and they continue to advance our knowledge [195]. In 2009, Chambers et al. [196] emphasized the useful contribution of this kind of study design when it comes to emerging technology and to informing decision-making when no other

higher level of evidence is available. There are increasing efforts of the scientific community to develop frameworks for approaching, appraising, synthesizing and applying evidence derived from case reports/series. For this purpose, the Case Report (CARE) guidelines were developed following a three-phase consensus process and provide a 13-item checklist that could assist researchers in publishing complete and meaningful exposition of medical information [174]. As this SR compiled studies from 1968 up to 2016, there was great heterogeneity regarding the quality of the diagnostic tools and the way of reporting the findings. Only two studies in our series mentioned the molecular diagnosis [182,191].

Of the 12 included case series, 4 studies had the best quality assessment when selection, ascertainment, causality and reporting parameters were considered [182–184,190]. They were followed by one study [181] that did not explore the eruption defects and the dental anomalies adequately. In addition, there were missing data related to the general intraoral examination. The poorest quality assessment was attributed to Trapnell et al. [192] mainly because of the non-detailed oro-dental features description based on lateral oblique radiographs, a technique that does not allow an appropriate evaluation. In a recent review, Van der Stelt [197] pointed out that panoramic radiograph is the appropriate technique suggested for the assessment of abnormalities that affect large areas in the maxillo-mandibular complex such as tumors or development disorders in jaws. In eight studies [182,184–188,190,192], the radiographic examination results were the inclusion criteria. In five studies the patients had not undergone a systemized examination and, most importantly, with regards to the findings of the oral screening, panoramic X rays were neither mentioned nor shown [185,188,189,191,192].

Ninety five patients were reviewed in the 12 revised studies and were distributed in the three types of autosomal dominant and recessive forms of osteopetrosis: ADO, ARO and ARO associated with renal tubular acidosis. In these patients, the most frequent oral manifestations described were osteomyelitis of both jaws (maxilla and mandible) in 75% of the studies in

patients with autosomal and recessive forms of osteopetrosis, eruption defects in 75% of the studies and dental anomalies in 66% of the studies. All patients with dental anomalies and eruption defects had autosomal recessive osteopetrosis. This was an expected result considering that ARO has an early onset during infancy, and is consistent with the fact that experimentally altered osteoclast activity during tooth formation induces substantial dental malformations [12,24].

Osteosclerosis results in decreased vascularity which predisposes the involved bones to infections such as osteomyelitis [198]. Osteomyelitis of the maxillo-mandibular complex is a very well documented and common infection complication of osteopetrosis described in the literature. It occurs mainly in the mandible due to its thick cortical bone and poor collateral blood supply. Teeth extractions and pulp necrosis are critical contributor factors to the development of osteomyelitis and the subsequent increased risk of pathological mandible fracture [199–204]. The predisposition to osteomyelitis is thought to be caused by a combination of the abnormal bony structure and the insufficiency of white blood cells [205]. The cause of osteomyelitis of the jaws is usually odontogenic and mostly related to high caries activity [193,206,207]. Patients affected with osteolytic and osteoporotic acquired conditions and in continuous use of drugs modulating bone resorption by targeting the osteoclasts such as the bisphosphonates, the monoclonal anti-RANKL antibody and antiangiogenic agents may present the same bone phenotype. This medication-induced bone phenotype is also triggered by teeth removal, pulp necrosis and periodontal infection [208]. In the present study, several reports showed also ARO children and adolescents with osteomyelitis [182,184,185,189–191]. This is an unusual finding in pediatric patients, therefore a special surveillance must be given to ARO patients.

The tooth eruption defects were mainly associated to recessive forms of osteopetrosis which present the most severe bone phenotypes. However, the reports did not describe

systematically the affected teeth. Tooth eruption depends directly of the bone remodeling surrounding the tooth. The tissue interactions involve the dental epithelium cells, the dental follicle and the apical papilla. The osteoclasts are the most important actors along with osteoblasts and by means of them, the eruption pathway is created through alveolar bone and overlying soft tissues. Experimentally, mouse models of altered osteoclast function and number provide a tooth phenotype involving tooth eruption failure in several levels, dental anomalies of number, size, shape and structure and root anomalies [7,8,12,24,87]. These findings emphasize the importance of the interface bone-teeth for all the development and growing of the maxillofacial site.

Concerning the other dental anomalies reported, tooth agenesis was reported in 9 patients [183–185,187,189,190]. Tooth agenesis is a common dental anomaly with prevalence between 1.6-9,6 % depending on the demographic origin [209,210]. At present, the molecular basis is partly elucidated and 10 genes have been identified in isolated and syndromic forms of dental agenesis [211]. The molecular analysis of patients with osteopetrosis and dental agenesis is essential in order to determine if this dental anomaly is part of the phenotypic spectrum or is another monogenic condition.

Enamel hypoplasia was also reported in 7 patients with ARO and ARO and renal tubular acidosis [183,187–189]. The causative gene of ARO and renal tubular acidosis is *CAII* [135] and experimental studies have shown the role of this protein in enamel formation [212,213]. Further studies are necessary in order to better understand the enamel defects observed in osteopetrotic patients with renal disorders. Although the molecular diagnosis for osteopetrosis is available at present, only 2 studies reporting oro-dental features had molecular analysis. Correlation of dental anomalies phenotype and the molecular basis of osteopetrotic patients may provide critical information on prognosis and clinical associations that will certainly have meaningful effects on management decisions.

In the future, well-designed studies with systematic phenotyping are necessary to classify the oro-dental findings in order to better determine the frequency of each described feature individually and in the different types of osteopetrosis. This knowledge will guide good clinical practices regarding the prevention of all the undesired outcomes in patients affected with osteopetrosis.

RANKL signaling implications in the physiopathology of orofacial skeleton.

Analysis in mouse of the consequences of RANKL invalidations.

RANKL was discovered as a cytoplasmic membrane-bound cytokine, but a soluble form was also evidenced [214]. Given the fact that RANKL is expressed in many tissues during embryonic development, and taking into account that soluble RANKL of maternal origin may cross the placenta, the question of the presence of an attenuated phenotype in young osteoclast-poor osteopetrotic patients, as well as in *Rankl* null mutants from heterozygous mothers, was raised.

In order to evaluate the maternal RANKL in young mice during embryonic development, the skeletal phenotype of *Rankl* null mutant mice was compared at one day post-natal between mouse pups obtained from heterozygous *versus* homozygous parents. Injections of a RANKL-blocking antibody were also performed on heterozygous mothers during the second half of gestation to enhance the demonstration. These experiments demonstrated that in craniofacial skeleton RANKL signaling is most solely implicated in the dysfunction/function of the osteoclast, and also in cell to cell communications during tooth development.

Interestingly, RANKL expression has been reported in several tissues, which also suggested implications in the cell-to-cell communications necessary for the morphogenesis of the corresponding organs, such as teeth, bones, thymus, thyroid glands, and lymphnodes [177]. So, RANKL signaling appears to have two main functions during the development: control of

osteoclast differentiation and the regulation of communication between the cells which has consequences on morphogenesis and histogenesis of different organs. Concerning the first function, in long bones such as the tibia, the total absence of osteoclasts was responsible for both a significant delay in development, and an absence of bone marrow space formation [177]. Regarding the craniofacial skeleton, the absence of osteoclasts made resorption of the Meckel cartilage impossible, which is an important step in mandible growth [215]. The significant delay in tooth morphogenesis, observed in the second-generation null mutants, validated the considerable involvement of RANKL signaling in the communication between mineral tissues forming cells, which is the second function of RANKL signalization during skeletal development. The existence of this function in teeth was initially suggested by the expression patterns of elements of RANKL signaling during the morphogenesis [9]. The absence of mandible curvature observed in the second-generation null mutants was also a consequence of the loss of the cell-to-cell communication function of RANKL signaling. Interestingly, similar flat mandibles were reported in mice invalidated for transcription factors known to have morphogenetic functions, such as MSX1[216,217] and PAX9 [218]. Crosstalk between RANKL signaling and these transcription factors may exist, as previously reported for other transcription factors, namely MSX2, EN1, and DLXs [8,219–221]. Further studies will be needed to demonstrate the veracity of such crosstalk and its implications in the morphogenesis of the whole skeleton.

In order to go further in the involvement of the RANKL signaling in the skeleton development, and following our experimental strategy regarding RANKL/RANK/OPG/LGR4 axis, the early stages of the first molars roots development (first post-natal week) were compared among *Rankl* null mutant mice, wild type controls and heterozygous mice, in order to establish that the observed radicular phenotype is not only consequence of defective osteoclasts but also of some cell-to-cell communication loss involving the RANKL signaling.

Expression patterns of the different receptors of RANKL have been characterized at post-natal day 5 revealing three distinct situations. Firstly, concerning the epithelial compartment more precisely the HERS cells, the RANKL response is driven by the receptor RANK, the most expressed. Secondly, concerning the mesenchymal compartment, dental pulp cells appeared to be responsive to RANKL through RANK receptor whereas dental follicle cells through LGR4 receptor [108]. Thirdly, in the bone compartment, osteoclasts and osteoblasts seem to respond by different receptors to RANKL at this age, more precisely, the osteoclasts through RANK and the osteoblasts through LGR4 activation was shown to promote bone mass by stimulating bone mesenchymal stem cells differentiation to osteoblast in response to R-spondin2, a competitor of RANKL for binding to LGR4.

The observed alveolar bone phenotype in the absence of RANKL was consistent with these two receptors expression patterns in bone cells. Indeed, the defective stimulation of RANK induced absence of osteoclast as widely described and the lack of RANKL might favor the binding of R-spondin 2 to LGR4 at the osteoblast surface and consequently enhancing bone formation.

Regarding the mesenchymal compartment, the complementary expression patterns of RANK and LGR4 respectively in the dental pulp and the dental follicle observed at day 5 in the first molars suggest the existence of a differential impact of RANKL onto mesenchymal cells of these two sites with a probable histogenesis function. Interestingly, the expression pattern of LGR4, in the complex formed by the tooth, the periodontium and the alveolar bone, appeared to be changing sequentially from the initial morphogenesis stage to the dental eruption stage suggesting a dynamic/evolutive function of this receptor to RANKL and R-spondin 2 during the whole dental development whose modalities remain to be elucidated in future studies.

Concerning the epithelial compartment, RANK is the main receptor expressed in HERS cells at day 5. In *Rankl*^{-/-} mouse comparatively to controls a decrease of the expression of the

proliferation marker PCNA in the HERS cells was associated with an increase of the expression of cell-cycle progression inhibitor P21, explaining the important reduction of the HERS cells proliferation observed. Interestingly, the RANKL/RANK signaling has already been implicated in the control of epithelial cells proliferation in various organs as the mammary, the thymus and the skin suggesting that the RANKL/RANK signaling may be cardinal for the epithelial cell proliferation control.

The dental root developmental alterations associated with functional RANKL/RANK signaling defect had so several origins that could be classified as intrinsic to dental tissues or extrinsic corresponding to bone remodeling perturbations. Regarding the extrinsic origins, regardless the way the bone remodeling was affected, deficiency in the case of RANKL/RANK loss of function inducing osteopetrosis or overactivation in the case of gain of function inducing osteolytic diseases, root formation was affected. The most representative feature of root developmental defects from extrinsic origin is the ankylosis observed in osteopetrosis.

Regarding the intrinsic origins, which correspond to perturbations of the dental cells proliferation/differentiation regulation by the RANKL/RANK/OPG/LGR4 system, the most representative feature of root developmental defect is the slowdown of the HERS elongation and finally its disruption, with late maintain of epithelial cells and defective cellular cementum formation. Interestingly, such a relationship between HERS cell permanence and absence of cellular cementum was observed in the continuously growing incisor, raising the question of the potential implication of RANKL/RANK/OPG/LGR4 system in the continuously growing character of the tooth.

The consequences of transient (first postnatal week) and permanent RANKL invalidations onto the first molars eruption and roots development were analyzed and compared at thirty five days postnatal, when all teeth development was normally due. Molar eruption and

root elongation were severely affected in both RANKL invalidated mice. However, degrees of the defects were different between the mice.

A great number of HERS cells and Epithelial Rests of Malassez (ERM) cells observed in the transiently invalidated mice compared to permanently invalidated mice, had an evident relationship with the length of the root. Indeed, an incomplete root elongation, further supported by the absence of cellular cementum formation was observed in molars of transiently RANKL invalidated mice. In contrast, an early interruption of the root formation and an ankylosis were observed in the *Rankl*^{-/-} mice as previously reported by Huang et al. [222]. Altogether, these results revealed that RANKL transitory invalidation during the first post-natal week was enough on one hand to block the first molar eruption, and on the other to arrest the root elongation in absence of either ankylosis or compression inside osteopetrotic alveolar bone.

The molar primary retention observed in clinic corresponds to a still non-explained absence of molar eruption despite a large eruption pathway with no physical obstacle [91]. Interestingly, this resemble to the situation associated to transient inhibition of RANKL during the first postnatal week described above, raising the question of the implication of the RANKL signaling in the occurrence of molar primary retention. In order to demonstrate such an implication, the experimental strategy used was first to assess in mouse the impact of different transient inhibitions of RANKL, realized by injections of the IK22.5 antibody during different post-natal periods, onto the eruption and the root elongation processes of molars, and secondly to compare the obtained craniofacial phenotypes with those of human patients with molar primary retention.

Two periods of RANKL inhibitions were chosen, from postnatal days 1 to 7 (PND1 group) and 7 to 13 (PND7 group) in order to respectively target the first and the second molars. The wild type and the *Rankl* KO mice were used as negative and positive controls.

Concerning the molar eruption, a significant heterogeneity of the alterations was observed for the first and second molars of mice injected at post-natal day seven (PND7). In contrast for all mice injected from the first postnatal day (PND1), a severe first and second molar retentions were reported. Interestingly, the severity of the phenotype was less important and less generalized in mice of the PND7 group than in those of the PND1 group. These observations suggest the presence of a spatio-temporal window of major importance for molar eruption. Indeed, the first post-natal week would seem very important for the development and dental eruption of the first and second molars considering RANKL signaling functions. Later during growth, from postnatal day 7, the developmental window of the dentoalveolar is almost complete and the program responsible for the eruption, including the RANKL signaling associated functions, would be already set.

A histological analysis was performed to study the effects of the transient inhibitions of RANKL on the mandible alveolar bone remodeling necessary to the molars eruption and on the mandible molars organogenesis. Compared to the wild type group, mice from the PND1 group had the most severe phenotype with the first and the second retained molars with severe surrounding tissue disorganization. Interestingly, regardless the inhibition window considered, the third molars were always erupted evidencing an important delay of the third molars eruption window comparatively to the first and the second molars. Mice from the PND7 group evidenced variable and heterogeneous phenotypes with mild/light forms and severe forms. In the severe forms, the first molars were mainly retained but severe tissues disorganization were observed for both first and second molars. In the mild/light forms limited tissues disorganization were visible in the molar root area.

The TRAP histoenzymology staining remarkably evidenced that the number of TRAP positive cells was more important in the alveolar bone when the molar phenotype was severe. Indeed, the higher TRAP staining was visible around the first and second molars of mice from

the PND1 group then around those of mice from the PND7 group with severe phenotype. The TRAP histoenzymology also enabled to observe, in the coronary region, the formation of an eruption pathway in mice of the PND1 group despite the intra-osseous retention of the molars. These histological analyses demonstrated that transient invalidation of the RANKL signaling has an impact on the molars eruption and roots formation processes in which the intensity is dependent on the period during which this inhibition is effective.

Considering the craniofacial morphometric parameters, the decrease in craniofacial measurements is related to the alteration of the bone remodeling. The constitutive inhibition of RANKL (*Rankl* KO) leads to osteopetrosis with presence of a significant growth retardation, some alterations of bone metabolism due to a decrease in osteoclastic differentiation, and alterations of the dental eruption [223].

Interestingly, transient inhibitions of RANKL during the first postnatal week induces craniofacial morphometric defects very close from those observed in *Rankl*^{-/-} mice whereas the inhibition during the second postnatal week induces a less severe phenotype with most of the measured parameters close from those of the wild type mice. The two craniofacial morphometric parameters that are the most affected in relationship with the defective molar eruption are the total skull length and the craniofacial vault length. So, in the case of a RANKL signaling perturbation during growth, if a tooth retention or a tooth eruption delay are observed, reduction of some craniofacial morphometric parameters are highly probable suggesting that primary molar retention may be part of a more global craniofacial growth alteration associated to transitory disruption of the RANKL signaling.

In this context, the intervention of an environmental factor disturbing the RANKL signaling would have consequences on the dental and craniofacial development, with a heterogeneity that depends on the stage of intervention of this factor and its local or systemic application. In the case of a systemic intervention, the craniofacial growth and the dental

eruption are therefore closely related processes that depend on the osteoclastogenesis, itself regulated in time and space [11,224].

Histologically, the transient inhibition of RANKL on the development of the dentoalveolar complex led to an intra-osseous retention of the first and second molars, comparable to primary retentions present in a generalized form for osteopetrotic patients [1], or in a localized form for patients without syndromes or associated diseases [225]. Alteration of bone remodeling and the absence of dental eruption are related to the absence of functional osteoclasts. In our study, transient inhibition of RANKL by the antibody paradoxically has a distant opposite effect. Indeed, one month after the last injection, the alveolar bone surrounding the crown and the roots of the molars of the injected mice presented an increased number of TRAP positive cells, compared with the molars of control mice. The inhibition of RANKL during the first postnatal days would inhibit osteoclast differentiation during this period, resulting in a complete but transient alteration of the tooth eruption process. Nevertheless, it seems that one month after stopping the treatment, the osteoclastic differentiation tries to restore the defect.

The transient inhibition of RANKL could alter signaling pathways involved in alveolar bone modeling and root formation, such as tumor growth factors/ bone morphogenetic protein (Tgf β /Bmp) pathway, Wingless/ β -catenin (Wnt/ β -catenin) pathway, fibroblast growth factor (Fgf) pathway, Sonic hedgehog (Shh) pathway or insulin-like growth factor (IGF) pathway [53,226], leading to an alteration of the root formation and an absence of eruption despite the presence of osteoclasts.

The PTHrP signaling pathway has been strongly implicated in some molars retentions. PTHrP, a peptide linked to parathyroid hormone, and its PTH1R receptor were identified in dental follicle mesenchymal cells and at the root surface. PTH1R is strongly expressed by osteoblasts adjacent to the dental germ, whereas PTHrP is expressed by the epithelial cells of

the dental lamina and in the stellate reticulum just before the formation of the eruption pathway [227]. It has been proposed that PTHrP and PTH1R play an important role in the regulation of root morphogenesis and maintenance of the periodontium [228]. A role of PTHrP / PTH1R in the formation and activation of osteoclasts has also been suggested through RANKL signaling, as in the process of root formation in mouse molars [227]. In humans, mutations in the gene encoding PTHrP have been identified in patients with primary eruption abnormalities [229]. The primary failure of eruption has been described as a non-syndromic alteration of eruption. The tooth presents a total or partial absence of the eruption with no mechanical obstacle identified [230]. It is a defect that mainly affects permanent molars (first and second molars) and, despite a low prevalence (0.06%), different analyses show that it is an alteration which prevalence actually demonstrate a gradual increase [231,232]. Its etiology has not been fully clarified. For some authors, it is a genetic disease with autosomal dominant transmission. Mutated mice for PTHrP show normal differentiation of osteoclasts in molar bone crypt. These animals do not present osteopetrosis, however, the molar eruption is disturbed. The authors evoke an epithelio-mesenchymal disruption at the origin of the tooth retention [233]. As previously shown, several signaling pathways have been identified as crucial for root formation and tooth eruption. The factors involved in the interactions of epithelial cells and mesenchymal cells during the formation of the dentoalveolar complex have been largely described; however, there are still many particular questions concerning the etiology of molar retention, other than an alteration of bone modeling. We found here that the injection of an anti-RANKL antibody has effects on dental development, particularly root formation. An alteration in the size, shape and structure of the root is evident in injected mice. Other studies on the effects of the RANKL mutation have reported alterations in the formation of the Hertwig's epithelial root sheath inducing an arrest of root elongation in the absence of osteoclasts and the lack of alveolar bone modeling when the tooth is forming [53].

Human molar primary retention as part of craniofacial development alteration

The craniofacial diagrams of patients with primary molar retentions were compared to those of patients with mechanical impactions. In order to identify a craniofacial phenotype associated with primary retentions, it would have been possible to choose a control group without particular alterations but a bias would have persisted. However, the simple fact that one or more molars did not erupt could influence the craniofacial measures. Thus, designating patients with "molar mechanical impactions" as a control group makes it possible to reduce this bias of the full molar eruption. A total of 42 patients were included in our analysis, 24 with molar primary retention and 18 with mechanical retention.

Two cephalometric analyses were applied to the patients radiographs in order to provide as much information as possible. Indeed, Delaire's analysis makes it possible to qualitatively highlight the craniofacial typology of the patient and to confront him with what his structural or dento-skeletal optimum could have been. Whereas, Tweed's analysis uses standard measures that make it possible to compare the patient to a cephalometric standard: the quantitative study is thus easier. In addition, the use of two different analyses, makes it possible to compare the results obtained in each of them, and thus, to be able to judge their coherence.

The results of the qualitative study according to Delaire's analysis showed a statistically significant difference in the distribution of skeletal classes and anteroposterior position of the mandible between the two groups ($p = 0.078$). Indeed, a higher occurrence of skeletal classes II (96%) associated with retromandibulism, in 78% of cases, is found in the group of primary retentions compared to the control group.

These results are consistent with those found in Tweed's analysis. Indeed, an angle ANB greater than 4° represents, according to Tweed, a skeletal class II. The average ANB angle in the group of primary retentions (5.58°) is not only higher than this norm, but it is also

significantly different ($p = 0.0112$) from the one of the control group (3.5°). Similarly, patients with primary retentions have, on average, retromandibulism (mean SNB = 76.6° , which is below the 80° norm) compared with control patients ($p = 0.006$).

Several articles in the literature have also listed the different skeletal patterns found in patients with eruption defects. In 2010, Frazier-Bowers and colleagues count 2 class III cases out of 4 patients studied with primary failure of eruption [234]. In 2013, Rhoads et al. reported 18 skeletal class III cases among the 58 patients included in the study, and found a more frequent tendency to class III when the patient had primary failure eruption. However, these patients had only PFE (and no other primary retention alterations) and were divided into 2 groups: 11 subjects with genetically confirmed PFE (*PTH1R* mutations) and 63.7% of them with Skeletal class III; and 47 subjects with clinically diagnosed PFE and only 23.4% of them with class III. Other skeletal classes have not been listed. It should also be noted that no specific cephalometric analyses were reported in this study: the results were determined from "good quality" clinical images by reporting the Dental Angle class, and profile telerradiographs when they were available in the orthodontic file without specifying the analysis methods [235]. Finally, Sharma et al. found 7 skeletal class III cases out of the 15 patients studied (with PFEs). However, they also relied on orthodontic records without specifying the protocol or the documents used [180]. Thus, a significant divergence of the results obtained in our study compared to the articles of the literature is noticed. Such a divergence can be explained by:

- only patients with PFE were analysed in the literature whereas in the present study all patients with primary retention of eruption (including PFE and other alterations) were included, the study population is therefore in part different;

- no study has reported before the use of cephalometric analysis from lateral telerradiographs, whereas in our study two different analyses (Delaire and Tweed) were used to determine the skeletal pattern.

Regarding the vertical measurements, neither of the two cephalometric analyzes used revealed a significant difference between the two groups.

For dental measurements, Delaire's analysis ($p = 0.018$) and Tweed's analysis ($p = 0.0001$) found significant statistically palatoversion of the upper incisor in patients with primary retentions (in mean I / FR = 104.7°) compared to control patients. These observations are in agreement with those found clinically (in the description of the population). In fact, patients in the "primary retention" group had a higher prevalence of class II.2 associated with anterior overbite (75%) compared to the control group ($p = 0.0043$). Although it is not a skeletal measure, it is interesting to note that this malocclusion is particularly preponderant in these patients.

These results lead us to assume the existence of a particular craniofacial phenotype in patients with primary retentions of molars: a retromandibular skeletal class II typology associated with reduced mandibular dimensions (short ascending ramus, short mandible body and, brachygnathism), which manifests itself at the dental level by a class II/2 with palatoversion of the upper incisors and anterior overbite.

This association reinforces the link between craniofacial growth and dental eruption and will be a starting point for further research.

For the moment, it is difficult to know if these two phenomena share a common etiology, or if a general defect of growth could locally cause an alteration of the eruption; but this phenotype could eventually become a clinical predictive sign of the primary retention of molars.

Finally, taken together all our results obtained in patients and in our mouse models of RANKL signaling invalidations, we may conclude that molar primary retentions are part of a large craniofacial skeleton phenotype whose origin is a transitory alteration of the RANKL functions during the initial step of the dental root elongation and tooth eruption. Further studies

will be necessary to integrate the notion of systemic versus local in the link between RANKL invalidation, molar primary retention and craniofacial morphometric alterations.

8. CONCLUSION

Based on a systematic review, we showed that the most frequent oro-dental findings in 95 patients with AD and AR osteopetrosis consisted in osteomyelitis of the jaws regardless the type of osteopetrosis, whereas eruption defects and dental anomalies were more frequent in AR osteopetrosis patients. These observations have raised the question of the origin of such variations in the dento-alveolar phenotype associated to osteopetrosis other than just a defective osteoclastic function. In order to respond this question, we have chosen to work with osteopetrosis models in mouse corresponding to global and transient invalidations of the master factor of the osteoclastogenesis, RANKL.

The series of experiments performed in an osteopetrotic context of permanent invalidation of RANKL enabled us to state that the maternal soluble RANKL can cross the placenta barrier and therefore it may participate in the morphogenesis/histogenesis of the craniofacial skeleton, mostly through its implication in cell-to-cell communications and the osteoclast differentiation control. During tooth later development, the *Rankl* null mutant mice showed important root alterations. Our comparative analyses of the dentoalveolar consequences of transient (during the first postnatal weeks) and permanent invalidations of RANKL have enabled the demonstration that, in addition to the defective osteoclastogenesis, perturbations in cell-to-cell communications are present affecting the HERS cells proliferation and differentiation with a gradual severity related to the penetrance of RANKL invalidation in terms of intensity (total with a genetic model versus transient with a pharmacological model of blocking antibody) and timing (continuous, first postnatal week or second postnatal week). So the variations of penetrance of the osteopetrotic phenotype observed in human patients may be explained by defect in cell-to-cell communications necessary to the root elongation and the tooth eruption processes in addition to the osteoclastic alterations, as established here for the RANKL signaling.

Despite the observations relative to the osteopetrotic pathology, our results obtained in mouse models demonstrated that defective molar eruptions, more specifically primary molar retentions characterized by an absence of physical obstacle on the eruption pathway, are part of general craniofacial growth alterations. This was confirmed by our clinical data evidencing that the patients with primary eruption retentions presented a craniofacial phenotype statistically different from patients with molar mechanical impactions (a retrognathism class II, associated with reduced mandibular dimensions, which manifested at the dental level by a class II division 2 with overbite).

Finally, the body of evidence suggested that any retained teeth in patients could be the consequence of systemic or localized perturbations in either the space or the time of the RANKL signaling by external actors that remain to be defined.

9. PERSPECTIVES

A more precise identification of the expression patterns of the elements of the RANKL signaling, RANKL, RANK, OPG and LGR4 in the dentoalveolar complex cells during physiological root formation and tooth eruption may enable to define precisely the developmental stages (ages) at which perturbations of this signaling in patients will have repercussions on each tooth type (second premolar, first molar, second molar...) with an evident interest in the management of the patients.

An identification of the factors inducing the local or systemic perturbations of the RANKL signaling will be necessary with an evident preventive interest. These factors may be of intrinsic origin such as hormones, cytokines and growth factors. In this respect, the PTHR1 mutations have been implicated in some molar primary retentions, as an interesting primary candidate whose impact on the RANKL signaling remain to be identified. These factors may on the contrary be of extrinsic origin such as local or systemic pharmacologic drugs. In that way, observations of tooth retentions reported in young patients treated with chemotherapy agents (including bone protective agents like bisphosphonates), antibiotics and anti-inflammatory agents will guide future investigations. Finally, we may not exclude chemical factors like endocrine disruptors, pesticides and herbicides whose involvement remains to be established.

10. REFERENCES

1. Fleischmannova J, Matalova E, Sharpe P, Misek I, Radlanski R. Formation of the tooth-bone interface. *J Dent Res*. 2010;89:108–15.
2. Hung Y, Huang X, Chai Y. Molecular regulatory mechanism of root development. *J Calif Dent Assoc*. 2011;39:321–4.
3. Kumakami-Sakano M, Otsu K, Fujiwara N, Harada H. Regulatory mechanisms of Hertwig's epithelial root sheath formation and anomaly correlated with root length. *Exp Cell Res*. Elsevier; 2014;325:78–82.
4. Kjær I. Mechanism of Human Tooth Eruption: Review Article Including a New Theory for Future Studies on the Eruption Process. *Scientifica (Cairo)*. Hindawi Publishing Corporation; 2014;1–13.
5. Heinrich J, Bsoul S, Barnes J, Woodruff K, Abboud S. CSF-1, RANKL and OPG regulate osteoclastogenesis during murine tooth eruption. *Arch Oral Biol*. 2005;50:897–908.
6. Everts V, de Vries TJ, Helfrich MH. Osteoclast heterogeneity: lessons from osteopetrosis and inflammatory conditions. *Biochim Biophys Acta*. Elsevier B.V.; 2009;1792:757–65.
7. Castaneda B, Simon Y, Jacques J, Hess E, Choi YWY, Blin-Wakkach C, et al. Bone resorption control of tooth eruption and root morphogenesis: Involvement of the receptor activator of NF-KB (RANK). *J Cell Physiol*. 2011;226:74–85.
8. Castaneda B, Simon Y, Ferbus D, Robert B, Chesneau J, Mueller C, et al. Role of RANKL (TNFSF11)-dependent osteopetrosis in the dental phenotype of *Msx2* null mutant mice. *PLoS One*. 2013;8.
9. Ohazama a, Courtney J-M, Sharpe PT. *Opg*, *Rank*, and *Rankl* in tooth development: co-ordination of odontogenesis and osteogenesis. *J Dent Res*. 2004;83:241–4.
10. Rani CS, MacDougall M. Dental cells express factors that regulate bone resorption. *Mol Cell Biol Res Commun*. 2000;3:145–52.
11. Berdal A, Castaneda B, Aïoub M, Néfussi J, Mueller C, Descroix V, et al. Osteoclasts in the dental microenvironment: A delicate balance controls dental histogenesis. *Cells Tissues Organs*. 2011;194:238–43.
12. Aïoub M, Lézot F, Molla M, Castaneda B, Robert B, Goubin G, et al. *Msx2* *-/-* transgenic mice develop compound amelogenesis imperfecta, dentinogenesis imperfecta and periodontal osteopetrosis. *Bone*. 2007;41:851–9.
13. Nanci A. Ten Cate's Oral Histology Development, Structure and Function. 6th ed. Rudolph P, Alvis K, editors. St. Louis, Missouri, USA: Mosby, Inc.; 2012.
14. Thesleff I, Sharpe P. Signalling networks regulating dental development. *Mech Dev*. 1997;67:111–23.
15. Thesleff I. Current understanding of the process of tooth formation: Transfer from the laboratory to the clinic. *Aust Dent J*. 2014;59:48–54.
16. Thesleff I. The genetic basis of tooth development and dental defects. *Am J Med Genet A*. 2006;140:2530–5.
17. Li J, Parada C, Chai Y. Cellular and molecular mechanisms of tooth root development.

Development. 2017;144:374–84.

18. Sharpe PT. Homeobox genes and orofacial development. *Connect Tissue Res.* 1995;32:17–25.

19. Suryadeva S, Begum M, Khan MB. Role of homeobox genes in tooth morphogenesis: A review. *J Clin Diagnostic Res.* 2015;9:ZE09-ZE12.

20. Miletich I, Sharpe PT. Normal and abnormal dental development. *Hum Mol Genet.* 2003;12:R69–73.

21. Mitsiadis TA, Graf D. Cell fate determination during tooth development and regeneration. *Birth Defects Res Part C - Embryo Today Rev.* 2009;87:199–211.

22. Thesleff I. Epithelial-mesenchymal signalling regulating tooth morphogenesis. *J Cell Sci.* 2003;116:1647–8.

23. Fleischmannova J, Matalova E, Tucker AS, Sharpe PT. Mouse models of tooth abnormalities. *Eur J Oral Sci.* 2008;116:1–10.

24. Gama A, Navet B, Vargas JWJW, Castaneda B, Lézot F. Bone resorption : an actor of dental and periodontal development ? *Front Physiol.* 2015;6:1–7.

25. Luan X, Ito Y, Diekwisch TGH. Evolution and development of Hertwig's Epithelial Root Sheath. *Dev Dyn.* 2006;235:1167–80.

26. Zeichner-David M, Oishi K, Su Z, Zakartchenko V, Chen L-S, Arzate H, et al. Role of Hertwig's epithelial root sheath cells in tooth root development. *Dev Dyn.* 2003;228:651–63.

27. Huang X-FF, Chai Y. Molecular regulatory mechanism of tooth root development. *Int. J. Oral Sci.* 2013 p. 177–81.

28. Huang X, Bringas P, Slavkin HC, Chai Y. Fate of HERS during tooth root development. *Dev Biol.* Elsevier Inc.; 2009;334:22–30.

29. Huang X, Xu X, Bringas P, Hung YP, Chai Y. Smad4-Shh-Nfic signaling cascade-mediated epithelial-mesenchymal interaction is crucial in regulating tooth root development. *J Bone Miner Res.* 2010;25:1167–78.

30. Nam H, Kim J-H, Kim J-W, Seo B-M, Park J-C, Kim J-W, et al. Establishment of Hertwig's epithelial root sheath/epithelial rests of Malassez cell line from human periodontium. *Mol Cells.* 2014;37:562–7.

31. Fong HK, Foster BL, Popowics TE, Somerman MJ. The crowning achievement: getting to the root of the problem. *J Dent Educ.* 2005;69:555–70.

32. Sakano M, Otsu K, Fujiwara N, Fukumoto S, Yamada A, Harada H. Cell dynamics in cervical loop epithelium during transition from crown to root: Implications for Hertwig's epithelial root sheath formation. *J Periodontal Res.* 2013;48:262–7.

33. Wang J, Feng J. Signaling Pathways Critical for Tooth Root Formation. *J Dent Res.* 2017;96:1221–8.

34. Itaya SI, Ka KO, Gata KO, Amura ST, Atsuoka MKIRA, Ujiwara NF, et al. Hertwig ' s epithelial root sheath cells contribute to formation of periodontal ligament through epithelial-mesenchymal transition by TGF- β . *Biomed Res.* 2017;38:61–9.

35. Yamamoto T, Hasegawa T, Yamamoto T, Hongo H, Amizuka N. Histology of human

cementum: Its structure, function, and development. *Jpn Dent Sci Rev. Japanese Association for Dental Science*; 2016;52:63–74.

36. Foster BL. Methods for studying tooth root cementum by light microscopy. *Int J Oral Sci*. 2012;4:119–28.

37. Salmon CR, Tomazela DM, Gonzales K, Ruiz S, Foster BL, Franco A, et al. Proteomic analysis of human dental cementum and alveolar bone. *J Proteomics*. 2013;91:544–55.

38. Salmon CR, Paula A, Giorgetti O, Franco A, Leme P, Domingues RR, et al. Global proteome profiling of dental cementum under experimentally-induced apposition. *J Proteomics*. 2016;141:12–23.

39. Nanci A, Bosshardt DD. Structure of periodontal tissues in health and disease. *Periodontol*. 2000. 2006. p. 11–28.

40. Nemoto E, Koshikawa Y, Kanaya S, Tsuchiya M, Tamura M, Somerman MJ, et al. Wnt signaling inhibits cementoblast differentiation and promotes proliferation. *Bone*. 2009;44:805–12.

41. Cao Z, Zhang H, Zhou X, Han X, Ren Y, Gao T, et al. Genetic evidence for the vital function of Osterix in Cementogenesis. *J Bone Min Res*. 2014;27:1080–92.

42. Kim THH, Bae CHH, Lee JCC, Kim JEE, Yang X, de Crombruffhe B, et al. Osterix Regulates Tooth Root Formation in a Site-specific Manner. *J Dent Res*. 2015;92:215–21.

43. He YD, Sui BD, Li M, Huang J, Chen S, Wu LA, et al. Site-specific function and regulation of Osterix in tooth root formation. *Int Endod J*. 2016;49:1124–31.

44. Zhang H, Jiang Y, Qin C, Liu Y, Ho SP, Feng JQ. Essential role of Osterix for tooth root but not crown dentin formation. *J Bone Miner Res*. 2014;

45. Marks Jr SC, Schroeder HE. Tooth eruption: Theories and Facts. *Anat Rec*. 1996;245:374–93.

46. Marks SC, Cahill DR. Experimental study in the dog of the non-active role of the tooth in the eruptive process. *Arch Oral Biol*. 1984;29:311–22.

47. Cahill DR, Marks SC. Tooth eruption: evidence for the central role of the dental follicle. *J Oral Pathol*. 1980;9:189–200.

48. Wang X-P. Tooth eruption without roots. *J Dent Res*. 2013;92:212–4.

49. Ehlen HW a, Buelens L a, Vortkamp A. Hedgehog signaling in skeletal development. *Birth Defects Res C Embryo Today*. 2006;78:267–79.

50. Lian JB, Stein GS, Javed A, Van Wijnen AJ, Stein JL, Montecino M, et al. Networks and hubs for the transcriptional control of osteoblastogenesis. *Rev Endocr Metab Disord*. 2006;7:1–16.

51. Hassan MQ, Tare RS, Suk HL, Mandeville M, Morasso MI, Javed A, et al. BMP2 commitment to the osteogenic lineage involves activation of Runx2 by DLX3 and a homeodomain transcriptional network. *J Biol Chem*. 2006;281:40515–26.

52. Alfaqeeh S a, Gaete M, Tucker a S. Interactions of the tooth and bone during development. *J Dent Res*. 2013;92:1129–35.

53. Helfrich M. Osteoclast diseases and dental abnormalities. *Arch Oral Biol*. 2005;50:115–22.

54. Yamada S, Tomoeda M, Ozawa Y, Yoneda S, Terashima Y, Ikezawa K, et al. PLAP-1/asporin, a novel negative regulator of periodontal ligament mineralization. *J Biol Chem.* 2007;282:23070–80.
55. Ueda M, Kuroishi KN, Gunjigake KK, Ikeda E, Kawamoto T. Expression of SOST/sclerostin in compressed periodontal ligament cells. *J Dent Sci. Elsevier Taiwan LLC;* 2016;11:272–8.
56. Capulli M, Paone R, Rucci N. Osteoblast and osteocyte: Games without frontiers. *Arch. Biochem. Biophys.* 2014. p. 3–12.
57. Otto F, Thornell AP, Crompton T, Denzel A, Gilmour KC, Rosewell IR, et al. *Cbfa1*, a candidate gene for cleidocranial dysplasia syndrome, is essential for osteoblast differentiation and bone development. *Cell.* 1997;89:765–71.
58. Komori T, Yagi H, Nomura S, Yamaguchi A, Sasaki K, Deguchi K, et al. Targeted disruption of *Cbfa1* results in a complete lack of bone formation owing to maturational arrest of osteoblasts. *Cell.* 1997;89:755–64.
59. Zaidi S, Young D, Choi J. Intracellular trafficking: organization and assembly of regulatory machinery for combinatorial biological control. *J Biol Chem.* 2004;279:43363–6.
60. Pratap J, Galindo M, Zaidi S. Cell growth regulatory role of *Runx2* during proliferative expression of preosteoblasts. *Cancer Res.* 2003;63:5357–62.
61. Ducy P, Zhang R, Geoffroy V, Ridall A, Karsenty G. *Osf2/Cbfa1*: a transcriptional activator of osteoblast differentiation. *Cell.* 1997;89:747–54.
62. Harada H, Tagashira S, Fujiwara M, Ogawa S, Katsumata T, Yamaguchi A, et al. *Cbfa1* isoforms exert functional differences in osteoblast differentiation. *J Biol Chem.* 1999;274:6972–8.
63. Kubota T, Michigami T, Ozono K. Wnt signaling in bone metabolism. *J Bone Min Metab.* 2009;27:265–71.
64. Karner CM, Long F. Wnt signaling and cellular metabolism in osteoblasts. *Cell Mol Life Sci.* 2017;74:1649–57.
65. Otsuki Y, Li, Masaaki L, Moriwaki K, Okada M, Ueda K, Asahi M. W9 peptide enhanced osteogenic differentiation of human adipose-derived stem cells. *Biochem Biophys Res Commun.* 2018;495:904–10.
66. Portal-Núñez S, Mediero A, Esbrit P, Sánchez-Pernaute O, Largo R, Herrero-Beaumont G. Unexpected Bone Formation Produced by RANKL Blockade. *Trends Endocrinol Metab.* 2017;28:695–703.
67. Cao X. RANKL-RANK signaling regulates osteoblast differentiation and bone formation. *Bone Res.* 2018;6:1–2.
68. Ikebuchi Y, Aoki S, Honma M, Hayashi M, Sugamori Y, Khan M, et al. Coupling of bone resorption and formation by RANKL reverse signalling. *Nature.* 2018;561:195–200.
69. Dallas SL, Prideaux M, Bonewald LF. The Osteocyte: An Endocrine Cell . . . and More. *Endocr Rev.* 2013;34(5):658–90.
70. Schaffler MB, Cheung W-Y, Majeska R, Kennedy O. Osteocytes: Master Orchestrators of Bone. *Calcif Tissue Int.* 2014;94:5–24.

71. Honma M, Ikebuchi Y, Kariya Y, Suzuki H. Regulatory mechanisms of RANKL presentation to osteoclast precursors. *Curr Osteoporos Rep.* 2014;12:115–20.
72. O'Brien CA, Nakashima T, Takayanagi H. Osteocyte Control of Osteoclastogenesis. *Bone.* 2013;54 (2):258–63.
73. Xiong J, Piemontese M, Onal M, Campbell J, Goellner J, Dusevich V, et al. Osteocytes, not osteoblasts or lining cells, are the main source of the RANKL required for osteoclast formation in remodeling bone. *PLoS One.* 2015;10.
74. Yasuda H, Shima N, Nakagawa N, Yamaguchi K, Kinosaki M MS. Osteoclast differentiation factor is a ligand for Osteoprotegerin/osteoclastogenesis-inhibitory factor and is identical to TRANCE: RANKL. *Proc Natl Acad Sci USA.* 95:3597–602.
75. Charles JF, Aliprantis AO. Osteoclasts: more than "bone eaters. *Trends Mol Med.* 2014;20:449–59.
76. Chen X, Wang Z, Duan N, Zhu G, Schwarz EM, Xie C. Osteoblast-Osteoclast Interactions. *Connect Tissue Res.* 2018;59:99–107.
77. Malhotra V, Erlmann P. The Pathway of Collagen Secretion. *Annu Rev Cell Dev Biol.* 2015;31:109–24.
78. Unal M, Creecy A, Nyman JS. The Role of Matrix Composition in the Mechanical Behavior of Bone. *Curr Osteoporos Rep.* 2018;16:205–15.
79. Wise GE, He H, Gutierrez DL, Ring S, Yao S. Requirement of alveolar bone formation for eruption of rat molars. *Eur J Oral Sci.* 2011;119:333–8.
80. Wise G, Frazier-Bowers S, D'Souza R. Cellular, Molecular, and Genetic Determinants of Tooth Eruption. *Crit Rev Oral Biol Med.* 2002;13:323–35.
81. Berkovitz B. Le mécanisme de l'éruption dentaire: bilan des recherches et des théories actuelles. *Rev d'Orthopedie Dento-Faciale.* 1990;24:13–32.
82. Rabea AA. Recent advances in understanding theories of eruption (evidence based review article). *Futur Dent J.* 2018;4:189–96.
83. Gowgiel J. Eruption of irradiation-produced rootless teeth in monkeys. *J Dent Res.* 1961;40:538–47.
84. Marks SJ, Cahill D, Wise G. The cytology of the dental follicle and adjacent alveolar bone during tooth eruption in the dog. *Am J Anat.* 1983;168:277–89.
85. Marks J, Sandy C. Tooth eruption and bone resorption: experimental investigation of the ia (osteopetrotic) rat as a model for studying their relationships. *J Oral Pathol.* 1976;5:149–63.
86. Marks SJ, Cahill D. Regional control by the dental follicle of alterations in alveolar bone metabolism during tooth eruption. *J Oral Pathol.* 1987;16:164–9.
87. Wang Z, Mccauley LK. Osteoclasts and odontoclasts: Signaling pathways to development and disease. *Oral Dis.* 2011;17:129–42.
88. Bondemark L, Tsiopa J. Prevalence of ectopic eruption, impaction, retention and agenesis of the permanent second molar. *Angle Orthod.* 2007;77:773–8.
89. Moulis E, Thierrens C, Goldsmith M-C, Torres J-H. Anomalies de l'éruption. *Encycl Med Chir - Pédiatrie - Maladies infectieuses.* 2003.

90. Raghoobar G, Boering G, Vissink A, Stegenga B. Eruption disturbances of permanent molars: a review. *J Oral Path Med.* 1991;20:159–66.
91. Cohen-Lévy J, Cohen N. Anomalies d'éruption des molaires permanentes: diagnostic différentiel et explorations radiographiques. *Rev Orthop Dento Faciale.* 2015;49:217–30.
92. Palma C, Coelho A, González Y, Cahuana A. Failure of eruption of first and second permanent molars. *J Clin Pediatr Dent.* 2003;27:239-45.
93. Cassetta M, Altieri F, Di Mambro A, Galluccio G, Barbato E. Impaction of permanent mandibular second molar: a retrospective study. *Med Oral Patol Oral Cir Bucal.* 2013;18:e564-8.
94. Proffit W, Vig K. Primary failure of eruption: a possible cause of posterior open bite. *Am J Orthod.* 1981;80:173–90.
95. Yamaguchi T, Hosomichi K, Narita A, Shirota T, Tomoyasu Y, Maki K, et al. Exome resequencing combined with linkage analysis identifies novel PTH1R variants in primary failure of tooth eruption in Japanese. *J Bone Miner Res.* 2011;26:1655–61.
96. Mannstadt M, Juppner H, Gardella TJ. Receptors for PTH and PTHrP: their biological importance and functional properties. *Am J Physiol.* 1999;277:F665-675.
97. Ohazama A, Sharpe PT. TNF signalling in tooth development. *Curr Opin Genet Dev.* 2004;14:513–9.
98. Branco J, Silva I. Rank/Rankl/Opg : Literature Review. *Acta Reum Port.* 2011;36:209–18.
99. Walsh MC, Choi Y. Biology of the RANKL/RANK/OPG System in Immunity, Bone, and Beyond. *Front Immunol.* 2014;5:1–11.
100. Leibbrandt A, Penninger JM. RANK/RANKL: regulators of immune responses and bone physiology. *Ann N Y Acad Sci.* 2008;1143:123–50.
101. O'Brien C a. Control of RANKL gene expression. *Bone. Elsevier B.V.;* 2010;46:911–9.
102. Theoleyre S, Wittrant Y, Tat SK, Fortun Y, Redini F, Heymann D. The molecular triad OPG/RANK/RANKL: Involvement in the orchestration of pathophysiological bone remodeling. *Cytokine Growth Factor Rev.* 2004;15:457–75.
103. Xiong J, O'brien CA. Osteocyte RANKL: New Insights into the Control of Bone Remodeling. *J Bone Min Res.* 2012;27:499–505.
104. Bellido T. Osteocyte-driven bone remodeling. *Calcif. Tissue Int.* 2014. p. 25–34.
105. Bi H, Chen X, Gao S, Yu X, Xiao J, Zhang B, et al. Key Triggers of Osteoclast-Related Diseases and Available Strategies for Targeted Therapies: A Review. *Front Med.* 2017;4.
106. Luo J, Yang Z, Ma Y, Yue Z, Lin H, Qu G, et al. LGR4 is a receptor for RANKL and negatively regulates osteoclast differentiation and bone resorption. *Nat Med.* 2016;22:539–46.
107. Jin Y, Yang Y. LGR4: A new receptor for a stronger bone. *Sci China Life Sci.* 2016;59:735–6.
108. kawasaki M, Porntaveetus T, Kawasaki K, Oommen S, Otsuka-Tanaka Y, Hishinuma M, et al. R-spondins/Lgrs expression in tooth development. *Dev Dyn.* 2014;243:844–51.
109. Bhatt R, Hibbert S, Munns C. The use of bisphosphonates in children: review of the

literature and guidelines for dental management. *Aust Dent J.* 2014;59:9–19.

110. Grier RL, Wise GE. Inhibition of tooth eruption in the rat by a bisphosphonate. *J Dent Res.* 1998;77:8–15.

111. Bradaschia-Correa V, Massa LF, Arana-Chavez VE. Effects of alendronate on tooth eruption and molar root formation in young growing rats. *Cell Tissue Res.* 2007;330:475–85.

112. Tuncer, Ibrahim, Delilbasi çagri, Deniz Ediz, Soluk-Tekkesin Merva, Olgaç Vakur SK. Effects of pamidronate administration on tooth eruption and mandibular growth in new born rats. *J Istanbul Univ Fac Dent.* 2017;51:8–14.

113. Bradaschia-Correa V, Moreira MM, Arana-Chavez VE. Reduced RANKL expression impedes osteoclast activation and tooth eruption in alendronate-treated rats. *Cell Tissue Res.* 2013;353:79–86.

114. Kamoun-Goldrat A, Ginisty D, Le Merrer M. Effects of bisphosphonates on tooth eruption in children with osteogenesis imperfecta. *Eur J Oral Sci.* 2008;116:195–8.

115. Christou J, Johnson AR, Hodgson TAIMA. Bisphosphonate-related osteonecrosis of the jaws and its relevance to children – a review. *Aust Dent J. Springer US;* 2014;59:9–19.

116. Lézot F, Chesneau J, Navet B, Gobin B, Amiaud J, Choi Y, et al. Skeletal consequences of RANKL-blocking antibody (IK22-5) injections during growth: Mouse strain disparities and synergic effect with zoledronic acid. *Bone. Elsevier Inc.;* 2015;73:51–9.

117. Lézot F, Chesneau J, Battaglia S, Brion R, Farges J-C, Lescaille G, et al. Preclinical evidence of potential craniofacial consequences of ZOL. *Bone.* 2014;Nov:146–52.

118. Forlino A, Marini JC. Osteogenesis imperfecta. *Lancet.* 2016;387:1657–71.

119. Barrence FAC, Ferreira LB, Massa LF, Paulo S. Effect of alendronate on endochondral ossification in mandibular condyles of growing rats. 2012;56:149–53.

120. Vuorimies I, Arponen H, Valta H, Tiesalo O, Ekholm M, Ranta H, et al. Timing of dental development in osteogenesis imperfecta patients with and without bisphosphonate treatment. *Bone.* 2017;94:29–33.

121. Soares AP, do Espirito Santo RF, Line SRP, Pinto M das GF, Santos P de M, Toralles MBP, et al. Bisphosphonates: Pharmacokinetics, bioavailability, mechanisms of action, clinical applications in children, and effects on tooth development. *Environ Toxicol Pharmacol.* 2016;42:212–7.

122. Hernandez M. Use of new targeted cancer therapies in children : effects on dental development and risk of jaw osteonecrosis : a review. *J Oral Pathol Med.* 2017;46:321–6.

123. Del Fattore A, Cappariello A, Teti A. Genetics, pathogenesis and complications of osteopetrosis. *Bone.* 2008;42:19–29.

124. Palagano E, Menale C, Sobacchi C, Villa A. Genetics of Osteopetrosis. *Curr Osteoporos Rep.* 2018;16:13–25.

125. Coudert AE, De Vernejoul M-C, Muraca M, Del Fattore A. Osteopetrosis and its relevance for the discovery of new functions associated with the skeleton. *Int J Endocrinol.* 2015;

126. Wu CC, Econs MJ, Dimeglio LA, Insogna KL, Levine MA, Orchard PJ, et al. Diagnosis and Management of Osteopetrosis: Consensus Guidelines From the Osteopetrosis Working

- Group. *J Clin Endocrinol Metab.* 2017;102:3111–23.
127. Teti A, Econs MJ. Osteopetroses, emphasizing potential approaches to treatment. *Bone.* 2017;102:50–9.
128. Funck-Brentano OT, Collet C, Coudert AE, Cohen-Solal M. Les ostéopétroses. *Rev du Rhum Monogr.* 2019;86:26–30.
129. Van Wesenbeeck L, Cleiren E, Gram J, Beals RK, Bénichou O, Scopelliti D, et al. Six Novel Missense Mutations in the LDL Receptor-Related Protein 5 (LRP5) Gene in Different Conditions with an Increased Bone Density. *Am. J. Hum. Genet.* 2003.
130. Brunetti G, Rucci N, Galliera E, Penna S, Capo V, Palagano E, et al. One Disease, Many Genes: Implications for the Treatment of Osteopetroses. *Front Endocrinol (Lausanne).* 2019;10.
131. Frattini A, Pangrazio A, Susani L, Sobacchi C, Mirolo M, Abinun M, et al. Chloride Channel CLCN 7 Mutations are responsible for severe recessive, dominant and intermediate osteopetrosis. *J Bone Miner Res.* 2003;18:1740–7.
132. Villa A, Guerrini MM, Cassani B, Pangrazio A, Sobacchi C. Infantile Malignant, Autosomal Recessive Osteopetrosis: The Rich and The Poor. *Calcif Tissue Int.* 2009;84:1–12.
133. Pangrazio A, Pusch M, Caldana E, Frattini A, Lanino E, Tamhankar PM, et al. Molecular and clinical heterogeneity in CLCN7-dependent Osteopetrosis: Report of 20 novel mutations. *Hum Mutat.* 2010;31:E1071-1080.
134. Stark Z, Savarirayan R. Osteopetrosis. *Orphanet J Rare Dis.* 2009;4:1–12.
135. Sly WS, Whyte MP, Sundaram V, Tashian RE, Hewett-Emmett D, Guibaud P, et al. Carbonic anhydrase II deficiency in 12 families with the autosomal recessive syndrome of osteopetrosis with renal tubular acidosis and cerebral calcification. *N Engl J Med.* 1985;313:139–45.
136. Sobacchi C, Frattini A, Guerrini MM, Abinun M, Pangrazio A, Susani L, et al. Osteoclast-poor human osteopetrosis due to mutations in the gene encoding RANKL. *Nat Genet.* 2007;39:960–2.
137. Balemans W, Van Wesenbeeck L, Van Hul W. A Clinical and Molecular Overview of the Human Osteopetroses. *Calcif Tissue Int.* 2005;77:263–74.
138. Dupuis-Girod S, Corradini N, Hadj-Rabia S, Fournet J-C, Faivre L, Le Deist F, et al. Osteopetrosis, Lymphedema, Anhidrotic Ectodermal Dysplasia, and Immunodeficiency in a Boy and Incontinentia Pigmenti in His Mother Sophie. *Pediatrics.* 2002;109:1–6.
139. Roberts CML, Angus JE, Leach IH, McDermott EM, Walker DA, Ravenscroft JC. A novel NEMO gene mutation causing osteopetrosis, lymphoedema, hypohidrotic ectodermal dysplasia and immunodeficiency (OL-HED-ID). *Eur J Pediatr.* 2010;169:1403–7.
140. Bacon S, Crowley R. Developments in rare bone diseases and mineral disorders. *Ther Adv Chronic Dis.* 2018;9:51–60.
141. Fontino M, Haymovits A, Falk C. Evidence for linkage between HLA and Paget's disease. *Transplantation Proceedings* 1977, 9, p. 1867-1868. 1977. 9AD;1867–8.
142. Daroszewska A, Ralston S. Clinical of Paget's disease of bone. *Clin Sci.* 2005;109:257–63.

143. Osterberg P, Wallace R, Adams D. Familial expansile osteolysis : a new dysplasia. *J Bone Jt Surg.* 1988;70:255–60.
144. Whyte M, Mills B, Reinus W. Expansile skeletal Hyperphosphatasia: A new familial metabolic bone disease. *J Bone Miner Res.* 2000;15:2330–44.
145. Ralston S, Langston A, Reid I. Pathogenesis of Paget’s disease of bone. *Lancet.* 2008;372:155–63.
146. Mitchell C, Wallace R. Dental abnormalities associated with familial expansile osteolysis: A clinical and radiographic study. *Oral Surg Oral Med Oral Pathol.* 1990;70:301–7.
147. Font N. Familial expansile osteolysis ontological and dental manifestations of genetic origin. *Ann d’oto-laryngologie Chir cervico faciale Bull la Soc d’Oto-laryngologie des Hôpitaux Paris.* 2004;121:360–72.
148. Baron R, Ferrari S, Russell RGG. Denosumab and bisphosphonates: different mechanisms of action and effects. *Bone.* Elsevier Inc.; 2011;48:677–92.
149. Boyce AM. Denosumab : an Emerging Therapy in Pediatric Bone Disorders. *Curr Osteoporos Rep.* 2017;15:283–92.
150. Anastasilakis AD, Polyzos S a, Anastasilakis CD, Toulis K a, Makras P. Denosumab and bisphosphonates: rivals or potential “partners”? A “hybrid” molecule hypothesis. *Med Hypotheses.* 2011;77:109–11.
151. Dahiya, Navdeep; Khadka, Anjan; Sharma, A.K.; Gupta, A.K.; Singh, Nishith; Brashier DBS. Denosumab : A bone antiresorptive drug. *Med J Armed Forces India.* 2015;1:71–5.
152. Weinstein RS, Roberson PK, Manolagas SC. Giant Osteoclast Formation and Long-Term Oral Bisphosphonate Therapy. *N Engl J Med.* 2009;360:53–62.
153. Hiraga T, Ninomiya T, Hosoya A, Nakamura H. Administration of the bisphosphonate zoledronic acid during tooth development inhibits tooth eruption and formation and induces dental abnormalities in rats. *Calcif Tissue Int.* 2010;86:502–10.
154. Hoyer-kuhn H, Netzer C, Koerber F, Schoenau E, Semler O. Two years ’ experience with denosumab for children with Osteogenesis imperfecta type VI. *Orphanet J Rare Dis.* 2014;9:1–8.
155. Hoyer-Kuhn H, Franklin J, Allo G, Kron M, Netzer C, Eysel P, et al. Safety and efficacy of denosumab in children with osteogenesis imperfecta - A first prospective trial. *J Musculoskelet Neuronal Interact.* 2016;16:24–32.
156. Ebetino FH, Hogan A-ML, Sun S, Tsoumpra MK, Duan X. The relationship between the chemistry and biological activity. *Bone.* 2011;49:20–33.
157. Fleisch H. Bisphosphonates--history and experimental basis. *Bone.* 1987;8 Suppl 1:S23-8.
158. Baroncelli GI, Bertelloni S. The Use of Bisphosphonates in Pediatrics. *Horm Res Paediatr.* 2014;82:290–302.
159. Grigoriadis AE, Wang Z, Cecchini MG, Hofstetter W, Felix R, Fleisch H a, et al. c-Fos: A Key Regulator of Osteoclast-Macrophage Lineage Determination and Bone Remodeling. *Science (80-).* 1994;266:443–8.

160. Graham R, Russell G. Bisphosphonates: The first 40years. *Bone*. 2011;49:2–19.
161. Cremers S, Papapoulos S. Pharmacology of biphosphonates. *Bone*. 2011;49:42–9.
162. Russell RGG, Watts NB, Ebetino FH, Rogers MJ. Mechanisms of action of bisphosphonates: similarities and differences and their potential influence on clinical efficacy. *Osteoporos Int*. 2008;19:733–59.
163. Bregou A, Aubry-rozier B, Bonafé L, Ann L, Pioletti DP, Zambelli P. Osteogenesis imperfecta : from diagnosis and multidisciplinary treatment to future perspectives. *Swiss Med Wkly*. 2016;146:1–10.
164. Bowden SA, Mahan JD. Zoledronic acid in pediatric metabolic bone disorders. *Transl Pediatr*. 2017;6:256–68.
165. Rijks EBG, Bongers BC, Vlemmix MJG, Boot AM, Van Dijk ATH, Sackers RJB, et al. Efficacy and safety of bisphosphonate therapy in children with osteogenesis imperfecta: A systematic review. *Horm Res Paediatr*. 2015;84:26–42.
166. Maasalu K, Haviko T, Märtson A, Märtson A. Treatment of children with Osteogenesis imperfecta in Estonia. *Acta Paediatr*. 2003;92:452–5.
167. Otaify GA, Aglan MS, Ibrahim MM, Elnashar M, Banna RAS El. Zoledronic acid in children with osteogenesis imperfecta and Bruck syndrome : a 2-year prospective observational study. *Osteoporos Int*. 2016;27:81–92.
168. Sordillo EM, Pearse RN. RANK-Fc: A therapeutic Antagonist for RANK-L in Myeloma. *Cancer Suppl*. 2003;97:802–12.
169. Sone E, Noshiro D, Ikebuchi Y, Nakagawa M, Khan M, Tamura Y, et al. The induction of RANKL molecule clustering could stimulate early osteoblast differentiation. *Biochem Biophys Res Commun*. 2019;509:435–40.
170. Petticrew M, Shekelle P, Stewart LA, Group P. Preferred reporting items for systematic review and meta-analysis protocols (PRISMA-P) 2015 : elaboration and explanation. *BMJ*. 2015;349:1–25.
171. Hutton B, Salanti G, Caldwell DM, Chaimani A, Schmid CH, Cameron C, et al. The PRISMA Extension Statement for Reporting of Systematic Reviews Incorporating Network Meta-analyses of Health Care Interventions : Checklist and Explanations. *Ann Intern Med*. 2015;162:777–84.
172. Booth A, Clarke M, Ghera D, Moher D, Petticrew M, Stewart L. An international registry of systematic-review protocols. *Lancet*. 2011;377:108–9.
173. Ouzzani M, Hammady H, Fedorowicz Z, Elmagarmid A. Rayyan-a web and mobile app for systematic reviews. *Syst Rev*. 2016;5:1–10.
174. Murad MH, Sultan S, Haffar S, Bazerbachi F. Methodological quality and synthesis of case series and case reports. *BMJ Evidence-Based Med*. 2018;23:60–3.
175. Moola S, Munn Z, Tufanaru C, Aromataris E, Sears K, Sfetcu R, et al. Chapter 7: Systematic reviews of etiology and risk. *Joanna Briggs Inst Rev Man*. 2017.
176. Munn Z, Moola S, Lisy K, Riitano D, Tufanaru C. Methodological guidance for systematic reviews of observational epidemiological studies reporting prevalence and incidence data. *Int J Evid Based Heal*. 2015;13:147–53.

177. Navet B, Vargas-Franco J, Gama A, Amiaud J, Choi Y, Yagita H, et al. Maternal RANKL Reduces the Osteopetrotic Phenotype of Null Mutant Mouse Pups. *J Clin Med*. 2018;7:426.
178. Vora SR, Camci ED, Cox TC. Postnatal Ontogeny of the Cranial Base and Craniofacial Skeleton in Male C57BL / 6J Mice : A Reference. *Front Physiol*. 2016;6:1–14.
179. Xiaoxi W, Neil T, Nan EH, Min H, Fei L. Postnatal Craniofacial Skeletal Development of Female C57BL/6NCrl Mice. *Front Physiol*. 2017;8:1–18.
180. Sharma G, Kneafsey L, Ashley P, Noar J. Failure of eruption of permanent molars: a diagnostic dilemma. *Int J Paediatr Dent*. 2016;26:91-9.
181. Bénichou O., Laredo J., de Vernejoul M. Type II autosomal dominant osteopetrosis (Albers-Schönberg disease): clinical and radiological manifestations in 42 patients. *Bone*. 2000;26:87–93.
182. Bjorvatn K, Gilhuus-Moe O, Aarskog D. Oral aspects of osteopetrosis. *Eur J Oral Sci*. 1979;87:245–52.
183. Detailleur V, Vansteenkiste G, Renard M, Verdonck A. Dental care approach in patients with osteopetrosis. *Eur Arch Paediatr Dent*. 2016;17:435–43.
184. Imanimoghaddam M, Davachi B, Nemati S, Johari M. Dental radiographic findings of malignant osteopetrosis: Report of four cases. *Iran J Radiol*. 2009;6:141–5.
185. Kahler SG, Burns JA, Aylsworth AS. A mild autosomal recessive form of osteopetrosis. *Am J Med Genet*. 1984;17:451–64.
186. Wong ML, Balkany TJ, Reeves J, Jafek BW. Head and neck manifestations of malignant osteopetrosis. *Otolaryngol Neck Surg*. 1978;86:585–94.
187. Krithika C, Neelakandan RS, Sivapathasundaram B, Koteeswaran D, Rajaram PC, Shetkar GS. Osteopetrosis-associated osteomyelitis of the jaws: a report of 4 cases. *Oral Surgery, Oral Med Oral Pathol Oral Radiol Endodontology*. 2009;108:56–65.
188. Ohlsson A, Stark G, Sakati N. Marble Brain Disease: Recessive Osteopetrosis, Renal Tubular Acidosis and Cerebral Calcification in Three Saudi Arabian Families. *Dev Med Child Neurol*. 1980;22:72–84.
189. Ohlsson A, Cumming WA, Paul A, Sly WS. Carbonic Anhydrase II Deficiency Syndrome: Recessive Osteopetrosis With Renal Tubular Acidosis and Cerebral Calcification. *Pediatrics*. 1986;77:371–80.
190. Rikhotso E, Reyneke JP, Ferretti C. Osteopetrosis: literature review and report of three cases. *SADJ*. 2008;63:302–7.
191. Sonia H-L, Mohamed F, Mohamed B, Rafika A, Dehmani F, Kossay D, et al. L'ostéopetrose par déficit en anhydrase carbonique II: A propos de 24 observations. *Tunis Med*. 2005;83:409–13.
192. Trapnell DH. Periodontal manifestations of osteopetrosis. *Br J Radiol*. 1968;41:669–71.
193. Sobacchi C, Schulz A, Coxon FP, Villa A, Helfrich MH, Sobacchi C, et al. Osteopetrosis: genetics, treatment and new insights into osteoclast function. *Nat Rev Endocrinol*. Nature Publishing Group; 2013;9:522–36.
194. Schulz AS, Moshous D, Steward CG, Villa A, Sobacchi C. Osteopetrosis Consensus

guidelines for diagnosis , therapy and follow-up. ESID EBMT. 2011. p. 1–33.

195. Sayre JW, Toklu HZ, Ye F, Mazza J, Yale S. Case Reports , Case Series – From Clinical Practice to Evidence-Based Medicine in Graduate Medical Education. *Cureus*. 2017;9:1–5.

196. Chambers D, Rodgers M, Woolacott N. Not only randomized controlled trials, but also case series should be considered in systematic reviews of rapidly developing technologies. *J Clin Epidemiol*. 2009;62:1253-1260.e4.

197. Van der Stelt P. Panoramic radiographs in dental diagnostics. *Ned Tijdschr Tandheelkd*. 2016;123:181–7.

198. Ambika G, Shikha K, Premdeep G, Virendra S. Maxillary osteomyelitis secondary to osteopetrosis - a rare case report. *J Clin diagnostic Res*. 2010;4:3261–5.

199. Sun HJ, Xue L, Wu C Bin, Zhou Q. Clinical Characteristics and Treatment of Osteopetrosis Complicated by Osteomyelitis of the Mandible. *J Craniofac Surg*. 2016;27:e728–30.

200. Arumugam E, Harinathbabu M, Thillaigovindan R, Prabhu G. Marble Bone Disease: A Rare Bone Disorder. *Cureus*. 2015;7:1–11.

201. Infante-Cossio P, Gonzalez-Perez LM, Martinez-De-Fuentes R, Infante-Cossio M, Castaño-Seiquer A, Jimenez-Castellanos E. Maxillomandibular osteomyelitis associated with osteopetrosis. *J Craniofac Surg*. 2014;25:2012–5.

202. García CM, García MAP, García RG, Gil FM. Osteomyelitis of the Mandible in a Patient with Osteopetrosis. Case Report and Review of the Literature. *J Maxillofac Oral Surg*. 2013;12:94–9.

203. Junquera L, Rodríguez-Recio C, Villarreal P, García-Consuegra L. Autosomal dominant osteopetrosis and maxillomandibular osteomyelitis. *Am J Otolaryngol - Head Neck Med Surg*. 2005;26:275–8.

204. Mikami T, Miake Y, Bologna-Molina R, Takeda Y. Ultrastructural analyses of alveolar bone in a patient with osteomyelitis secondary to osteopetrosis: A review of the literature. *J Oral Maxillofac Surg*. 2016;1–48.

205. Tabrizi R, Arabi AM, Arabion HR, Gholami M. Jaw osteomyelitis as a complication in osteopetrosis. *J Craniofac Surg*. 2010;21:136–41.

206. Dick HM, Simpson WJ. Dental changes in osteopetrosis. *Oral Surgery, Oral Med Oral Pathol*. 1972;34:408–16.

207. Athani NA, Kakaraddi MP, Kallalli BN, Ramesh D. Osteopetrosis : Report of a Rare Case. *J Indian Aca Oral Med Radiol*. 2012;24:206–8.

208. King R, Tanna N, Patel V. Medication-related osteonecrosis of the jaw unrelated to bisphosphonates and denosumab-a review. *Oral Surg Oral Med Oral Pathol Oral Radiol*. 2019;127:289–99.

209. Vastardis H. The genetics of human tooth agenesis: New discoveries for understanding dental anomalies. *Am J Orthod Dentofac Orthop*. 2000;117:650–6.

210. Polder B, Van't Hof M, FPGM V der L, Kuijpers-Jagtman A. A meta-analysis of the prevalence of dental agenesis of permanent teeth. *Community Dent Oral Epidemiol*. 2004;32:217–26.

211. Fournier B, Bruneau M, Toupenay S, Kerner S, Berdal A, Cormier-Daire V, et al. Patterns of Dental Agenesis Highlight the Nature of the Causative Mutated Genes. *J Dent Res*. 2018;97:1306–16.
212. Lacruz RS, Hilvo M, Kurtz I, Paine ML. A survey of carbonic anhydrase mRNA expression in enamel cells. *Biochem Biophys Res Commun*. 2010;393:883–7.
213. Xiaogu W, Tetsuo S, Hirotada O, Baohong Z, Yoichi M, Tomohiko M, et al. Carbonic anhydrase II regulates differentiation of ameloblasts via intracellular pH-dependent JNK signaling pathway. *J Cell Physiol*. 2010;225:709–19.
214. Ikeda T, Kasai M, Utsuyama M, Hirokawa K. Determination of Three Isoforms of the Receptor Activator of Nuclear Factor-Ligand and Their Differential Expression in Bone and Thymus*. 2001.
215. Parada C, Chai Y. Mandible and Tongue Development. *Curr Top Dev Biol*. 2015;115:31–58.
216. Orestes-Cardoso S, Nefussi JR, Lezot F, Oboeuf M, Pereira M, Mesbah M, et al. Msx1 is a regulator of bone formation during development and postnatal growth: In vivo investigations in a transgenic mouse model. *Connect Tissue Res*. 2002;43:153–60.
217. Nassif A, Senussi I, Meary F, Loiodice S, Hotton D, Robert B, et al. Msx1 role in craniofacial bone morphogenesis. *Bone*. Elsevier Inc.; 2014;66:96–104.
218. Anthwal N, Peters H, Tucker AS. Species-specific modifications of mandible shape reveal independent mechanisms for growth and initiation of the coronoid. *Evodevo*. BioMed Central; 2015;6:1–14.
219. Lézot F, Thomas BL, Blin-Wakkach C, Castaneda B, Bolanos a., Hotton D, et al. Dlx homeobox gene family expression in osteoclasts. *J Cell Physiol*. 2010;223:779–87.
220. Deckelbaum RA, Majithia A, Booker T, Henderson JE, Loomis CA. The homeoprotein engrailed 1 has pleiotropic functions in calvarial intramembranous bone formation and remodeling. *Development*. 2006;133:63–74.
221. Briana D, Boutsikou M, Baka S, Hassiakos D, Gourgiotis D, Malamitsi-Puchner A. Circulating osteoprotegerin and sRANKL concentrations in the perinatal period at term. The impact of intrauterine growth restriction. *Neonatology*. 2009;96:132–6.
222. Huang H, Wang J, Zhang Y, Zhu G, Li Y, Ping J, et al. Bone resorption deficiency affects tooth root development in RANKL mutant mice due to attenuated IGF-1 signaling in radicular odontoblasts. *Bone*. 2018;114:161–71.
223. Kong YY, Yoshida H, Sarosi I et al. OPGL is a key regulator of osteoclastogenesis. *Nature*. 1999;397:315–23.
224. Wise GE. Cellular and molecular basis of tooth eruption. *Orthod Craniofac Res*. 2009;12:67–73.
225. Wise GE, Lin F. The Molecular Biology of Initiation of Tooth Eruption. *J Dent Res*. 1995;74:303–6.
226. Li C, Lan Y, Jiang R. Molecular and Cellular Mechanisms of Palate Development. *J Dent Res*. 2017;96:1184–91.
227. Kitahara Y, Suda N, Kuroda T, Beck F, Hammond VE, Takano Y. Disturbed Tooth

- Development in Parathyroid Hormone-related Protein (PTHrP) -Gene Knockout Mice. *Bone*. 2002;30:48–56.
228. Ono W, Sakagami N, Nishimori S, Ono N, Kronenberg H. Parathyroid hormone receptor signalling in osterix-expressing mesenchymal progenitors is essential for tooth root formation. *Nat Commun*. 2016;1–16.
229. Decker E, Stellzig-Eisenhauer A, Fiebig B, Rau C, Kress W, Saar K, et al. PTHR1 Loss-of-Function Mutations in Familial, Nonsyndromic Primary Failure of Tooth Eruption. *Am J Hum Genet*. 2008;83:781–6.
230. Proffit W, Frazier-Bowers S. Mechanism and control of tooth eruption: overview and clinical implications. *Orthod Craniofac Res*. 2009;12:59–66.
231. Frazier-Bowers SA, Hendricks HM, Wright JT, Lee J, Long K, Dibble CF, et al. Novel Mutations in PTH1R associated with primary failure of eruption and osteoarthritis. *J Dent Res*. 2014;93:134–9.
232. Silva MAD, Vasconcelos DFP, Marques MR, Barros SP. Parathyroid hormone intermittent administration promotes delay on rat incisor eruption. *Arch Oral Biol*. 2016;69:102–8.
233. Piattelli A, Eleuterio A. Primary failure of eruption. *Acta Stomatol Belg*. 1991;88:127–30.
234. Frazier-Bowers S, Simmons D, Wright JT, Proffit W, Ackerman J. Primary failure of eruption and PTH1R: The importance of a genetic diagnosis for orthodontic treatment planning. *Am J Orthod Dentofac Orthop*. 2010;137:160.e1-160.e7.
235. Rhoads SG, Hendricks HM, Frazier-Bowers SA. Establishing the diagnostic criteria for eruption disorders based on genetic and clinical data. *Am J Orthod Dentofac Orthop*. 2013;144:194–202.

11. ANNEXES

Supplementary table 1. Primary and secondary antibodies used in this study.

Primary antibodies			
Anti-mouse RANK	Goat polyclonal IgG	R&D AF692	1/20
Anti-human/mouse RANKL	Rabbit polyclonal IgG	Abcam ab62516	1/20
Anti-mouse OPG	Goat polyclonal IgG	R&D AF805	1/10
Anti-mouse LGR4	Rabbit polyclonal IgG	ThermoFischer PA5-67868	1/100
Anti-mouse PCNA	Rabbit polyclonal IgG	Abcam ab2426	1/500
Anti-mouse P21	Rabbit polyclonal IgG	Santa Cruz Biotechnology SC-397	1/50
Anti-mouse KERATIN-14	Rabbit polyclonal IgG	Covance AF64	1/500 - 1/1000
Anti-mouse CD146	Rabbit monoclonal IgG	Abcam ab75769	1/100
Anti-mouse SOX9	Rabbit polyclonal IgG	Abcam ab3697	1/100
Anti-mouse CD68	Rat monoclonal IgG	MCA1957	1/100
Secondary antibodies			
Bovine anti-goat	Biotin-SP conjugated polyclonal whole IgG	Jakson Immuno Research 805-065-180	1/400
Goat anti-rabbit	Peroxidase conjugated polyclonal IgG	Dako P0448	1/200 – 1/500

Horse anti-rabbit	Biotin conjugated polyclonal IgG	Vector laboratories BA-1100	7/1000
Goat anti-rabbit	Alexa Fluor 594 conjugated polyclonal IgG	Life Technologies A-11072	1/500
Donkey anti-rat	Biotin-SP conjugated polyclonal whole IgG	Jackson ImmunoResearch 712-065-153	1/400

Supplementary table 2. Excluded articles and reasons for exclusion

Author(s), Year	Reason for exclusion
Al Ibrahim et al., 2003	2
Ata and Gustafson, 1961	9
Barry et al., 2003	4
Barry et al., 2007	9
Bertoin and Drouin, 1966	9
Cadenat and Hemous, 1958	9
Cainelli et al., 2017	1
Ciaramella et al., 1979	8
Déchaume et al., 1954	1
Dick and Simpson, 1972	9
Dyson, 1970	9
García et al., 2013	9
Gwinn et al., 1972	1
Hoppe and Wandel, 1967	9
Kaslick and Brustein, 1962	9
Khochtali et al., 1991	1
Leblebisatan et al., 2015	8
Lee et al., 2008	3
Leone et al., 1982	2
Lindenberg et al., 1982	1
Long et al., 2001	9
Mahdi et al., 1987	7
Makarem et al., 2012	9
Medvedev et al., 2016	3
Ocal et al., 2001	8
Ozmen et al., 1997	9
Plotz and Chakales, 1954	9
Rajathi et al., 2010	1
Reichenbach, 1954	9
Rey et al., 1971	9
Ruprecht et al., 1988	2

Saigal et al., 2015	9
Sarper et al., 2002	2
Shah et al., 1996	8
Sly et al., 1985	2
Smith R. et al., 1965	8
Steiner et al., 1983	9
Sutadi et al., 1999	3
Thomas et al., 1952	1
Thompson et al., 1969	2
Ullah et al., 2015	9
Younai et al, 1988	5
Zhang et al., 2017	8

- (1) Reviews, letters, personal opinions, book chapters, conference abstracts, posters, short communications and patents (n= 7);
- (2) Studies without maxillomandibular manifestations, dental and/or oral findings (n= 6);
- (3) Non roman languages (n= 3)
- (4) Studies with the same sample (n= 1);
- (5) *In vivo*, *Ex vivo* and *In vitro* studies (n= 1)
- (6) Osteopetrosis associated to other syndromes or pathological conditions (n= 0)
- (7) Studies with only caries reported as oral findings (n= 1)
- (8) Studies without clinical and/or radiological exams (n= 6)
- (9) Studies reporting less than 3 cases (n=18)

Supplementary table 3. Summary of the descriptive characteristics of included studies (N=12).

Authors, Year/ Country	Study design/sample	Sex (F/M)	Age /Age of diagnosis (y/mo)	Diagnostic Methods	Type of Osteopetrosis	Main skeletal and extra-skeletal features
Bénichou et al., 2000/France	Case Series/ N=42	20F/22M	Mean age: 39,5y/17, 8y	Clinical and radiographic examination	ADO type II	All patients included in the case series report had sandwich vertebrae. The radiographic bone within bone appearance was present in 94.4% of the patients. The radiographical penetrance of the disease was 90% and increased after 20 years of age. Clinical data were available from 37 patients. The most common clinical complications were fractures: 123/28 (78%), the femur was the most frequent fracture site. Besides, hip osteoarthritis: 10 patients (27%), 16 hips and thoracic or lumbar scoliosis: 9 (24%) and bone/ joint hip sepsis: 4 (11%) (8.1%) were reported. Extraskelatal features included: stomatologic manifestations; cranial nerves involvement responsible for facial palsy, hearing loss and visual loss.
Bjorvatn et al., 1979/Norway	Case Series/ N=4	1F/3M	1: 11y 2: 7y 3: 9y 4: 3y	Clinical and radiographic examination	Malignant Osteopetrosis	All four patients showed generalized osteopetrosis with typical radiographic features: hypermineralization, increased bone density, poor development of marrow space and « bone in bone » phenomenon. Besides, all had short stature and macrocephaly. Extra-skeletal manifestations included: enlarged liver and spleen, generalized lymphadenopathies, hemolytic anemia, thrombocytopenia, myelocytosis, blindness, buphthalmos, oral findings. Patients 3 and 4 have facial paresis and Patients 1 and 3 had a reduced sense of taste and smell. Homozygous mutations in the <i>TCIRG</i> gene were identified in three patients.

Détailleur et al., 2016/Belgium	Case Series N=4	F/M/F/NR	1: 31y/NR 2: 14y/3mo 3: 10y 4: 2.5y/3mo	Clinical and radiographic examination	1: Osteopetrosis without classification 2-4: ARO	All four patients showed increased bone density, bone marrow failure, blindness and deafness due to compression of cranial nerves. Also, dental manifestations with varying severity and extent.
Imanimoghaddam et al., 2009/Iran	Case Series N=4	1F/3M	1: 6y 2: 7y 3: 7y 4: 7y	Clinical and radiographic examination	Malignant osteopetrosis	All patients showed increased bone density. Patients 1 and 2 were siblings and both presented mental retardation, anemia, hepatosplenomegaly, impairment of vision, hearing loss and short stature. Craniofacial features such as hypertelorism, front bossing, exophthalmus, broad face, and snubbed nose were also observed. Patient 3 presented history of spleen removal, hypertelorism, frontal bossing and exophthalmos. Finally, Patient 4 presented short stature, broad face, frontal bossing, hypertelorism, snubbed nose, exophthalmus.
Kahler et al., 1984/USA	Case Series N=4	M/F/M/F	1: 8y 2: 13y 3: 10y 4: 21y	Clinical and radiographic examination CT scan	Mild ARO	Four individuals of the same kindred having intrafamilial variability of clinical and radiographic findings were reported. All of them presented radiographic changes of osteopetrosis: sclerosis of the cranial base, generally increased bone density, sclerosis of the vertebral end plates, and transverse bands and poor diaphyseal modelling of the long bones. Also, relative or absolute short stature; increased upper/lower segment ratio with decreased arm span; fractures, and mandibular prognathism. Extra-skeletal features such as moderate anemia with extramedullary hematopoiesis, and dental abnormalities were also observed.
Krithika et al., 2009/India	Case Series N=4	4M	1:18y 2:47y 3:8y	Clinical and radiographic and CT scan examination,	Not defined the type of osteopetrosis	All four reported individuals had generalized increased bone density and fractures. Patients 3,4 presented also stunted growth, genu

			4:16y			valgum. Vision and hearing impairment was observed in patient 1 and anemia, hepatosplenomegaly were reported in Patients 1 and 2.
Ohlsson et al., 1980/Saudi Arabia	Case Series N=4	M/F/M/F	1: 17 Mo 2: 3y8mo 3: 5y7Mo 4: 7y	Clinical and radiographic examination	ARO with renal tubular acidosis and cerebral calcifications.	Four individuals of three unrelated families were described. All patients had generalized increased bone density and renal tubular acidosis. Besides, all had slow psychomotor development. Patient 2 presented recurrent fractures and calcification in the basal ganglia. Both patients 2 and 4 presented genu valgum anemia.
Ohlsson et al., 1986/Canada	Case Series N=4	4M	1: 2y 2: 10y 3: 8y 4: 23 days	Clinical and radiographic examination	ARO with renal tubular acidosis and cerebral calcifications.	Four individuals from two unrelated Saudi Arabian families were reported. All patients had slow physical and psychomotor development, generalized osteosclerosis and renal tubular acidosis. Patients 2 and 3 presented genu valgum without biochemical evidence of rickets. Optic atrophy was observed in three (patients 1-3). Also, patients 1 and 2 had iron deficiency anemia and patient 2 presented intracranial calcifications in the basal ganglia. The 23 days old child (patient 4) also had slight sclerosis of the distal ends of the phalanges and fifth digit and clinodactyly with middle phalangeal hypoplasia.
Rikhotso et al., 2008/South Africa	Case Series N=3	2M/1F	1: 12y/6mo 2: 26y 3: 18y	Clinical and radiographic examination	1: Malignant ARO 2: Benign osteopetrosis 3: Benign osteopetrosis	Three unrelated individuals were reported. Patient 1 had short stature, valgus deformity and spontaneous long bone fractures. Craniofacial findings included macrocephaly and frontal bossing and jaw osteomyelitis. Extra-skeletal features such as hepatosplenomegaly, anemia, blindness and decreased auditory acuity was reported. Patients 2 and 3 reported neuralgic facial pain and hearing impairment.
Sonia et al., 2005/Tunisia	Case Series N=24	10F/14M	Age range: 7 days - 17y	Clinical, radiographic examination	Carbonic anhydrase II deficiency osteopetrosis	All 24 individuals in the series case report had osteosclerosis, defective skeletal remodeling, metabolic acidosis, facial dysmorphia, proptosis, frontal bossing. Genetically, all

						patients had a homozygous splice junction mutation in intron 2 of the CA 2 gene and 18 cases had reduction of carbonic anhydrase II activity in erythrocytes. Twenty patients reported one or more fractures. Short stature was frequently reported (85.5%) as well as cerebral calcifications (70.8%) and mental retardation (52%). Optic nerve atrophy and visual impairment was observed in 25% and 33.3% respectively.
Trapnell et al., 1968 England	Case Series N=3	1M/2F	1: 24y 2: 28y 3: 26y	Clinical and radiographic examination	Not defined the type of osteopetrosis	Three individuals with osteopetrosis and jaw osteomyelitis were reported. Two individuals reported multiple fractures (patients 1 and 3) while patient 2 had typical mild radiopacity changes.
Wong et al., 1978 USA	Case Series N=6	1F/5M	Diagnosis age range: soon after birth to 8 months	Clinical and radiographic, CT scan, ultrasonography examination	Malignant Osteopetrosis	All six patients in the case series report presented generalized dense bone, growth and developmental retardation, chronic nasal congestion and anemia. Craniofacial findings included hydrocephalus (5/6), frontal bossing, proptosis and hypertelorism (1/6). Besides, hepatosplenomegaly (4/6), blindness (4/6), facial nerve paresis/paralysis (3/6) were reported.

Abbreviation: NR: Not Reported; ADO: Autosomal Dominant Osteopetrosis; ARO: Autosomal Recessive Osteopetrosis; F/M: Female/Male; CT: Computed Tomography; mo: months; y: years

Supplementary table 4. The JBI critical appraisal modified checklist for case series and prevalence studies – quality assessment

	Bénichou et al., 2000	Bjorvatn et al., 1979	Détailleux et al., 2016	Imanimoghaddam et al., 2009	Kahler et al., 1984	Krithika et al., 2009	Ohlsson et al., 1980	Ohlsson et al., 1986	Rikhotso et al., 2008	Sonia et al., 2005	Trapnell et al., 1968	Wong et al., 1978
1. Were the clear criteria for inclusion in the case series?	Y	Y	Y	Y	Y	Y	Y	Y	Y	Y	Y	Y
2. Was the sample frame appropriate to address the target population?	Y	Y	Y	Y	Y	Y	Y	Y	Y	Y	Y	Y
3. Was the condition measured in a standard, reliable way for all participants included in the case series?	Y	Y	Y	Y	U	Y	Y	Y	Y	Y	U	Y
4. Were valid methods used for identification of the condition for all participants included in the case series?	Y	Y	Y	Y	U	Y	N	N	Y	U	N	Y
5. Was there clear reporting of clinical information of the participants?	Y	Y	Y	Y	U	Y	Y	Y	Y	Y	N	Y
6. Was there clear reporting of the demographics of the participants in the study?	Y	Y	Y	Y	Y	Y	Y	Y	Y	Y	N	Y
7. Were the outcomes and follow up results of cases clearly reported?	Y	Y	Y	Y	U	U	U	Y	Y	Y	N	U
8. Were the subjects and setting described in detail?	U	Y	Y	Y	Y	Y	U	U	Y	N	N	Y
9. Was the data analysis conducted with sufficient coverage of the identified sample?	U	Y	Y	Y	Y	Y	N	N	Y	N	U	Y

The Joanna Briggs Institute. Joanna Briggs Institute Reviewers' Manual: 2016 edition. Australia: The Joanna Briggs Institute; 2016
 Abbreviation: JBI: Joanna Briggs Institute; Yes (Y); No (N); Unclear (U).

Supplementary table 5. Descriptive summary of the oral and dental findings in the included studies (N=12)

AUTHOR/YEAR/ COUNTRY	SAMPLE	TYPE OF OSTEOPETROSIS	DIAGNOSTIC METHODS	ORAL AND DENTAL FINDINGS			
				Osteomyelitis	Eruption defects	Dental Anomalies	Other oral findings
Bénichou et al., 2000 France	N=31	ADO type II	Clinical and radiographic examination	Mandibular osteomyelitis: 4/31 (12.9%).	NR	NR	Multiple dental abscesses: 3/31 (9.7%). Multiple non trauma-related tooth fractures: 1/31. 123 total fractures: Tooth fractures: 3/123.
Bjorvatn et al., 1979 Norway	N=4	Malignant osteopetrosis	Clinical and radiographic examination	Mandibular osteomyelitis (patients 1,2 and 3)	ND	Malformed primary molars and permanent teeth No root formation in posterior teeth.	Reduced temporomandibular joints movements Broad alveolar ridges Lower palate vault Mobile erupted teeth, poor fibrous attachment, periodontitis Spontaneous crown fracture of incisors (Patients 1, 2 and 4)
Détailleur et al., 2016 Belgium	N=4	1: Osteopetrosis without classification 2-4: ARO	Clinical and radiographic examination	NR	1 : Slow eruption process and unerupted teeth in permanent dentition. 2 : Upper lateral primary incisors unerupted. lower left primary molar retention. Slower eruption rate in permanent dentition. 3 : Impacted molar in the third quadrant and two impacted molars in the fourth quadrant in primary dentition. Ankylosis and infraocclusion of primary first molars Slow rate eruption, impacted second upper right molars and first premolar in permanent dentition. 4 : NR	1 : Lower central incisors, lower canines and right upper canine agenesis, and crown malformation in primary dentition. Teeth agenesis, supernumerary teeth in anterior maxilla, crown and root malformations, lower quality enamel in permanent dentition. Primary dentition indistinguishable from the permanent dentition. 2 : Lower lateral incisor agenesis, smaller crowns and shorter roots in primary teeth. Left lower premolars agenesis, malformed crowns, aberrant tooth formation at the region of the lateral upper incisors and the upper right second molar, malformed or absent roots in permanent dentition. 3 : Left lower incisors fused, abnormal crown forms, pits and decalcifications, shorter and malformed roots in primary dentition.	1 : NR 2 : NR 3 : NR 4 : NR

						Multiple premolars agenesia, hypercalcified teeth with pits and grooves, malformed crowns and roots in permanent dentition. 4 : Enamel pits, lingual notch on four molars, sharp forms in primary dentition.	
Imanimoghaddam et al., 2009 Iran	N=4	Malignant osteopetrosis	Clinical and radiographic examination (Panoramic Rx)	3 : Chronic osteomyelitis in the mandible. 4 : Mandibular osteomyelitis.	1 and 2 : Impacted and unerupted teeth 4: Delayed eruption of permanent teeth, impacted teeth, retention of primary teeth.	3: Absence of lower premolars. Few malformed erupted teeth. 4 : Defect in periodontal ligament and missing roots in the mandibular molar	1 and 2 : Sclerotic maxilla and mandible. 3: Generalized radiopacity. 4 : Bone expansion due to periosteal reaction.
Kahler et al., 1984 USA	N=4	Mild ARO	Intraoral and radiographic examination CT scan	1: Chronic osteomyelitis in the mandible 2: Chronic osteomyelitis in the mandible 3: NR 4: NR	1: Retained primary teeth, impacted permanent teeth 2: NR 3: Retained primary and impacted teeth 4: Primary and impacted permanent teeth in the mandible and maxilla.	1: Deformed crowns 2: Oligodontia, severe crown deformities 3: Misshapen teeth 4: Misshapen teeth, oligodontia	1: NR 2: NR 3: Slight mandibular prognathism 4: Mandibular prognathism
Krithika et al., 2009 India	N=4	Not defined the type of osteopetrosis	Intraoral, extraoral and radiographic examination, CT scan	1: Maxillary osteomyelitis 2: Mandibular osteomyelitis. 3: Maxillary osteomyelitis bilaterally. 4: Maxillary osteomyelitis.	1: Lower second primary molar retained 2: NR 3: NR 4: Multiple retained deciduous teeth, missing permanent second molars and premolars, retained and ankylosed left second deciduous molar, unerupted premolars and permanent second molars	1: Multiple missing permanent teeth 2: NR 3: NR 4: Generalized enamel hypoplasia	1: NR 2: Generalized osteosclerosis of the maxilla and mandible 3: NR 4: NR
Ohlsson et al., 1980 Canada	N=4	ARO with renal tubular acidosis and cerebral calcifications	Clinical and radiographic examination	1: NR 2: NR 3: NR 4: NR	1: Delayed eruption 2: NR 3: NR 4: NR	1: NR 2: Peg-shaped teeth 3: Peg-shaped teeth	1: NR 2: Malocclusion 3: Malocclusion 4: NR

						4: Peg-shaped primary teeth, enamel hypoplasia	
Ohlsson et al., 1986 Saudi Arabia	N=4	ARO with renal tubular acidosis and cerebral calcifications	Clinical examination	1: NR 2: Maxillary osteomyelitis. 3: NR 4: NR	1 : NR 2: NR 3: NR	1: Abnormal teeth with enamel hypoplasia 2: Abnormal teeth with several teeth missing, enamel hypoplasia. 3: Abnormal peg-shaped teeth with enamel hypoplasia.	1: Malocclusion. 2: Small lower jaw. 3: Small lower jaw.
Rikhotso et al., 2008 South Africa	N=3	1: Malignant ARO 2: Benign osteopetrosis 3: Benign osteopetrosis	Clinical and radiographic examination	1: Mandibular/ maxillary osteomyelitis 2: NR 3: NR	1: Only maxillary premolars erupted, multiple unerupted teeth. 2: NR 3: NR	1: NR 2: Multiple missing teeth. 3: NR	1: NR 2: Mid-face deficiency, prognathism, posterior mandibular alveolous enlargement, large bilateral mandibular lingual tori, hyperdense mandibular and maxillary bones. 3: Broad and flat face with a prominent chin, diffuse hyperdense maxilla and mandible, compression of the inferior alveolar nerve.
Sonia et al., 2005 Tunisia	N=24	Carbonic anhydrase II deficiency osteopetrosis	Clinical, radiographic examination, Classic PCR, asymmetric PCR	Maxillary osteomyelitis (2/24)	Impacted teeth	Odontoma-like structures	Micrognathism, hyperdense maxilla and mandible
Trapnell, 1968 England	N=3	Not defined the type of osteopetrosis	Clinical and radiographic examination	1: Mandibular osteomyelitis 2: Maxillary osteomyelitis 3: NR	1: NR 2: NR 3 :NR	1: NR 2: NR 3 :NR	1: Thickened lamina dura 2: Dense and thick lamina dura around each tooth. 3: Thickened lamina dura around the teeth and the margins of the mandibular canal.
Wong et al., 1978 USA	N=6	Malignant Osteopetrosis	Clinical and radiographic examination, CT Scan, Ultrasonography	NR	Delayed dental eruption: 2/6 (no teeth by one year of age)	NR	Prominent alveolar ridges: 2/6 Hypoplastic mandible: 3/6 High-arched palate: 6/6

Abbreviation: NR: Not Reported; F/M: Female/Male; CT: Computed Tomography; Mo: Months; Y: years ; ND : Not Described /mentioned feature but not quantified in the sample ; NR : Not Reported ; ADO : Autosomal Dominant Osteopetrosis ; ARO : Autosomal Recessive Osteopetrosis.

Supplementary Table 6. Eruption defects distribution in the overall sample (N=95 patients)

STUDY	SAMPLE	TYPE OF OSTEOPETROSIS	ERUPTION DEFECTS					GENERAL ERUPTION DEFECTS
			DELAYED ERUPTION PROCESS	UNERUPTED TEETH	ANKYLOSIS	INFRAOCCCLUSION	RETENTION OF PRIMARY TEETH	
Bénichou et al., 2000	N=31	ADO type II	-	-	-	-	-	-
Bjorvatn et al., 1979	N=4	Malignant osteopetrosis	-	-	-	-	-	ND
Détailleux et al., 2016	N=4	1: Osteopetrosis without classification 2-4: ARO	3/4	3/4	1/4	1/4	-	-
Imanimoghaddam et al., 2009	N=4	Malignant osteopetrosis	1/4	3/4	-	-	1/4	-
Kahler et al., 1984	N=4	Mild ARO	-	3/4	-	-	2/4	-
Krithika et al., 2009	N=4	Not defined the type of osteopetrosis	-	1/4	1/4	-	2/4	-
Ohlsson et al., 1980	N=4	ARO with renal tubular acidosis and cerebral calcifications	1/4	-	-	-	-	-
Ohlsson et al., 1986	N=4	ARO with renal tubular acidosis and cerebral calcifications	-	-	-	-	-	-
Rikhotso et al., 2008	N=3	1: Malignant ARO 2: Benign osteopetrosis 3: Benign osteopetrosis	-	1/3	-	-	-	-
Sonia et al., 2005	N=24	Carbonic anhydrase II deficiency osteopetrosis	-	ND	-	-	-	-
Trapnell, 1968	N=3	Not defined the type of osteopetrosis	-	-	-	-	-	-
Wong et al., 1978	N=6	Malignant Osteopetrosis	2/6	-	-	-	-	-

Abbreviation : ND: Not Described or mentioned features not quantified in the sample; - : Not Reported ; ADO : Autosomal Dominant Osteopetrosis ; ARO : Autosomal Recessive Osteopetrosis.

Supplementary table 7. Oral and dental findings distribution in the overall study sample (N=95 patients)

STUDY	SAMPLE	TYPE OF OSTEOPETROSIS	ORAL FINDINGS DISTRIBUTION														
			OSTEOMYELITIS		ERUPTION DEFECTS	DENTAL ANOMALIES				ROOT ANOMALIES	OTHER ORAL FINDINGS						
			MAXILLA	MANDIBLE		NUMBER	SIZE	SHAPE	STRUCTURE		BONE DEVELOPMENT DISORDERS	PERIODONTAL INFLAMMATORY DISORDERS	TMJ DISORDERS	NON-TRAUMA RELATED TOOTH FRACTURE	MALOCCLUSION		
									TEETH AGENESIS							SUPERNUMERARY TEETH	ENAMEL
Bénichou et al., 2000	N=31	ADO type II	-	4/31	-	-	-	-	-	-	-	-	-	3/31	-	1/31	-
Björvatn et al., 1979	N=4	Malignant osteopetrosis	-	3/4	ND	-	-	ND	-	-	ND	ND	ND	ND	ND	3/4	-
Détailleur et al., 2016	N=4	1: Osteopetrosis without classification 2-4: ARO	-	-	3/4	3/4	1/4	1/4	4/4	2/4	-	3/4	-	-	-	-	1/4
Imanimoghdam et al., 2009	N=4	Malignant osteopetrosis	-	2/4	3/4	1/4	-	1/4	-	-	1/4	3/4	1/4	-	-	-	-
Kahler et al., 1984	N=4	Mild ARO	-	2/4	3/4	2/4	-	4/4	-	-	-	2/4	-	-	-	-	-
Krithika et al., 2009	N=4	Not defined the type of osteopetrosis	3/4	1/4	2/4	2/4	-	-	-	1/4	-	1/4	-	-	-	-	-
Ohlsson et al., 1980	N=4	ARO with renal tubular acidosis and cerebral calcifications	-	-	1/4	-	-	-	3/4	1/4	-	-	-	-	-	-	2/4
Ohlsson et al., 1986	N=4	ARO with renal tubular acidosis and cerebral calcifications	1/4	-	-	-	-	-	3/4	3/4	-	-	3/4	-	-	-	1/4
Rikhotso et al., 2008	N=3	1: Malignant ARO 2: Benign osteopetrosis 3: Benign osteopetrosis	1/3	1/3	1/3	1/3	-	-	-	-	-	-	2/3	-	-	-	-
Sonia et al., 2005	N=24	Carbonic anhydrase II deficiency osteopetrosis	2/24	-	ND	-	-	-	ND	-	-	ND	-	-	-	-	-
Trapnell et al., 1968	N=3	Not defined the type of osteopetrosis	1/3	1/3	-	-	-	-	-	-	-	-	2/3	3/3	-	-	-
Wong et al., 1978	N=6	Malignant Osteopetrosis	-	-	2/6	-	-	-	-	-	-	6/6	-	-	-	-	-

Abbreviations : ND: Not described or mentioned features not quantified in the sample. ; - : Not Reported ; ADO : Autosomal Dominant Osteopetrosis ; ARO : Autosomal Recessive Osteopetrosis.

Supplementary Table 8. Quantification of epithelial cells of the Hertwig's epithelial root sheath (HERS) based on keratin-14 staining by genotype and age in both the lingual and the buccal regions.

		<i>Rankl^{+/+}</i>	<i>Rankl^{+/-}</i>	<i>Rankl^{-/-}</i>	<i>Rankl^{Tg}</i>
LINGUAL	3 days	0.0±0.0	0.0±0.0	0.0±0.0	5.8±0.8
	5 days	11.4±1.1	13.2±0.8	5.4±1.1	17.2±0.8
	7 days	17.2±1.5	15.0±1.6	7.2±0.8	13.4±1.1
BUCCAL	3 days	10.0±2.0	13.8±1.9	0.0±0.0	13.6±1.5
	5 days	14.8±1.3	27.4±0.9	6.8±1.3	34.8±1.1
	7 days	22.8±1.9	21.0±1.0	4.4±1.1	12.4±1.8

Supplementary Table 9. Evaluation of the PCNA labeling intensity in the apical area of the mandible first molar root according to genotype and age

		PCNA labeling intensity			
		-	+	++	+++
Rankl^{+/+}	3 days			1	4
	4 days		1	3	1
	5 days		2	2	1
	6 days		1	2	2
	7 days		3	2	
Rankl^{+/-}	3 days		1	2	2
	4 days		2	1	2
	5 days		1	3	1
	6 days		2	2	1
	7 days		3	2	
Rankl^{-/-}	3 days	3	2		
	4 days	4	1		
	5 days	5			
	6 days	5			
	7 days	5			

Quantification was realized on sections of five different mice for each group (genotype) and each age (all from post-natal day 3 to 7). -: no detection; +: low staining intensity; ++: intermediary staining intensity; +++: high staining intensity.

Supplementary Table 10. Evaluation of P21 labeling intensity in the apical area of the mandible first molar root according to genotype and age.

		P21 labeling intensity			
		-	+	++	+++
Rankl^{+/+}	3 days		1	4	
	4 days	1	4		
	5 days	1	4		
	6 days	1	4		
	7 days	1	3	1	
Rankl^{+/-}	3 days	5			
	4 days	1	4		
	5 days	1	4		
	6 days	1		4	
	7 days	2	3		
Rankl^{-/-}	3 days				5
	4 days				5
	5 days				5
	6 days				5
	7 days				5

Quantification was realized on sections of five different mice for each group (genotype) and each age (all from post-natal day 3 to 7). -: no detection; +: low staining intensity; ++: intermediary staining intensity; +++: high staining intensity.




12. PUBLISHED PAPERS

12.1. PAPER 1



Article

Maternal RANKL Reduces the Osteopetrotic Phenotype of Null Mutant Mouse Pups

Benjamin Navet ^{1,†}, Jorge William Vargas-Franco ^{1,2,†}, Andrea Gama ^{3,†}, Jérôme Amiaud ¹, Yongwon Choi ⁴, Hideo Yagita ⁵, Christopher G. Mueller ⁶ , Françoise Rédini ¹, Dominique Heymann ^{7,8} , Beatriz Castaneda ³ and Frédéric Lézet ^{1,*} 

¹ INSERM, UMR 1238, Faculté de Médecine, Université de Nantes, F-44035 Nantes, France; Benjamin.navet@univ-nantes.fr (B.N.); jerome.amiaud@univ-nantes.fr (J.A.); Françoise.redini@univ-nantes.fr (F.R.)

² Department of Basic Studies, Faculty of Odontology, University of Antioquia, Medellin AA 1226, Colombia; jorge.vargas@udea.edu.co

³ INSERM, UMR-1138, Equipe 5, Centre de Recherche des Cordeliers, F-75006 Paris, France; dea.gama10@gmail.com (A.G.); Bea.castaneda.1@gmail.com (B.C.)

⁴ Department of Pathology and Laboratory Medicine, School of Medicine, University of Pennsylvania, Philadelphia, PA 19104, USA; ychoi3@penmedicine.upenn.edu

⁵ Department of Immunology, School of Medicine, Juntendo University, Tokyo 113-8421, Japan; hyagita@med.juntendo.ac.jp

⁶ CNRS, UPR-9021, Laboratoire Immunologie et Chimie Thérapeutiques, Institut de Biologie Moléculaire et Cellulaire (IBMC), Université de Strasbourg, F-67084 Strasbourg, France; c.mueller@ibmc-cnrs.unistra.fr

⁷ INSERM, LEA Sarcoma Research Unit, Department of Oncology and Human Metabolism, Medical School, University of Sheffield, Sheffield S10 2RX, UK

⁸ INSERM, UMR 1232, LabCT, Université de Nantes, Université d'Angers, Institut de Cancérologie de l'Ouest, site René Gauducheau, F-44805 Saint-Herblain, France; Dominique.Heymann@univ-nantes.fr

* Correspondence: frederic.lezet@univ-nantes.fr; Tel.: +33-240-412-846; Fax: +33-240-412-860

† These authors contributed equally.

Received: 12 October 2018; Accepted: 6 November 2018; Published: 8 November 2018



Abstract: RANKL signaling is implicated in the morphogenesis of various organs, including the skeleton. Mice invalidated for *Rankl* present an osteopetrotic phenotype that was less severe than anticipated, depending on RANKL's implication in morphogenesis. The hypothesis of an attenuated phenotype, as a result of compensation during gestation by RANKL of maternal origin, was thus brought into question. In order to answer this question, *Rankl* null mutant pups from null mutant parents were generated, and the phenotype analyzed. The results validated the presence of a more severe osteopetrotic phenotype in the second-generation null mutant with perinatal lethality. The experiments also confirmed that RANKL signaling plays a part in the morphogenesis of skeletal elements through its involvement in cell-to-cell communication, such as in control of osteoclast differentiation. To conclude, we have demonstrated that the phenotype associated with *Rankl* invalidation is attenuated through compensation by RANKL of maternal origin.

Keywords: RANKL; skeletal growth; morphogenesis; osteoclast; bone; mandible; tooth

1. Introduction

RANKL (TNFSF11) signaling is implicated in the development, histogenesis, and functional homeostasis of various tissues, particularly lymphoid tissues, skin appendages (hair, teeth, and mammary glands) and skeletal components [1–8]. During development, expression of RANKL, as well as expressions of its receptors RANK and OPG, have been reported in the spleen [9],

thymus [10,11], lymph nodes [12,13], hair [14], teeth [15,16], mammary glands [17,18], and bones, regardless of the ossification process involved: endochondral [19–21] or intramembranous [19,20]. In bone development, during endochondral ossification, RANKL expression by the pre-hypertrophic and hypertrophic chondrocytes is crucial for the differentiation and activation of osteoclasts that resorb the primary spongiosa, making trabecula formation possible [21–23]. During intramembranous ossification, RANKL is expressed by mesenchymal cells and actively synthesizes osteoblasts [19], which are of importance for woven bone resorption and replacement by lamellar bone. It was, therefore, unsurprising that loss of RANKL function was associated with osteoclast-poor osteopetrosis in young patients with RANKL mutations (autosomal recessive form, OPTB2; OMIM #259710; [24]) and in *Rankl* null mutant mice [1,5], as well as in monkeys or mice injected with a powerful RANKL-blocking antibody [25–27].

On the contrary, when RANKL was overexpressed, for instance, when produced genetically in pigs [28] and mice [29], a severe osteolytic phenotype was observed that led to premature death. This phenotype was in line with those associated with the gains in RANK function observed in patients with mutations (duplications) in the RANK signal peptide, leading to three seemingly homologous pathologies (familial expansile osteolysis, Paget disease of bone 2, expansile skeletal hyperphosphatasia) [30,31], as well as in mice overexpressing RANK [16,32].

All these observations underline the fact that finely tuned control of RANKL expression/function is required during the entire skeletal development process, from the early stages (antenatal) to adulthood.

RANKL was discovered as a cytoplasmic membrane-bound cytokine, but a soluble form was also evidenced [33]. Given the fact that RANKL is expressed in many tissues during embryonic development, and taking into account that soluble RANKL of maternal origin may cross the placenta, the question of the presence of an attenuated phenotype in young OPTB2 patients, as well as in *Rankl* null mutants from heterozygous mothers, was raised.

In order to answer this question, the skeletal phenotype of *Rankl* null mutant mice was compared at one day post-natal between mouse pups obtained from heterozygous vs. homozygous parents. Injections of a RANKL-blocking antibody were also performed on heterozygous mothers during the second half of gestation, to enhance the demonstration.

2. Materials and Methods

2.1. Animals and Drug Administration

All C57BL/6J mice used in the experiments were housed in pathogen-free conditions at the Experimental Therapy Unit at the medical faculty at the University of Nantes (Nantes, France), in accordance with the institutional guidelines of the French Ethical Committee (CEEA-PdL-06, accepted protocol number 00165.01) and under the supervision of authorized investigators. Newborn mice were used for the experiments.

The *Rankl* heterozygous mice were generated as previously described [5] by homologous recombination. Genotyping was carried out using PCR with the following primers 5'-*Rankl*: CCAAGTAGTGGATTCTAAATCCTG; 3'-*Rankl*: CCAACCTGTGGACTTACGATTAAAG; and 3'-insert: ATTCGACGCGCATCGCCTTCTATC.

First- and second-generation null mutant pups were obtained by mating heterozygous and homozygous animals, respectively. The nomenclature used for the different animals obtained is presented in Supplementary Figure S1.

Some heterozygous pregnant mice were injected IP three times during the second part of gestation with 2 mg/kg of a mouse-specific RANKL-blocking antibody, IK22.5, following a protocol summarized in Supplementary Figure S1D.

2.2. MicroCT Analysis

Analyses of the bone microarchitecture were performed using a Skyscan 1076 in vivo microCT scanner (Skyscan, Kontich, Belgium). Tests were performed after sacrifice on the tibias and heads of each animal. All tibias and heads were scanned using the same parameters (pixel size 9 μm , 50 kV, 0.5 mm Al filter, 10 minutes of scanning). The reconstructions were analyzed using NRecon and CTan software (Skyscan, Kontich, Belgium). 3D visualizations of the tibias and heads were made using ANT software (Skyscan, Kontich, Belgium).

2.3. Histology

Whole skeletons, collected from euthanized one-day pups, were fixed in 4% buffered paraformaldehyde. Samples were decalcified in 4.13% EDTA/0.2% paraformaldehyde pH 7.4 over 4 days in KOS sw10 (Milestone, Sorisole, Italy). The specimens were dehydrated and embedded in paraffin. Then, 3 μm -thick sagittal sections stained with Masson's trichrome were observed using a DMRXA microscope (Leica, Nussloch, Germany). Tartrate-resistant acid phosphatase (TRAP) staining was performed on sample sections to identify multinucleated osteoclast-like cells after 90 min' incubation in 1 mg/mL of Naphthol AS-TR phosphate, 60 mmol/L *N,N*-dimethylformamide, 100 mmol/L sodium tartrate, and 1 mg/mL Fast Red TR Salt solution (all from Sigma Chemical Co., St. Louis, MO, USA), and counterstained with hematoxylin.

2.4. Immunohistochemistry

Immunohistochemistry was performed as previously described [34], using antibodies from Abcam (Cambridge, UK; ab75769 for CD146 and ab3697 for SOX9) and Bio-Rad (Marnes-la-Coquette, France; MCA1957 for CD68).

3. Results

3.1. Second-Generation Rankl Null Mutants Had a More Severe Craniofacial Phenotype

At birth, first-generation *Rankl* null mutants ($N = 5$) had a craniofacial osteopetrotic phenotype with an open foramen, due to delayed mineralization of the calvaria and delayed tooth development, associated with an absence of osteoclasts (Figures 1 and 2). As part of the craniofacial skeleton develops during the second half of gestation, and taking into account that secreted forms of RANKL of maternal origin may be active in the embryo, the question of an attenuated craniofacial phenotype in first-generation *Rankl* null mutants was raised. In order to answer this question, second-generation *Rankl* null mutant pups were generated by mating male and female *Rankl* null mutants. The craniofacial phenotype of the second-generation null mutants ($N = 5$) was more severe than the phenotype of the first-generation mutants, with a more open foramen (Figure 1) and more delayed tooth morphogenesis (Figure 2). In addition, a loss in mandible curvature was observed (Figure 1), associated with defective disruption of the Meckel cartilage (Figure 2). A similar craniofacial phenotype was observed in null mutant pups ($N = 2$) from null mutant females mated with heterozygous males (Figure 3), confirming the importance of RANKL of maternal origin.

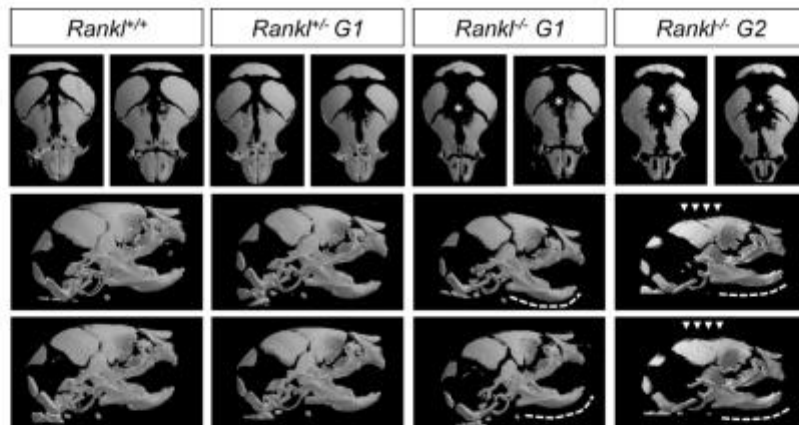


Figure 1. MicroCT comparative analysis of the craniofacial skeletons of first- and second-generation *Rankl* null mutant mice. Second-generation null mutants had enlarged foramen (stars and arrowheads) compared with first-generation null mutants. Percentage of closure measures (surface) for the different genotypes are 89 ± 2 for $+/+$, 84 ± 3 for $+/-$, 67 ± 4 for $G1-/-$ and 57 ± 5 for $G2-/-$. Moreover, the mandibles of second-generation null mutants appeared flat, with missing proximo-distal curvature (dotted lines). Angle of the mandible curvature measures (opening degrees) for the different genotypes are 134 ± 9 for $+/+$, 136 ± 11 for $+/-$, 139 ± 9 for $G1-/-$ and 163 ± 7 for $G2-/-$. No difference was observed between the wild type and heterozygous pups. Numbers of pups: 4 $+/+$, 8 $G1+/-$, 5 $G1-/-$, and 5 $G2-/-$.

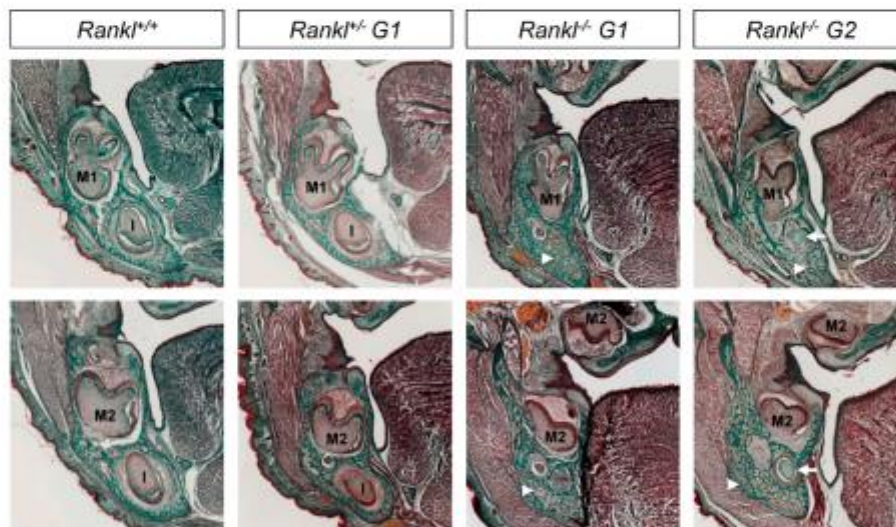


Figure 2. Histological comparative analysis of the craniofacial skeletons of first- and second-generation *Rankl* null mutant mice. Frontal sections of the head in planes of first (M1) and second (M2) molars revealed more severe osteopetrosis in the second-generation ($Rankl^{-/-} G2$) compared to the first-generation ($Rankl^{-/-} G1$) null mutants. While both null mutants revealed increased bone density compared to wild type and heterozygous mice (arrowheads), the second-generation null mutants had a remnant Meckel cartilage (arrow) and a very significant delay in the development of first and second molars, with the second molar appearing to be blocked between the cap and bell stages. Comparison of sections from wild type and heterozygous pups revealed a pre-osteopetrotic phenotype in the heterozygous mice, with increased bone density and delayed moving back of the incisor (I) in the mandible. Magnification $40\times$ for all images. Numbers of pups: 4 $+/+$, 8 $G1+/-$, 5 $G1-/-$, and 5 $G2-/-$.

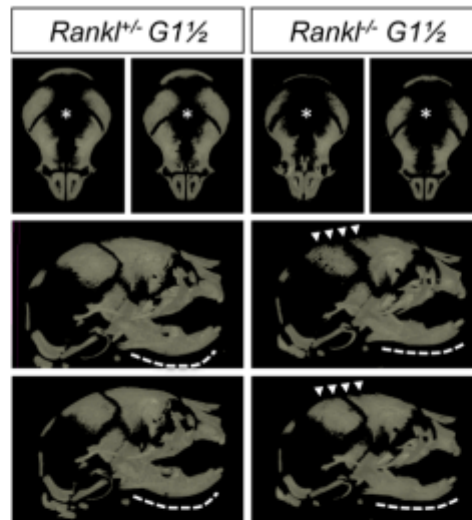


Figure 3. MicroCT comparative analysis of the craniofacial skeleton of pups born from null mutant females and heterozygous males. Heterozygous and null mutant pups revealed craniofacial phenotypes that were respectively similar to first- and second-generation null mutants. Enlarged foramina (stars) were present, more pronounced in the null mutants (arrowheads), and the mandibles of the null mutants appeared flat (dotted lines) as in the second-generation null mutants. Percentage of closure measures (surface) for the two genotypes are 65 ± 4 for $+/-$ and 54 ± 7 for $-/-$. Angle of the mandible curvature measures (opening degrees) for the two genotypes are 133 ± 10 for $+/-$, 159 ± 12 for $1 -/-$. Numbers of pups: 4 $+/-$ and 2 $-/-$.

3.2. Second-Generation *Rankl* Null Mutants Had a More Severe Long Bone Phenotype

At birth, first-generation *Rankl* null mutants had a long bone osteopetrotic phenotype with delayed formation of the bone medullary cavity, as clearly seen by microtomography and histology (Figure 4). This appeared to be secondary to an absence of resorption of the spongy bone in the primary ossification center at the diaphysis site (TRAP staining in Figure 4). Interestingly, an intermediary phenotype was observed in the heterozygous mice, suggesting probable haplo-insufficiency (Figure 4). This was supported by graduated decreases in TRAP staining and CD68 monocyte/macrophage lineage immunodetection from the wild type through the heterozygous to the null mutant mice (Figure 4; Enlargements in Supplementary Figure S2). Moreover, a grade increase in detection of the vasculature marker (CD146) was revealed using immunohistochemistry from the WT through the heterozygous to the null mutant mice (Figure 4). The long bone phenotype of the second-generation null mutants was more severe than the phenotype of first-generation mutants (Figure 4; Enlargements in Supplementary Figure S2), suggesting an attenuated long bone phenotype in the first-generation null mutants. Interestingly, while no TRAP-positive cells were detected in the second-generation null mutant, small round CD68 cells seemed to accumulate in the restricted subchondral area (Figure 4), and there was significant CD146 staining. Surprisingly, immunohistochemistry revealed an almost complete lack of SOX9 expression, but only in the second-generation null mutants, with very weak staining in just a few chondroblastic cells, and no staining in the periosteal osteoblastic cells (Figure 5), whereas both mutants evidenced an apparently normal growth plate thickness with, however, disorganized chondrocyte columns (Figure 5).

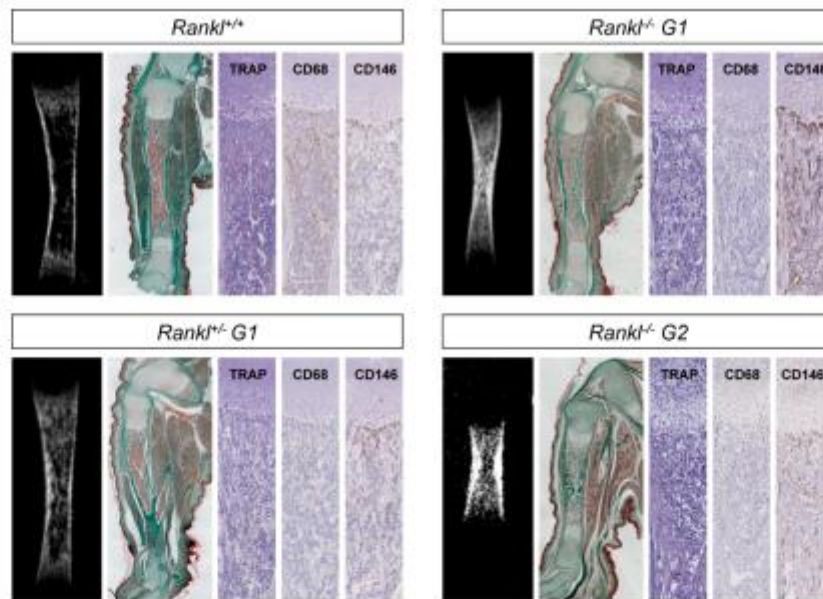


Figure 4. MicroCT (mCT) and histological comparative analysis of the appendicular skeleton of first- and second-generation *Rankl* null mutant mice. Tibias were chosen as representative bone of the appendicular skeleton. Second-generation null mutants revealed significantly delayed tibia development in comparison with first-generation null mutants, as shown by mCT and Masson trichrome staining. Interestingly, comparing the mCT and histological sections of wild type and heterozygous pups revealed a pre-osteopetrotic phenotype in the heterozygous pup. TRAP staining was observed in wild type and heterozygous pups, with a lower number of stained cells in the heterozygous pups. CD68 immunostaining decreased gradually (in intensity and number of stained-cells) from the wild type to the first-generation null mutant pups. No TRAP expression was observed in the second-generation null mutants, while small, round CD68 cells were visible in the subchondral area. CD146 immunostaining increased gradually (in terms of intensity and number of stained cells) from wild type to first-generation null mutant pups, while it was comparable in first- and second-generation null mutant pups. Masson trichrome magnification 10×; TRAP, CD68, and CD146 magnification 40×. Numbers of pups: 4 +/+, 8 G1+/-, 5 G1-/-, and 5 G2-/-.

SOX 9

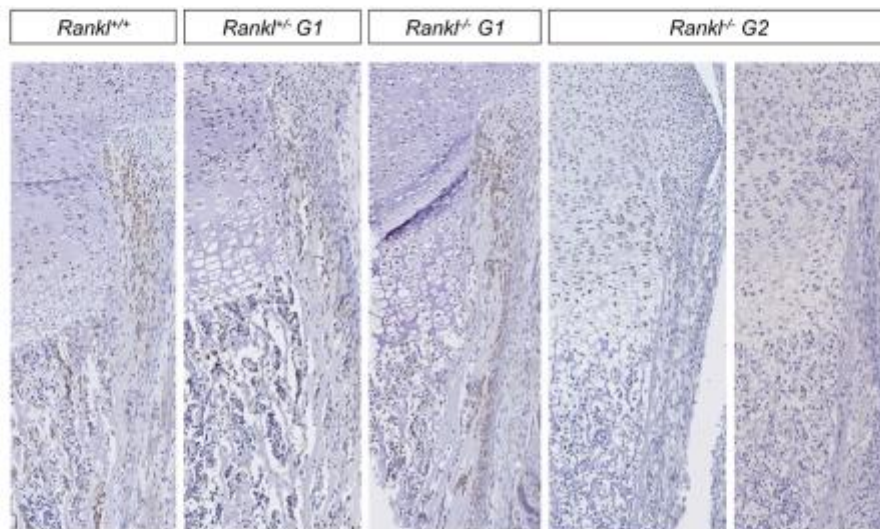


Figure 5. Immunohistochemical comparative analysis of SOX9 expression in the tibias of first- and

second-generation *Rankl* null mutant mice. A graduated decrease in SOX9 expression was observed from wild type to first-generation null mutant pups in either chondroblastic cells or periosteal osteoblastic cells. In the tibias of second-generation null mutant pups, very weak staining was present in rare chondroblastic cells, while no staining was observed in periosteal osteoblastic cells. Magnification 100 \times . Numbers of pups: 4 +/+, 8 G1+/-, 5 G1-/-, and 5 G2-/-.

3.3. IK22-5 RANKL-Blocking Antibody Injections in Pregnant Heterozygous Mice Induced a Second-Generation-Like Phenotype in Null Mutant Pups

In order to validate the importance of RANKL of maternal origin in the attenuated osteopetrotic phenotype of the null mutant pups, IK22-5-blocking antibody was injected into heterozygous pregnant females during the second part of gestation, and the consequences on the whole skeleton of the pups were analyzed (Figures 6 and 7). A noticeable aggravation in either craniofacial or long bone phenotypes was observed for the different genotypes, with WT being comparable to first-generation heterozygous mutants and first-generation to second-generation null mutants. Surprisingly, while a more open foramen (Figure 6) and severe tooth morphogenesis delay (Figure 7) was observed in the null mutants from injected mothers, the curvature of the mandible appeared unaffected (Figure 6), suggesting that this craniofacial osteopetrotic feature was secondary to a loss of RANKL function before mid-gestation.

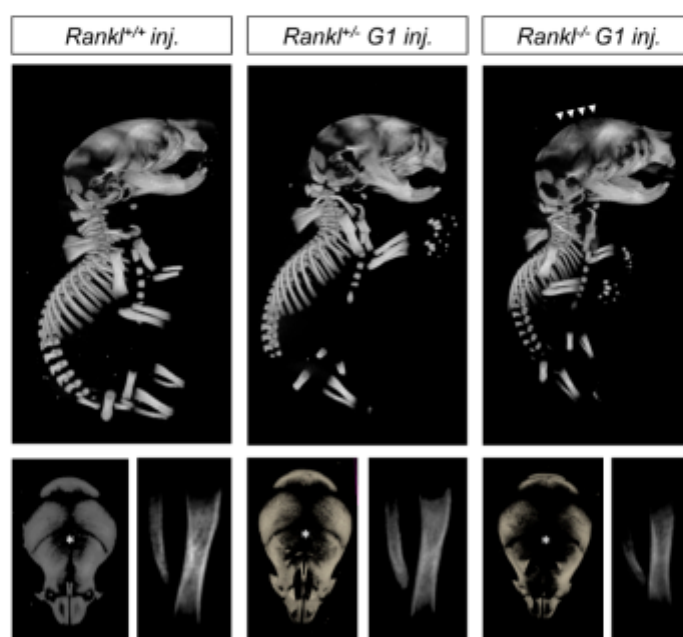


Figure 6. MicroCT comparative analysis of the skeletons of wild type, heterozygous, and first-generation *Rankl* null mutant pups born from females treated with IK22-5 during the second half of pregnancy. A graduated skeleton phenotype was observed from wild type to null mutant pups, with the presence of an enlarged foramen (star and arrowheads) in all genotypes. Percentage of closure measures (surface) for the different genotypes are 87 ± 3 for +/+, 68 ± 4 for +/-, and 60 ± 4 for -/-. Globally, it seems that injections of IK22-5 increased the phenotype of each genotype to the next in terms of severity, wild type being comparable to non-injected heterozygous, heterozygous to non-injected first-generation null mutants, and first-generation null mutants to second-generation phenotypes. Numbers of pups: 3 +/+, 6 +/-, and 2 -/-.

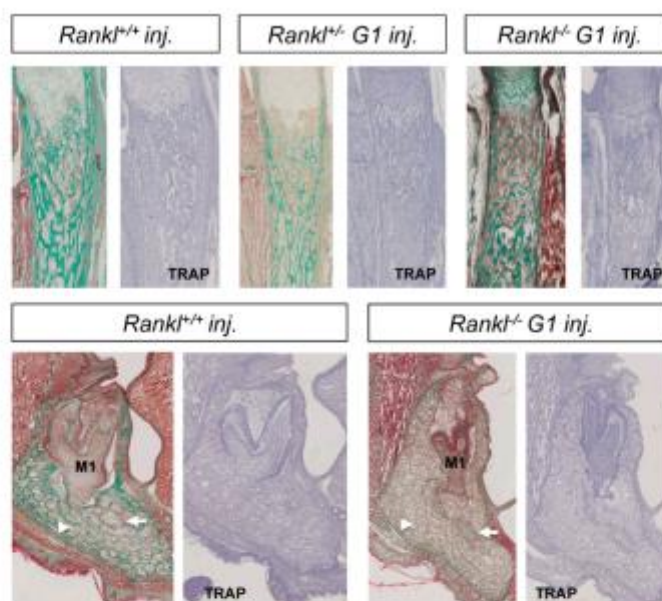


Figure 7. Histological comparative analysis of the skeletons of wild type, heterozygous, and first-generation *Rankl* null mutant pups born to females treated with IK22-5 during the second half of pregnancy. Masson trichrome staining of longitudinal sections of tibias made it possible to observe an osteopetrotic phenotype in all genotypes with, however, graduated severity from wild type to null mutant. TRAP staining was negative in all sections, signaling the absence of osteoclasts, induced by the IK22-5 injections. Masson trichrome staining of mandible frontal sections in the plane of the first molar (M1) revealed the induction of an osteopetrotic phenotype in the wild type pup with significant mandibular bone density (arrowhead), an absence of incisor in this section plane, remnant Meckel cartilage (arrow), and abnormal tooth morphology. TRAP staining of adjacent sections revealed a total absence of osteoclasts. Concerning the null mutant pups, a phenotype similar to the second-generation mutant pup was observed, with significant mandibular bone density (arrowhead), remnant Meckel cartilage (arrow), and abnormal tooth morphology. Magnification 40 \times . Numbers of pups: 3 +/+, 6 +/-, and 2 -/-.

4. Discussion

During embryonic development, RANKL expression has been reported in several tissues, with suggested implications in the cell-to-cell communications necessary for the morphogenesis of the corresponding organs, such as teeth, bones, thymus, thyroid glands, and lymph nodes. Surprisingly, RANKL invalidation in mice did not induce premature lethality, despite a severe osteopetrotic phenotype and alterations to the immune system (for reviews, see [8,35]). Moreover, the *Rankl* null mutant osteopetrotic phenotype appears less severe than that reported for its main receptor, *Rank* null mutant [36]. Depending on the existence of soluble forms of RANKL that may cross the placenta, the question of an attenuated phenotype in the null mutant due to partial compensation by RANKL of maternal origin was raised. In order to answer this question, second-generation null mutants were generated, and the osteopetrotic phenotype compared with first-generation mutants. The data obtained validated the existence of partial compensation of this type in the entire skeleton, suggesting that soluble RANKL of maternal origin does, indeed, cross the placenta.

Second-generation null mutants were difficult to obtain because of considerable embryonic lethality, as also reported by another group and explained by defects in decidual M2 macrophage polarization, essential for maternal-fetal tolerance [37]. The mutants that survived until birth did not survive more than 30 h, even if adopted by wild type lactating females (to deal with the fact that mammary gland development was defective in the null mutant mother). These observations validated the notion that normal embryonic development requires RANKL. Considering the fact that early lethality was also reported in transgenic pigs and mice following overexpression of

RANKL [28,29], it appeared that, during embryonic development, the RANKL expression level required a strict regulation.

Blood concentrations of RANKL and its decoy receptor OPG were analyzed throughout normal and pathological pregnancies, supporting the role played by RANKL signalization in communications between the mother and the fetus [38–43]. Alterations to RANKL and OPG expressions were associated with severe gestational pathologies, such as pre-eclampsia [38,40,41], intrauterine growth restriction [39,42], and premature labor [43], negatively impacting the life expectancy of both the mother and infant. Further studies are needed to decipher the complex role played by RANKL signalization during gestation, bearing in mind that RANKL has at least three receptors, two at the membrane of target cells, RANK and LGR4 [44], and one secreted, OPG.

Based on the data presented concerning skeletal development, RANKL signalization appears to have two main functions: controlling osteoclast differentiation, and in communication between mineral tissues forming cells. It has consequences on morphogenesis and histogenesis.

For the first function, in long bones such as the tibia, the total absence of osteoclasts was responsible for both a significant delay in development, and an absence of bone marrow space formation. The initial vascularization appeared to be maintained, and an accumulation of potential osteoclast precursors, CD68 cells, could be observed around the vessels. Moreover, the expression of SOX9, a major factor in endochondral bone formation [45], was severely decreased in the second-generation null mutants, outlining that the absence of osteoclasts completely blocked long bone formation. With regard to the craniofacial skeleton, the absence of osteoclasts made resorption of the Meckel cartilage impossible, which is an important step in mandible growth (for a review, see [46]).

The significant delay in tooth morphogenesis, observed in the second-generation null mutants, validated the considerable involvement of RANKL signalization in the communication between mineral tissues forming cells, which is the second function of RANKL signalization during skeletal development. The existence of such a function in teeth was initially suggested by the expression patterns of elements of RANKL signalization during morphogenesis [15]. Further studies are needed to decipher the modalities of this type of function, and the ability of the RANKL-blocking antibody to cross the placenta will be helpful. The absence of mandible curvature observed in the second-generation null mutants was also a consequence of the loss of the cell-to-cell communication function of RANKL signalization. Similar flat mandibles were reported in mice invalidated for transcription factors known to have morphogenetic functions, such as MSX1 [47] and PAX9 [48]. Crosstalk between RANKL signalization and these transcription factors may exist, as previously reported for other transcription factors, namely MSX2, EN1, and DLXs [32,49,50]. Further studies are needed to demonstrate the veracity of such crosstalk and its implications in morphogenesis of the whole skeleton.

5. Conclusions

To conclude, second-generation *Rankl* null mutants made it possible to demonstrate that the pediatric osteopetrotic phenotype associated with loss of RANKL function was reduced, thanks to partial compensation by RANKL of maternal origin during gestation. Those animals also made it possible to validate the involvement of RANKL signalization functionally in the communications between the mother and the embryo, but also in the morphogenesis/histogenesis of different organs through its implication in cell-to-cell communication and osteoclast differentiation control.

Supplementary Materials: The following are available online at <http://www.mdpi.com/2077-0383/7/11/426/s1>, Figure S1, Nomenclature used to distinguish the different mutants based on the genotypes of the parents, both heterozygous (A), both homozygous (B), and only the mother homozygous (C). The chronogram used for IK22-5 injections in pregnant heterozygous mice is also presented (D); Figure S2, Enlargements of Figures 4 and 7 enabling to visualize the different tibia growth plate cartilage phenotypes at the cellular level. Magnification 100×.

Author Contributions: Conceptualization, B.N., J.W.V.-F., A.G., D.H., B.C. and F.L.; Formal analysis, B.N., J.W.V.-F., A.G., J.A., F.R., D.H., B.C. and F.L.; Funding acquisition, D.H. and F.L.; Investigation, B.N., J.W.V.-F., A.G., J.A., F.R., B.C. and F.L.; Methodology, F.L.; Resources, Y.C., H.Y., C.G.M. and F.L.; Validation, B.N., J.W.V.-F., A.G., J.A., F.R., D.H., B.C. and F.L.; Writing-original draft, B.N., J.W.V.-F., A.G. and F.L.; Writing-review & editing, D.H., B.C. and F.L. F.L. takes responsibility for the integrity of the data analysis.

Funding: The project received the financial support of the French National Cancer Institute (Funding INCa-6001). B.N. has received a grant from the French Ministry for Higher Education and Research. A.G. is a grantee of INSERM-SFODE.

Acknowledgments: The authors wish to thank G. Hamery and J. Pajot from the Therapeutic Experimental Unit (Nantes, France) for their technical assistance.

Conflicts of Interest: None of the authors have any disclosures to make with regard to the work being considered here for publication.

References

- Kong, Y.Y.; Yoshida, H.; Sarosi, I.; Tan, H.L.; Timms, E.; Capparelli, C.; Morony, S.; Oliveira-dos-Santos, A.J.; Van, G.; Itie, A.; et al. OPG is a key regulator of osteoclastogenesis, lymphocyte development and lymph-node organogenesis. *Nature* **1999**, *397*, 315–323. [[CrossRef](#)] [[PubMed](#)]
- Kong, Y.Y.; Boyle, W.J.; Penninger, J.M. Osteoprotegerin ligand: A common link between osteoclastogenesis, lymph node formation and lymphocyte development. *Immunol. Cell Biol.* **1999**, *77*, 188–193. [[CrossRef](#)] [[PubMed](#)]
- Fata, J.E.; Kong, Y.Y.; Li, J.; Sasaki, T.; Irie-Sasaki, J.; Moorehead, R.A.; Elliott, R.; Scully, S.; Voura, E.B.; Lacey, D.L.; et al. The osteoclast differentiation factor osteoprotegerin-ligand is essential for mammary gland development. *Cell* **2000**, *103*, 41–50. [[CrossRef](#)]
- Kim, D.; Mebius, R.E.; MacMicking, J.D.; Jung, S.; Cupedo, T.; Castellanos, Y.; Rho, J.; Wong, B.R.; Josien, R.; Kim, N.; et al. Regulation of peripheral lymph node genesis by the tumor necrosis factor family member TRANCE. *J. Exp. Med.* **2000**, *192*, 1467–1478. [[CrossRef](#)] [[PubMed](#)]
- Kim, N.; Odgren, P.R.; Kim, D.K.; Marks, S.C.; Choi, Y. Diverse roles of the tumor necrosis factor family member TRANCE in skeletal physiology revealed by TRANCE deficiency and partial rescue by a lymphocyte-expressed TRANCE transgene. *Proc. Natl. Acad. Sci. USA* **2000**, *97*, 10905–10910. [[CrossRef](#)] [[PubMed](#)]
- Xing, L.; Schwarz, E.M.; Boyce, B.F. Osteoclast precursors, RANKL/RANK, and immunology. *Immunol. Rev.* **2005**, *208*, 19–29. [[CrossRef](#)] [[PubMed](#)]
- Sugiyama, M.; Nakato, G.; Jinnohara, T.; Akiba, H.; Okumura, K.; Ohno, H.; Yoshida, H. Expression pattern changes and function of RANKL during mouse lymph node microarchitecture development. *Int. Immunol.* **2012**, *24*, 369–378. [[CrossRef](#)] [[PubMed](#)]
- Walsh, M.C.; Choi, Y. Biology of the RANKL-RANK-OPG System in Immunity, Bone, and Beyond. *Front. Immunol.* **2014**, *5*, 511. [[CrossRef](#)] [[PubMed](#)]
- Habbedine, M.; Verthuy, C.; Rastoin, O.; Chasson, L.; Bebien, M.; Bajenoff, M.; Adriouch, S.; den Haan, J.M.M.; Penninger, J.M.; Lawrence, T. Receptor Activator of NF- κ B Orchestrates Activation of Antiviral Memory CD8 T Cells in the Spleen Marginal Zone. *Cell Rep.* **2017**, *21*, 2515–2527. [[CrossRef](#)] [[PubMed](#)]
- Hikosaka, Y.; Nitta, T.; Ohigashi, I.; Yano, K.; Ishimaru, N.; Hayashi, Y.; Matsumoto, M.; Matsuo, K.; Penninger, J.M.; Takayanagi, H.; et al. The cytokine RANKL produced by positively selected thymocytes fosters medullary thymic epithelial cells that express autoimmune regulator. *Immunity* **2008**, *29*, 438–450. [[CrossRef](#)] [[PubMed](#)]
- Desanti, G.E.; Cowan, J.E.; Baik, S.; Parnell, S.M.; White, A.J.; Penninger, J.M.; Lane, P.J.L.; Jenkinson, E.J.; Jenkinson, W.E.; Anderson, G. Developmentally regulated availability of RANKL and CD40 ligand reveals distinct mechanisms of fetal and adult cross-talk in the thymus medulla. *J. Immunol.* **2012**, *189*, 5519–5526. [[CrossRef](#)] [[PubMed](#)]
- Mueller, C.G.; Hess, E. Emerging Functions of RANKL in Lymphoid Tissues. *Front. Immunol.* **2012**, *3*, 261. [[CrossRef](#)] [[PubMed](#)]

13. Hess, E.; Duheron, V.; Decossas, M.; Lézot, F.; Berdal, A.; Chea, S.; Golub, R.; Bosisio, M.R.; Bridal, S.L.; Choi, Y.; et al. RANKL Induces Organized Lymph Node Growth by Stromal Cell Proliferation. *J. Immunol.* **2012**, *188*, 1245–1254. [[CrossRef](#)] [[PubMed](#)]
14. Duheron, V.; Hess, E.; Duval, M.; Decossas, M.; Castaneda, B.; Klöpffer, J.E.; Amoasii, L.; Barbaroux, J.-B.; Williams, I.R.; Yagita, H.; et al. Receptor activator of NF-kappaB (RANK) stimulates the proliferation of epithelial cells of the epidermo-pilosebaceous unit. *Proc. Natl. Acad. Sci. USA* **2011**, *108*, 5342–5347. [[CrossRef](#)] [[PubMed](#)]
15. Ohazama, A.; Courtney, J.-M.; Sharpe, P.T. Opg, Rank, and Rankl in tooth development: Co-ordination of odontogenesis and osteogenesis. *J. Dent. Res.* **2004**, *83*, 241–244. [[CrossRef](#)] [[PubMed](#)]
16. Castaneda, B.; Simon, Y.; Jacques, J.; Hess, E.; Choi, Y.-W.; Blin-Wakkach, C.; Mueller, C.; Berdal, A.; Lézot, F. Bone resorption control of tooth eruption and root morphogenesis: Involvement of the receptor activator of NF-κB (RANK). *J. Cell. Physiol.* **2011**, *226*, 74–85. [[CrossRef](#)] [[PubMed](#)]
17. Kim, N.-S.; Kim, H.-J.; Koo, B.-K.; Kwon, M.-C.; Kim, Y.-W.; Cho, Y.; Yokota, Y.; Penninger, J.M.; Kong, Y.-Y. Receptor activator of NF-kappaB ligand regulates the proliferation of mammary epithelial cells via Id2. *Mol. Cell. Biol.* **2006**, *26*, 1002–1013. [[CrossRef](#)] [[PubMed](#)]
18. Tanos, T.; Brisken, C. What signals operate in the mammary niche? *Breast Dis.* **2008**, *29*, 69–82. [[CrossRef](#)] [[PubMed](#)]
19. Kartsogiannis, V.; Zhou, H.; Horwood, N.J.; Thomas, R.J.; Hards, D.K.; Quinn, J.M.; Niforas, P.; Ng, K.W.; Martin, T.J.; Gillespie, M.T. Localization of RANKL (receptor activator of NF kappa B ligand) mRNA and protein in skeletal and extraskeletal tissues. *Bone* **1999**, *25*, 525–534. [[CrossRef](#)]
20. Sakakura, Y.; Tsuruga, E.; Irie, K.; Hosokawa, Y.; Nakamura, H.; Yajima, T. Immunolocalization of receptor activator of nuclear factor-kappaB ligand (RANKL) and osteoprotegerin (OPG) in Meckel's cartilage compared with developing endochondral bones in mice. *J. Anat.* **2005**, *207*, 325–337. [[CrossRef](#)] [[PubMed](#)]
21. Xiong, J.; Onal, M.; Jilka, R.L.; Weinstein, R.S.; Manolagas, S.C.; O'Brien, C.A. Matrix-embedded cells control osteoclast formation. *Nat. Med.* **2011**, *17*, 1235–1241. [[CrossRef](#)] [[PubMed](#)]
22. Odgren, P.R.; Witwicka, H.; Reyes-Gutierrez, P. The cast of clasts: Catabolism and vascular invasion during bone growth, repair, and disease by osteoclasts, chondroclasts, and septoclasts. *Connect. Tissue Res.* **2016**, *57*, 161–174. [[CrossRef](#)] [[PubMed](#)]
23. Atkins, G.J.; Kostakis, P.; Pan, B.; Farrugia, A.; Gronthos, S.; Evdokiou, A.; Harrison, K.; Findlay, D.M.; Zannettino, A.C.W. RANKL expression is related to the differentiation state of human osteoblasts. *J. Bone Miner. Res.* **2003**, *18*, 1088–1098. [[CrossRef](#)] [[PubMed](#)]
24. Sobacchi, C.; Frattini, A.; Guerrini, M.M.; Abinun, M.; Pangrazio, A.; Susani, L.; Bredius, R.; Mancini, G.; Cant, A.; Bishop, N.; et al. Osteoclast-poor human osteopetrosis due to mutations in the gene encoding RANKL. *Nat. Genet.* **2007**, *39*, 960–962. [[CrossRef](#)] [[PubMed](#)]
25. Boyce, R.W.; Varela, A.; Chouinard, L.; Bussiere, J.L.; Chellman, G.J.; Ominsky, M.S.; Pyrah, I.T. Infant cynomolgus monkeys exposed to denosumab in utero exhibit an osteoclast-poor osteopetrotic-like skeletal phenotype at birth and in the early postnatal period. *Bone* **2014**, *64*, 314–325. [[CrossRef](#)] [[PubMed](#)]
26. Lézot, F.; Chesneau, J.; Navet, B.; Gobin, B.; Amiaud, J.; Choi, Y.; Yagita, H.; Castaneda, B.; Berdal, A.; Mueller, C.G.; et al. Skeletal consequences of RANKL-blocking antibody (IK22-5) injections during growth: Mouse strain disparities and synergic effect with zoledronic acid. *Bone* **2015**, *73*, 51–59. [[CrossRef](#)] [[PubMed](#)]
27. Okamatsu, N.; Sakai, N.; Karakawa, A.; Kouyama, N.; Sato, Y.; Inagaki, K.; Kiuchi, Y.; Oguchi, K.; Negishi-Koga, T.; Takami, M. Biological effects of anti-RANKL antibody administration in pregnant mice and their newborns. *Biochem. Biophys. Res. Commun.* **2017**, *491*, 614–621. [[CrossRef](#)] [[PubMed](#)]
28. Klymiuk, N.; Böcker, W.; Schönitzer, V.; Bähr, A.; Radic, T.; Fröhlich, T.; Wunsch, A.; Keßler, B.; Kurome, M.; Schilling, E.; et al. First inducible transgene expression in porcine large animal models. *FASEB J.* **2012**, *26*, 1086–1099. [[CrossRef](#)] [[PubMed](#)]
29. Mizuno, A.; Kanno, T.; Hoshi, M.; Shibata, O.; Yano, K.; Fujise, N.; Kinoshita, M.; Yamaguchi, K.; Tsuda, E.; Murakami, A.; et al. Transgenic mice overexpressing soluble osteoclast differentiation factor (sODF) exhibit severe osteoporosis. *J. Bone Miner. Metab.* **2002**, *20*, 337–344. [[CrossRef](#)] [[PubMed](#)]

30. Hughes, A.E.; Ralston, S.H.; Marken, J.; Bell, C.; MacPherson, H.; Wallace, R.G.; van Hul, W.; Whyte, M.P.; Nakatsuka, K.; Hovy, L.; et al. Mutations in TNFRSF11A, affecting the signal peptide of RANK, cause familial expansile osteolysis. *Nat. Genet.* **2000**, *24*, 45–48. [[CrossRef](#)] [[PubMed](#)]
31. Palenzuela, L.; Vives-Bauza, C.; Fernández-Cadenas, I.; Meseguer, A.; Font, N.; Sarret, E.; Schwartz, S.; Andreu, A.L. Familial expansile osteolysis in a large Spanish kindred resulting from an insertion mutation in the TNFRSF11A gene. *J. Med. Genet.* **2002**, *39*, E67. [[CrossRef](#)] [[PubMed](#)]
32. Castaneda, B.; Simon, Y.; Ferbus, D.; Robert, B.; Chesneau, J.; Mueller, C.; Berdal, A.; Lézet, F. Role of RANKL (TNFSF11)-dependent osteopetrosis in the dental phenotype of Msx2 null mutant mice. *PLoS ONE* **2013**, *8*, e80054. [[CrossRef](#)] [[PubMed](#)]
33. Ikeda, T.; Kasai, M.; Utsuyama, M.; Hirokawa, K. Determination of three isoforms of the receptor activator of nuclear factor-kappaB ligand and their differential expression in bone and thymus. *Endocrinology* **2001**, *142*, 1419–1426. [[CrossRef](#)] [[PubMed](#)]
34. Sojod, B.; Chateau, D.; Mueller, C.G.; Babajko, S.; Berdal, A.; Lézet, F.; Castaneda, B. RANK/RANKL/OPG Signaling Implication in Periodontitis: New Evidence from a RANK Transgenic Mouse Model. *Front. Physiol.* **2017**, *8*, 338. [[CrossRef](#)] [[PubMed](#)]
35. Leibbrandt, A.; Penninger, J.M. RANK/RANKL: Regulators of immune responses and bone physiology. *Ann. N. Y. Acad. Sci.* **2008**, *1143*, 123–150. [[CrossRef](#)] [[PubMed](#)]
36. Xing, L.; Chen, D.; Boyce, B.F. Mice Deficient in NF- κ B p50 and p52 or RANK Have Defective Growth Plate Formation and Post-natal Dwarfism. *Bone Res.* **2013**, *1*, 336–345. [[CrossRef](#)] [[PubMed](#)]
37. Meng, Y.-H.; Zhou, W.-J.; Jin, L.-P.; Liu, L.-B.; Chang, K.-K.; Mei, J.; Li, H.; Wang, J.; Li, D.-J.; Li, M.-Q. RANKL-mediated harmonious dialogue between fetus and mother guarantees smooth gestation by inducing decidual M2 macrophage polarization. *Cell Death Dis.* **2017**, *8*, e3105. [[CrossRef](#)] [[PubMed](#)]
38. Shaarawy, M.; Zaki, S.; Ramzi, A.-M.; Salem, M.E.; El-Minawi, A.M. Feto-maternal bone remodeling in normal pregnancy and preeclampsia. *J. Soc. Gynecol. Investig.* **2005**, *12*, 343–348. [[CrossRef](#)] [[PubMed](#)]
39. Briana, D.D.; Boutsikou, M.; Baka, S.; Hassiakos, D.; Gourgiotis, D.; Malamitsi-Puchner, A. Circulating osteoprotegerin and sRANKL concentrations in the perinatal period at term. The impact of intrauterine growth restriction. *Neonatology* **2009**, *96*, 132–136. [[CrossRef](#)] [[PubMed](#)]
40. Vitoratos, N.; Lambrinouadaki, I.; Rizos, D.; Armeni, E.; Alexandrou, A.; Creatsas, G. Maternal circulating osteoprotegerin and soluble RANKL in pre-eclamptic women. *Eur. J. Obstet. Gynecol. Reprod. Biol.* **2011**, *154*, 141–145. [[CrossRef](#)] [[PubMed](#)]
41. Shen, P.; Gong, Y.; Wang, T.; Chen, Y.; Jia, J.; Ni, S.; Zhou, B.; Song, Y.; Zhang, L.; Zhou, R. Expression of osteoprotegerin in placenta and its association with preeclampsia. *PLoS ONE* **2012**, *7*, e44340. [[CrossRef](#)] [[PubMed](#)]
42. Tenta, R.; Bourgiezi, I.; Aliferis, E.; Papadopoulou, M.; Gounaris, A.; Skouroliaou, M. Bone metabolism compensates for the delayed growth in small for gestational age neonates. *Organogenesis* **2013**, *9*, 55–59. [[CrossRef](#)] [[PubMed](#)]
43. Rzepka, R.; Dołęgowska, B.; Sałata, D.; Rajewska, A.; Budkowska, M.; Domański, L.; Kwiatkowski, S.; Mikołajek-Bedner, W.; Torbé, A. Soluble receptors for advanced glycation end products and receptor activator of NF- κ B ligand serum levels as markers of premature labor. *BMC Pregnancy Childbirth* **2015**, *15*, 134. [[CrossRef](#)] [[PubMed](#)]
44. Luo, J.; Yang, Z.; Ma, Y.; Yue, Z.; Lin, H.; Qu, G.; Huang, J.; Dai, W.; Li, C.; Zheng, C.; et al. LGR4 is a receptor for RANKL and negatively regulates osteoclast differentiation and bone resorption. *Nat. Med.* **2016**, *22*, 539–546. [[CrossRef](#)] [[PubMed](#)]
45. Hattori, T.; Müller, C.; Gebhard, S.; Bauer, E.; Pausch, F.; Schlund, B.; Bösl, M.R.; Hess, A.; Surmann-Schmitt, C.; von der Mark, H.; et al. SOX9 is a major negative regulator of cartilage vascularization, bone marrow formation and endochondral ossification. *Dev. Camb. Engl.* **2010**, *137*, 901–911. [[CrossRef](#)] [[PubMed](#)]
46. Parada, C.; Chai, Y. Mandible and Tongue Development. *Curr. Top. Dev. Biol.* **2015**, *115*, 31–58. [[CrossRef](#)] [[PubMed](#)]
47. Orestes-Cardoso, S.; Nefussi, J.R.; Lezet, F.; Oboeuf, M.; Pereira, M.; Mesbah, M.; Robert, B.; Berdal, A. Msx1 is a regulator of bone formation during development and postnatal growth: In vivo investigations in a transgenic mouse model. *Connect. Tissue Res.* **2002**, *43*, 153–160. [[CrossRef](#)] [[PubMed](#)]

48. Anthwal, N.; Peters, H.; Tucker, A.S. Species-specific modifications of mandible shape reveal independent mechanisms for growth and initiation of the coronoid. *EvoDevo* **2015**, *6*, 35. [[CrossRef](#)] [[PubMed](#)]
49. Lézot, F.; Thomas, B.L.; Blin-Wakkach, C.; Castaneda, B.; Bolanos, A.; Hotton, D.; Sharpe, P.T.; Heymann, D.; Carles, G.F.; Grigoriadis, A.E.; et al. Dlx homeobox gene family expression in osteoclasts. *J. Cell. Physiol.* **2010**, *223*, 779–787. [[CrossRef](#)] [[PubMed](#)]
50. Deckelbaum, R.A.; Majithia, A.; Booker, T.; Henderson, J.E.; Loomis, C.A. The homeoprotein engrailed 1 has pleiotropic functions in calvarial intramembranous bone formation and remodeling. *Dev. Camb. Engl.* **2006**, *133*, 63–74. [[CrossRef](#)] [[PubMed](#)]



© 2018 by the authors. Licensee MDPI, Basel, Switzerland. This article is an open access article distributed under the terms and conditions of the Creative Commons Attribution (CC BY) license (<http://creativecommons.org/licenses/by/4.0/>).

Effets de l'inhibition post-natale de RANKL sur l'éruption et la formation radiculaire des molaires de souris C57BL/6

Andrea GAMA^{1,5*}, Linamary PEREA², Catalina YEPES², Jhon J BETANCUR², Jorge VARGAS², Jérôme AMIAUD³, Sylvie BABAJKO¹, Frédéric LEZOT³, Beatriz CASTANEDA^{1,4}

¹ Centre de Recherche des Cordeliers, INSERM, Sorbonne Université, USPC, Université Paris Descartes, Université Paris Diderot, Équipe BERDAL, 75006 Paris, France

² Faculté d'Odontologie, Université d'Antioquia, Medellín, Colombia

³ INSERM UMRS 1238, Faculté de Médecine, Nantes, France

⁴ Service d'Orthopédie Dento-faciale, Hôpital la Pitié Salpêtrière, Paris, France

⁵ Laboratoire d'Histopathologie orale, Faculté des sciences de la santé, Université de Brasilia, Brasilia, Brésil

Projet ayant obtenu le 1^{er} prix de recherche SFODF / INSERM 2017

(Reçu le 29 mai 2018, accepté le 10 février 2019)

MOTS CLÉS :

RANK /
 RANKL /
 Follicule dentaire /
 Défauts primaires
 d'éruption

RÉSUMÉ – Introduction : Des observations récentes effectuées dans le service d'ODF de la Pitié-Salpêtrière à Paris montrent une augmentation des altérations de l'éruption des molaires permanentes non-familiales. Nos travaux récents au laboratoire montrent l'implication des ostéoclastes (OC) dans les processus d'éruption et de rétention dentaires avec implication de la voie de signalisation RANKL/RANK/OPG. Ces faits nous ont amenés à émettre l'hypothèse d'une étiologie environnementale à l'origine de ces défauts d'éruption qui correspondrait à la perturbation des voies de signalisation cellulaires autocrines/paracrines telles que la voie RANKL/RANK/OPG. **Matériels et méthodes :** Des souris C57BL/6 ont subi des injections d'anticorps anti-RANKL à intervalles réguliers au cours des neuf premiers jours après la naissance. Une comparaison phénotypique avec les souris transgéniques RANK a permis la caractérisation fonctionnelle de la voie RANK/RANKL. Le complexe dento-alvéolaire a été analysé par micro-CT pour la densité osseuse, et la coloration au trichrome de Masson pour les examens histologiques. **Résultats :** L'inactivation transitoire de RANKL a conduit à un arrêt du développement radiculaire des molaires et l'inhibition de l'éruption dentaire contrairement au phénotype des souris surexprimant RANK. Le recrutement et l'activité des ostéoclastes ont été fortement altérés. **Discussion :** Ces recherches présentent un intérêt clinique tant direct concernant la compréhension des pathologies de l'éruption qu'indirect pour l'établissement des protocoles de traitements orthodontiques pour les cas particuliers.

KEYWORDS:

RANK /
 RANKL /
 Dental follicle /
 Primary failure of eruption

ABSTRACT – Effects of post-natal inhibition of RANKL on molar eruption and root formation in C57BL/6 mice. Introduction: Recent observations performed in the orthodontic department of La Pitié-Salpêtrière hospital in Paris reported an increase of non-familial eruption defects of permanent molars. Our recent data have evidenced the involvement of osteoclasts (OC) in both the eruption and the dental retention processes through the RANKL/RANK/OPG signaling pathway. These facts are at the origin of the hypothesis of the existence of an environmental etiology for those eruption defects that would correspond to the perturbation of cellular autocrine/paracrine signaling pathways as the RANKL/RANK/OPG. **Materials and methods:** C57BL/6 mice were submitted to repeated injections with anti-RANKL neutralizing antibody during the nine days following birth. A phenotypic comparison with transgenic mice overexpressing RANK was

* Auteur pour correspondance : dea.gama10@gmail.com

performed for the functional characterization of the RANKL/RANK/OPG pathway. The dento-alveolar complex was analyzed using micro-CT for bone density and Masson's trichrome staining for histological examination. Results: The RANKL transient invalidation of RANKL stopped the molar root development and tooth eruption contrary to transgenic mice overexpressing RANK. The recruitment and the OC activity were strongly impacted. Discussion: This research is of direct clinical interest in understanding the pathology of eruption as indirect in establishing orthodontic treatment protocols for particular cases.

1. Introduction

L'éruption dentaire est un processus complexe qui implique l'interaction, dans le temps et dans l'espace, des cellules de l'organe de l'email, du follicule dentaire et de l'os alvéolaire²⁹. Concernant le modelage de l'os alvéolaire, deux processus physiologiques interdépendants sont nécessaires au cours de l'éruption dentaire : d'une part, la résorption osseuse de l'os alvéolaire qui entoure la couronne de la dent, responsable de la formation d'une voie d'éruption et, d'autre part, un processus d'apposition osseuse, qui contribue au déplacement de la dent via cette voie d'éruption^{29,30}. Ces processus dépendent de signaux qui proviennent du sac folliculaire et du follicule dentaire²⁹. Le follicule dentaire (FD) est un sac de tissu conjonctif comprenant des cellules souches à l'origine de l'unité dento-parodontale^{30,31}.

Des expériences réalisées au cours des années 80 ont démontré l'importance du FD dans l'éruption dentaire dont l'excision chirurgicale conduit à son absence. Inversement, si le FD est laissé intact, mais la dent remplacée par une vis en métal, celle-ci se déplace dans la voie d'éruption²⁹. Le FD est donc nécessaire non seulement pour la phase intra-osseuse de l'éruption, mais aussi comme source de signalisation durant la formation de la racine, la prolifération des cellules de la pulpe et la formation de l'os alvéolaire qui contribuent à l'éruption dentaire^{30,31}. Le FD est un tissu cible pour l'attraction et la prolifération des cellules précurseurs mononucléées et un milieu dans lequel ces cellules fusionnent pour former des ostéoclastes. Localisé entre l'os alvéolaire et le germe dentaire, il permet de réguler les événements cellulaires lors de l'éruption. Wise et ses collègues ont montré, chez le rat, un flux maximal de cellules progénitrices mononucléées au troisième jour post-natal dans le FD de la première molaire mandibulaire³³. Après ce pic, le nombre de cellules précurseurs mononucléées et d'ostéoclastes diminue fortement³¹.

Certaines molécules induisant l'ostéoclastogénèse, telles que le facteur de stimulation des colonies-1 (CSF-1) et RANKL, sont libérées dans le FD, d'autres, comme le peptide apparenté à l'hormone parathyroïdienne (PTH-rP), sont sécrétées dans le réticulum étoilé et sont responsables de l'induction de facteurs intra- et extra-cellulaires au sein du FD³². Une fois que les cellules précurseurs mononucléées ont été recrutées dans le FD, elles fusionnent et forment les ostéoclastes. Le proto-oncogène c-FOS(c-Fos), le facteur nucléaire kappa-B (NF-kB) et la protéine chimio-attractante des monocytes - 1 (MCP-1) sont des éléments clés nécessaires à cette étape⁸.

L'expression maximale de CSF-1 induit l'ostéoclastogénèse par augmentation de l'expression de RANK dans les précurseurs ostéoclastiques, et ensuite la signalisation RANKL/RANK favorise la survie, la prolifération et la fusion des précurseurs ostéoclastiques^{15,30}. RANKL, RANK et OPG sont ainsi les facteurs constituant la voie principale d'activation de l'ostéoclastogénèse. RANKL est une protéine exprimée par les ostéoblastes et les cellules stromales qui induit la formation d'ostéoclastes via l'activation des cellules précurseurs par liaison au récepteur membranaire RANK exprimé par ces précurseurs²⁷. OPG est un récepteur leurre, dont la structure est similaire à RANK mais incapable de transmettre un signal. OPG, en liant RANKL, bloque son activité et, par conséquent, la différenciation des ostéoclastes. Il a été montré que son expression dans le FD est réduite lors du pic de différenciation des ostéoclastes²⁷. Bien que l'implication des facteurs RANKL/RANK/OPG ait été amplement démontrée dans l'inflammation, la réponse immunitaire et la résorption osseuse, seules quelques études rapportent leur implication dans la morphogénèse et l'éruption dentaire^{18,20}.

Concernant la morphogénèse et l'histogénèse du germe dentaire, RANKL est exprimé dans les cellules mésenchymateuses du FD tout au long du développement dentaire. Il est co-exprimé avec OPG dans les

cellules épithéliales au stade du bourgeon, puis dans toutes les cellules dentaires, les cellules pulpaires, les améloblastes et les odontoblastes, au stade plus avancé de la cloche. RANK est exprimé dans l'épithélium du germe dentaire au stade de bourgeon et dans les cellules mésenchymateuses du FD au stade de la cloche. Le récepteur RANK est essentiel non seulement pour stimuler l'ostéoclastogénèse nécessaire à l'éruption dentaire, mais aussi pour la formation normale de la dent, en particulier de la racine²⁰.

Chez l'homme, les altérations de l'éruption dentaire telles que la rétention primaire et l'ankylose de la molaire peuvent être associées à des anomalies du développement dentaire comme l'hypodontie², l'agénésie¹⁹ ou les malformations radiculaires²⁸. Leur étiologie est complexe. Il apparaît que la mutation du récepteur de l'hormone parathyroïdienne (PTHr1)^{3,22,23} est à l'origine de la plupart de ces formes familiales de rétentions d'éruption⁴. Or, les ostéoclastes n'expriment pas PTHr1. De plus, la prévalence des rétentions molaires sporadiques (non familiales) semble augmenter ces dernières années. Ces deux observations nous ont amenés à poser l'hypothèse d'une étiologie environnementale avec un facteur exogène capable de perturber les signalisations autocrines/paracrines nécessaires à l'éruption dentaire, telles que la voie RANKL/RANK/OPG. En effet, des facteurs environnementaux non-héréditaires comme certains médicaments ou certaines pathologies inflammatoires (telles que les kystes, abcès, otites...) ont également été associés à des pathologies d'éruption¹¹.

La méconnaissance de l'étiologie et du développement de cette pathologie rend son approche thérapeutique particulièrement difficile. En effet, dans ce cas, la traction orthodontique n'est pas efficace et entraîne souvent une ankylose de la dent^{6,25}. La caractérisation des anomalies d'éruption s'avère donc indispensable pour une prise en charge thérapeutique adaptée.

Ce travail vise à comprendre le rôle des ostéoclastes, et de la voie de signalisation RANKL/RANK/OPG dans la communication entre les cellules osseuses et les cellules dentaires au cours de l'éruption dentaire. Pour cela, nous comparons l'impact de l'inhibition constitutive et transitoire de RANKL dans l'éruption dentaire et la formation radulaire des souris C57BL/6 afin d'évaluer l'implication de RANK/RANKL dans les différentes formes de rétentions dentaires.

2. Méthodes

2.1. Collecte des échantillons biologiques

Les souris C57BL/6 utilisées dans cette étude sont élevées et maintenues à l'Unité de Thérapeutique Expérimentale (UTE) de la faculté de médecine de l'Université de Nantes dans le respect des règles en vigueur régissant l'expérimentation animale, selon un protocole validé par le comité d'éthique des Pays de la Loire (CEEA 06) et approuvé par le Ministère de l'Enseignement et de la Recherche (APAFIS#11208).

Une série de quatre injections sous-cutanées de l'anticorps bloquant RANKL (IK22-5) est réalisée à deux jours d'intervalle à partir du premier jour post-natal (PN). Les souris contrôles sont injectées avec du sérum physiologique 0,9 %. Les souris sont sacrifiées au jour 39 (PN), soit 30 jours après la dernière injection.

Les échantillons sont conservés dans du paraformaldéhyde (PFA) 4 % pour les analyses en micro-tomographie (μ -CT). Pour les techniques d'histologie, les échantillons sont décalcifiés dans une solution de PBS 1X contenant 4,13 % d'acide éthylène diamine tétra-acétique (EDTA) pH 7,6 pendant une période variant entre 10 et 15 jours. Après la décalcification, les échantillons sont déshydratés dans l'alcool absolu à concentrations croissantes puis inclus en paraffine.

2.2. Analyse par micro-CT (μ -CT)

L'analyse de la microarchitecture osseuse est réalisée à l'aide d'un scanner Skyscan1076 (Skyscan, Kontich, Belgium). Toutes les têtes ont été scannées en utilisant les mêmes paramètres (Pixel de 9 μ m, 49 kV, filtre aluminium de 0,5-mm, scan de 20 minutes). Les reconstructions ont été réalisées et analysées par NRecon puis CTVox (Skyscan).

2.3. Histomorphologie

Les coupes sériées de 7 μ m d'épaisseur sont réalisées à l'aide d'un microtome RM 2245 (Leica, France) avec une orientation frontale par rapport à l'axe de la mandibule. Toutes les coupes sont soumises à une étape de déparaffinage préalable à toute expérimentation ultérieure. Toutes les lames sont observées et photographiées au microscope photonique DMRB (Leica, France).

2.4. Trichrome de Masson

Après le déparaffinage et la réhydratation, les coupes sont immergées dans l'hématoxyline ferrique de Weigart pendant 10 min. Elles sont ensuite rincées à l'eau courante puis placées dans de l'eau ammoniacale 1 % jusqu'à bleuissement, et finalement rincées et placées de nouveau dans de l'eau distillée. Chaque lame est immergée durant 10 min dans la fuchsine Ponceau puis rincée à l'eau distillée. Les lames sont ensuite plongées dans l'acide phosphomolybdique pendant 3 minutes avant d'être colorées dans le vert lumière pendant une minute. Enfin, elles sont plongées rapidement dans de l'eau acétifiée pour éliminer l'excès de colorant, puis dans deux bains d'éthanol 100 % suivie de deux bains de clearene. Le montage est effectué après déshydratation dans un milieu résine DPX.

2.5. Histoenzymologie de la phosphatase acide résistante au tartrate (TRAP)

Après déparaffinage et fixation des coupes avec du PFA 4 %, les lames sont passées dans la solution de révélation de l'activité TRAP (Tampon acétate PH 5,2 contenant 1 mg/ml de Naphtol AS-TR-phosphate, 0,5 % N-N diméthylformamide, 1 mg/ml de FastRed TR salt et 100 mM de tartrate de sodium) à température ambiante et en chambre noire et humide jusqu'à l'obtention d'un marquage rouge. Les lames sont ensuite rincées en eau stérile pendant 5 minutes à température ambiante et les coupes sont contre colorées à l'hématoxyline (5 secondes). Les lames sont montées ensuite en Aquamount.

3. Résultats

3.1. Phénotype alvéolo-dentaire des souris ayant reçu quatre injections d'anticorps anti-RANKL

Les radiographies permettent d'observer à 39 jours PN l'absence d'éruption des premières et deuxième molaires chez les souris injectées avec l'anticorps anti-RANKL, alors que les souris contrôles présentent les trois molaires dans la cavité buccale (Fig. 1a). Ces molaires retenues ne présentent pas de racines radiographiquement visibles. Ce phénotype est opposé à celui rapporté pour les souris surexprimant RANK (RTg) qui ont une éruption plus précoce

que les contrôles, ainsi qu'une élévation radiculaire accélérée (Fig. 1b).

3.2. Morphologie dento-alvéolaire des souris injectées avec l'anticorps anti-RANKL

Afin de comparer l'histologie dento-alvéolaire des souris invalidées transitoirement pour RANKL et des souris du groupe contrôle, une coloration au Trichrome de Masson a été réalisée. Ce réactif permet d'identifier les matrices collagéniques (os et dentine) en bleu/vert et les cellules en rouge. La couronne présente une morphologie similaire dans les deux groupes, mais sa taille est réduite chez les souris injectées (Fig. 2). La dentine radiculaire présente une épaisseur non homogène, avec une apparence de type hyperplasique (Fig. 2). La frontière tissulaire avec le ciment radiculaire est difficile à observer. De plus, l'espace desmodontal n'est pas homogène. Les fibres du ligament parodontal présentent une orientation désordonnée et une insertion radiculaire indéfinie (Fig. 2).

3.3. Présence d'ostéoclastes dans l'os alvéolaire des souris injectées avec l'anticorps anti-RANKL

L'histoenzymologie TRAP permet d'analyser les ostéoclastes présents dans l'os alvéolaire. Au niveau coronaire, la formation d'une voie d'éruption osseuse chez les souris du groupe expérimental est repérée malgré la rétention intra-osseuse des molaires (Fig. 3a). Aucun marquage TRAP n'est observé dans cette voie (Fig. 3a). Dans l'os alvéolaire entourant les dents incluses, on observe la présence de cellules TRAP positives, plus nombreuses chez les souris invalidées pour RANKL que chez les souris témoins (Fig. 3b).

4. Discussion

Le complexe dento-alvéolaire est constitué par la dent, l'os alvéolaire de soutien et le ligament parodontal. Les éléments de cette unité sont interdépendants, que ce soit d'un point de vue développemental ou fonctionnel. En effet, une altération dans la formation ou le maintien de l'un de ces éléments a des répercussions sur les autres. Une altération du développement dentaire s'accompagne d'une altération ou d'une absence de formation osseuse alvéolaire⁷.

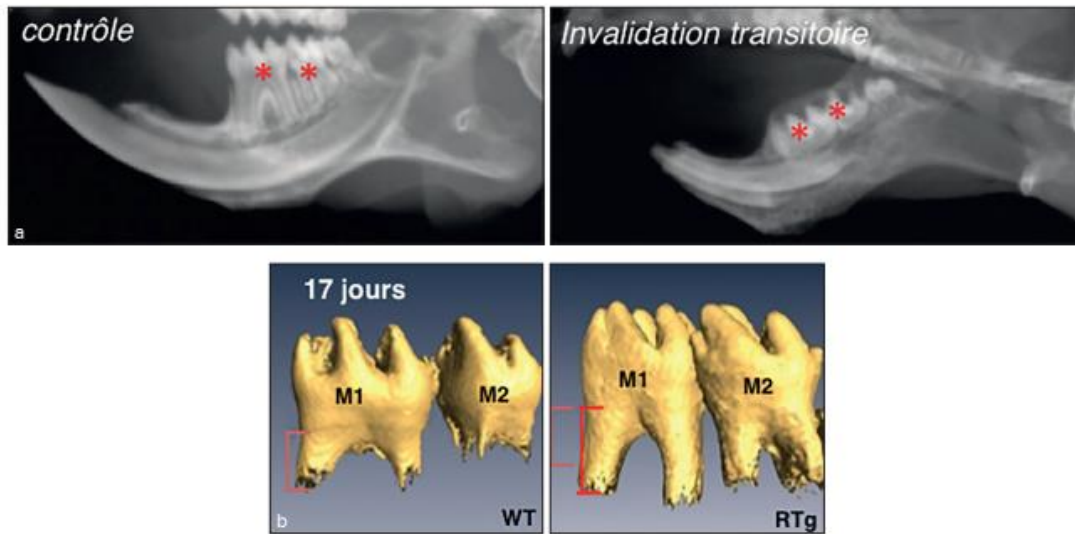


Figure 1

Coupe sagittale de la radiographie craniofaciale des souris contrôle et injectées avec l'anticorps anti-RANKL. La figure 1a montre l'absence dans la cavité buccale de la première et de la deuxième molaire mandibulaires des souris injectées. Les souris contrôle présentent toutes les molaires avec leur éruption complète dans la cavité buccale. La figure 1b met en évidence, par scanner, la formation radriculaire plus précoce chez les souris RANK-Tg en comparaison avec les souris sauvages.

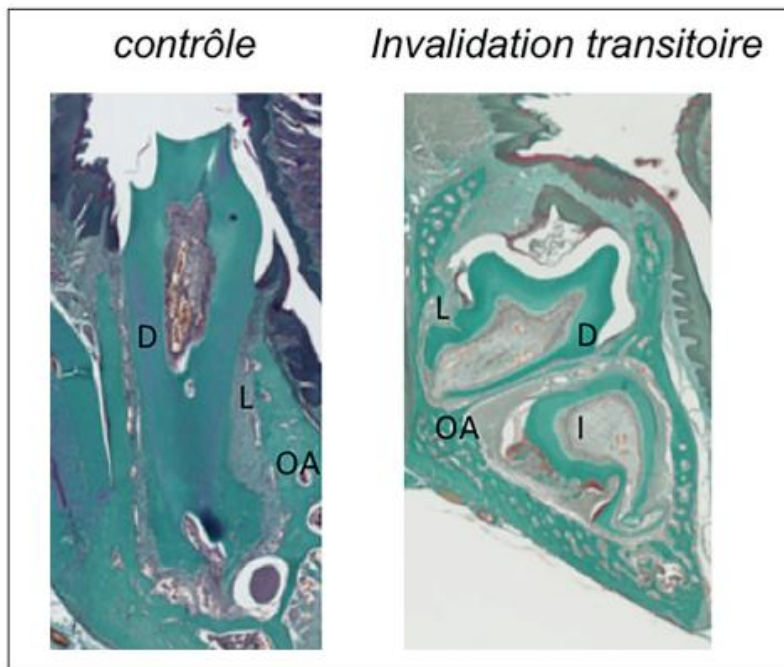


Figure 2

Coloration par Trichrome de Masson des coupes frontales de la première molaire mandibulaire des souris de 39 jours PN, contrôle et injectées avec l'Ac anti-RANKL. La figure met en évidence en 10X l'altération de la morphologie radriculaire des molaires du groupe des souris injectées. D : dentine ; L : ligament parodontal ; OA : os alvéolaire ; I : incisif.

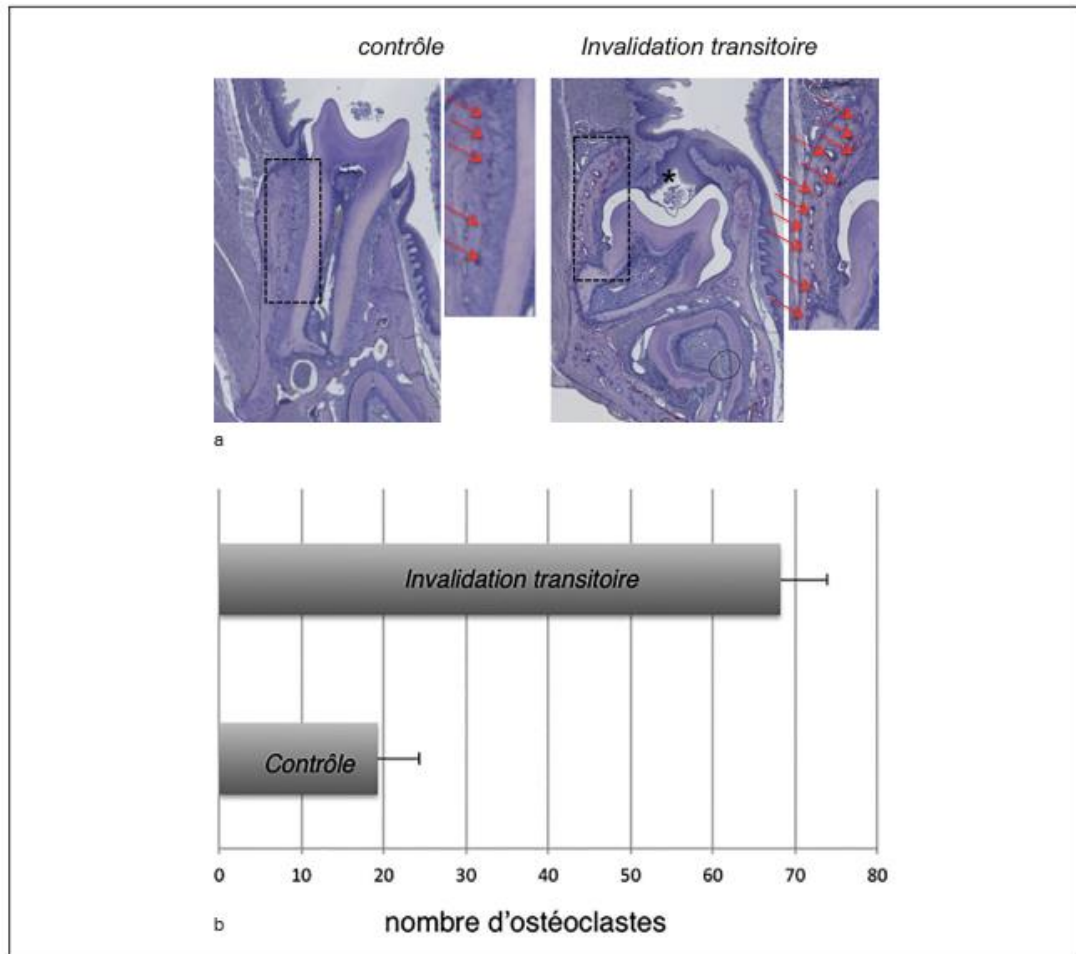


Figure 3

Histoenzymologie TRAP des coupes frontales de la première molaire des souris contrôles et injectées avec l'Ac anti-RANKL. (a) Image à 10X et son grossissement à 20X. Les flèches montrent les cellules TRAP positives présentes dans l'os alvéolaire adjacent au ligament parodontal. (b) Graphique de la quantification du nombre des cellules TRAP positives présentes en la paroi osseuse de l'os alvéolaire adjacente au ligament parodontal. La barre représente la moyenne avec l'écart type correspondant à chaque groupe de souris.

Réciproquement, une diminution du modelage osseux, comme dans l'ostéopétrose, provoque une interruption prématurée ou une altération du développement et de l'éruption dentaire, en relation avec la gravité de l'altération osseuse⁵.

La formation du complexe dento-alvéolaire correspond à une coordination dans l'espace et le temps, entre le développement de la dent à l'intérieur de la crypte osseuse et le modelage de l'os alvéolaire qui l'entoure. Les modalités de cette coordination sont peu connues, mais il est admis qu'il existe des inte-

ractions réciproques entre les cellules osseuses et les cellules dentaires^{5,12}.

Au cours du développement précoce de la dent, les interactions réciproques et séquentielles entre l'épithélium et le mésenchyme conduisent finalement à la formation de la dentine, de la racine, du ciment et des tissus parodontaux. Le follicule dentaire joue un rôle fondamental dans ces interactions^{13,14}.

Concernant les acteurs moléculaires impliqués dans les communications et coordinations au cours de l'éruption dentaire, des pistes ont émergé des études

menées chez des patients atteints de dysplasie cléido-crânienne. En effet, cette pathologie est caractérisée par de multiples dents retenues, avec non seulement une altération de l'ostéogenèse du fait de la mutation du facteur de transcription Runt - 2 (RUNX2), mais également une diminution de la formation d'ostéoclastes, associée à un ratio RANKL/OPG diminué^{10,26}.

RANKL est le composant clef de la triade RANKL/RANK/OPG, principale voie d'activation des ostéoclastes^{1,20}. L'activation de son récepteur RANK, présent dans la membrane des précurseurs, est fondamentale pour la différenciation et l'activation des ostéoclastes. Les ostéoclastes sont nécessaires au remodelage de l'os alvéolaire. Un défaut d'activation des ostéoclastes conduit à une altération de l'éruption dentaire et à des altérations de la formation des dents, notamment dans la partie radiculaire¹². Par contre, une sur-activation RANKL/RANK produit une accélération du développement et de l'éruption de la dent, avec un impact sur la forme finale de la racine²⁰.

L'impact de RANKL sur le développement du complexe dento-alvéolaire a été étudié chez des modèles animaux mutés pour RANKL. Dans ces modèles animaux, l'altération ostéopétrotique, qui correspond à une augmentation de la densité osseuse, est permanente car liée à l'inactivation complète du gène RANKL¹². Dans notre étude, nous avons évalué les conséquences d'une inhibition transitoire de RANKL sur le développement du complexe dento-alvéolaire. L'inhibition transitoire de RANKL conduit à une rétention intra-osseuse de la première et de la deuxième molaire, comparable aux rétentions primaires présentes sous une forme généralisée chez les patients ostéopétrotiques⁵, ou sous une forme localisée chez les patients sans syndromes ou maladies associées³².

L'altération du remodelage osseux et l'absence d'éruption dentaire sont liées à l'absence d'ostéoclastes fonctionnels dans les modèles d'ostéopétrose constitutifs. Dans notre étude, l'inhibition transitoire de RANKL par l'anticorps a paradoxalement un effet opposé à distance. En effet, un mois après la dernière injection, l'os alvéolaire entourant la couronne et les racines des molaires des souris injectées présente un nombre augmenté des cellules TRAP positives, en comparaison avec les molaires des souris contrôle.

Plusieurs explications peuvent être avancées : 1. L'inhibition de RANKL activerait une voie alternative compensatoire pour l'activation des ostéoclastes telle que la voie ostéo-immunitaire par exemple. 2.

L'inhibition de RANKL durant les premiers jours post-nataux inhiberait la différenciation des ostéoclastes durant cette période, ce qui entraîne une altération complète mais transitoire du processus d'éruption de la dent. En effet, un mois après l'arrêt du traitement, la différenciation OC reprend son cours pour tenter de restaurer le défaut. 3. L'inhibition de RANKL pourrait avoir modifié d'autres voies de signalisation, en plus de l'ostéoclastogénèse. Ainsi, les voies de signalisation impliquées dans le modelage de l'os alvéolaire et dans la formation des racines, telles que celles des facteurs de croissance transformant la protéine morphogénétique osseuse (Tgfb/Bmp), Wingless/ β -caténine (Wnt/ β -catenin), facteur de croissance des fibroblastes (Fgf) et *Sonic hedgehog* (Shh), facteur de croissance semblable à l'insuline (IGF)^{12,17}, pourraient être inhibées, ce qui conduirait à l'altération de la formation radiculaire et l'absence d'éruption malgré la présence d'ostéoclastes.

En écho à ce dernier scénario, la voie de signalisation du PTHrP s'est avérée fortement impliquée dans certains types de rétention. Le PTHrP, un peptide lié à l'hormone parathyroïdienne, et son récepteur PTH1R ont été identifiés dans les cellules mésenchymateuses du FD et à la surface radiculaire. PTH1R est fortement exprimé par les ostéoblastes adjacents au germe dentaire, tandis que PTHrP est exprimé dans les cellules épithéliales de la lame dentaire et dans le reticulum étoilé juste avant la formation de la voie d'éruption¹⁶. Il a été proposé que PTHrP et PTH1R pourraient jouer un rôle important dans la régulation de la morphogénèse de la racine et du maintien du parodonte²¹. Un rôle de PTHrP/PTH1R dans la formation et l'activation des ostéoclastes a été suggéré à travers la signalisation de RANKL et dans le processus de formation radiculaire des molaires de souris¹⁶. Chez l'homme, des mutations du gène codant PTHrP ont été identifiées chez des patients présentant des anomalies de l'éruption primaire⁴. Le défaut primaire de l'éruption a été décrit comme une altération non-syndromique de l'éruption. La dent présente une absence totale ou partielle de l'éruption en l'absence d'un obstacle mécanique²⁴. C'est un défaut qui touche principalement les molaires permanentes (M1 et M2) et, malgré une faible prévalence (0,06), les différentes études montrent qu'il s'agit d'une altération dont la fréquence augmente progressivement^{9,25}. Son étiologie n'a pas été complètement clarifiée. Pour certains auteurs, il s'agit d'une maladie génétique à transmission autosomique dominante.

Les souris mutées pour le PTHrP présentent une différenciation normale des ostéoclastes dans la crypte osseuse des molaires. Ces animaux ne présentent donc pas d'ostéopétrose. Cependant, l'éruption des molaires est perturbée. Les auteurs évoquent une perturbation épithélio-mésenchymateuse à l'origine de la rétention de la dent²³.

Comme indiqué précédemment, un certain nombre de voies de signalisation ont été identifiées comme étant importantes pour la formation radiculaire et l'éruption dentaire. Les facteurs impliqués dans les interactions des cellules épithéliales et des cellules mésenchymateuses, au cours de la formation du complexe dento-alvéolaire, ont été amplement décrits. Cependant, il reste encore de nombreuses questions notamment concernant l'étiologie de la rétention des molaires, autre qu'une altération du modelage osseux.

Nous avons constaté que l'application de l'anticorps anti-RANKL a des effets sur le développement dentaire, en particulier la formation radiculaire. Une altération de la taille, de la forme et de la structure de la racine est évidente chez les souris injectées. D'autres études sur les effets de la mutation de RANKL ont associé les altérations de la formation de la gaine épithéliale de Hertwig et l'arrêt de l'élongation radiculaire à l'absence d'ostéoclastes et au défaut du modelage de l'os alvéolaire lors de la formation de la dent¹².

5. Conclusion

L'étude des mécanismes de la formation des racines et de l'éruption des dents est essentielle pour la compréhension des troubles de l'éruption dans les syndromes congénitaux et dans les altérations isolées localisées non syndromiques. Nos travaux qui portent sur le rôle de la signalisation RANKL/RANK/OPG ont montré que toute altération de cette voie de signalisation, cardinale pour les ostéoclastes, pendant les premiers jours de vie chez la souris C57BL/6, aboutit à la rétention des molaires. Cela suggère que, chez nos patients, les dents retenues pourraient être la conséquence d'une atteinte localisée dans l'espace et dans le temps de cette signalisation par des facteurs qui restent à définir.

Conflit d'intérêt

Les auteurs déclarent n'avoir aucun lien d'intérêt concernant les données publiées dans cet article.

Bibliographie

1. Berdal A, Castaneda B, Aioub M, Néfussi JR, Mueller C, Descroix V, Lezot F. Osteoclasts in the dental microenvironment: A delicate balance controls dental histogenesis. *Cells Tissues Organs* 2011;194:238-243.
2. Castañeda B, Simon Y, Jacques J, Hess E, Choi YW, Blin-Wakkach C, et al. Bone resorption control of tooth eruption and root morphogenesis: Involvement of the receptor activator of NF- κ B (RANK). *J Cell Physiol* 2011;226:74-85.
3. Cobourne MT, Sharpe PT. Diseases of the tooth: the genetic and molecular basis of inherited anomalies affecting the dentition. *Wiley Interdiscip Rev Dev Biol* 2013;2(2):183-212.
4. Decker E, Stellzig-Eisenhauer A, Fiebig BS, Rau C, Kress W, Saar K, et al. PTHR1 Loss-of-Function Mutations in Familial, Nonsyndromic Primary Failure of Tooth Eruption. *Am J Hum Genet* 2008;83(6):781-786.
5. Fleischmannova J, Matalova E, Sharpe PT, Misek I, Radlanski RJ. Formation of the tooth-bone interface. *J Dent Res* 2010;89(2):108-115.
6. Frazier-Bowers SA, Koehler KE, Ackerman JL, Proffit WR. Primary failure of eruption: Further characterization of a rare eruption disorder. *Am J Orthod Dentofac Orthop* 2007;131(5):1-11.
7. Frazier-Bowers S, Puranik P, Mahaney MC. The etiology of eruption disorders - further evidence of a genetic paradigm. *J Semin* 2010;16(3):180-185.
8. Frazier-Bowers SA, Simmons D, Wright JT, Proffit WR, Ackerman JL. Primary failure of eruption and PTH1R: The importance of a genetic diagnosis for orthodontic treatment planning. *Am J Orthod Dentofac Orthop* 2010;137(2):160-167.
9. Frazier-Bowers SA, Hendricks H, Wright JT, Lee J, Largo K, Dibble C. Novel mutations in PTH1R associated with primary failure of eruption and osteoarthritis. *J Dent Res* 2014;93(2):134-139.
10. Ge J, Guo S, Fu Y, Zhou P, Zhang P, Du Y, et al. Dental follicle cells participate in tooth eruption via the RUNX2-MiR-31-SATB2 loop. *J Dent Res* 2015;94(7):936-944.
11. Hanisch M, Hanisch L, Kleinheinz J, Jung S. Primary failure of eruption (PFE) : a systematic review. *Head Face Med* 2018;14(1):5.
12. Helfrich MH. Osteoclast diseases and dental abnormalities. *Arch Oral Biol* 2005;50(2):115-122.
13. Honda M, Imaizumi M, Suzuki H, Ohshima S, Tsuchiya S, Satomura K. Stem cells isolated from human dental follicles have osteogenic potential. *Oral Surgery, Oral Med Oral Pathol Oral Radiol Endod* 2011;111(6):700-708.
14. Huang H, Wang J, Zhang Y, Zhu G, Li YP, Ping J, Chen W. Bone resorption deficiency affects tooth root development in RANKL mutant mice due to attenuated IGF-1 signaling in radicular odontoblasts. *Bone* 2018;114:161-171.
15. Kim J-Y, Kim M-R, Kim S-J. Modulation of osteoblastic/odontoblastic differentiation of adult mesenchymal stem cells through gene introduction: a brief review. *J Korean Assoc Oral Maxillofac Surg* 2013;39(2):55-62.

16. Kitahara Y, Suda N, Kuroda T, Beck F, Hammond V, Takano Y. Disturbed Tooth Development in Parathyroid Hormone-related Protein (PTHrP) - Gene Knockout Mice. *Bone* 2002;30(1):48-56.
17. Li J, Parada C, Chai Y. Cellular and molecular mechanisms of tooth root development. *Development* 2017;144(3):374-384.
18. Martin TJ. Historically significant events in the discovery of RANK/RANKL/OPG. *J Orthop* 2013;18(4):186-197.
19. Mattheeuws N, Dermaut L, Martens G. Has hypodontia increased in Caucasians during the 20th century? A meta-analysis. *Eur J Orthod* 2004;26(1):99-103.
20. Ohazama A, Courtney JM, Sharpe PT. Expression of TNF-Receptor-associated factor genes in murine tooth development. *Gene Expr Patterns* 2003;3(2):127-129.
21. Ono W, Sakagami N, Nishimori S, Ono N, Kronenberg HM. Parathyroid hormone receptor signalling in osteoblast-expressing mesenchymal progenitors is essential for tooth root formation. *Nat Commun* 2015;1-16.
22. Philbrick W, Dreyer B, Nakchbandi I, Karaplis A. Parathyroid hormone-related protein is required for tooth eruption. *Proc Natl Acad Sci USA* 1998;95(20):11846-11851.
23. Piattelli A, Eleuterio A. Primary failure of eruption. *Acta Stomatol Belg* 1991;88(3):127-130.
24. Proffit W, Frazier-Bowers SA. Mechanism and control of tooth eruption : overview and clinical implications. *Orthod Craniofac Res* 2009;12(2):59-66.
25. Silva MA, Vasconcelos DF, Marques MR, Barros SP. Parathyroid hormone intermittent administration promotes delay on rat incisor eruption. *Arch Oral Biol* 2016;69:102-108.
26. Sun X, Wang X, Zhang C, Liu Y, Yang X, Yan W, et al. RUNX2 mutation impairs bone remodelling of dental follicle cells and periodontal ligament cells in patients with cleidocranial dysplasia. *Mutagenesis* 2016;31(6):677-685.
27. Van Wesenbeeck L, Odgren PR, MacKay CA, D'Angelo M, Safadi FF, Popoff SN, et al. The osteopetrotic mutation toothless (tl) is a loss-of-function frameshift mutation in the rat *Csf1* gene: Evidence of a crucial role for CSF-1 in osteoclastogenesis and endochondral ossification. *Proc Natl Acad Sci USA* 2002;99(22):14303-14308.
28. Vieira AR. Oral clefts and syndromic forms of tooth agenesis as models for genetics of isolated tooth agenesis. *J Dent Res* 2003;82(3):162-165.
29. Wise GE, Frazier-Bowers S, D'Souza RN. Cellular, Molecular and Genetic Determinants of Tooth Eruption. *Crit Rev Oral Biol Med* 2002;13(4):323-335.
30. Wise GE. Cellular and molecular basis of tooth eruption. *Orthod Craniofac Res* 2009;12(2):67-73.
31. Wise GE, King GJ. Mechanisms of tooth eruption and orthodontic tooth movement. *J Dent Res* 2008;87(5):414-434.
32. Wise GE, Lin F. The molecular biology of initiation of tooth eruption. *J Dent Res* 1995;74(1):303-306.
33. Yao S, Pan F, Prpic V, Wise GE. Differentiation of stem cells in the dental follicle. *J Dent Res* 2008;87(8):767-771.